



Targeted and Untargeted Metabolomic Profiling of Human Serum, Urine and Brain by Liquid Chromatography-Mass Spectrometry (LC-MS)

A thesis presented in fulfilment of the Degree of Doctor of Philosophy in
Pharmacy and Biomedical Sciences at the University of Strathclyde

By

ALI MUHSEN ALI

BSc Chemistry, MSc Clinical Biochemistry

Strathclyde Institute of Pharmacy & Biomedical Sciences

Faculty of Sciences, University of Strathclyde

161 Cathedral Street, Glasgow, G4 0RE

United Kingdom

December, 2018

AUTHOR'S DECLARATION:

I declare that this thesis is the result of the author's original research. It has been composed by the author and has not been previously submitted for examination which has led to the award of a degree.

The copyright of this thesis belongs to the author under the terms of the United Kingdom Copyright Acts as qualified by University of Strathclyde Regulation 3.50. Due acknowledgement must always be made of the use of any material contained in, or derived from, this thesis.

Signed: -----

Date: -----

ACKNOWLEDGEMENTS

I would firstly like to express my sincerest gratitude to my lord ‘‘Allah’’ for providing me with health, commitment and patience to complete my PhD study. I am very grateful for my supervisor Dr Dave Watson for his outstanding supervision and his continuous guidance, support and encouragement throughout the three years of my study. I would also like to thank him for making my PhD period a most enjoyable and fulfilling experience. My gratitude goes to the laboratory technical staff and the other post graduate students in the group for being all round nice folks and being great fun to work with, as well as all that hard work we carried out together. My heartfelt thanks go to all the other people who have volunteered to help with the experimental work of the thesis. I would like to thank Colin Smith, Robert Walker and Chris-Anne McKenzie of the MRC Sudden Death Brain and Tissue Bank for their assistance in sample provision. I would also like to thank the Scottish Life Sciences Alliance for funding mass spectrometry instruments. My thanks are also extended to my colleagues we worked together in our publications that were part in this thesis.

I am indebted and thankful to my parents, may Allah rest their soul, who provided me with the opportunities to self-discover since my childhood and guided me forward to achieve my scientific ambition. In particular, I would like to take this opportunity to express my sincerest appreciation to my dear wife, WAFAA, for her incessant support and encouragement during the difficult times of my academic and social life. Also my thanks are owed to my brothers and sisters and to all my friends for their support during my study.

Finally, I wish to thank the ministry of higher education and scientific research, Iraqi government for funding for my PhD study.

CONTENTS

Author's Declaration:	I
Acknowledgements:	II
List of Figures:	X
List of Tables:.....	XIV
Abbreviation List:.....	XVI
Published papers and presented posters:.....	XVII
Abstract:	XVIII
CHAPTER 1 GENERAL INTRODUCTION	1
1.1 Metabolism and Metabolites	1
1.2 Metabolomics	3
1.2.1 Targeted Metabolomics.....	5
1.2.2 Untargeted Metabolomics	6
1.3 Metabolomics in Biomedical Research	7
1.3.1 Potential applications of Metabolomics.....	8
1.3.2 The Pathological Factors Effects on Metabolic Phenotype	10
1.3.3 The Physiological Factors Relevant to the Metabolic Phenotype.....	13
1.4 Metabolomic Approaches Workflow	14
1.4.1 Data Acquisition.....	15
1.4.2 Data Processing.....	17
1.4.3 Data Analysis	23
1.4.4 Data Validation	27
1.4.5 Data Interpretation	30

1.5	Analytical Tools	32
1.5.1	Separation Technology.....	32
1.5.2	Mass Spectrometry (MS)	37
1.5.3	Gas Chromatography/Mass Spectrometry (GC/MS)	40
1.5.4	Liquid Chromatography-Mass Spectrometry (LC-MS).....	42
1.6	Aims of Study.....	44
CHAPTER 2 MATERIALS AND METHODS.....		46
2.1	Chemicals and Solvents.....	47
2.2	Biological Samples Preparation	47
2.3	Standard Solutions Preparation:	47
2.4	Pooled Samples Preparation	48
2.5	HPLC Conditions	48
2.5.1	Mobile Phase Solutions for ZIC-pHILIC Chromatography.....	48
2.5.2	Mobile Phase for C18 Chromatography	49
2.5.3	HPLC Setup	49
2.5.4	MS Setup of Exactive and LTQ-Orbitrap	51
2.6	LC-MS Data Extraction and Processing	52
2.6.1	Data Processing by MZmine 2-14.....	52
2.7	Metabolomics Profiling	59
2.7.1	Statistical Software.....	59
2.7.2	Pre-Treatment.....	59
2.7.3	Data Visualisation and Biomarkers Identification	59
2.7.4	Diagnostics and Validation	61
2.7.5	Putative Biomarker Selection Workflow	62

CHAPTER 3 METABOLOMIC PROFILING OF THE EFFECTS OF SUBMAXIMAL EXERCISE AT A STANDARDISED RELATIVE INTENSITY IN HEALTHY ADULTS IN ORDER TO DETERMINE MARKERS OF PHYSICAL FITNESS RELATED TO VO₂MAX..... 63

3.1	Introduction	65
3.1.1	Urine Metabolome	67
3.1.2	Metabolomic profiling of Exercise Urine Samples as A Predictor of VO ₂ max	70
3.1.3	Aim of Study	72
3.2	Materials and Methods	72
3.2.1	Chemicals and Solvents	72
3.2.2	Subjects and Experimental Design.....	72
3.2.3	Experimental Design.....	73
3.2.4	VO ₂ max Test	74
3.2.5	Submaximal Test.....	75
3.2.6	Sample Collection and Preparation.....	75
3.2.7	LC-MS Method	76
3.3	LC-MS Data Processing and Statistical Analysis	77
3.4	Results	78
3.4.1	Physiological Responses to Submaximal Exercise	78
3.4.2	Metabolite Profiling	78
3.5	Discussion	99
3.6	Conclusion.....	104

CHAPTER 4 METABOLOMIC PROFILING OF POST-MORTEM BRAIN IN ORDER DETERMINE DIAGNOSTIC MARKERS CLASSIFYING DIFFERENT TYPES OF MENTAL ILLNESS..... 105

4.1	Introduction	107
4.1.1	Aims of Study	108
4.2	Materials and Methods	109
4.2.1	Chemicals and Solvents	109
4.2.2	Post-Mortem Brain Samples:	109
4.2.3	Sample Extraction	110
4.2.4	HILIC–HRMS Analysis.....	111
4.2.5	Analysis of Sugar Acids and Polyols by GC-MS	111
4.2.6	Data Extraction and Metabolite Identification.....	112
4.2.7	Univariate and Multivariate Analysis	113
4.2.8	Diagnostics and Validation of Models.....	114
4.3	Results	115
4.3.1	The Effect of the HPLC Column Used on the Results.....	115
4.3.2	Comparison of Control and Schizophrenic/Depressive/Bipolar/Diabetic Brains Using PCA.....	116
4.3.3	Comparison of SDB and SDBDI Samples against Controls Using OPLSDA.....	118
4.3.4	SDB Samples Show Differences in Branched Amino Acid, Neurotransmitter and Sugar Metabolism Compared With Controls	121
4.3.5	The Effect of Age on Metabolite Profiles of Brain Tissue	121
4.3.6	Inclusion of Diabetic Brains in the OPLSDA Model	123
4.3.7	Preparation of the PCA Model with a Reduced Metabolite List	126
4.3.8	Refining the OPLSDA Models	128

4.3.9	GC-MS Analysis to Quantify and Identify Polyols and Polyol Acids in Brain	132
4.4	Discussion	137
4.4.1	High Levels of BCAs and Other Liphilic Amino Acids in SDB Samples	137
4.4.2	Alterations in Sugar Metabolism	138
4.4.3	Elevation of Polyols and Oxidative Stress	139
4.4.4	Altered Purine Metabolism	141
4.4.5	Gamma-aminobutyric acid (GABA) Deficiency	142
4.4.6	Alterations in Biogenic Amine Metabolism	142
4.4.7	Differences in a Sub-group of SDB Samples.....	143
4.4.8	OPLS-DA Models Based on Reduced Metabolites	144
4.5	Conclusion.....	145

CHAPTER 5 THE ANALYSIS OF SUGARS IN POST-MORTEM HUMAN BRAIN IN ORDER TO DETERMINE WHETHER OR NOT PERTURBED SUGAR METABOLISM IS ASSOCIATED WITH MENTAL ILLNESS 146

5.1	Introduction	148
5.1.1	Aim of the Study	152
5.2	Materials and Methods	152
5.2.1	Chemicals and Materials	152
5.2.2	Biological Samples	152
5.2.3	Sugar Derivatisation.....	153
5.2.4	Profiling of Biological Samples	154
5.2.5	LC-MS Analysis	154
5.3	Results	155

5.3.1	Underivatised Sugars	155
5.3.2	Tagging with Deuterated Aniline (² H ₅ -aniline)	156
5.3.3	Quantification and Profiling of Sugars in Post-Mortem Human Brain	159
5.4	Discussion:	171
5.5	Conclusion.....	173

CHAPTER 6 DEVELOPMENT OF AN LC-MS METHOD FOR THE ENHANCED DETECTION OF OXIDISED FATTY ACIDS IN PLASMA AND ITS APPLICATION TO DETERMINE THE EFFECTS OF THE INGESTION OF THE ANTI-OXIDANT BEETROOT JUICE..... 174

6.1	Introduction	176
6.1.1	Derivatisation in Mass Spectrometric Analysis	177
6.1.2	Aim of the Study	179
6.2	Materials and Methods	180
6.2.1	Chemical and Materials.....	180
6.2.2	Plasma Samples Collection:.....	181
6.2.3	Preparation of Plasma Solutions and Reagents.....	182
6.2.4	Native and Internal Standards	182
6.2.5	Standard Curve Preparation	183
6.2.6	Fatty Acids and its Oxidised Derivatisation	183
6.2.7	LC-MS Analysis	184
6.3	Results	185
6.3.1	Underivatised Oxidised Fatty Acids	185
6.3.2	Fatty Acids Derivatisation.....	187
6.3.3	Oxidised Fatty Acids Derivatisation	190

6.3.4	Oxylipin Quantification and Profiling of Plasma Samples from Healthy Human	194
6.4	Discussion	204
6.5	Conclusion.....	207
CHAPTER 7	GENERAL DISCUSSION.....	208
7.1	Discussion	209
REFERENCES	215
APPENDIX-1: SUPPLEMENTARY DATA	233
APPENDIX-II: POSTER PRESENTED IN CONFERENCES	292

LIST OF FIGURES:

Figure 1-1: The untargeted metabolomic workflow is divided into three major steps which include seven sub steps for identification and quantification of metabolites in biological samples by LC/MS-based metabolomics.	15
Figure 1- 2: The schematic layout of the steps of data processing.	17
Figure 1-3: The chemical structure (A) ZIC-HILIC and (B) ZIC-cHILIC stationary phases.	37
Figure 1-4: Gas Chromatography/Mass Spectrometry diagram.	41
Figure 2-1: The setting of mass detection parameters..	53
Figure 2-2: The setting of chromatogram builder parameters.	54
Figure 2-3: The setting of chromatogram deconvolution parameters.	54
Figure 2-4: The setting of de-isotoping module parameters.	55
Figure 2-5: The setting of required parameters for the alignment method.	56
Figure 2-6: The parameters setup dialog of gap filling.	56
Figure 2-7: The setting of filtering module parameters.	57
Figure 2-8: the parameters setup dialog of Identification method.	58
Figure 3-1: Indicative representation of urine collection schematic. The first urine sample on each day was the first pass after waking (typically 6 am–8 am).	74
Figure 3- 2: PCA comparing D2S1 (green) and D2S3 (blue) samples based on the peak areas for the raw data (un-normalised).	80
Figure 3-3: Separation of D2S1 (green) from the post exercise D2S3 (blue) samples by using PCA.	81
Figure 3-4: Separation of day 1 first void (D1S1-green) and third samples (D1S3-blue) by using PCA.	81
Figure 3-5: Separation of D2S1 (green) and D2S3 (blue) samples by using OPLSDA based on 3078 features.	86
Figure 3-6: Cross validation model for the classification of D2S1and D2S3 by OPLSDA.	87
Figure 3-7: Separation of D1S1 (green) and D1S3 (blue) by OPLSDA based on 3540 features.	87
Figure 3-8: Cross validation of the separation of D1S1 and D1S3 by OPLSDA.	88
Figure 3-9: S-plot for OPLSDA model of D2S3 vs D2S1 highlighting the metabolites listed in Table 3-S2.	89
Figure 3-10: S-plot for OPLSDA model of D1S3 vs D1S1 highlighting the metabolites listed in Table 3-S3.	89
Figure 3-11: Plot of measured against predicted VO ₂ max against normalised levels of OHA.	94
Figure 3-12: Extracted ion trace for OHA isomers in urine comparing a pre- and post-exercise sample for samples D2S1 and D2S3 for a subject with VO ₂ max 53.4.	94

Figure 3-13: MS2 of oxoaminohexanoic acid obtained with a collision energy of 35V.....	96
Figure 3-14: Plot of (area OHA D2S3/area OHA isomer D2S3)/ (area OHA D2S1/area OHA isomer D2S1).....	96
Figure 3-15: a diagrammatic model of the biochemistry for metabolites differing between D2S1 and D2S3 in comparison with D1S1 and D1S3.....	103
Figure 4-1: PCA plot for control, SDB and DI samples (R2X cum 0.61, Q2 (cum) 0.464, and three components) based on 755 metabolites from positive and negative ion modes.	117
Figure 4-2: OPLS-DA model (R2 (cum) 0.976, Q2 (cum) 0.671 and Six components) of control (n = 17) compared to SDB (n = 19) brain samples based on 755 metabolites from positive and negative ion modes	119
Figure 4-3: Permutation plot for the OPLS-DA model compared to control and SDB brain samples based on 755 metabolites from positive and negative ion modes as shown in Figure 4-2.	119
Figure 4-4: OPLS correlation of brain metabolite profiles to the age of the subjects (R2X (cum) 0.706), R2Y (cum) 0.979, Q2 (cum) 0.476).	122
Figure 4-5: OPLS-DA model (R2 (cum) 0.850, Q2 (cum) 0.534, four components) including six of the DI samples. Green control and blue SDB + DI brain samples based on 755 metabolites from positive and negative ion modes.....	124
Figure 4-6: Permutations plot for the OPLS-DA model compared to control and SDB-DI brain samples based on 755 metabolites from positive and negative ion modes shown in figure 4-5.	124
Figure 4-7: PCA model (R2X=0.68, Q2X=0.283 and five components) based on the metabolites with P-values <0.05 (table 4-S2) when the control and SDB samples are compared and hierarchical cluster analysis (Fig. 4-S2).	126
Figure 4-8: OPLSDA model (R2Y (cum) 0.725, Q2 (cum) 0.638, and five components) of 18 controls (green) compared to 20 SDB brain samples (blue) based on the filtered 120 metabolites.....	129
Figure 4-9: Permutations plot for the OPLS-DA model shown in Fig. 4-8.....	129
Figure 4-10: OPLSDA model of 18 controls (green) compared to 27 SDBDI brain samples (blue) based on the filtered 120 metabolites.	130
Figure 4-11: Permutations plot for the OPLS-DA model shown in Fig. 4-10.....	131
Figure 4-12: GC-MS analysis of polyol standards at 0.8µg/0.2ml (A and C) in comparison with polyols in brain (B and D).....	134
Figure 4-13: Separation of SDB + DI brain samples (green) and controls (blue) on the basis of the GC-MS analysis of sugar alcohols.....	135
Figure 4-14: Cross validation by permutation plot for Figure 4-13.....	135

Figure 5-1: The equilibrium forms of glucose where the aldehyde group can react to form 5 (furan) or six membered ring via formation of a hemiacetal. The hydroxyl group generated can be in the α - or β -position.....	148
Figure 5-2: Reductive amination of a sugar and its derivatives using deuterio- $^2\text{H}_5$ aniline and picoline borane.	153
Figure 5-3: Extracted ion chromatograms for glucose and galactose in negative ion mode on a ZICpHILIC column (150×4.6 mm, 5 μm) with a gradient between acetonitrile and ammonium carbonate pH 9.2.	155
Figure 5-4: Comparison of the separation of (A) aniline and (B) $^2\text{H}_5$ -aniline derivatives galactose and mannose run on a ZICHILIC column in ACN/water containing 0.01% (v/v) formic acid at 0.6 ml/min.	157
Figure 5-5: $^2\text{H}_5$ -aniline of 1 μg amounts of hexose standards run on a ZICHILIC column in ACN/water containing 0.01% (v/v) formic acid at 0.6 ml/min.	157
Figure 5-6: Calibration curve for glucose (0.5-8.0 μg).....	161
Figure 5-7: Calibration curve for galactose (0.1-1.6 μg).....	161
Figure 5-8: Calibration curve for mannose (0.1-1.6 μg).....	162
Figure 5-9: Calibration curve for fructose (0.1-1.6 μg).....	162
Figure 5-10: Calibration curve for glucuronic acid (0.1-1.6 μg).....	163
Figure 5-11: Calibration curve for galacturonic acid (0.1-1.6 μg).....	163
Figure 5-12: Calibration curve for ribose (0.1-1.6 μg).....	164
Figure 5-13: Calibration curve for xylose (0.1-1.6 μg).....	164
Figure 5-14: Calibration curve for N-acetyl glucosamine (0.1-1.6 μg).....	165
Figure 5-15: Calibration curve for N-acetylneuraminic (0.1-1.6 μg).....	165
Figure 5-16: Hexoses extracted from brain tissue obtained from an individual with bipolar disorder and a control sample.	169
Figure 5-17: Pentose extracted from brain tissue obtained from an individual with bipolar disorder and a control sample.	170
Figure 5-18: Additional sugar isomers extracted from brain tissue obtained from an individual with bipolar disorder.....	170
Figure 6-1: Scheme for the time-points of plasma collection.....	181
Figure 6-2: Choline coupling of carboxylic acids scheme.....	184
Figure 6-3: Extracted ion chromatograms for the standard mixture of LAO in positive ion mode by non-derivatisation LC-MS method on a ACE 3 C18 column (150 x 3.0mm, 5 μm).....	186
Figure 6-4: Extracted ion chromatograms for the standard mixture of ArAO in positive ion mode by non-derivatisation LC-MS method on a ACE 3 C18 column (150 x 3.0mm, 5 μm).....	186
Figure 6-5: The coupling reaction outline and the exact mass of the coupled fatty acids, palmitic acid and myrestic acid after derivatisation method.	187

Figure 6-6: Extracted ion chromatograms and the mass spectral analysis for derivatives of palmitic acid by coupling with choline using FMP reagent on a C18 column.....	188
Figure 6-7: Extracted ion chromatograms and the mass spectral analysis for derivatives of myristic acid by coupling with choline using FMP reagent on a C18 column.....	188
Figure 6-8: Calibration curve of palmitic acid in the range of 0.01-1 μ g/ml.....	189
Figure 6-9: The discrimination between LAO isomers.....	191
Figure 6-10: The chromatographic separation among the standard mixture components of LAO under derivatisation conditions.	193
Figure 6-11: The chromatographic separation among the standard mixture components of ArAO under derivatisation conditions.	193
Figure 6-12: LAO isomers extracted from plasma samples	195
Figure 6-13: the calibration curves of 13-oxo-9Z,11E-octadecadienoic acid in the range (2.5-160.0 ng).....	196
Figure 6-14: The calibration curves of 9-oxo-10E,12Z-octadecadienoic acid in the range (2.5-160.0 ng).....	196
Figure 6-15: the calibration curves of 9S-hydroxy-10E,12Z-octadecadienoic acid in the range (2.5-160.0 ng).....	197
Figure 6-16: the calibration curves of 13S-hydroxy-9Z, 11E-octadecadienoic acid in the range (2.5-160.0 ng).....	197
Figure 6-17: the calibration curves of (\pm) 9, 10-epoxy-12Z-octadecenoic acid in the range (2.5-160.0 ng).....	198
Figure 6-18: the calibration curves of (\pm) 12, (13) epoxy-9Z-octadecenoic acid in the range (2.5-160.0 ng).....	198
Figure 6-19: the calibration curves of (\pm) 9, 10-dihydroxy-12Z-octadecenoic acid in the range (2.5-160.0 ng).....	199
Figure 6-20: the calibration curves of (\pm) 12, 13-dihydroxy-9Z-octadecenoic acid in the range (2.5-160.0 ng).....	199
Figure 6-21: the calibration curves of 5-oxo-6E, 8Z, 11Z, 14Z-eicosatetraenoic acid in the range (2.5-160.0 ng).....	200
Figure 6-22: the calibration curves of 12-oxo-5Z, 8Z, 10E, 14Z-eicosatetraenoic acid in the range (2.5-160.0 ng).....	200
Figure 6-23: the calibration curves of 15-oxo-5Z, 8Z, 11Z, 13E-eicosatetraenoic acid in the range (2.5-160.0 ng).....	201
Figure 6-24: the calibration curves of 5S-hydroxy-6E, 8Z, 11Z, 14Z-eicosatetraenoic acid in the range (2.5-160.0 ng).	201
Figure 6-25: the calibration curves of 12S-hydroxy-5Z, 8Z, 10E, 14Z-eicosatetraenoic acid in the range (2.5-160.0 ng).	202
Figure 6-26: the calibration curves of 15S-hydroxy-5Z, 8Z, 11Z, 13E-eicosatetraenoic acid in the range (2.5-160.0 ng).	202

LIST OF TABLES:

Table 2-1: Gradient elution programme applied for ZICpHILIC column in LC-MS analysis.....	50
Table 2-2: Gradient elution programme applied for C18-AR in LC-MS analysis. ..	50
Table 3-1: Participant Characteristics. Values are mean \pm SD; n, number of subjects; F, female; M, male; aerobic capacity (VO_{2max}) and maximal cycling work rate (WR_{max}).....	73
Table 3-2: The gradient programme.....	77
Table 3-3: Summarises univariate comparisons for all the metabolites that are appeared in comparison between first sample post-exercise (S3) with the rest of samples in both days (D1 and D2).	82
Table 3-4: Metabolites differing between D2S1 and D2S3 in comparison with D1S1 and D1S3.....	90
Table 3-5: Predicted VO_{2max} values for all samples of day-2 based on normalised response for OHA.	97
Table 4-1: Summary information for the different groups of brain samples.	110
Table 4-2: Metabolites with high impact on the LOPS-DA model separating control (17) from SDB (19) samples.....	120
Table 4-3: Most significant metabolite changes with the age of brain tissue.	122
Table 4-4: Metabolites with high impact on the model separating controls from SDB brains combined with diabetic brains.....	125
Table 4-5: Important metabolites defining the sub-group of nine SDB brains shown in Figure 4-7.....	127
Table 4-6: Marker compounds resulted of the OPLSDA model shown in Figure 4-8. *For the 38 samples used in the model.....	128
Table 4-7: Marker compounds resulting from the OPLSDA model shown in Figure 4-10. *For the 45 samples used in the model.....	131

Table 4-8: Retention data for polyol isomers and acids analysed by GC-MS in EI mode.....	133
Table 4-9: Calibration curve data for sugar alcohols and gluconic acid over the range 1-16µg with pinitol as an internal standard.....	136
Table 4-10: The amounts of sugar alcohols and gluconic acid in post-mortem brain samples.....	136
Table 5-1: Retention and molecular ion data for some sugar standards tagged with of ² H ₅ - aniline and run on a ZICHILIC column in ACN/water containing 0.01% (v/v) formic acid at 0.6 ml/min.	159
Table 5-2: Summary table showing peaks areas and peak-area ratios of A: glucose with (0.5-8µg) and B: other sugar standards with (0.1-1.6µg) to ¹³ C ₆ - glucose as internal standard (InS).....	160
Table 5-3: Calibration data based on ratio of response of derivatised sugars to response for derivatised internal standard (13C-glucose) over the range 0.1-1.6µg.	166
Table 5-4: Summary table showing amount of the major sugars tagged with of ² H ₅ - aniline in 200mg of control, and SDB brain tissue.	167
Table 5-5: Summarises the average of the amounts of hexose, pentose, NANA and gluconic acid in post-mortem brain samples with schizophrenia, depression, bipolar and control.....	169
Table 6-1: The chemical formula, molar mass and retention time for the oxylipin metabolites after carrying out derivatisation procedure.....	192
Table 6-2: Calibration data based on ratio of response of derivatised oxylpins to response for derivatised internal standard (13(S)-HODE-d4) over the range 2.5-160.0 ng.....	203
Table 6-3: Concentrations (ng/100ul) for oxylipin metabolites derived from LAO and ArAO in plasma samples at pre- and post-ingested beetroot.....	203

ABBREVIATION LIST:

BMI	Body mass index
CVD	Cardiovascular disease
GABA	Gamma-aminobutyric acid
GC	Gas chromatography
HILIC	Hydrophilic Interaction Liquid Chromatography
HRMS	High Resolution Mass Spectrometer
HGPRT	Hypoxanthine-guanine phosphoribosyl transferase
JS	Jaundice syndrome
LC	Liquid chromatography
MS	Mass spectrometer
M/Z	Mass-to-Charge Ratio
NAAG	N-acetyl aspartyl glutamate
OHA	Oxoaminohexanoic acid
OPLS	Orthogonal Partial Least Squares
OPLSDA	Orthogonal Partial Least Squares Discriminant Analysis
PCA	Principle Components Analysis
PK	Pantothenate kinase
ROS	Reactive oxygen species
RP	Reversed Phase
RT	Retention time
TOF	Time of Flight

PUBLISHED PAPERS AND PRESENTED POSTERS:

Papers

- 1) **Ali Muhsen Ali**, Mia Burleigh, Evangelia Daskalaki, Tong Zhang, Chris Easton and David G. Watson. Metabolomic Profiling of Submaximal Exercise at a Standardised Relative Intensity in Healthy Adults. *Metabolites Journal*. 2016 Feb 26; 6 (1).
- 2) Rong Zhang, Tong Zhang, **Ali Muhsen Ali**, Mohammed Al Washih, Benjamin Pickard, David G. Watson. Metabolomic Profiling of Post-Mortem Brain Reveals Changes in Amino Acid and Glucose Metabolism in Mental Illness Compared with Controls. *Computational and Structural Biotechnology Journal*. 2016 Feb 26; Vol (14); Pages (106–116).
- 3) Sami Bawazeer, **Ali Muhsen Ali**, Aliyah Alhawiti, Abedawn Khalaf, Colin Gibson, Jonans Tusiimire, David G. Watson. A method for the analysis of sugars in biological systems using reductive amination in combination with hydrophilic interaction chromatography and high resolution mass spectrometry. *Talanta*. 13 January 2017; Vol (166); Pages (75–80).

Posters

- 1) The Impact of Exercise on the Urinary Metabolome. *University of Edinburgh, Edinburgh, Scotland, UK*. Scottish Metabolomics Network Inaugural Meeting; 30th November and 1st December 2015. (**Appendix-II-1**)
- 2) Metabolomic Changes in Plasma and Urine Following Exposure to Ultraviolet Radiation by Using Liquid Chromatography - Mass Spectrometry (LC-MS). *University of the Highland and Island, Inverness, Scotland, UK*. Scottish Metabolomics Network Meeting, 16th and 17th November 2016. (**The runner-up poster award**). (**Appendix-II-2**)
- 3) An Enhanced LC-MS Approach to Detection Carboxylic Acid in Biological Samples by Derivatisation with Choline Coupling. *City of Glasgow College, Glasgow, Scotland, UK*. Scottish Metabolomics Network Symposium, 2nd and 3rd of November 2017. (**Appendix-II-3**)

ABSTRACT

Four projects were undertaken in the current study to apply, and in some cases develop, metabolomic profiling methods based on LC-HRMS for application to different human biofluid and tissue samples.

In the first study concerns the potential of metabolic changes to give an indication of physical fitness. Urine samples were collected from ten physically active subjects who underwent two cycling exercise trials. Firstly, their aerobic capacity (VO_{2max}) was determined and the second was a 45 min submaximal exercise test. One hundred and twenty urine samples were collected in total over two days at regular time intervals: on day 1 where there was no exercise intervention; on day 2 where there was an exercise session and on day 3 where there was no exercise intervention. The metabolites affected by the exercise included a range of purine metabolites and several acyl carnitines. Some metabolites including bile acids and several amino acids were subject to diurnal variation during the rest day (day 1). Using OPLS modelling it proved possible to identify a single abundant urinary metabolite provisionally identified as oxo-aminohexanoic acid (OHA) as being strongly correlated with VO_{2max} .

Secondly, metabolomic profiling was carried out on 53 post-mortem brain samples from subjects diagnosed with schizophrenia (S), depression (D), bipolar (B), diabetes (Di) and controls (C) in order determine whether or not there were clear metabolites distinguishing these conditions. The most important metabolites producing discrimination were the lipophilic amino acids leucine/isoleucine, proline, methionine, phenylalanine, and tyrosine; the neurotransmitters gamma-aminobutyric acid (GABA)

and N-acetyl aspartyl glutamate (NAAG) and sugar metabolites sorbitol, gluconic acid, xylitol, ribitol, arabinotol, and erythritol. For the determination of the sugar polyols it was necessary to develop and new GC-MS method. There appears some commonality between metabolic perturbations resulting from diabetes and from SDB. This study concluded that the changes in sugar alcohol levels which were quantified in physiological fluids confirm the metabolic similarity between mental illness and diabetes. This leads to the question regarding whether or not antidiabetic drugs might have a role in treating mental illness?

In a third project a reductive amination method was used in combination with hydrophilic interaction liquid chromatography and high resolution mass spectrometry to analyse the sugars in post-mortem human brain. The samples were collected from six control brain samples and eighteen samples from individuals who had suffered from schizophrenia, depression and bipolar (SDB) disorder. This method was applied to confirm the important role of sugar metabolism through evaluation of relation between the changes in sugar levels and psychiatric. The best separation and quantification of the common hexoses (glucose, fructose, mannose and galactose) by this method was achieved when $^2\text{H}_5$ -aniline was used as a tagging agent. Additionally, it succeeded in tagging a range of other sugars including pentoses (ribose and xylose) and sugar derivatives (N-acetylneuraminic acid and glucuronic acid). The results highlighted a relationship between the increases in the levels of sugars and psychiatric disorders (SDB). This relation which matched with other studies once again supported our results project 2 suggesting that in that sugar metabolism has an important role in distinguishing the control and SDB brains.

Oxidised fatty acids such as oxylipins and prostaglandins have profound effects on human physiology and are present at low levels in biological fluids. In project 4 a novel tagging method for the analysis of oxidised fatty acids was developed. Fatty acids give a relatively weak response in negative ion ESI-MS. In untargeted metabolomics studies, it is important to obtain a good response from molecules of interest. A derivatisation method using choline as a tag to put a positive charge on the analytes succeeded for the quantification of oxidised fatty acids, especially oxylipins, in plasma samples collected from seven participants before and after taking of beetroot juice (strong anti-oxidant and a source of nitrate). The current results concluded that this derivatisation method improved the sensitivity and selectivity of LC-MS analysis by increasing the response factors for the positively tagged oxidised fatty acids by more than 100 times in comparison to those for the untagged compounds in negative ion. There was no clear effect of beetroot juice on the levels of oxidised fatty acids in plasma.

CHAPTER ONE

GENERAL INTRODUCTION

Chapter 1 Introduction

1.1 Metabolism and Metabolites

Thousands of chemical reactions are performed inside body to keep its cells alive and healthy. These chemical reactions occurring within cells are regularly classified under set of pathways and are defined as the cell's metabolism. Thus, Metabolism covers a vast set of chemical reactions within organism that enable them to maintain life through the breakdown of molecules to product the energy (catabolism) and the synthesis of all compounds to build cellular blocks (anabolism). Energy formation is one of the vital components of metabolism which is closely linked to nutrition and the availability of nutrients. Metabolism significantly reflects the influences of endogenous and exogenous factors and their interactions within a biological system. In order to understand the interactions between those biological systems and the environment, considerable effort has gone into determining the metabolic processes associated with the production and breakdown of essential biochemical components involved in metabolism (Fell and Cornish-Bowden, 1997).

During metabolism, there are many of chemical components produced as result of these reaction are called metabolites. Metabolites are the biochemical substances include organic, inorganic, and elemental species such as carbohydrates, amino and fatty acids, vitamins, and lipids as well as inorganic anions and cations that formed as intermediates, precursors or changes into metabolism processes. Those substances, metabolites, are small simple structures absorbed in a diet and their accumulations show the end point of the response of an organism to a stimulus. Generally, Metabolites produced from metabolism divided to essential, are called primary

metabolites and are necessary for the growth and maintenance of cellular function, and non-essential or secondary metabolites, are the end biochemical that produced of the essential metabolism and are not required for the growth and maintenance of the cellular functions. Primary metabolites such as vitamins, carbohydrates, proteins and lipids play the significant role in the cell growth, reproduction and development (Djoumbou-Feunang *et al.*, 2019). In metabolomic studies, the complete set of metabolites produced by metabolism processes into cells has been defined as metabolome. Kell and Oliver (2016) cited that the first use of the term ‘metabolome’ was by Oliver and his colleagues in 1998 as a term for metabolomic profiling (Kell and Oliver, 2016).

A comprehensive and quantitative analysis of metabolites is important to understand the changes in metabolome of the biological system through the comparison between diseased and healthy conditions. Metabolomic tools are an essential part of the study of all small molecules in biological samples due to the massive number, complexity, diversity and dynamic concentration of metabolites (Dettmer *et al.*, 2007). The metabolome is a major challenge to a metabolomic analysis in the quantitative analysis of all metabolites, its understanding of human metabolome will be immensely useful in the development and support of the science of metabolomics. Over the past two decades, a number of very effective scientific tools have been developed to devote the efforts for prediction the essential metabolism products, primary metabolites, without non-essential metabolism, secondary metabolites (Beecher, 2003).

1.2 Metabolomics

Metabolomics is the scientific term describing an optimal approach to identify and quantify small-molecule metabolites within biological systems (Fiehn, 2002). It is a promising method for understanding the dynamics of how living systems deal with metabolic changes and offers a new investigative way of studying mechanistic biochemistry related to natural processes in health and disease. Global analysis of metabolites has been facilitated considerably by the application of recent analytical technique developments (Vinaixa *et al.*, 2012). The metabolomic field was described by Jeremy Nicholson who defined the metabolomic approach as a holistic profiling and analysis method to determine the effective change of metabolites within a biological system which occur as a result of many outside conditions such as diet, lifestyle and genetic factors (Nicholson *et al.*, 1999). Although fundamental metabolomics techniques go back to the 1960s, the term itself formally came into use during the first ten years of the twenty-first century. The greater efficacy of mass spectrometry and nuclear magnetic resonance techniques in data extraction and manipulation techniques has led to an increased number of publications on the subject (Ellis *et al.*, 2007).

Generally, metabolomics can be classified as two discrete strategies: (a) targeted metabolomics, i.e. as a result of a specific biochemical question or hypothesis with a defined set of metabolites related to one or more pathways, or (b) untargeted metabolomics which uses an unbiased approach which attempts to assign as many compounds or metabolites as possible by either analytical identification or ideally, by achieving high confidence levels in identification by utilising reference standards, (Patti *et al.*, 2012). Information on biochemical processes which are obtained from

changes in metabolites can provide details on specific pathways which may relate to disease processes. Thus, the applications of metabolomics have the most important role in the quantification of known metabolites and the identification of new metabolites as biomarkers to predict and diagnose diseases. Biomarkers in biomedical research related to the discovery of biological molecules in a variety of body fluids which can be used as tools to improve diagnosis of disease and understand its pathological mechanisms. The National Institutes of Health Biomarker Definitions Working group and the World Health Organization defined a biomarker as: “a characteristic that is objectively measured and evaluated as an indicator of normal biological processes, pathogenic processes, or pharmacologic responses to a therapeutic intervention” (Biomarkers Definitions Working, 2001) and “almost any measurement reflecting an interaction between a biological system and a potential hazard, which may be chemical, physical or biological. The response may be functional and physiological, biochemical at the cellular level, or a molecular interaction” (WHO, 1993), respectively.

Quantifiable biomolecules characteristic of biological processes, biomarkers, are used as clinical and diagnostic tools for a normal physiological state or changes in an individual in relation to a pathophysiological process or a treatment. Biomarkers can be (a) proteins indicating cellular and enzymatic changes, or (b) small biological molecules (metabolites) which highlight physiological endpoints, which help in disease management with reference to the early detection of disease, disease process markers, monitoring of drug response and therapeutic intervention, and outcome measurement.

The search for biomarkers in the untargeted biochemical profiling of metabolites, basically depends on powerful analytical techniques for separation such as chromatographic methods and identification of the greatest number of endogenous compounds possible by mass spectrometry as the method of choice. Significantly, it is possible to use the same equipment in peak generation and structure determination, as the coupling of mass spectrometers (MS/MS) allows a fragmentation of the metabolites, with subsequent structure elucidation, whereby the qualification of the biomarker may involve established methods different from the analytical technique used to discover it.

1.2.1 Targeted Metabolomics

The functional understanding of many biochemical pathways is utilised in one of the approaches to metabolomics, usually known as targeted metabolomics. It is the identification and quantification of defined sets of structurally known and biochemically annotated metabolites which provide an invaluable source of background information facilitating evidence-based interpretation of metabolomics data sets results from so many biochemical pathways having been explored in considerable detail. It has been possible to elucidate most of these pathways, substrates and products of enzymatic reactions, reaction mechanisms, equilibria and kinetics of these reactions, as well as cofactors or compartmentalisation. Thanks to this information, instant functional interpretation of the data set and, thus, analysed cell or organism phenotyping, a straightforward process, is facilitated (Lundin *et al.*, 2011). Quantitative information which is generally provided by targeted metabolomics constitutes a further significant advantage for this approach. An immediate

understanding of any alterations between different biological states, the molar concentrations of the metabolites involved in a pathway, and for comparison and meta-analysis of several independent studies is made possible by such quantitative data. Through the use of targeted metabolomics a wide range of relevant molecule classes in cells, tissues, or clinically relevant fluids can be systematically quantified. An automated sample preparation workflow in conjunction with sensitive mass spectrometric methods and a customised software solution are the components of the technology, which is a novel platform facilitating the identification and quantification of many hundreds of metabolites. It is also well suited where high-throughput and routine applications are concerned. There are certain similarities between targeted metabolomics and conventional multiplexed bioanalytical assays through analytes which have been previously selected, based on the underpinnings of known biology and chemistry, are measured. (Enot *et al.*, 2011).

1.2.2 Untargeted Metabolomics

Untargeted metabolomics applications represent the main method for improving biomedical research by providing potential chemical biomarkers in clinical practice. The effective and reliable results of the untargeted metabolomic approach can be obtained by various analytical techniques. These techniques included nuclear magnetic resonance spectroscopy (NMR) (Bharti and Roy, 2014) and mass spectrometry (MS) which can be used alone or in conjunction with one of a number of different separation techniques such as liquid chromatography (LC), gas chromatography (GC) and capillary electrophoresis (CE) (Pham-Tuan *et al.*, 2003, Plumb *et al.*, 2002).

The wide variation in the physicochemical properties and abundance of the metabolites in a biological sample renders untargeted metabolite profiling a major challenge in metabolomics. The inaccessibility of purified standards has seriously hindered the identification and quantification of a large proportion of unknown metabolites in complex biological samples by metabolomics. Mass-to-charge ratio (m/z), retention time (RT), fragmentation patterns, using standards and databases, are generally determining factors in metabolite identification or confirmation (Patti, 2011). Thus, the quantification and identification of metabolites still presents significant challenges to determine metabolic changes related to genetic differences, environmental influences and disease or drug perturbations. Maximum coverage of classes of compounds in conjunction with relatively high throughput is facilitated by means of the analytical methodology. The analytical methodology is employed and all endogenous metabolite related features, characterised by their m/z and RT, are included in a subsequent multivariate analysis procedure used to study metabolic differences between the different groups of samples and to identify putative biomarkers (Dunn *et al.*, 2011).

1.3 Metabolomics in Biomedical Research

Metabolomics studies have provided new and complementary insights in biomedical research and for developing a better understanding for many diseases related to metabolic disorders. The main goals of metabolomics is the assessment of biochemical products of metabolism, metabolites, in proportion to the phenotypic and biocompatible activity of the organism.

1.3.1 Potential applications of Metabolomics

Applications of metabolomics can be found in a huge diversity of research fields, including environmental perturbations of biological systems and toxicology. Metabolomics is recently being applied as the well-established procedure of human screening in biomarker and diagnostics research. Biomarkers are measurable biological indicators that can be used for instance in clinical screenings to stratify patients according to the characteristics of their phenotype (Serkova et al., 2011).

There is a widespread range of potential applications of metabolomics in the areas of biomedical research such as pharmaceutical and clinical diagnostics. The diagnostic potential of metabolomics is not confined to typical metabolic disorders, but rather extends into fields such as cancer (Osl et al., 2008) and neurologic disorders (Urban et al., 2010). Metabolomics can also be applied in drug development where it is used to uncover new drug targets, prioritize lead compounds and assess drug toxicity, enabling the development of novel, smarter and safer drugs (Weinberger and Graber, 2005). In addition, metabolomics has the possibility to identify individuals likely to benefit from a given therapy, minimizing the risk of side effects and avoiding unnecessary drug use. Biochemical approaches typically focused on a very limited amount of metabolites keeping the results manually interpretable by the researchers. However, being a very active field of research, metabolomics has made rapid progress nowadays allowing modern instrumentation to measure thousands of metabolites simultaneously. This growing complexity of high throughput small molecule measurements now constitutes a substantial challenge to the researchers (Bhattacharya et al., 1995, Tweeddale et al., 1998). Changes in the metabolite concentrations, determined by a different metabolomic strategies, reflect changeable in health and the response to external and

internal influences on the metabolomic profile. Metabolic dysfunctions are directly related to the risk of developing many diseases such as cardiovascular disease, kidney disorders, type 2 diabetes and psychiatric illnesses (Malik *et al.*, 2010, Felizola, 2015, Kaur, 2014). Metabolic disorders involve abnormal biochemical reactions in living organisms and the biomolecular damage caused by the accumulation of oxidant products, and reactive species. It is not only very well suited for biomarker discovery in different diseases, metabolomics is also important to explain the pathophysiological effects behind the disease, e.g., inhibition of or upregulation of an enzyme in a specific pathway (Bartel *et al.*, 2013). Many researches have suggested that biomolecular conditions such as oxidative stress and the abnormality in fatty acids, amino acids and sugars metabolism are considered to be the most common factors associated with development of metabolic abnormalities (Di Marzo *et al.*, 1994, Fukuchi *et al.*, 2004, Kelley *et al.*, 2017, Newgard *et al.*, 2009). On the other hand, the metabolic phenotype may be affected by physiologically relevant factors including dietary modifications and regular physical activity and lifestyle changes, which have the potential benefits in treatment of metabolic disturbances (Pitsavos *et al.*, 2006, Lenz *et al.*, 2004). Also, ultraviolet radiation derived from sunlight exposure may be one of natural effects which can stimulate or inhibit the biosynthesis of biologically active molecules (Park *et al.*, 2014).

1.3.2 The Pathological Factors Effects on Metabolic Phenotype

Dysregulation in metabolic processes may be evolved by abnormal chemical reactions or deviation of metabolic pathways and produce the cumulative damage for the etiology of many pathological conditions and diseases. Some of the pathological factors which can be causes the metabolic disorders are:

1.3.2.1 Oxidative Stress

Oxidative stress is a condition in which more oxidants are produced than can be scavenged and this leads to an imbalance in the oxidant-antioxidant equilibrium in a biological system. Persistent oxidative stress causes harm to cellular structures including nucleic acids, lipids and proteins resulting in oxidative damage. An imbalance between the oxidants and antioxidants is exacerbated by an increase in free radical generation. A radical can be defined as 'reactive chemical species possessing an unpaired electron and can be considered as fragments of molecules and which are generally very reactive' (Sies, 1997). Highly reactive oxygen and nitrogen species, ROS and RNS, and free radicals derived from them, such as the superoxide anion, the hydroxyl radical, and nitric oxide, can impair key enzymes and biomolecules in cells. However, oxidative stress and mitochondria dysfunction have been implicated in various pathological conditions in humans and may lead to disturbances in many metabolic pathways (Lobo *et al.*, 2010). The inferences of oxidative stress on metabolism have been shown in many biological studies which focused on their effects on metabolism in biological disorders. In addition, to contributing to oxidative damage in metabolism disorders in the pathophysiology of these diseases, oxidative status may also influence metabolism dysregulation during various physiological functions such

as nutrition, exercise and exposure to sunlight. Recently, metabolome analysis has been used to discover metabolite biomarkers for many diseases in human biological samples and contributed to understanding the link between oxidative dysfunction and metabolism (Bridi *et al.*, 2003, Celi and Gabai, 2015).

1.3.2.2 Fatty Acid Dysregulation

A fatty acid is a biological molecule consisting of various hydrocarbon attached to a carboxylic acid, carboxylic acid is an organic acid containing COOH as functional group. Aliphatic monocarboxylic acids are derived from or contained in esterified form in an animal or vegetable fat, oil or wax. Natural fatty acids commonly have a chain of 4 to 28 carbons (usually unbranched and even-numbered), which may be saturated or unsaturated (Moss *et al.*, 1995). The major source of essential fatty acids, which cannot be produced in the body, can be found with various concentrations in many different food types. Fatty acids play an important role in energy metabolism because they are a major dietary source of fuel and energy storage to provide adequate quantities of adenosine triphosphate (ATP), is a high-energy molecule found in every cell, when glucose is not available for this purpose (Schönfeld and Wojtczak, 2016). The toxicity of fatty acids and derivatives caused by their accumulation may be related to mitochondrial dysfunction and worsening of metabolic decompensation. In fatty acid oxidation defects, many metabolite changes have been reported as a result of the toxicity of the accumulation of long-chain fatty acids, aliphatic tails of 13 to 21 carbons, in high concentrations (Wajner and Amaral, 2016). Previous studies indicated that dysregulation of fatty acid metabolism has been detected in the pathophysiology of many diseases. Thus, understanding metabolomic changes may contribute to the

assessment of impaired fatty acid or amino acid metabolism in different health conditions as a result of environmental factors such as nutrition, exercise and light.

1.3.2.3 Amino Acid Dysregulation

An amino acid is any biological molecule consisting of a carbon atom bonded to two fixed functional groups, the basic amino group (the substituent $-NH_2$) and the acidic carboxylic group (the substituent $-COOH$), as well as a hydrogen atom (H) and an organic side-chain group (R), which is a specific group related to the name of the amino acid. The primary use of amino acids is as the building blocks of polypeptides and proteins and the participation in the synthesis of other nitrogenous substances (Vickery and Schmidt, 1931). Not all amino acids can be synthesised by the body, therefore a good diet is considered a major source for essential amino acids. Amino acids are necessary compounds in many biological activities in an organism such as neurotransmission, nutritional influences on physiology and lipid transport and have important roles in energy metabolism and the regulation of metabolic pathways in cells. The essential roles of amino acids in metabolism and the proteome encouraged researchers to use metabolomic tools to provide a better understanding of the amino acid pathways and metabolic responses of living systems to external or internal perturbations (Gu *et al.*, 2015).

1.3.2.4 Dysregulation of Sugar Metabolism

Carbohydrates, are biological molecules consisting of three types of atoms including carbon (C), hydrogen (H) and oxygen (O) with a formula $C_m(H_2O)_n$, where $n=m$ only

in the fundamental units of carbohydrates. Generally, saccharides are divided into three main groups including sugars (monosaccharides, disaccharides and polyols), oligosaccharides and polysaccharides. Monosaccharides, or simple sugars, are relatively small molecules having the empirical formula $C_nH_{2n}O_n$ and are the most basic units which can be further linked together to build other large carbohydrates (Moss *et al.*, 1995). Sugars are soluble carbohydrates and are classified into groups based on a number of carbon atoms as in common compounds such as hexose groups ($C_6H_{12}O_6$), e.g. glucose, fructose, mannose and galactose, and pentose groups ($C_5H_{10}O_5$), e.g. ribose, xylose and arabinose. Saccharides are an important source of energy for the body's cells as well as having major roles in many human systems and vital processes such as the immune system, fertilization, homeostasis, blood clotting, brain functions and metabolism. Metabolism of sugars and their derivatives such as sugar alcohols and sugar acids, is of major interest in metabolomics studies. It became apparent that sugar metabolism had an important role in brain function where the prevalence of metabolic syndrome has been observed in patients diagnosed with mental illness (Newcomer, 2007).

1.3.3 The Physiological Factors Relevant to the Metabolic Phenotype

In addition to pathological factors, it is thought that the metabolic phenotype may be influenced by many physiological and environmental factors such as lifestyle modifications and the exposure to sunlight. Previous studies suggested that nutrient stimuli and physical activity had clear effects on a number of metabolic pathways and influence health through reducing or increasing the risk of diseases. Pitsavos and his colleagues in their review have summarised the effects of lifestyle modifications such

as following a more active lifestyle and dietary modifications on the development of metabolic dysregulation (Pitsavos *et al.*, 2006).

The modern lifestyle and regular exercise may positively impact on human health or may be the cause of disability and disorders such as mental illness, hormonal disorders, inflammation and oxidative stress (Jacka *et al.*, 2012). Also, the effects of ultraviolet radiation resulting from sunlight exposure, as one of the environmental factors, were identified on the metabolic pathways for various metabolites in a given biological sample (biofluid, tissue, cells). According to Matus's minireview, several metabolomic studies were conducted on wide types of plants in order to detect the impacts of ultraviolet radiation on metabolic processes (Matus, 2016).

1.4 Metabolomic Approaches Workflow

Practically, metabolomic profiling strategies are performed by three main processes including data acquisition, data processing and data analysis and interpretation to obtain tangible and reliable outcomes. With the advancement in analytical techniques, the detection of thousands of metabolites from biological samples is one of the challenges in untargeted phenotyping. Obtaining the best analytical results in untargeted metabolomics can be achieved by applying an integrated metabolomic workflow as shown in Figure 1. The optimisation of the metabolomics workflow has been managed by the subdivision of main processes into six sub steps including selection and preparation of biological samples, analytical methods, metabolites identification, data treatment, statistical analysis and validation of data and biomarkers (Fukushima and Kusano, 2013).

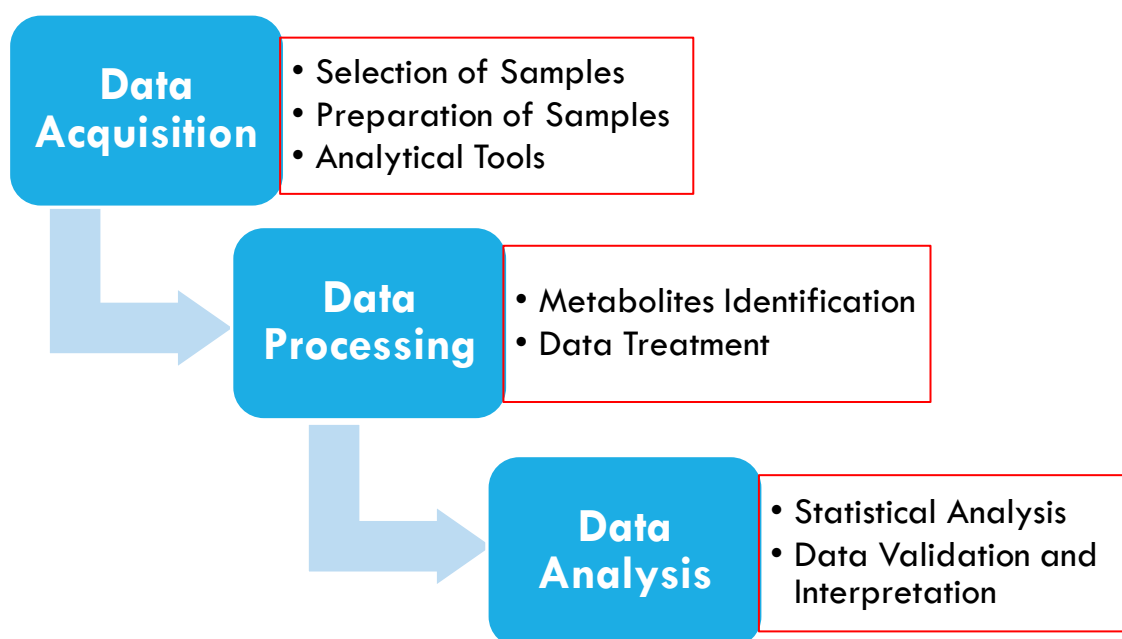


Figure 1-1: The untargeted metabolomic workflow is divided into three major steps which include seven sub steps for identification and quantification of metabolites in biological samples by LC/MS-based metabolomics.

1.4.1 Data Acquisition

The general workflow of metabolomic analysis is initiated by the acquisition of metabolomic data, data acquisition, through the selection and preparation of samples and applying of appropriate analytical tools. Metabolomic profiling studies are conducted to monitor and reveal the metabolite changes to provide a unique metabolomic fingerprint for understanding the complex transitions of metabolic pathways. The first and important step in these studies is choosing the type and number of biological fluid samples. Due to their properties such as being easily obtained and prepared, urine and plasma are the most commonly used biofluids for obtaining a metabolic fingerprint. Also brain tissue, cells and other biofluids such as cerebrospinal

fluid and saliva have been examined in the study of metabolic perturbations associated with different disease states (de Paiva *et al.*, 2014). In addition to the type of biological samples, the number of subjects per group, high or low sample size, has an important role on the design of study and may lead to a waste of resources or a lack of the accuracy for information, respectively. The next step of data acquisition is choosing a suitable method of analysis. Thus, the preparation method of the sample will be designed depending on the type of samples and the determined analytical tools. Analysis and detection in metabolomic studies necessitates picking an optimal analytical strategy to obtain a clear metabolite spectrum and reliable data. Many analytical and instrument strategies can be used separately or coupled such as mass spectrometry, gas chromatography and liquid chromatography to identify the biochemical signature of samples, these analytical tools will be described later (section 1.5). Generally, data acquisition has several problems which the most important of them are related to analytical noise changes (van Velzen *et al.*, 2009), a signal intensity of metabolite (Shurubor *et al.*, 2005), and sampling variability or systematic drift (van der Kloet *et al.*, 2009). Thus, normalisation before analysis, pre-acquisition, or after analysis, post-acquisition, and the use of quality control (QC) samples are important actions to avoid the abnormalities and deflections which occur in analytical measurements (Edmands *et al.*, 2014). After tackling all the unwanted challenges which accompany data acquisition, data processing is the next process which is applied to preliminary data to extract quantified data and can be handled by analytical tools and statistical analysis software.

1.4.2 Data Processing

The data obtained from available analytical tools requires some processing in order to facilitate data analysis through extraction of clear information and disposal of unwanted effects. Metabolomics technologies can provide large amounts of data in different formats to be used in investigation of a thousands of different metabolites. Therefore regulation of data and file format conversion from special formats to more common formats is the start of the series of processes to be carried out on raw data. Depending on the type of the extracted data, data processing may be necessary to avoid insufficient correction for background ions, retention time shifts and emergence of phantom metabolites (Sugimoto *et al.*, 2012). Figure 1-2 shows the schematic layout of data processing which aim to extract biological information from the acquired data. Data processing by MZmine will be detailed in section 2-6-1.

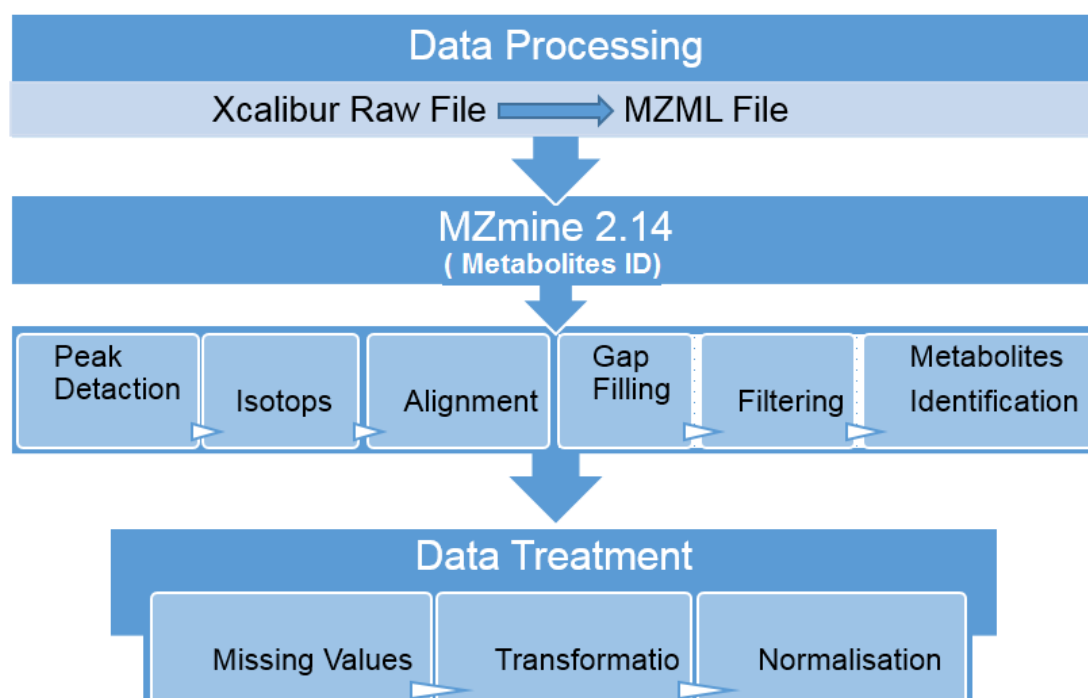


Figure 1- 2: The schematic layout of the steps of data processing.

1.4.2.1 Metabolite Identification

The starting step of data processing is metabolite identification which aims to identify numerous metabolites from mixtures of compounds in biological samples. After data acquisition is completed, the results produced from metabolomic analytical tools contains hundreds of metabolites which have great variability in their biochemical structures and concentrations. Metabolite identification is one of the most important and more difficult steps in metabolomics studies based on NMR, GC-MS and LC-MS techniques (Moco *et al.*, 2007). The raw data extracted from deferent metabolomic approaches, GC-MS and LC-MS, should be handled by several metabolomic commercial or non-commercial software, such as SIEVE (Thermo Fisher, Germany) and MZmine 2 software, to provide methods for differential analysis. M/Zmine software can be applied to assign the huge quantities of intermediate organic compounds or metabolites and is suitable to be utilised in both targeted and untargeted LC-MS-based metabolomic data (Katajamaa and Orešič, 2005). Untargeted metabolomics, especially through its use of LC/MS-based methods, is comprehensive in scope and outputs complex data sets and can routinely detect thousands of so called metabolites, based on their features such as peaks corresponding to individual ions with a unique m/z and RT, in biological samples. Furthermore, each m/z and RT feature in the dataset is associated with an intensity value (or area under the peak), indicating its relative abundance in the sample. Overall, this complexity imposes the implementation of metabolomic software such as XCMS (Smith *et al.*, 2006), MZmine (Katajamaa and Orešič, 2005) or Metalign (Lommen, 2009) capable of providing automatic methods for peak picking, RT alignment and for correcting experimental drifts in instrumentation, and relative quantification.

In metabolomics analysis, the Metabolomics Standards Initiative (MSI) can be used to identify the metabolites according to the information provided for the compound characterization within four different levels of MSI as described by Sumner and his colleagues (Sumner *et al.*, 2007). Compounds identified by level 1 (MSI1) are a minimum of two independent and orthogonal types of data relative to an authentic compound analysed under identical experimental conditions. Level 2 (MSI2) is used to identify putatively annotated compounds, without chemical reference standards, based on physicochemical properties and/or spectral similarity with public or commercial spectral libraries. Putatively characterized compound classes, level 3 (MSI3), are the identification of compounds based on characteristic physicochemical properties of a chemical class of compounds, or by spectral similarity to known compounds of a chemical class. Finally, there are unidentified or unclassified metabolites, unknown compounds, cannot be covered by previous three levels (MSI 1-3). Level 4 (MSI4) can be employed to classify these compounds according to spectral data then enabling relative quantification (Sumner *et al.*, 2007). In metabolomics studies, according to MSI levels, metabolites can be identified based on their exact mass, chemical formula, structure, and possible adducts facilitating their prediction based on mass tolerance, head group, and precursor ions of MS data. These information for metabolites are provided by various database sets compatible the instrumentation used in the metabolomics experiments (Dunn *et al.*, 2011). The output from data extraction in current study will be matched according to MSI levels 1 or 2 to identify the metabolites.

1.4.2.2 Data Treatment

Raw data collected from metabolomics analytical techniques are analysed by appropriated software to identify and quantify the metabolites depending on their mass to charge ratio and retention time. During data treatment, the resulting data are processed by many statistical steps to resolve analytical variation from sample preparation and instrumental drifts. Also, abnormalities in the data which were previously detected such as the effect of missing values and the effect of noise may be needed to handle. The ideal method of data treatment to provide the robust and quality of outcomes in untargeted metabolomic studies can be achieved by using QC samples.

1.4.2.2.1 Missing Values

Data produced from the metabolite identification step should be treated to reduce the deviations and unwanted values in metabolomics data caused by biological and/or technical causes. A major deviation in updated data is zero values which appear in the variable matrix and it would give a misleading result and are called missing values. Missing values may occur as a result of many causes either the metabolite appears in one sample but not in others, or the limit of detection for the analytical method exceeds the concentration of metabolite in sample, or the used metabolomics' software may identify some metabolites which are not detected (Hrydziuszek and Viant, 2012).

Gromski and his colleagues reported that the missing values can be replaced either with the half of the minimum peak intensity, small values (SV), or mean of all intensities, mean (MN), or median (MD) of all intensities or K-nearest neighbour imputation (KNN), which is the mean of the nearest 10 non-missing values. Another approach solves these effects by generation of an adjacent matrix as a source of

iterative imputation of missing values through applied Random Forest Imputation (RF) approach (Gromski *et al.*, 2014).

1.4.2.2.2 Normalisation

The analysis of metabolomics data is plagued with different limitations which may prevent the achievement of the main aims of the metabolomics study. The major challenge in metabolomics experiments is systematic variabilities related to biological differences, caused by experimental and environmental factors, and technical deviations, produced by instability in samples and instrument conditions. For systematic variations removal, the selection of the ideal normalisation technique is related to the variability of the instrument as well as the type of analysed sample and its content. The differences in contents of samples such as the variations of protein content in urine in comparison to plasma or other samples, tissue, cell, sweat and saliva, and the variations of volume, strength and density of these samples may generate doubts in the metabolomic output. Thus, this variance may lead to the use of several indicators such as protein content, cell count, osmolality, and creatinine (Wu and Li, 2016). In addition to the type of sample analysed and its content, specific normalisation techniques to remove systematic variations may be influenced by many other co-factors which should be observed such as gender, age, stress, disease, training modality, diet and ethnicity. The normalisation of systematic changes can be performed internally by using internal standards, which is a common practice and these should be stable compounds that are not present in biological matrices, or externally via addition a pooled sample to the run sequence as QC. The use of QC sample in the external normalisation as a representative of the samples is necessary in order to

monitor progress within and between batches as well as instrument drift. Despite the internal and external normalisation may possess the capability to overcome the variations in practical aspects, biological and technical deviations, but normalisation of obtained data after these normalisation methods is required to gain the ideal metabolic fingerprinting (Warrack *et al.*, 2009).

Data normalisation is a successful strategy to remove the effects of systematic variability on the full spectral data and to eliminate the variances in concentrations between the observations in order to ensure that samples are comparable. Ejigu and his team reported that there are seven approaches of data normalisation that can be applied in eliminating outliers or variability removal including the normalisation by: (1) linear baseline, the median intensity of each metabolite for all runs is calculated to construct the baseline in this normalisation method; (2) sum or analogous to total ion count, It is applied through the sums of the intensities for each experimental run are forced to be equal to one another. Due to the arithmetic means and median of the runs are equated, this method is not similar to the normalisation by the mean and by the median; (3) median (middle value when data is ranked into ascending order); (4) cyclic-Loess, non-linear local regression is used to fit the normalization curve in this method; (5) quantile, the data must have the same distribution to be normalised in this approach which could be done by projecting the original data onto a unit diagonal vector; (6) probabilistic quotient, Instead of the median value of a particular metabolite across different experimental run as applied in linear baseline normalization, this method is applied to normalise the data based on the construction of the reference metabolite (baseline) by taking the median intensity value at each experimental run; and (7) cubic-spline, this method was explained by Ejigu and his colleagues as

following “This normalization method assumes the existence of non-linear relationships between a baseline and each experimental runs. In this work, the baseline experimental run is built by computing the geometric mean of the intensities of each metabolite over all experimental runs. To get the normalization curve, cubic splines are fitted between each run and the baseline. In order to fit a smooth cubic spline, a set of evenly distributed quantiles are taken from both the baseline experimental run and the experimental runs” (Ejigu *et al.*, 2013).

1.4.3 Data Analysis

A comprehensive covering for metabolomics workflow starting from data acquisition and data processing is an essential tool prior to biological interpretation. The extracted results of metabolites identification and data treatment steps are handed to new stage of metabolomic workflow called data analysis or biological interpretation which is divided to database search and biomarker validation. Biological interpretation is the way to manage the structure of data to describe the information obtained from wide range of qualitative data through matching these data with standard data network. This standard data network has been structured to provide an abundance of the information about metabolite features (Steuer, 2006).

1.4.3.1 Statistical Analysis

During the data analysis process, normalised data are analysed by using appropriate statistical approaches to evaluate significant observations obtained from the data (Issaq *et al.*, 2009). Statistical analysis in metabolomics can be applied by using different

statistical and bioinformatics software either commercial (e.g., Agilent MassHunter, Waters ProGenesis QI, ABSciex XCMSPlus) or freely available (i.g. Excel, MetaboAnalyst and SIMCA) designed to uncover the homogeneity in variables and approximate linear dependencies among them. Visualisation and interpretation of a metabolomic change is challenging and needs a robust statistical approach to accurately assess the data differences. Statistical platforms for metabolomics data involves two approaches which are univariate and multivariate analysis (Bartel *et al.*, 2013).

1.4.3.1.1 Univariate Analysis

There are many variables produced in the metabolomics data which should be examined to find the relationship between the metabolomic changes and either internal or external challenges to the biological system. Statistical analysis of variables using univariate analysis is the easiest method to analyse variables and may be designated as a deductive or descriptive approach. Univariate analysis has been used for dealing with one variable to determine significant differences in metabolite concentration between two or more groups. In this statistical approach, paired t-test (p-value), fold changes (ratio) and one or two-way ANOVA have been calculated in order to investigate appropriate significant metabolites through reducing a lot of interrelated analytes. Contrary to multivariate analysis, univariate analysis is not related to causal relationships such as outlier variables and regression analysis and it may fail in acquiring understanding of biological changes (Bartel *et al.*, 2013). Univariate analysis also generally assumes normal distribution of the variables unless non-parametric methods are used.

1.4.3.1.2 Multivariate Analysis

Extensive data collection and analysis is possible by employing global metabolic analysis methods to determine the critical features of for the biological components. For this purpose, univariate analysis should be followed by the most common steps of multivariate analysis. Advances in a metabolic statistical methods by the use of multivariate analysis has allowed unparalleled biomarker detection and may offer a variety of novel biomarkers. The most commonly used analytical methods for the applying of multivariate analysis the unsupervised technique, principal component analysis (PCA), and supervised techniques which include partial least squares projection (PLS) or orthogonal partial least squares projection (Worley and Powers, 2013).

1.4.3.1.2.1 Unsupervised Techniques

Accurate analysis of data is possible which can be achieved by an appropriate and adequate statistical approach to reduce the dimensionality of the input space in the samples into groups with similar characteristics. Unsupervised statistical patterns such as PCA and Hierarchical Cluster Analysis (HCA) are created to reduce the complexity of the data and to graphically represent patterns or clusters identified in the data (Kirwan *et al.*, 2012).

PCA is the most widely used unsupervised model to find the clustering of variables regardless of the classification of the observations. The PCA approach is usually carried out as the first step in the multivariate analysis method to combine the variables associated with each other to detect outlying values in order to extract meaningful information for data sets. For metabolic fingerprinting, the objective of PCA has been

utilised in the analysis of metabolomics data to provide a linear transformation that maintains lower dimensionality output data for the same amount of the variance that can be measured in original data (Nyamundanda *et al.*, 2010). PCA, aims to achieve an unprejudiced dimensional reduction in data and is applied to show only the structure of the group and an overview of the dataset. While these characteristics of a PCA model may be sufficient to detect the deviations within- and among the groups, but it may not be able to provide a useful regression model if the expected changes in the data are affected by some confounding factors such as diet, environment and genetics (Abdi and Williams, 2010). Therefore, the supervised form is necessary to provide good predictions and improved data interpretation.

1.4.3.1.2.2 Supervised Techniques

In addition to the robust PCA method, supervised methods have been mainly performed to improve the ability to better distinguish the classification results between the actual samples and the outlier samples in order to solve the regression problem. A biased regression model can be obtained when the analyst uses a partial least squares (PLS) as a supervised model that explicitly specifies the response value for each variable. PLS regression problem is known as Partial Least Squares-Discriminant Analysis (PLS-DA) when there is a desired prediction between measurements taken in two or more experimental groups. Therefore, supervised models such as PLS-DA and its extension Orthogonal Partial Least Squares-Discriminant Analysis (OPLS-DA) have been applied to preserve the scores, loadings, and residual-based parameters with a familiar meaning and to address the regression problem (Worley and Powers, 2016).

OPLS-DA is a powerful technique used to identify differences between groups. It helps to understand pathophysiology and future therapeutic goals by identifying reliable biomarkers that have a significant relationship with segregation between groups and are associated with changes in the metabolic pathway. The appearance of spectral signals which are very diverse and may not be connected to the variation between study groups is inevitable in complex studies such as metabolomics (Wold *et al.*, 2001). Due to this reason, OPLS-DA has been employed instead of PLS-DA to separate prediction groups and changes unrelated to the groups in the extracted data. Thus, OPLS-DA is advantageous over PLS-DA because it can separate not only the individual variants of X that do not belong to Y-horizontally, predictive variation, but also produce separation of X variants uncorrelated to Y-orthogonal. The quality of the supervised model, OPLS-DA, is evaluated by a symmetric validation method that determines the importance of the model with the goodness of fit (R^2), the goodness of prediction (Q^2) and the p-value of the model (P-CV-ANOVA) (Triba *et al.*, 2015).

1.4.4 Data Validation

The statistical models thus, created however, do not always stand true as predictive models unless validation of the model has been carried out. Without validation, there is always an associated risk of over-fitting the data. Such over-fitted data stands out to be unreliable if considered for any clinical situations. Two main approaches to data validation in multivariate statistics are model validation and biomarkers identification.

1.4.4.1 Model Validation

The validation of data modelling is an important step to obtain the reliable results. The most powerful tools to validate the applied model are the quality parameters including the variance explained (R²) and the variance predicted (Q²). A quantitative measure of the goodness of fit relates observations on Y-axis to variables on X-axis by quantifying the fraction of Y explained by the variation in x. Thus, the fraction of the total variation of the X block (R²X) that can be explained by each component will be valid when the value of R² of this kind is close to one, the maximal value, which may be achieved through an increase the number of components. The considerable number of variables compared with relatively few observations might result in data overfitting. In other words, the results could be too optimistic. By means of cross validation (CV), which constitutes omitting a predefined number of observations (by default 1/7th) and subsequently refitting the model, a quality of prediction parameter (Q²) can be obtained (Kirwan *et al.*, 2012). Comparing the average value of the refitted models Q² with the R² of that model can show that it predicts more effectively than relying on chance (Steuer, 2006).

In addition to internal validation tools (R² and Q²), the validation of supervised model which has been built using SIMCA-P may be carried out by two external methods include the permutation test and analysis of variance of the cross validated (CV-ANOVA). Applying a permutations test can establish if a specifically classifying observations into two groups is better to any significant degree than any other arbitrary division into two classes (Westerhuis *et al.*, 2008). This test compares the R² and a parameter derived from the original model with the new permutations of R² and Q², and constitutes a process which may be repeated in order to achieve new quality

parameters, which should all have lower values than the originals. Furthermore, the regression line of the predictive model should cross the horizontal line zero. CV-ANOVA is used to test the significance of the variation predicted by the model under supervision. CV-ANOVA is the test which investigates the variation the model predicts against an H_0 hypothesis of equal cross validated predictive residuals around the mean (Eriksson *et al.*, 2008).

1.4.4.2 Biomarker Identification

Many statistical steps may be used to identify and validate biomarkers based on a supervised model and statistical software used in it. The variable importance in the projection (VIP) and corrected p-values are tools used for this purpose.

VIP is utilised to examine the contribution of each metabolite in a given model. The importance of each variable (metabolite) in the projection can be estimated and rated using the calculated value for this parameter in this way. In addition, it is often employed in variable selection during metabolomics. If $VIP > 1$, metabolites are generally seen as making a high contribution to the model. A value for each metabolite in terms of its difference between groups (VIP_{pred}) results from VIP, as does its contribution to the variability within the group (VIP_{ortho}). Metabolites with high VIP_{pred} and low VIP_{ortho} values are sensitive and specific (Chong and Jun, 2005).

Corrected p-values, the p-value is a tool used in statistics to evaluate the statistical significance of a variable. This value at α level = 0.05 has been the most used level which means that a difference in the risk may be due to chance is lower than 5%. For corrected p values, the number of variables (k) signifies a positive risk relationship

with a greater risk of false positive discoveries. To minimise this risk or α -alterred, the Bonferroni correction is used. The Bonferroni correction compensates for that increase by testing each variable at a significance level of ($\alpha_{\text{altered}} = \alpha_{\text{original}} / k$) (Simes, 1986). In metabolomics variables are in the hundreds so when $k=100$, $\alpha=0.0005$, this significance level might be acceptable when for example human cell lines are used as a matrix of metabolomics profiling in which almost all the condition are under control, but in the case of human plasma which is a complex matrix, which renders level of metabolites among individuals of the same group disease/control highly variable and this will affect the significance level of these variables (Dunn *et al.*, 2011). Hence for human biological samples it is preferable to utilise a less stringent tool such as false discovery rate (FDR). Benjamin-Hochberg defined FDR as “the proportion of errors committed by falsely rejecting null hypotheses that can be viewed through the random variable $Q = V/(V + S)$ the proportion of the rejected null hypotheses which are erroneously rejected. Naturally, we define $Q = 0$ when $V + S = 0$, as no error of false rejection can be committed. Q is an unobserved (unknown) random variable, as we do not know v or s , and thus $q = v/(v + s)$, even after experimentation and data analysis. The FDR of Q is defined to be the expectation of Q ” (Benjamini and Hochberg, 1995).

1.4.5 Data Interpretation

The interpretation of metabolomics changes and validation of practical conclusions should be taken into account in order to detect the biological function of the metabolite which can be useful as a biomarker. After identifying and determining metabolic changes induced by extrinsic and intrinsic interventions on metabolism processes, many metabolites that may display no significant change in their levels between two

different experimental conditions or study groups may show a correlation or intervention with other metabolites. These observations lead to the final step of metabolomics workflow, the biochemical interpretation and validation of metabolomics data, to provide an overview of all metabolic changes identified by specific conditions of the analysis model and biomarker validation (Steuer, 2006).

The benefit of using metabolomics results combined with pathway topological measures is that it helps with understanding the relevance of each individual change and makes pathway analysis results interpretable. The interpretation of data is based largely on statistical approaches that have been established in order to determine the interdependencies between metabolites and metabolic pathway changes, such as principal and independent component analysis (Scholz *et al.*, 2004), clustering techniques (Sumner *et al.*, 2003), discriminant function analysis and multidimensional scaling (Arkin *et al.*, 1997). The computational methods are the essential key to make the data visualisation and interpretation much easier to detect the significant metabolites closely associated with the affected biochemical pathways or biological processes. These procedures are used in assess the impact of the unbalanced metabolites within the over-represented pathway as well as the detection of biochemical relationships between the components. Metabolomics researchers currently have a wide variety of software tools at their disposal for the analysis of metabolomic data at the pathway level. A highly versatile pathway analysis tool which a recent development is Metaboanalyst. It offers a considerable range of metabolite set analysis methods and provides the web server to permit comprehensive metabolomic data analysis, visualisation and interpretation (Xia *et al.*, 2015).

1.5 Analytical Tools

The use of different technologies and methodologies is required in the metabolomics approach because of the considerable variability of metabolites in their chemical structures. Among the techniques metabolomics analysis toolbox are metabolite separation techniques (e.g. GC and LC) and spectroscopic detection techniques (e.g. Fourier-transform infrared spectroscopy, MS, and NMR), for determining metabolite variations in biological samples (Dettmer *et al.*, 2007).

1.5.1 Separation Technology

Chromatography is a physical separation method involving the distribution of metabolites between two phases: the stationary phase and the mobile phase. A high efficiency to provide good shape and high resolution of peaks along with stable retention times are the required features from the ideal chromatography systems to achieve their main purpose. Generally, chromatography techniques are classified based on stationary phase either GC or LC. Depending on the nature of the analytes, volatile compounds can be separated by gas chromatography; while the separation of non-volatile compounds, whether weakly ionisable or neutral, require high performance liquid chromatography (HPLC). Mobile phases in these techniques are particularly significant in metabolome analysis and are selected depending on targeted metabolites and samples, since the number of metabolites is not the same in different biological samples. Chromatographic resolution and sensitivity is affected by the nature of the stationary phase or column chemistry. The most commonly used columns are silica-based or monolithic based for reversed-phase (RP)-chromatographic

columns. For RP-HPLC of metabolite mixtures, the mobile phase gradient necessitates a long gradient with a slow process. The mobile phase begins with high in water content and the final solvent has a high organic content. RP columns for analysing the metabolome have an advantage in that the analysis of non-polar compounds is easy, but many metabolites such as polar amino acids are not retained in RP chromatography (Iwasaki *et al.*, 2007). An alternative to RP chromatography is hydrophilic interaction liquid chromatography (HILIC), which may be silica-based with a hydrophilic stationary phase. The HILIC mobile phase mode uses organic solvents with volatile buffers or water where the gradient mobile phase begins at a high organic solvent concentration such as 95% acetonitrile. Ammonium acetate and formic acid are suitable buffers. The zwitterionic-HILIC (ZIC-HILIC) column is being used extensively in the metabolomic field, the sulfobetaine zwitterionic functional group coats the silica and so permits polar analytes to separate by partitioning into a hydrophilic environment (Jandera, 2008). Thus, the properties of the metabolite establish the choice of separation tool.

1.5.1.1 Normal Phase Liquid Chromatography (NPLC)

Normal phase liquid chromatography (NPLC) uses a non-polar mobile phase, such as hexane, and a polar stationary phase, such as unmodified silica gel or silica gel with diol, cyano-alkyl, amide-alkyl or amino-alkyl groups attached, in order to retain the polar analytes. The commonest solvent mixtures are non-polar solvents with a slightly polar one as a modifier, for example hexane/ethyl acetate or hexane/isopropanol.

The retention mechanism involves polar compounds adsorbed onto the stationary phase more strongly than the non-polar ones. The adsorption forces are mainly due to

hydrogen bonding between polar analytes and the polar stationary phase. NPLC has a different selectivity when compared to the reversed phase although the latter has a wider applicability. In fact, NPLC has several limitations including: poor solubility of polar analytes in the highly non-polar mobile phases used; difficulty in ionising analytes when interfaced with an electrospray mass spectrometer; slow equilibration between analytes and stationary phase leading to peak tailing, fronting, or variable retention times as concentration changes; and phase instability. Due to these problems there has been an increased popularity of RP systems whose mode of separation is opposite to that of NPLC (Watson, 2015).

1.5.1.2 Reversed Phase Liquid Chromatography (RPLC)

This offers an opposite mode of operation when compared to the normal phase type. The mobile phase is a polar one, containing a high proportion of water with an organic modifier, while the amount the stationary phase is hydrophobic, such as octadecyl (C18), octyl (C8) or butyl (C4) bonded to a silica support.

The RPLC type offers a reliable and excellent method of separation of non-polar compounds as these can partition easily into the lipophilic stationary phase for separation to occur. However, the retention of the polar ones is a challenging process in RPLC. The solution might be to use a high amount of water in the mobile phase, however, this also leads to phase collapse, or phase de-wetting, and thus loss of all chromatographic efficiency. This frequently results in unstable retention times and poor resolution of peaks resulting from poor wettability in highly aqueous mobile phase compositions (Majors and Przybyciel, 2002).

Polar analyte retention in RP chromatography may be possible if the analyte is ionisable and therefore can form charged species in a reasonable pH range. The charged ions can in turn be made for form neutral ion pairs with ion-pair reagents such as alkyl sulfonates (if the analyte is positively charged) or tetrabutylammonium (for negatively charged analyte ions). The other setbacks are: (a) the possibility for complexation between the ions and, (b) slow equilibration rates with the ion pair reagent which might lead unstable retention times. An alternative approach to this is the HILIC technique (Watson, 2015, Gama *et al.*, 2012).

1.5.1.3 Hydrophilic Interaction Liquid Chromatography (HILIC)

HILIC is a technique used to separate polar analytes using a polar stationary phase and a less polar mobile phase. It works in an orthogonal manner to RP chromatography, for example, whereas the organic solvent is the strong solvent in RP partition, water is the stronger one in HILIC. It has recently established itself as the method of choice for highly polar and hydrophilic compounds instead of RPLC.

An advantage of HILIC is that it can increase MS sensitivity in electrospray ionisation (ESI) mode due to increased ionisation efficiency (Gama *et al.*, 2012). The latter occurs as a result of a high proportion of organic solvent (such as acetonitrile) in HILIC mobile phase. This high organic content of the mobile phase in HILIC also means that biological samples need not be evaporated and re-constituted following protein precipitation with acetonitrile. This simplifies the whole process of sample preparation in bioanalysis. The other advantages include ability to separate counter ions including chloride, sodium and potassium that are common components of pharmaceuticals formulated in salt forms; low viscosity of the high organic mobile phase permits the

use of higher flow rates and leads to lower back pressures; and a wide selection of HILIC stationary phases is now available. Many challenges such as column overload leading to peak fronting, longer equilibration times may hinder the HILIC mechanism and also may be there mixed mechanisms in the separation process which are not easily understood and therefore not easily controllable (Martin and Synge, 1977).

The main mechanism of separation in HILIC is the partitioning of polar compounds between a layer of water adhering on the polar stationary phase and the mobile phase that is less polar. The approaches that have used HILIC have demonstrated that the retention time for polar compounds will be longer than for non-polar. Other factors that increase retention times are: increased stationary phase polarity and decreased percentage of water in the mobile phase. The activity of column is impacted by the partitioning effect between the non-polar mobile phase and an aqueous layer which adsorbs onto the surface of the polar stationary phase. Thus the HILIC separation mechanism is dependent on solute characteristics as type and nature of the stationary phase and mobile phase composition (Gama *et al.*, 2012).

Due to the problems of mixed interactions and the need to reduce ion exchange interactions in HILIC, zwitterionic phases which are charge neutral have been developed. The ZICHILIC, zwitterionic phase, is the least affected by pH change and provides a totally different selectivity as well as it contains a strongly basic (a quaternary amino group) linked to a strongly acidic sulfonic acid group via a short alkyl spacer (Figure 1-3). Furthermore, the ability of zwitterionic phase surfaces to form a hydration layer do not exhibit strong ion exchange interactions because of cancellation of the positive and negative charge effects (Weber *et al.*, 2008).

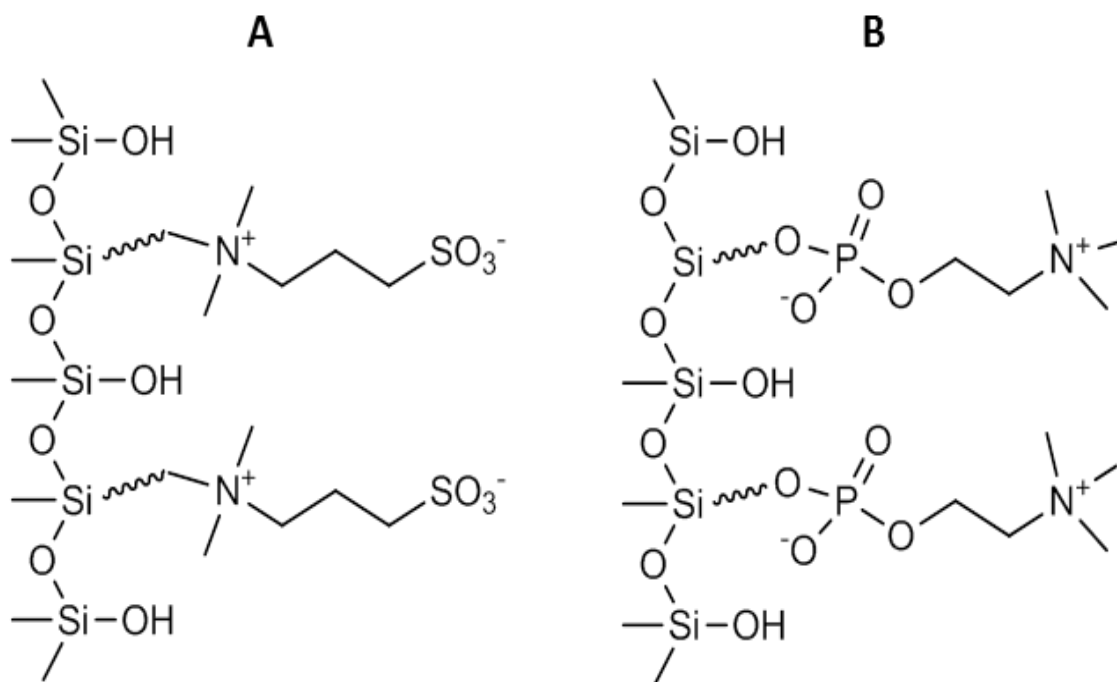


Figure 1-3: The chemical structure (A) ZIC-HILIC and (B) ZIC-cHILIC stationary phases. ZIC-HILIC has a sulfobetaine functional group while ZIC-cHILIC has a phosphorylcholine.

1.5.2 Mass Spectrometry (MS)

Mass spectrometry (MS) is the most commonly used tool in metabolome analysis as a spectroscopy detection technique. It comprises different ionisation sources such as ESI, atmospheric pressure chemical ionisation (APCI), and matrix assisted laser desorption/ionisation (MALDI). Furthermore, there are different analysers for MS such as quadrupole (Q), ion trap (IT), time of flight (TOF), and Fourier-transform ion cyclotron resonance (FT-ICR), in addition to the Orbitrap technique which was developed (Katajamaa and Orešič, 2005). The experimental sequence for measurements of the extent of mass accuracy the orbitrap mass analyser was depicted by Makarov and his colleagues in Fig. 1 from their paper (Makarov *et al.*, 2006). One of the systems commercially utilizing the Orbitrap analyser is available as a hybrid

linear ion trap/Orbitrap mass spectrometer (LTQ Orbitrap) which consists of three major parts. The first part of LTQ system after the ionisation source is a linear ion trap which can produce MS and MSⁿ spectra (n= the number of steps of MS). The ions are then focused in a quadrupole called the C-trap due to it is like letter C shape. Finally the ions injected into the third trap which is the Orbitrap. The ions tangentially cycle around an inner electrode and are trapped by applying a suitable voltage between outer and inner electrodes (Makarov *et al.*, 2006, Scigelova and Makarov, 2006). The Orbitrap is also available in the other commercial instrumentation such as the Exactive which is an easy-to-use benchtop LC/MS system that can measure wide mass range spectra at high resolution and with minimum supervision. The schematic layout of the Exactive high resolution instrument was shown in paper of Makarov and Scigelova (Fig. 4) (Makarov and Scigelova, 2010). In comparison with the LTQ Orbitrap, the Exactive Orbitrap cannot be used to do MS/MS because of it does not have the capability of performing selected ion fragmentation using collision induced dissociation (CID). These diversities between the mass analysers caused by the variation in the characteristics of these analysers including mass resolving power, mass accuracy, sensitivity, and capability of generating spectral fragment masses from compound ions. In order to achieve sophisticated and robust spectroscopy techniques for metabolome analysis, soft ionisation methods such as photo ionisation (APPI) or ESI have been added to improve MS systems (Nordstrom *et al.*, 2008). In order to achieve the benefit from the high-resolution, Orbitrap systems connect to liquid chromatography equipment to enhance separation of unknown compounds and enable high-throughput workflows. Essentially, the Orbitrap is an ion trap mass analyzer that consists of three electrodes. These electrodes are divided to two outer electrodes and a

central electrode which enable it to act as both an analyzer and detector. Orbitrap mass analyser work is described by Zubarev and Makarov as following “Ions are injected into the volume between the central and outer electrodes essentially along a tangent through a specially machined slot with a compensation electrode (a “deflector”) in one of the outer electrodes. With voltage applied between the central and outer electrodes, a radial electric field bends the ion trajectory toward the central electrode while tangential velocity creates an opposing centrifugal force. With a correct choice of parameters, the ions remain on a nearly circular spiral inside the trap, much like a planet in the solar system. At the same time, the axial electric field caused by the special conical shape of electrodes pushes ions toward the widest part of the trap initiating harmonic axial oscillations. Outer electrodes are then used as receiver plates for image current detection of these axial oscillations. The digitized image current in the time domain is Fourier-transformed into the frequency domain in the same way as in Fourier transform ion cyclotron resonance (FTICR) and then converted into a mass spectrum.” (Zubarev and Makarov, 2013). MS has become a major technique in the biomedical field through improvements in mass detectors because of their ability to detect low levels of compounds. Using a mass spectrometer can provide structural identity of the individual components with high molecular specificity and detection sensitivity. The value of metabolite data has been enhanced due to the achievement of accurate mass measurements by new technology, LTQ-Orbitrap and Exactive mass spectrometry, which are beneficial in the detection of the elemental composition of metabolites.

1.5.3 Gas Chromatography/Mass Spectrometry (GC/MS)

Metabolomics research has made considerable use of GC techniques for analysing compounds in biological samples, especially the quantitative and qualitative for volatile and heat stable compounds. After it is dissolved in an organic solvent, the sample is injected into a high temperature injection port for volatilisation. Once volatilised, the mobile phase, an inert gas such as helium or hydrogen, carries it over a long column coated with a liquid layer which is the stationary phase. The components of the sample separate according to their chemical and physical characteristics of the stationary phase (the gas mobile is inert so does not play a part). If the affinity of the component for the stationary phase is greater, it is held on the column longer. An important factor in component identifying is the determination of the retention time of each component on the column under particular experimental conditions. The sample traverses the column to move onto the next stage in which the compounds can be detected by various detectors. The MS source where the separated components are ionised by electron ionisation (EI) is the first part of the MS. The mass analyser (quadruples or ion traps) separates the ions produced by their mass/charge ratio. A mass spectrum is created by the mass detector, where the ion abundance is plotted against the M/Z ratio (Stauffer *et al.*, 2008).

Increased sensitivity, high chromatographic resolution and high specificity can be achieved by linking MS with gas chromatography, Figure 1-4 shows a diagram of GC/MS. An important role in GC-MS sensitivity is played by the choice of ion separation methods and high sensitivity and high resolution is provided by the time of flight separation. Nevertheless, the dynamic range for the quadrupole analyser is greater than for TOF analysers. Moreover, it is possible to optimise many parameters

in order to improve sensitivity in GC instruments. Samples are carried into the GC system using a splitless injector (Pasikanti *et al.*, 2008). The popularity of GC-MS in metabolomics studies can be explained in part by its accurate and reliable compound identification and the high resolution separations achievable on capillary gas chromatography columns. However, the variety of chemical structures and concentrations renders identification of metabolites somewhat challenging. Rapid progress in carbohydrate chemistry has in part been accelerated by the use of GC-MS. Current research on carbohydrate such as sugar acids and sugar alcohols has made ample use of these essential tools over the past ten years (Wiklund *et al.*, 2008) (Ruiz-Matute *et al.*, 2011).

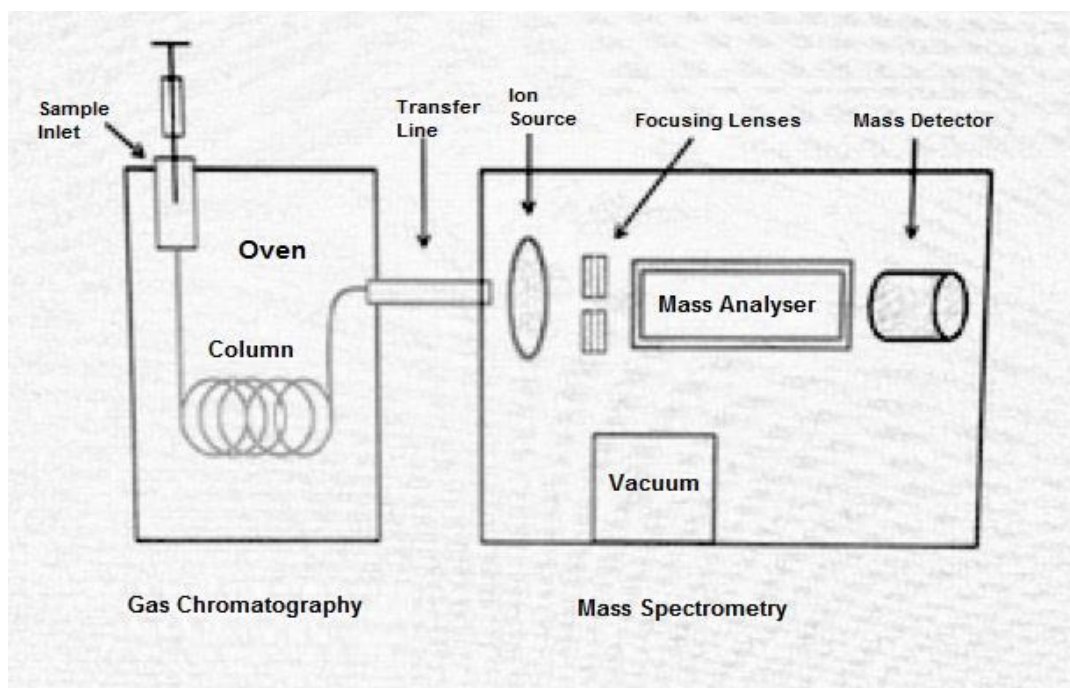


Figure 1-4: Gas Chromatography/Mass Spectrometry diagram. The injected sample is volatilised in the sample inlet and is carried by the mobile phase (inert gas) to the column where the components are separated. The retention time for each component on the column is important for identification. The separated elements are transferred to the MS detector where they are ionised. The ions are passed through the mass analyser to the mass detector and a mass spectrum is generated

1.5.4 Liquid Chromatography-Mass Spectrometry (LC-MS)

High resolution mass spectrometry (HRMS) (e.g. TOF or Orbitrap systems) alone are not qualified to provide identity information for metabolites. A chromatographic separation is required to distinguish isomeric metabolites possible and reduce ion suppression effects from the sample matrix. For this reason, a coupling of HRMS with the separation techniques, chromatographic methods such as GC and LC, is commonly used in HRMS-based metabolomics studies (Theodoridis *et al.*, 2012, Gika *et al.*, 2014). Dionex UltiMate 3000 LC Front End is one of liquid chromatographic approaches can be used in metabolomics studies in compelling with an HRMS. The ultimate 3000 delivers high productivity and performance across the full range of sample sizes, column dimensions, and flow rates to meet the growing diversity of MS applications. The ultimate 3000 optimizes separations for all LC/MS applications, providing a new level of productivity and versatility. All the benefits, classical binary to quaternary and dual-gradient micro systems, provided by this technology are available to improve performance and productivity. Approaches based on LC-HRMS present greater complexity, but result in a greater likelihood that potential biomarkers will be observed where authentic standards are unavailable or where the compounds are unknown. The first pass in global metabolomics screens based on LC-MS produces a list of features. Accurate masses of these features can be subsequently searched against a database containing the accurate masses of metabolites (Vinaixa *et al.*, 2012). The first LC separation technique hyphenated with HRMS and widely employed in metabolomics studies was RP, although there exists a limitation with regard to the retention and separation of polar metabolites - major components in all biological samples. There has been greater application of HILIC in recent HRMS-based

metabolomics studies (Cubbon *et al.*, 2010, Zhang *et al.*, 2012b). Furthermore, the occurrence of ion-suppression is more likely in polar metabolites present at trace levels. It has been reported that polar compounds can be separated by using HILIC, generally the LC performance of amines, sugars, phosphates and organic acids seems better under the conditions of the ZIC-pHILIC column, zwitterionic polymeric column, which can be used at high pH, and the sensitivity of ESI-MS is increased with the use of an organic solvent-rich mobile phase. Investigation of practical concerns in metabolomics have been carried out providing information on the number of repeatedly detected LC–HRMS features, isomer separation and the quality of the chromatographic peak shapes (Iwasaki *et al.*, 2012, Zhang *et al.*, 2014). In general, the accessibility of high quality data by using LC-MS techniques in metabolomic applications requires the control of unwanted deviations. The undesirable variations which accompanies the analysis of biological samples such as blood, plasma, saliva and urine by LC-MS methods can be caused by either unwanted variation or the specific properties of the analysed samples which are related to physiological factors (Edmands *et al.*, 2014). Control and correction of these measurements by good measurement designs are an important way to quantify sampling variability and identify the clear metabolite signals from the data. Additionally, optimal measurement designs produce an adequate answer on to biological queries and reduces the impacts of biological variation in order to increase the accuracy of the analysis. The possibility of conducting both biomarker discovery and validation on the same platform with LC-MS now arises by means of the application of stable isotope techniques for allowing relative quantification between differentially labelled samples or, absolute quantification via the inclusion of internal labelled standards or multiple reaction monitoring. During the

last quarter century, hundreds of LC/MS-based metabolomics studies have sought to detect and quantify many biomarkers in different animal and human biological fluids (Denoroy *et al.*, 2013).

1.6 Aims of Study

The current study aimed to apply and, in some cases, develop metabolomic profiling methods for application to different human biofluid and tissue samples.

1. The first aim of this thesis (Chapter 3) is to conduct an exploratory pilot study by using an untargeted LC-MS method to explore the effects of aerobic exercise challenge on the urinary metabolome of physically active individuals. An untargeted LC-MS method, using a well-established HILIC-MS procedure will be used to accomplish the analysis.
 - The objective of this part of the study is determine whether or not if there is a metabolite of metabolites which are correlated to VO_{2max} . For this purpose, PLS modelling will be used to identify urinary metabolites which may be strongly correlated with VO_{2max} .
2. The second aim (Chapter 4) was to apply LC-MS based untargeted metabolomics to the analysis of post mortem human brain tissue will be performed by applying an established LC-MS-based metabolomic profiling methods. The availability of a unique library of post-mortem brain samples with extensive associated medical information will allow investigating of whether or not these samples might reveal any underlying pathology which could be related to diagnostic differences.

- The objective of this part of the study is to correlate metabolic profile with different types of mental illness and to determine whether or not there is an overlap between metabolic perturbations in mental illness and diabetes as has been previously suggested.
3. The third aim was to apply a previously developed reductive amination method to separate the common hexoses fructose, glucose, galactose and mannose and in the identification of unknown sugars detected in post-mortem brain samples.
 - The objective of this part of the study is to further explore a proposed link between mental illness and diabetes could be established then this might give some rationale for the evaluation of medicines used in the treatment of diabetes in the treatment of mental illness.
 4. The fourth aim of the current study (Chapter 6) was to develop a novel strategy will be developed for the analysis of carboxyl-containing compounds, particularly oxidised fatty acids, in biological samples by ESI-LC-MS after coupling them to choline in order to enhance their detection limits via establishing a positive charge on the molecules.
 - The objective of this part of the study is to enhance the detection of a range of biologically active oxidised fatty acids and to determine their levels in human plasma pre- and post- ingestion of beetroot juice which is an anti-oxidant.

CHAPTER 2

MATERIALS AND METHODS

2.1 Chemicals and Solvents

HPLC grade ACN, chloroform and methanol were purchased from Fisher Scientific, UK. HPLC grade water was produced by a Direct-Q 3 Ultrapure Water System from Millipore, UK. AnalaR grade formic acid (98%) was obtained from Fisher Scientific, UK or from BDH-Merck (Poole, Dorset, UK). Sodium chloride, ammonium carbonate, ammonium acetate, ammonium hydroxide solution (30-33%) and all standard used to evaluate the column were purchased from Sigma-Aldrich, UK.

2.2 Biological Samples Preparation

The samples obtained from the subjects which were designated for each study were collected in pre-labelled sterilised containers. The unopened containers were transported by ice box to the laboratory to be stored at -20°C to -80 C, according to samples type, until are analysed. On the day of analysis, these samples were thawed at ambient temperature for 1-2 hours before further preparation for LC-MS analysis. The three types of biological samples were urine, plasma and brain tissue in this study. Metabolites in these specimens were extracted based on type of study samples as will be stated in the subsequent chapters wherever applicable for each study.

2.3 Standard Solutions Preparation:

The stock solution of each metabolite standard was prepared at 1 mg/ml with HPLC grade methanol and water (v/v) and stored at – 20°C. Four authentic stock standard mixtures for 220 compounds were prepared by mixing 100µl from each stock solution. In each mixture, about 56 metabolites were mixed and then the solution was made up to 10 ml with acetonitrile. Consequently, the final concentration for each metabolite

standard was 10µg/ml. Thus, 440 positive and negative ions for these metabolite standard mixtures, as detailed in supplementary material (Table 2-S1), were later used to determine the matched metabolites in biological samples. In order to avoid identity confusion, isomers were distributed into different standard solutions and in-source fragments were also carefully verified.

2.4 Pooled Samples Preparation

Pooled plasma samples were prepared by taking 20µl aliquots from 10 randomly selected non-extracted plasma samples, metabolites were extracted by transferring the 200µl to an Eppendorf tube with the addition of 800µl of ACN. After vortexing the samples were centrifuged at 10000 revolutions per minute (rpm) for 10 min. The supernatant was then collected into a HPLC vial as a final solution ready for LC-MS. A pooled sample was injected at the beginning, in the middle and at the end of the run to check for technical variation and to monitor the stability of the instrumentation. To quantify the precision of the measurements, the relative standard deviation (RSD) was calculated between the pooled samples based on total intensities in each sample and an RSD must not exceed 20%.

2.5 HPLC Conditions

2.5.1 Mobile Phase Solutions for ZIC-PHILIC Chromatography

All mobile phase solutions were freshly prepared and stored at room temperature for up to 48 hours. Mobile phase A (20mM ammonium carbonate (AC) buffer, pH 9.2) was prepared by addition of 1.92g of AC to 800 ml of HPLC-grade water followed by adjustment to pH 9.2 with ammonia solution and then more water was added to make

the volume up to 1L. Mobile phase B was HPLC- grade ACN only. The column used was a ZIC-pHILIC column (L150 x L.D. 4.6 mm, 5 μ m, polymeric bead support) from Hichrom Ltd, Reading, UK (Zhang *et al.*, 2013).

2.5.2 Mobile Phase for C18 Chromatography

All solutions were freshly prepared and were stored at room temperature for up to 48 hours. Mobile phase A (0.1 % formic acid (FA) in water (v/v), pH 3) was prepared by addition of 1ml of acid to 800 ml of HPLC-grade water followed by mixing then was completed to a volume to 1L with additional water. Mobile phase B (0.1 % FA in ACN (v/v), pH 3) was prepared by addition of 1ml of acid to 800 ml of HPLC-grade ACN followed mixing then was completed to a volume of 1L with more ACN, and the pH adjusted using a pH meter. The column used was an ACE C18-AR (150 x 4.6mm, particle size 5 μ m, pore size 100A) from Hichrom Ltd., Reading UK (Zhang *et al.*, 2013).

2.5.3 HPLC Setup

The HPLC was fitted with the appropriate mobile phase components. The auto-sampler needle and sample syringe were flushed with the syringe wash solution (methanol/water, 1:1). The system was initially purged, successively, with 100 % of each of mobile phases B followed by A at a flow at 5 ml/min for 5 min in each case. The purge valve was then closed and the selected HPLC column was conditioned with 50 % of mobile phase B at a flow rate of 0.3 ml / min for 10 min. The operating pump pressure was continuously monitored to ensure that it was below 2,000 pounds per square inch (p.s.i). Injection volume was 10 μ l per sample and chromatographic

separations were performed on both ZIC-pHILIC and C18-AR columns by applying two separate linear gradient elutions for 46 min as shown in Tables 2.1 and 2.2, respectively as described in sections 2.5.1 and 2.5.2. For both separations, the same operating conditions were employed for the ESI interface which was operated in a positive/negative polarity switching mode. While on the instrument, samples were kept on a vial tray which was set to a constant temperature of 4°C to avoid any possible degradation of samples.

Table 2- 1: Gradient elution programme applied for ZICpHILIC in LC-MS analysis.

Time (min)	Mobile Phase A% 20 mM AC	Mobile Phase B% ACN	Flow Rate (ml/min)
0	20	80	0.3
30	80	20	0.3
31	92	8	0.3
36	92	8	0.3
37	20	80	0.3
46	20	80	0.3

Table 2- 2: Gradient elution programme applied for C18-AR in LC-MS analysis.

Time (min)	Mobile Phase A% 0.1% aqueous FA	Mobile Phase B% 0.1% FA in ACN	Flow Rate (ml/min)
0	90	10	0.3
30	0	100	0.3
35	0	100	0.3
36	95	5	0.3
46	95	5	0.3

2.5.4 MS Setup of Exactive and LTQ-Orbitrap

LC-MS was performed on Dionex Ultimate 3000 HPLC connected to an Exactive (Orbitrap) mass spectrometer from Thermo Fisher Scientific (Bremen, Germany). The quality of data acquired from an instrument has an implication on the accuracy of the deductions that can be made from a study as a whole. To maintain enhanced instrument sensitivity, any residues in the ion source chamber were removed. This was achieved by sonicating the sample cone and the ion transfer capillaries in a 50:50 methanol/water solution (v/v) for 15 min.

The mass spectrometry was tuned and calibrated in accordance with the manufacturer's specifications using the Thermo Calmix standard solutions. The signals of ACN dimer ($2 \times \text{ACN} + \text{H}$) m/z at 83.0604 and 195.03765 for caffeine were used as lock masses for positive (PIESD) mode and a lock mass for negative (NIESI) mode was used at m/z 91.0037 ($2 \times \text{formate} - \text{H}$), during each analytical run. The MS accuracy was tested using standard analytes with intensities between 10^4 and 10^7 as calibrates. The calibration peaks were checked to make sure that the mass deviations were less than 3 part per million (p.p.m), otherwise the instrument was recalibrated to correct the mass errors. The spray voltage 4.5 kV for positive mode and -4.0 KV for negative mode. The temperature of the ion transfer capillary was 275°C and the sheath and auxiliary gases were set at 50 and 17 arbitrary units, respectively. The full scan range was 75 to 1200 m/z for both positive and negative modes.

The LTQ-Orbitrap is used to record full-scan mass spectra and sequential MS^2 (MS-MS) activation spectra from low-resolution precursor ion selection. Full-scan mass spectra are acquired in positive-ion mode with a resolving power of 60,000. MS/MS spectra can be obtained at 35 V by using the LTQ-Orbitrap, a parent ion intensity

threshold of 10,000, and targeting the three most abundant species in the full-scan spectrum or targeting selectively only predefined species on a parent ion list.

2.6 LC-MS Data Extraction and Processing

2.6.1 Data Processing by MZmine 2-14

All raw data files (Thermo-Xcalibur format) were manually sorted into folders according to study groups. Then they were converted to mzXML files using an open source software: msconvert (proteowizard.sourceforge.net). Polarity split was processed by using the MZMIN split function to separate the Exactive's positive and negative ion mass spectra. Prior to metabolite identification by MZmine 2-14. In order to identify the metabolites in the processed data was searched against an in house metabolite database as well describe in next section (2-6-2). The procedures and the setting of each step used in MZmine 2.14 are described below (Pluskal *et al.*, 2010, Zhang *et al.*, 2013).

1. Raw data import

The raw data were converted to mzML format to be imported into MZmine.

2. Peak detection

Three steps including mass detection, chromatogram builder and chromatogram deconvolution were performed for peak detection as follows.

➤ Mass detection:

A list of masses (ions) for each scan in the raw data file was generated by the mass detection module which can be provided by many mass detectors. The appropriate detector can be chosen depending on the raw data characteristics such as mass resolution, mass precision, peak shape and noise. The centroid mass detector was used

for mass detection in this study because of the raw data are already centroided, only one algorithm (centroid mass detector) can be used. All major three parameters of mass detection including mass detector, MS level and noise level were set in Figure 2-1.

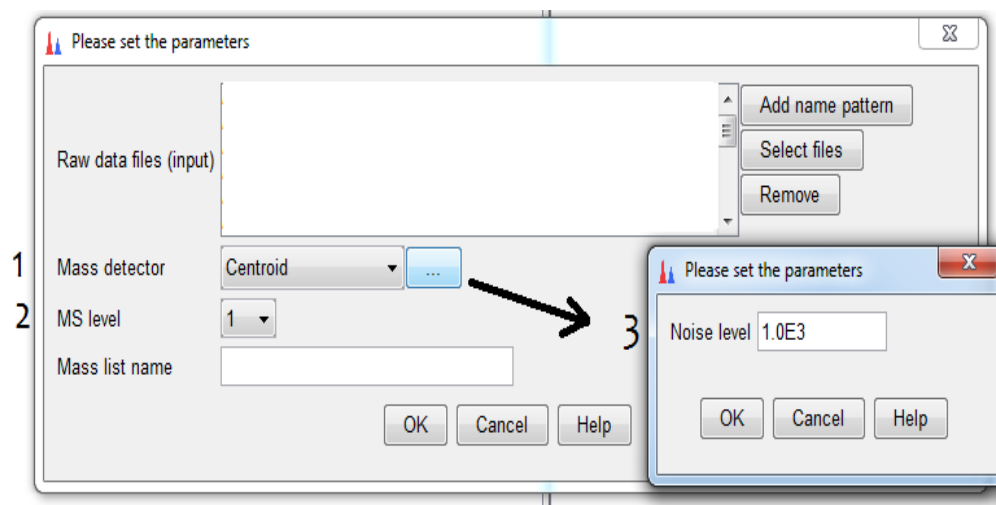


Figure 2-1: The setting of mass detection parameters. Algorithm is used for mass detection and its parameters. MS level of scans is one, for which the mass lists should be generated

➤ Chromatogram builder:

The mass lists obtained from mass detection were used to build the chromatogram algorithm for each mass that can be detected continuously over the scans. For building the chromatograms, only MS level 1 scans are considered for chromatogram algorithm which works by preserving a series of chromatograms coming cross consecutive scans. A chromatogram can be finished when no m/z peak is found to be connected to, its length (time span) and intensity (height) are checked according to the required parameters (Fig. 2-2) which were added to the final peak list.

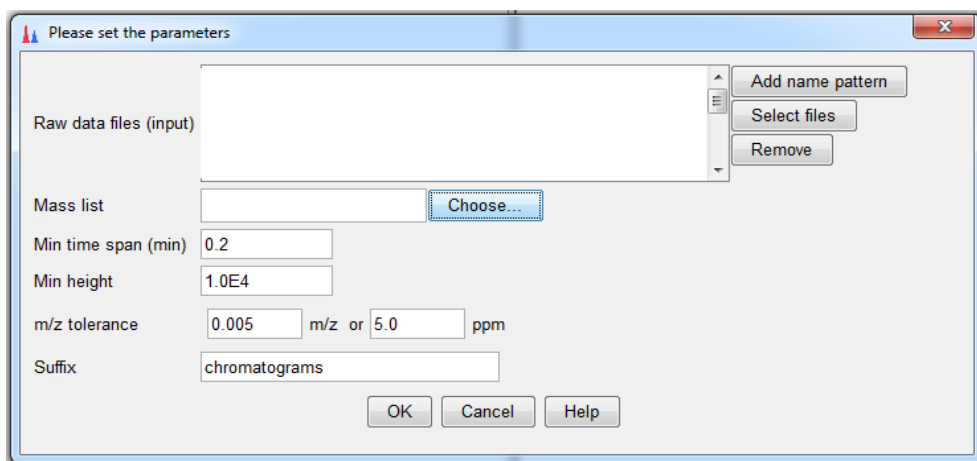


Figure 2-2: The setting of chromatogram builder parameters.

➤ Chromatogram deconvolution:

Chromatogram deconvolution module was conducted to establish individual peaks when the detection of chromatograms by the chromatogram builder has been finished. Due to several algorithms are provided for chromatograms have to be deconvoluted into individual peaks, the choosing of deconvolution algorithm should be suitable for study purpose. Algorithm of chromatogram deconvolution in this study was local minimum search. Figure 2-3 shows the setting of chromatogram deconvolution parameters.

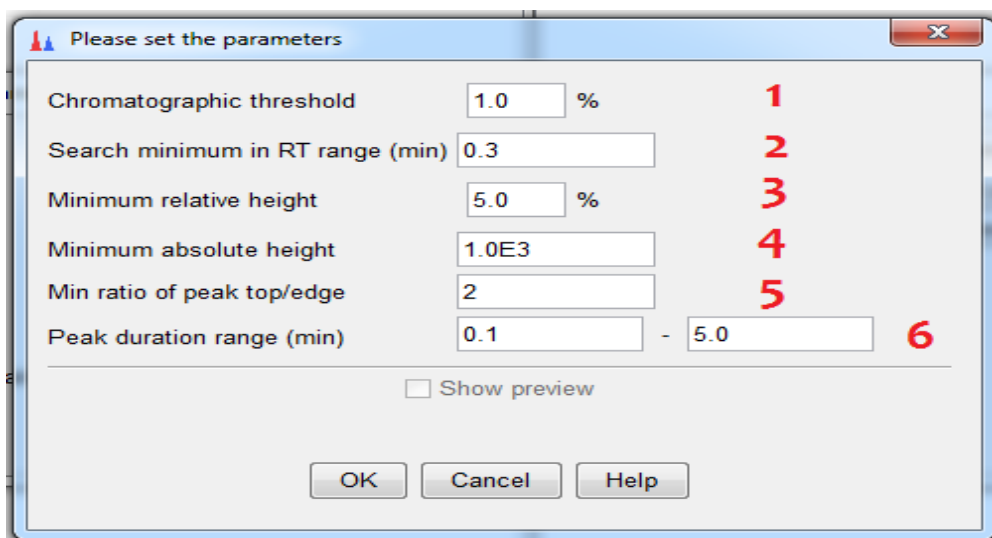


Figure 2-3: The setting of chromatogram deconvolution parameters.

3. Isotopes

In MZmine, isotope pattern (deisotoping) cannot be applied in individual scans. Therefore, it has been performed after the carrying out of chromatogram builder and deconvolution module. The main purpose of isotopes module is processing the peaks in the peak list by the order of decreasing height to find the most appropriate charge state by comparing the number of identified isotopes for each possible charge in each peak. For each charge state, peaks which fit the m/z and RT distance limits are considered as isotopes. Thus, only the most abundant isotope is kept while the additional isotopic peaks are removed from the peak list. Isotopes module which was performed by isotopic peaks grouper (deisotoped) was set based on parameters as explained in Figure 2-4.

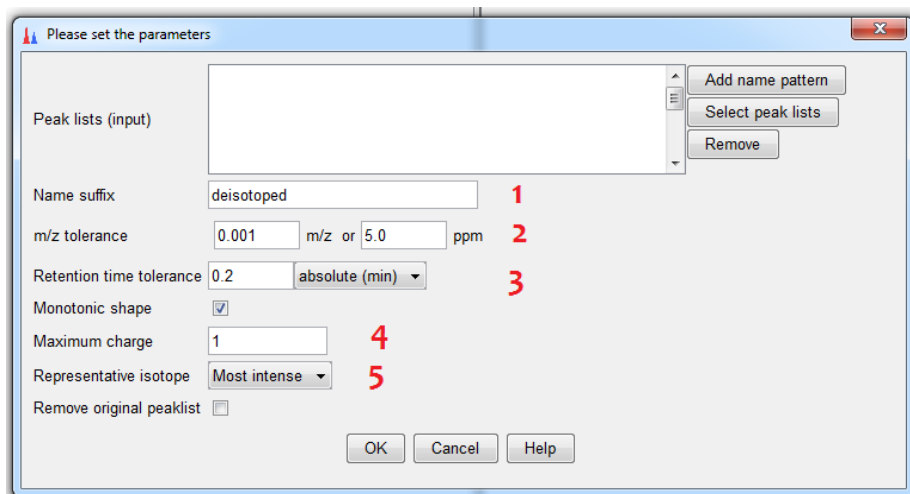


Figure 2-4: The setting of de-isotoping module parameters.

4. Alignment

Join aligner was used to align detected peaks in different samples through a match score which was calculated based on the mass and retention time of each peak and ranges of tolerance stipulated in the parameters setup dialog (Figure 2-5).

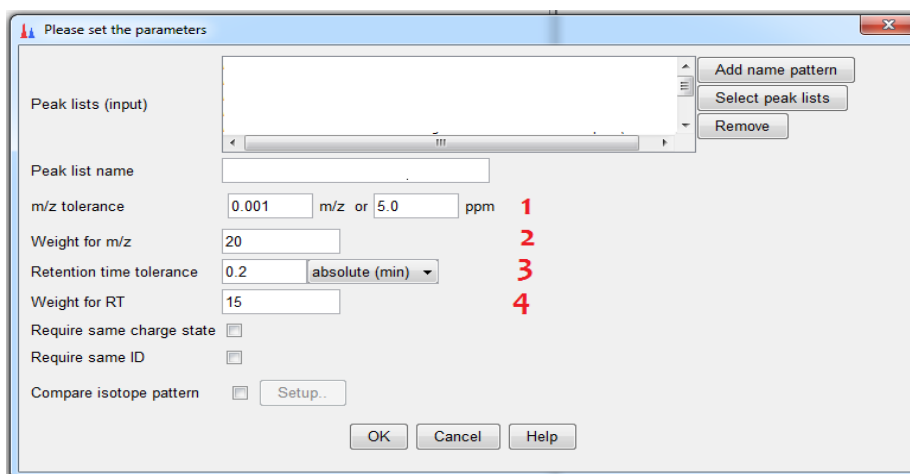


Figure 2-5: The setting of required parameters for the alignment method.

5. Gap filling

This method fills in gaps in each peak list row by using the same m/z and RT range as other peaks in the row (Fig 2-6). The m/z and RT ranges where the new peaks will be sought are obtained using the ranges of the rest of the peaks in the same row. The minimum value of these ranges is the minimum value in the range of all the peaks in the row and the same happens with the maximum value. The new peak is constructed using the highest data point of each scan within the determined m/z and RT ranges.

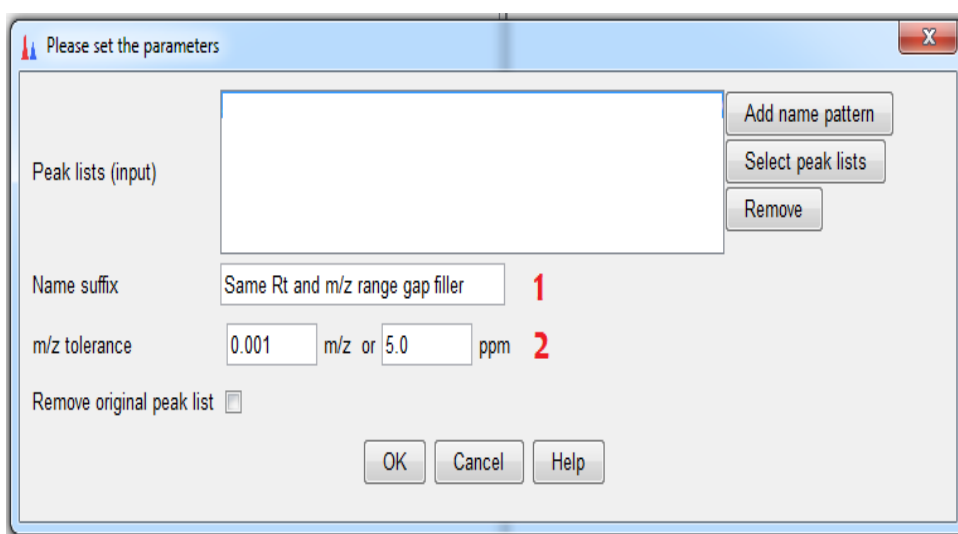


Figure 2-6: The parameters setup dialog of gap filling.

6. Filtering

Filtering module, peak list rows filter (Fig 2-7), removes all rows in the selected peak list that cannot achieve the user defined requirements. These requirements can be the minimum number of peaks in the row, the minimum number of peaks in an isotope pattern, peak duration or a m/z vs retention time window. When an aligned peak list, i.e. multiple peaks per row, is filtered then the average of each row's peak duration, m/z and RT values are used to filter the row.

The screenshot shows a dialog box titled "Please set the parameters" with the following settings:

- Peak lists (input): [Empty text box]
- Name suffix: filtered
- Minimum peaks in a row: 15 (with a red '1' next to the input field)
- Minimum peaks in an isotope pattern: 1 (with a red '2' next to the input field)
- m/z: 74.9998 - 1199.9869 (with a red '3' next to the input field)
- Retention time: 3.0 - 30.0 (with a red '4' next to the input field)
- Peak duration range: 0.0005 - 10.0 (with a red '5' next to the input field)
- Parameter: No parameters defined
- Only identified?:
- Remove source peak list after filtering:

Buttons: Add name pattern, Select peak lists, Remove, OK, Cancel, Help.

Figure 2-7: The setting of filtering module parameters.

7. Identification

Identity of peaks were allocated based on the values of m/z and RT of the peaks collected in custom database which previously designed in comma-separated values (CSV) format. The requirements of metabolites identification are stipulated in the parameters setup dialog as show in Figure 2-8. The filtered peaks were searched against a custom database, house metabolite database, which are provided from four common databases used for metabolites identification. These common databases used

for this purpose are: (1) Kyoto Encyclopaedia of Genes and Genomes (KEGG) (<http://www.genome-jp/kegs/>), (2) Human Metabolome Data Base (HMDB) (<http://www.hmdb.ca/>), (3) METACYC Metabolic Pathway Database (<http://metacyc.org/>) and (4) LIPID MAPS (<http://www.lipidmaps.org/>)

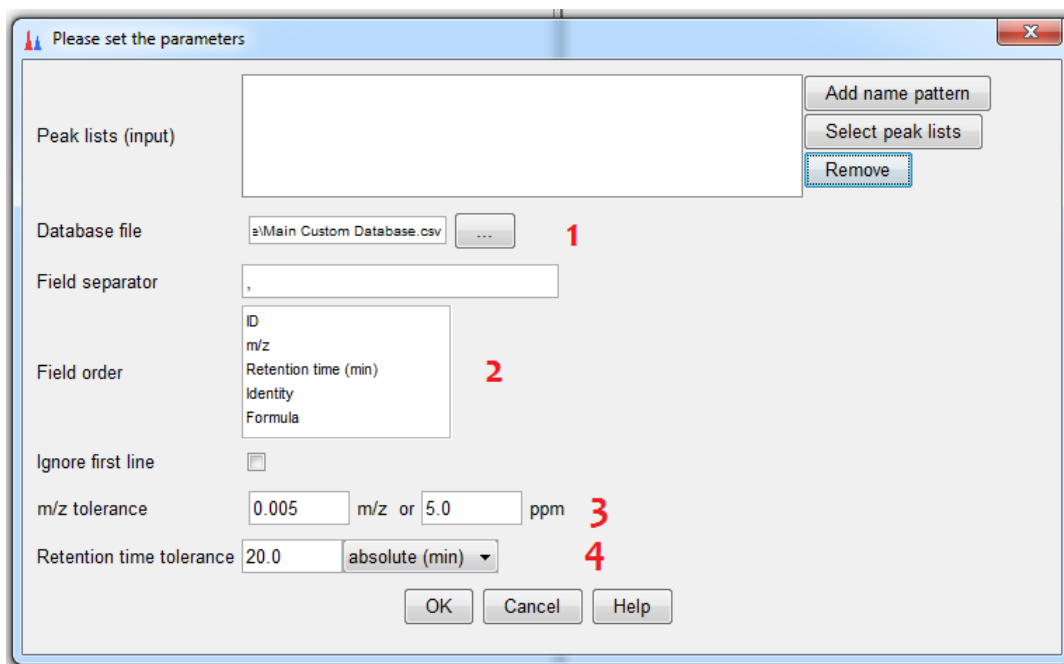


Figure 2-8: the parameters setup dialog of Identification method.

2.7 Metabolomics Profiling

2.7.1 Statistical Software

All data processing, including data visualisation, biomarker identification, diagnostics and validation, was implemented using SIMCA software v.14 (Umetrics AB, Umeå, Sweden) for multivariate analysis (Trivedi and Iles, 2012). Additionally, Metaboanalyst 3.0 (www.metaboanalyst.ca) (Xia *et al.*, 2015) and Excel (Microsoft Office 2013) were employed for univariate and multivariate analysis.

2.7.2 Pre-Treatment

Prior to multivariate analysis, LC-MS data was log transformed (base 2) and then Pareto scaled for variance (Par) so that the responses for each variable were centred by subtracting its mean value and then divided by the square root of its standard deviation. The variation of QC samples around their mean (CV_{QC}) is expected to be low since they are replicates of the same pooled samples. CV_{QC} was also calculated for each of the putatively identified metabolites among the pooled samples, metabolites with $CV_{QC} > 20\%$ were rejected. CV_{QC} applied as the last filter where the metabolites were removed if only detected in less than 80% of the biological samples in each defined group (Dunn *et al.*, 2011).

2.7.3 Data Visualisation and Biomarkers Identification

Prior to modelling the LC-MS data, Hotelling's T and DModx limits were employed to detect sample outliers which might affect the whole model. Samples were removed from the model if they were above the action limit (99 %) of Hotelling 's T₂ , red line, or if they exceeded the warning limit (95 %) of Hotelling 's T', orange line, plus critical

limit of DModX. PCA, an unsupervised model, was employed to explore how observations clustered based on their metabolic composition regardless of their grouping (Eriksson *et al.*, 2008). On the other hand, a supervised model, orthogonal partial least squares-discriminant analysis, was employed to examine the differences between groups while neglecting the systemic variation. The p values of the biomarkers were corrected using false discovery rate (FDR) (Benjamini and Hochberg, 1995). Variable importance in the projection was employed to assess the contribution of each variable in the observed metabolomics change to a given model compared to the rest of variables. VIP divided into VIPpred, which represent contribution of a metabolite to the difference between groups compared to other metabolites, and VIPortho, which indicates contribution of a metabolite to variability within group compared to other metabolites in the same model. The average VIP is equal to 1; thus a variable with VIP larger than 1 has more contribution in explaining y and vice versa (Chong and Jun, 2005). Also, unreliable metabolites can be filtered by jack-knifing, a method for finding the precision of an estimate, by calculation the confidence interval (CI). The 95% CI was calculated for each metabolite based on jack-knife of uncertainty which estimates the prediction error rate based on the cross validation rule used. Correlation coefficient of a metabolite in samples used to evaluate reliability of a metabolite (Wiklund *et al.*, 2008). Metabolites were then filtered based on their p-values and 95% CI so that all metabolites with p-values > 0.05 and / or 95 % CI crossing the zero point were filtered out.

2.7.4 Diagnostics and Validation

Diagnostics and validation of data modelling by PCA and OPLS-DA models were performed by internal and external diagnosis tools. In internal validation, the variance predicted- Q^2 (Cum) and variance explained- R^2 (Cum) were employed as internal validation tools for supervised and unsupervised models. The R^2 represents the percentage of variation explained by the model while Q^2 indicates the percentage of variation in response to cross validation. The R^2 value of the regression line in the plot represents the strength of the association between the observed and predicted Y values and was used to choose the number of latent variables (orthogonal axis). The R^2 represents quantitative measure of the goodness of fit and its value limited with minimum explanation (0) to maximum explanation (1). The goodness of model can be inferred through the rising of R^2 value to be close to the maximal value of one, whilst reduction this value to zero indicates to poor model. Unless the value of Q^2 more than 0.5 and close to a high R^2 value (close to 1), a large gap between R^2 and Q^2 values indicate poor model, model that cannot predict, and problems with variables (Worley and Powers, 2013). In additional to internal validation tools, the permutation test and CV-ANOVA as external diagnosis tools were performed to validate supervision model. In the process of validation by SIMCA-P, a permutations test was applied to evaluate whether the specific grouping of the observations in the two designated classes was significantly better than any other random grouping in two arbitrary classes. The criteria for validity are: All blue Q^2 -values to the left are lower than the original points to the right or regression line of the Q^2 -points intersects the vertical axis (on the left) at, or below zero. Note that the R^2 -values always show some degree of optimism. However, when all green R^2 -values to the left are lower than the original

point to the right, this is also an indication for the validity of the original model. Model validity was also assessed using CV-ANOVA which corresponds to H_0 hypothesis of equal cross validated predictive residual of the supervised model in comparison with the variation around the mean (Eriksson *et al.*, 2008).

2.7.5 Putative Biomarker Selection Workflow

The initial filtration of metabolites was carried out in data modelling step based on their VIP and FDR value as described in section 2-7-3. The selected metabolites which had assessed contribution in the observed metabolomics change ($VIP > 1.0$) were filtered again to select significant metabolites. Putative biomarker selection workflow was examined based on four main factors are their p-values, 95 % CI of mean difference, corrected p-values and VIP. Firstly, p-values and 95 % CI of mean difference were calculated for selected high VIP metabolites to be filtered. In this filtration, a metabolite was filtered out if it had a p - value > 0.05 and / or its 95 % CI crossed 0. Secondly, filtered metabolites were processed by using Metaboanalyst in order to obtain corrected p-values (Xia *et al.*, 2015). The metabolites which had a p-value (corr) > 0.05 and/or $VIP < 1.0$ were excluded from significant metabolites list.

CHAPTER 3

**METABOLOMIC PROFILING OF THE EFFECTS
OF SUBMAXIMAL EXERCISE AT A
STANDARDISED RELATIVE INTENSITY IN
HEALTHY ADULTS IN ORDER TO DETERMINE
MARKERS OF PHYSICAL FITNESS RELATED TO
VO₂MAX**

Abstract:

Ten physically active subjects underwent two cycling exercise trials. In the first, aerobic capacity (VO_{2max}) was determined and the second was a 45 min submaximal exercise test. Urine samples were collected separately the day before (day 1), the day of exercise (day 2), and the day after (day 3) the submaximal exercise test (12 samples per subject). Metabolomic profiling of the samples was carried out using HILIC column coupled to an Orbitrap Exactive mass spectrometer. Data were extracted, database searched and then subjected to PCA and OPLSDA modelling. The best results were obtained following normalisation the metabolites in each individual to their mean output over the five urine samples on days 1 and 2 of the trial proved the accepting of the current normalisation approach. This approach allowed PCA to separate the day 2 first void samples (D2S1) from the day 2 post-exercise samples (D2S3) PCA also separated the equivalent samples obtained on day 1 (D1S1 and D1S3). OPLSDA modelling separated both the D2S1 and D2S3 samples and D1S1 and D1S3 samples. The metabolites affected by the exercise samples included a range of purine metabolites and several acyl carnitines. Some metabolites were subject to diurnal variation these included bile acids and several amino acids, the variation of these metabolites was similar on day 1 and day 2 despite the exercise intervention on day 2. Using OPLS modelling it proved possible to identify a single abundant urinary metabolite provisionally identified as oxo-aminohexanoic acid (OHA) as being strongly correlated with VO_{2max} when the levels in the D2S3 samples were considered.

3.1 Introduction

Physical activity and exercise have a major impact on health (Sarris *et al.*, 2014) and can reduce the incidence of several diseases including cardiovascular disease (CVD), diabetes (WHO., 2009), and mild-to-moderate depression (Sarris *et al.*, 2014). The World Health Organisation has reported that CVDs are the leading cause of mortality (17.5 million deaths) followed by diabetes (1.5 million deaths) (WHO, 2014). In the UK this equates to more than 200,000 (37% of total) deaths due to CVD per annum (Allender *et al.*, 2007). The five major world risks for death are, to some degree, modifiable risk factors including high blood pressure (13%), the use of tobacco (9%), elevated blood glucose (6%), physical inactivity (6%) and overweight/obesity (5%) (WHO, 2014). Modifications to these risks can be achieved through consumption of fruit and vegetables (diet modification), moderation in the use of alcohol and physical activity. The indirect cost of physical inactivity in developed countries, Scotland is among the least physically active countries (Reilly *et al.*, 2014), equates to 1.5%-3% of total direct health care costs. Regular exercise which is relatively inexpensive cannot only modify, but also, more importantly, improve the overall quality of life and life expectancy (Scarborough *et al.*, 2011). There are uncertainties, however, connected with the duration, frequency and intensity, as well as the optimal type of exercise for persons of different cohorts (for example, sedentary or already active), and the nature of the molecular mechanisms underlying health improvement by means of exercise. A number of factors such as gender, age, life-style and body mass index (BMI) may be relevant in solving this issue. Lack of regular exercise may negatively impact on human health and may be the cause of disability or disrupt numerous abnormalities disorders such as mental illness, hormones disorder, inflammation and

oxidative stress (Jacka *et al.*, 2012). The use of metabolomics-based techniques to directly investigate the effects of exercise on the human metabolome, can lend new insight into novel phenotypic responses – which may lead to personalised training regimes related to an individual's initial metabolic status (Sarris *et al.*, 2014).

In the last quarter century, the greater availability of NMR, GC-MS and improved LC-MS techniques was reported in the majority of untargeted metabolomics studies on exercise and some studies which focused on pre-determined pathways such as the metabolic effects of exercise on steroid metabolism, purine metabolism, and oxidative stress. A large variation exists in the depth of the studies judging from their success in generating intriguing new hypotheses where a sense of the metabolome operating in a complex, dynamic fashion in a variety of exercise regimes becomes apparent. There are many metabolomics-based studies suggeste that exercise has a clear effect on the human metabolome as shown in the smaller study by our laboratory group (Daskalaki *et al.*, 2015b). These studies used several analytical metabolomics techniques to determine the changes in the levels of metabolites and search for novel biomarkers. Some of these studies included the measurement of aerobic capacity as an indicator associated with the impact of exercise on the human metabolic pathway. Aerobic capacity is the VO_{2max} which refers to the use of oxygen to adequately meet energy demands during exercise via aerobic metabolism. However, the changing in urine metabolomics before and after the acute various exercises was one of the main goals for several of metabolomics studies in clinical field

3.1.1 Urine Metabolome

Urine has long been used as one of the most important biological fluids to identify and monitor a variety of diseases because of some of its physical characterisation. Clinically, some of pathological conditions such as jaundice syndrome (JS), diabetes (DI), haemolytic anaemia and uraemia syndrome, can be predicted by the smell and colour of urine (Bouatra *et al.*, 2013). Additionally, the vast amount of biomarkers in urine, ease of collection the large amounts of sample and lower urinary protein or lipid content encouraged metabolomics researchers to use urinary metabolic profiling as the important clinical diagnostic tool (Zhang *et al.*, 2012a). Metabolomics studies reported that the estimation of metabolite biomarkers in urine samples is more advantageous than their estimation in other biological samples (Ellis *et al.*, 2007). Therefore, the discovery of novel biomarkers through the application of urine metabolomics has become a key element in metabolomics research which focuses on diagnosis of disease states and therapeutic efficacy.

One of common uses of LC-MS include analysis of human urine and its successful use in urine metabolomics studies for disease diagnostics and biomarker discovery. In this approach, HILIC is the major determinant in separation and retention of metabolites because of a significant number of highly polar metabolites such as amino acids, organic acids, sulphate and glucuronide conjugates, and sugars contained in human urine (Zhang *et al.*, 2012c). However, chromatographic performance of LC conditions with regard to repeatability and linearity for urinary metabolites in untargeted metabolomic studies were reviewed by Iwasaki and his colleagues (Iwasaki *et al.*, 2012).

Nasrallah and Al-Khalidi (1964) cited that the increase in “non-uric acid purine” in urine samples post-exercise was first observed in the early 1900s by Burian (Nasrallah and Al-Khalidi, 1964). Most investigations into these adenine nucleotides, effective as potent vasodilators and contributors to energy regulation, have their origins in the basic metabolomics techniques mentioned above, developed in the late 1960s and early 1970s (Mashego *et al.*, 2007). Forrester and Lind (1969), in their research on humans, investigated the role of ATP content from venous effluent of the forearm muscle after exercise (i.e. 10% and 20% maximal voluntary contractions), and demonstrated a comparative increase in ATP post-exercise as against resting values (Zhang *et al.*, 2013).

Recently, metabolomics studies have been improved to be one of the important approaches to identify the reliable biomarkers which contribute diagnosis and treatment of diseases. Urinary metabolomics has been evaluated as one of analytical method for detection of many of chronic diseases (Zhang *et al.*, 2013).

3.1.1.1 Purine Metabolism in Metabolomic-Exercise Studies

Most recurrent observations of the effects of exercise focus upon the effects on the purine pathway in both acute and prolonged exercise regimes. The metabolic effects of exercise on purine metabolism were frequently reported in most exercise-based metabolomics studies (Neal *et al.*, 2013, Pechlivanis *et al.*, 2010, Pechlivanis *et al.*, 2013, Sheedy *et al.*, 2014). More specifically, the greater efficiency of salvage of hypoxanthine, a purine derivative and intermediate in the adenosine metabolism, among trained individuals has been observed in several papers in this field as in relation to the important role of ATP in muscle function during exercise (Dudzinska

et al., 2010, Sahlin *et al.*, 1999, Zielinski *et al.*, 2013a, Zielinski *et al.*, 2011). Researchers have monitored changes in purine metabolism in long-distance runners during their yearly training cycle through decreases in levels of post-exercise xanthine together with higher levels of the salvage enzyme hypoxanthine-guanine phosphoribosyl transferase (HGPRT). The resulting principal observation in the study indicated that training produced reduced excretion of hypoxanthine (Zielinski *et al.*, 2009). In another study, the same authors then undertook a comparison of high-level sprinters and triathletes, establishing that reduced hypoxanthine levels occurred among the trained sprinters, as compared with the triathletes. HGPRT levels increased among sprinters, compared with the triathletes, suggesting a more effective use of anaerobic energy resources as a result of sprint training than from triathlon training (Zielinski and Kusy, 2012). Finally, significant changes in purine metabolism with time were only recorded after high-intensity exercise in their training schedules, there being no significant change subsequent to constant low-intensity exercise (Zielinski *et al.*, 2013b). It is interesting to note that in a study comparing triathletes, sprinters, middle- and long-distance runners, low post-exercise hypoxanthine levels corresponded with performance far more than lactate levels and aerobic capacity, maximal oxygen consumption (VO_{2max}).

3.1.1.2 Oxidative Stress in Metabolomic-Exercise Studies

Oxidative stress may play an important role in the development of complications and may be associated with metabolic changes which may due to accelerated generation of ROS and increases in oxidative chemical modification of lipids, DNA, and proteins in various tissues (Liu *et al.*, 2011). Correspondingly, the levels of antioxidants and

lipid peroxidation products were measured before and after submaximal exercise in two groups, resistance-trained and non-resistance-trained males. Elevated α -tocopherol, γ -tocopherol, β -carotene, and lycopene (fat soluble antioxidants) concentrations after exercise were noted. In both groups, the concentrations of the lipid peroxidation products malondialdehyde and conjugated dienes were also higher after exercise. A switch from xanthine dehydrogenase, which uses nicotinamide adenine nucleotide (H^+) as a co-factor, to xanthine oxidase, which uses oxygen as a co-factor, was classified as one of the mechanisms for exercise-induced free radical formation (Ramel *et al.*, 2004, Subudhi *et al.*, 2001). The oxidative stress related with free radical activity resulting from the exercise appears to be better tolerated during moderate intensity exercise in the trained subjects. In their article, Vollaard and his colleagues reported evidence suggesting that elevated oxygen consumption may increase free radical activity. They concluded that the elevation of oxygen consumption during exercise compared with rest may depend on the type of exercise and this is responsible for increased oxidative stress reactions (Vollaard *et al.*, 2005). Thus, among a number of mechanisms which may cause free radical production during exercise is increased VO_{2max} .

3.1.2 Metabolomic profiling of Exercise Urine Samples as A Predictor of VO_{2max} :

VO_{2max} is a measurement of capacity to take advantage of oxygen or the maximum level of oxygen consumption by individuals during maximal aerobic exercise. It has been used as a useful tool for predicting cardiovascular and other mortality causes (Sousa *et al.*, 2015). Given that cardiorespiratory fitness is strongly associated with

morbidity and mortality outcomes (Carnethon *et al.*, 2005), assessing the effects of exercise on the human metabolome may also yield vital diagnostic and prognostic indicators for clinicians. Cardiorespiratory fitness is most commonly expressed as the maximal rate of oxygen consumption which can be determined by measuring respiratory variables during an incremental exercise test to exhaustion. Of further interest is that VO_{2max} is also a primary determinant of endurance exercise performance (Joyner and Coyle, 2008). A positive correlation between VO_{2max} with tryptophan and metabolites related with increased tryptophan such as kynurenate, was evident in a study of individuals after running a 26.2-mile Boston marathon, as identified by Lustgarten *et al.* (2013). In another study, many differences were noted between persistently physically active and inactive individuals in the circulating metabolome, with results demonstrating a better cardio metabolic health in a more physically active twin (Kujala *et al.*, 2013). Based on the studies mentioned previously in the literature of similar study by our laboratory group (Daskalaki *et al.*, 2015a, Daskalaki *et al.*, 2015b), there have been very few comprehensive LCMS-based investigations utilising an untargeted metabolomics method that examine the acute effects of exercise. Meanwhile, new prospects are becoming available in understanding and coverage the metabolic changes because of the high resolution and high throughput monitoring systems. However, directly investigating the effect of exercise on the human metabolome, via metabolomics-based techniques, has the potential to provide new insights into novel phenotypic responses and might allow personalised training regimes that are reflective of the initial metabolic status of each individual.

3.1.3 Aim of Study

Conducting an exploratory pilot study by using an untargeted LC-MS method to explore the effects of aerobic exercise challenge in the urinary metabolome of physically active individuals was performed. The primary aim was to establish the effects of exercise on the human metabolome using a bout of exercise that was standardised to a relative intensity. The secondary aim was to explore potential predictive markers for VO_{2max} .

3.2 Materials and Methods

3.2.1 Chemicals and Solvents

HPLC grade ACN was purchased from Fisher Scientific, UK and HPLC grade water was produced by a Direct-Q 3 Ultrapure Water System (Millipore, UK). AnalaR-grade formic acid (98%) was obtained from BDH-Merck (Poole, Dorset, UK). Four authentic stock standard mixtures for 220 compounds were prepared as stated previously in section 2-3 and diluted 4 times with ACN before LC-MS analysis. Ammonium carbonate was purchased from Sigma-Aldrich, UK.

3.2.2 Subjects and Experimental Design

Ten healthy recreationally active adults, two females and eight males, volunteered and provided written informed consent to participate in the study. Participant characteristics such as age, stature, weight and aerobic capacity are shown in Table 3-1. Ten participants were entered into the study and this was approved by the ethics committee of the school of Science and Sport, University of the West of Scotland.

Participants recruited were staff and students from the University of the West of Scotland, Hamilton Campus. All procedures were conducted in accordance with the declaration of Helsinki.

Table 3-1: Participant Characteristics. Values are mean \pm SD; N, number of subjects; F, female; M, male; aerobic capacity (VO_{2max}) and maximal cycling work rate (WR_{max}).

Participant Characteristics					
Number (N) (F/M)	Age (Y)	Stature (cm)	Weight (kg)	VO_{2max} (ml/kg ⁻¹ /min ⁻¹)	WR_{max} (W)
10 (2 / 8)	28.3 \pm 6.7	168 \pm 30	68.53 \pm 14.7	197 \pm 5.4	134 \pm 61.3

3.2.3 Experimental Design

Each participant visited the laboratory on two separate occasions to complete two cycling exercise trials. The first was an incremental exercise test until exhaustion in order to determine VO_{2max} and the second was a 45 min submaximal exercise test. Urine samples were collected the day before, the day of and the day after the submaximal exercise test (Figure 3-1). Participants were asked not to exercise 24h prior to the maximal test and for the duration of the urine collection period other than the submaximal trial. They were also asked to refrain from the consumption of alcohol 24h before each test, caffeine for 6h before testing, or consume anything other than water for 3h before testing.

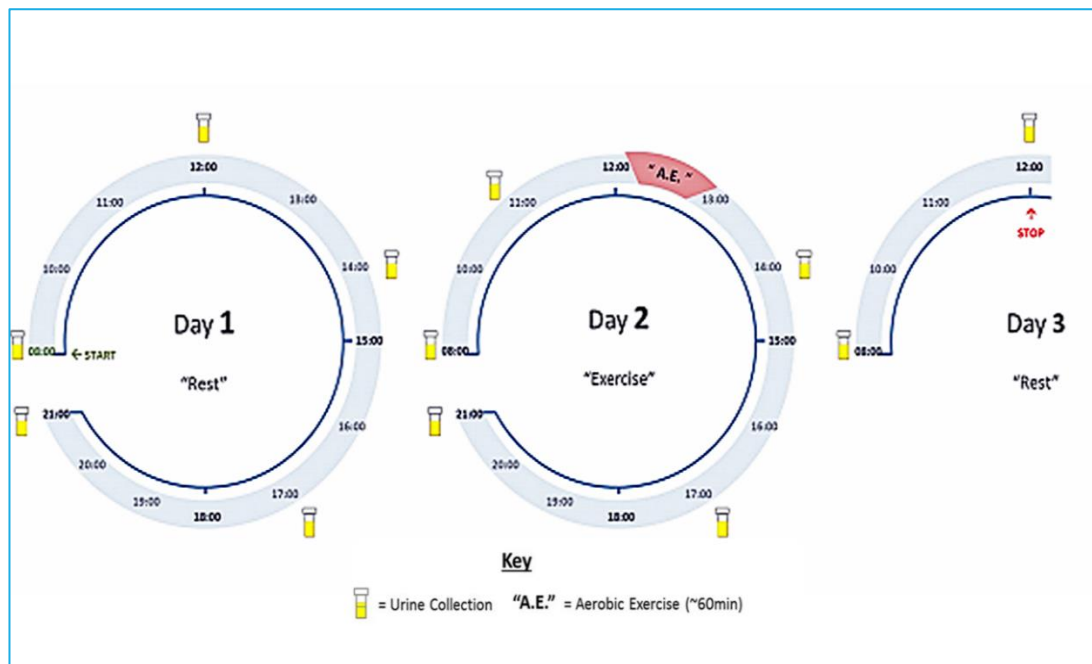


Figure 3-1: Indicative representation of urine collection schematic. The first urine sample on each day was the first pass after waking (typically 6 am–8 am). urine sample was collected at mid-stream on each time.

3.2.4 VO_{2max} Test

On their first visit after standard anthropological measurements, VO_{2max} and maximal cycling work rate (WR_{max}) were measured using a continuous graded exercise test on an electronically braked cycle ergometer (Lode Excalibur, Groningen, The Netherlands) maintaining an initial workload of 50 W. Work rate was increased in a ramp protocol at a rate of 15 W/min until the participant could no longer maintain a cadence of 50 rpm at which point the test was stopped. Throughout the test heart rate was measured by telemetry (Polar Electro, Oy, Finland) and expired gas was measured breath by breath via indirect calorimetry (Medgraphics, Milan, Italy) and analysed for respiratory variables. The indirect calorimeter was calibrated immediately prior to each test using calibration and reference gases (calibration gas: 12% O_2 , 5% CO_2 ; reference Gas: 21% O_2 , 0% CO_2). Volume was calibrated using a 3L syringe.

Following data collection, VO_{2max} data was filtered to delete values that were less than or greater than the rolling seven breathe mean \pm two standard deviations. All ten participants obtained a plateau in VO_{2max} (as determined by a rise in VO_{2max} of $<50\%$ of the expected increase for the given WR_{max}) fulfilling the criteria for VO_{2max} . Smoothed data was subsequently averaged over a rolling seven breath mean and the largest value obtained was determined as the participant's VO_{2max} .

3.2.5 Submaximal Test

Participants cycled on an electronically braked cycle ergometer at light and moderate intensities for a total duration of 45 min. The exercise protocol comprised of a 5min warm up at 50W, 15 min at 40% of WR_{max} (established from the initial VO_{2max} test), 15min at 50% WR_{max} , and 10 min at 60% WR_{max} . Heart rate and expired gas were continuously monitored throughout as previously described in section 3.2.4.

3.2.6 Sample Collection and Preparation

120 samples obtained from the subjects were collected at mid-stream on different drop-off points (Fig. 3-1) and moved on pre-labelled sterilised urine containers. The unopened urine containers were transported by ice box to the laboratory to be stored at -20°C until analysis. On the day of analysis, these samples were thawed at room temperature in order to be prepared for LC-MS analysis. Urine (200 μl) was thoroughly mixed with 800 μl of ACN, followed by centrifugation at 10000 rpm for 5min; 800 μl of supernatant was then transferred to a LC auto-sampler vial (Thermo Fisher, UK). The instrumental variation was also minimised by running the 12 samples for each subject in blocks followed by pooled samples. Due to the final normalisation is subject

specific, rather than being based on the full cohort this reduces the impact of technical variations in a long run. Samples were designated as follows D=day, S=sample number within a day e.g. D1S1 = day1 sample 1. Pooled samples were interspersed throughout the run to check for technical variation. Within the blocks of 12 the samples for each participant, ten pooled samples were randomised. Four standard mixtures containing 220 standards were run also with the samples. Details of the urine samples for LC-MS running order are given in Table 3-S1 in supplementary data (Appendix-1).

3.2.7 LC-MS Method

LC-MS data were acquired on Dionex Ultimate 3000 HPLC (Thermo Fisher Scientific) coupled to an Exactive Orbitrap (Thermo Fisher Scientific) in both positive and negative mode set at 50,000 resolution (controlled by Xcalibur version 2.1.0; Thermo Fisher Corporation). The mass scanning range was m/z 75–1200, the capillary temperature was 320 °C and the sheath and auxiliary gas flow rates were 50 and 17 arbitrary units, respectively. The separation was performed on a ZIC-pHILIC column (150 x 4.6mm, 5 μ m from HiChrom, Reading UK) in binary gradient mode. The used mobile phase was (A) 20 mM ammonium carbonate buffer (pH 9.2) and (B) pure ACN; the flow rate was 300 μ L.min⁻¹. The gradient was programmed for 46min as shown in Table 3-2. The injection volume was 10 μ L and the sample tray temperature was controlled at 12°C during the measurement. Samples were run in a stratified method with between subject samples placed in randomised order. Due to The Exactive Orbitrap does not have the capability of performing selected ion fragmentation using collision induced dissociation (CID), it cannot be used to do

MS/MS. Therefore MS² spectra were obtained with CID (35V) by using an LTQ-Orbitrap under the same conditions described in section 2-5-4.

Table 3-2: The gradient programme

Time (min)	Mobile Phase		Flow Rate (µl/min)
	A%	B%	
0.00	20	80	300
30.00	80	20	300
31.00	92	8	300
36.00	92	8	300
37.00	20	80	300
46.00	20	80	300

3.3 LC-MS Data Processing and Statistical Analysis

Raw files obtained from the LC-MS approach were converted to mzXML file (ProteoWizard) and separated into ESI positive and negative. Converted mzXML files were processed by using m/z Mine 2.14 (Pluskal *et al.*, 2010) and searched against an in house metabolite database in order to identify the metabolites. Graphical representations, tabular features and statistical analysis (p-value generation) were performed in Excel (Microsoft Office 2013). The mean of the peak areas for each metabolite across the samples within each day was calculated and then the area for each metabolite was divided by the mean. This provided a subject-specific normalisation within the non-exercise and exercise days. All subsequent metabolite responses, paired t-test and fold changes (ratio) were conducted on new data set. SIMCA-P version 14.0 (Umetrics, Sweden) was used for multivariate analysis which included PCA, OPLSDA and OPLS. The data were centred, and Pareto scaled for PCA

and OPLS-DA and OPLS in order to generate S-plots for visualisation of the components with significant influence in the dataset. In S-plot, the metabolites far to the upper right and to the lower left are closely associated with differences between assigned groups.

3.4 Results

3.4.1 Physiological Responses to Submaximal Exercise

The mean $\text{VO}_{2\text{max}}$ at 40%, 50%, and 60% of WR_{max} was $21.2 \pm 2.5 \text{ mL/kg}^{-1}/\text{min}^{-1}$, $25.8 \pm 2.5 \text{ mL/kg}^{-1}/\text{min}^{-1}$, and $30.8 \pm 4.1 \text{ mL/kg}^{-1}/\text{min}^{-1}$, respectively. The mean HR during the submaximal exercise test was $115 \pm 12.8 \text{ bpm}$, $156 \pm 14 \text{ bpm}$, and $169 \pm 13.6 \text{ bpm}$ and 40%, 50%, and 60% of WR_{max} , respectively.

3.4.2 Metabolite Profiling

Longitudinal sampling of urine provides a non-invasive method that provides rich data sets produces samples with greater volume than plasma as well as containing higher concentrations of particular metabolite over the period between samplings. In contrast, even if plasma is taken frequently, it will always represent an open system where taking a sample at a slightly different time might give a different answer. In this study, a 37h protocol was used (Figure 3-1) in order to generate an understanding of the acute effects of exercise and the duration of that response in the metabolite profiles. In addition, sampling on the pre-exercise day allowed observation of metabolite variations occurring as a diurnal rhythm. The output from data extraction followed by

searching against the data base yielded metabolites which were identified to MSI levels 1 or 2 (Sumner *et al.*, 2007) according to either exact mass (with <3 ppm deviation) or exact mass plus retention time matching to a standard (Table 2-S1).

Figure 3-2 shows the PCA analysis of the raw un-normalised peak area data for the comparison of the day 2 first (D2S1) and third (D2S3-first post-exercise) samples. There was no classification of the samples by PCA when the raw data was used as the basis of the model and it was also not possible to fit an OPLSDA model to this data set.

Thus in order to compare metabolites on the same axis the areas for each metabolite across all the time-points for day 1 and day 2 were averaged for each individual and then each metabolite area at each time-point was divided by the average to give the proportion contributed to the total output during the day. This approach was similar to that used in previous study of our group and was discussed at some length in that paper (Daskalaki *et al.*, 2015a). Figure 3-3 shows the PCA separation of 19 out 20 samples in the current study for the D2S1 and D2S3 following normalisation to individual metabolic output over the five urine samples taken collected during day 2. One sample was excluded because there were problems with the analytical run which may due to the fault in collection or preparation of sample. It is clear that there is a marked difference in metabolite profile between the two groups. The same comparison on day 1 between the first (D1S1) and third (D1S3) samples of the day, where there was no exercise intervention, did not yield as clear cut a separation although there was some evidence of division into two sample types. The PCA model shown in Figure 3-4 gave a clear separation when one individual's samples (GS) on day 2 were excluded from the model.

Table 3-3 summarises univariate comparisons for all the metabolites that are significantly changed between D2S3 in comparison with the rest (S1) of the day 2 (D2) samples and D1S3 with the rest (S1) of the day1 (D1) samples. OPLSDA models of the data were made in order to get a clearer picture of the differences between the first and third samples on day 2 and day 1. There are a large number of changes and such models emphasise the importance of key variables as VIPs.

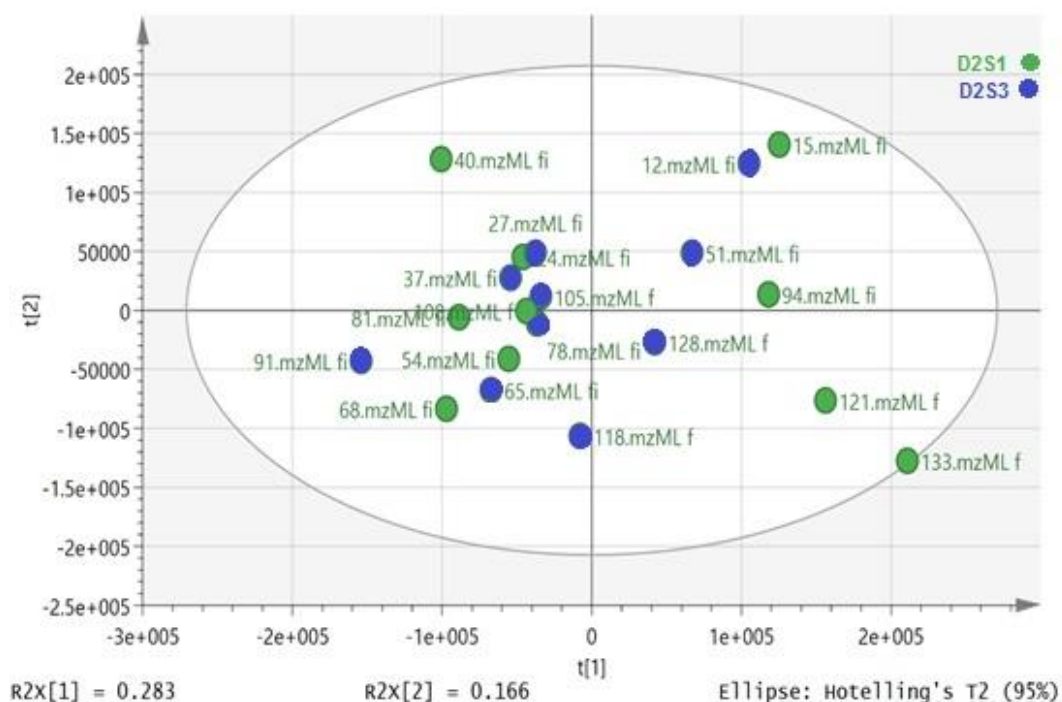


Figure 3- 2: PCA comparing D2S1 (green) and D2S3 (blue) samples based on the peak areas for the raw data (un-normalised). The samples are labelled according to Table 3-S1 as shown in Appendix-I.

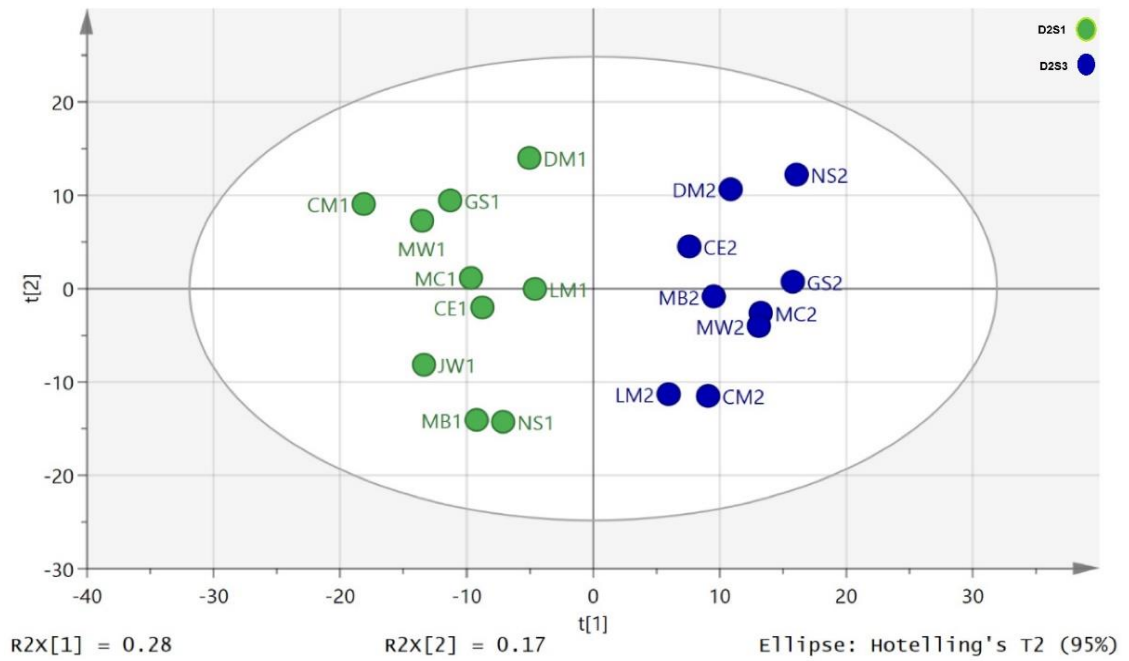


Figure 3-3: Separation of D2S1 (green) from the post exercise D2S3 (blue) samples by using PCA [$R^2X(cum)=0.548$, $Q^2(cum)=0.295$, three components] following normalisation to individual metabolic output on day 2

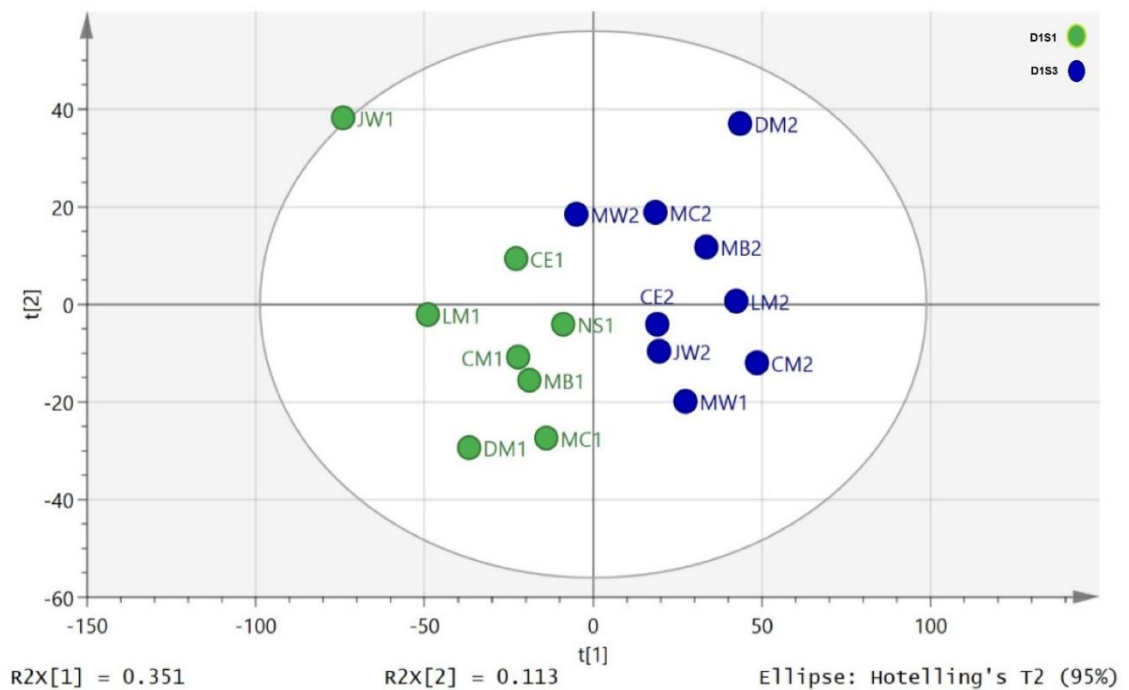


Figure 3-4: Separation of day 1 first void (D1S1-green) and third samples (D1S3-blue) by using PCA ($R^2X(cum)$ 0.536, $Q^2(cum)$ 0.263, three components).

Table 3-3: Summarises univariate comparisons for all the metabolites that are appeared in comparison between first sample post-exercise (S3) with the rest of samples in both days (D1 and D2).

Metabolites			Day 2 (D2)								Day 1 (D1)							
m/z	RT	Name	S3 - S1		S3 - S2		S3 - S4		S3 - S5		S3 - S1		S3 - S2		S3 - S4		S3 - S5	
			P value	Ratio	P value	Ratio	P value	Ratio	P value	Ratio	P value	Ratio	P value	Ratio	P value	Ratio	P value	Ratio
Purine metabolism																		
137.046	10.8	Hypoxanthine	<0.001	3.748	<0.001	3.463	<0.001	5.203	<0.001	5.934	0.516	0.832	0.374	0.713	0.679	0.846	0.772	0.898
152.057	13.1	Guanine	0.018	2.562	0.009	2.960	0.002	6.015	0.006	3.521	na	na	na	na	na	na	na	na
178.072	10.8	Methyl-H2-pterin	<0.001	3.942	0.000	3.462	0.000	5.422	0.000	6.094	0.564	0.848	0.379	0.718	0.643	0.830	0.729	0.882
253.093	9.2	Deoxyinosine	0.009	4.971	na	na	Na	na	na	na	na	na	na	na	na	na	na	na
165.042	13.8	Methylxanthine	0.030	0.768	0.254	1.163	0.900	0.987	0.421	1.089	0.089	0.787	0.916	1.017	0.958	0.992	0.532	0.896
165.042	8.9	Methylxanthine	0.035	0.673	0.135	1.409	0.112	1.446	0.741	0.935	0.068	0.735	0.699	1.074	0.998	1.000	0.533	0.896
167.021	13.5	Urate	0.015	0.748	0.688	0.959	0.663	0.948	0.931	0.989	<0.001	0.534	0.333	0.824	0.491	0.883	0.023	0.676
181.037	10.8	1-Methyluric acid	0.008	0.594	0.264	1.232	0.109	1.365	0.997	0.999	0.012	0.561	0.941	0.981	0.993	1.002	0.333	0.798
269.088	11.5	Inosine	0.025	16.274	0.040	7.292	Na	na	0.032	9.781	0.947	0.967	0.667	1.240	0.331	1.699	0.477	1.472
285.083	13.1	Xanthosine	0.011	2.327	0.002	3.983	0.002	3.933	0.012	2.440	0.012	0.506	0.350	0.737	0.290	0.708	0.183	0.641
296.135	17.7	N6,N6-Dimethyladenosine	0.197	2.390	0.104	3.656	0.047	9.091	0.036	19.294	0.002	0.491	0.192	0.769	0.508	0.903	0.350	0.851
Carnitines																		
202.109	5.8	Hydroxyhepanoylglycine	0.003	1.763	0.001	2.117	0.006	1.805	0.002	1.863	0.238	1.276	0.981	1.003	0.574	0.875	0.165	0.751
218.139	6.0	Propanoylcarnitine	0.032	0.359	0.048	10.710	0.153	3.112	0.277	2.292	0.095	0.732	0.363	1.124	0.143	0.762	0.009	0.710
248.149	12.1	Hydroxybutyrylcarnitine	0.414	1.213	0.059	1.402	0.886	1.035	0.350	0.820	0.304	0.824	0.464	0.857	0.359	0.781	0.074	0.643
274.201	6.9	Heptanoylcarnitine	0.220	1.206	0.003	1.751	0.014	1.526	0.465	1.106	0.120	0.779	0.547	0.902	0.741	0.942	0.626	0.913
314.234	5.6	Decanoyl carnitine	0.010	1.562	0.000	2.046	0.001	2.153	0.007	1.744	0.079	0.682	0.391	0.825	0.742	0.914	0.659	0.897
300.218	6.0	Nonanoylcarnitine	0.015	1.632	0.003	2.096	0.003	2.083	0.057	1.450	0.064	0.604	0.499	0.850	0.789	0.932	0.682	0.890
330.227	6.6	Keto-decanoylcarnitine	0.032	1.606	0.001	2.143	0.003	2.022	0.269	1.222	<0.001	0.453	0.345	0.814	0.588	0.896	0.481	0.871
368.279	5.1	Tetradecadienecarnitine	0.158	1.719	0.004	4.727	0.004	4.243	0.041	2.177	na	na	na	na	na	na	na	na
Steroids																		
539.25	6.7	Tetrahydroaldosterone-3-glucuronide	0.007	1.618	0.038	1.423	0.002	1.799	0.000	2.082	0.369	1.211	0.847	1.037	0.531	1.128	0.189	1.316
539.25	7.9	Tetrahydroaldosterone-3-glucuronide	0.157	1.364	0.009	1.736	0.007	1.797	0.002	1.949	0.699	1.089	0.616	0.885	0.618	1.106	0.335	1.230
413.2	4.2	Tetrahydrocorticosterone sulfate or isomer	0.124	1.371	0.412	1.188	0.023	1.724	0.032	1.647	0.672	1.098	0.980	0.995	0.198	1.337	0.053	1.563
367.158	3.9	Hydroxyandrosteneone sulfate	0.037	1.572	0.806	0.949	0.171	1.395	0.147	1.442	0.319	1.227	0.453	0.872	0.208	1.275	0.031	1.499

Metabolites			Day 2 (D2)								Day 1 (D1)							
m/z	RT	Name	S3 - S1		S3 - S2		S3 - S4		S3 - S5		S3 - S1		S3 - S2		S3 - S4		S3 - S5	
			P value	Ratio	P value	Ratio	P value	Ratio	P value	Ratio	P value	Ratio	P value	Ratio	P value	Ratio	P value	Ratio
Bile acids																		
405.265	5.6	Dihydroxy-oxo-cholanate	0.004	0.441	0.783	0.924	0.144	1.582	0.437	1.210	0.078	0.512	0.869	0.930	0.765	1.153	0.297	0.613
583.312	10.3	Cholicacidglucuronide	0.000	0.273	0.246	0.608	0.657	1.227	0.347	1.564	0.006	0.170	0.775	0.790	0.676	1.495	0.120	0.338
583.312	11.5	Cholicacidglucuronide	0.003	0.227	0.262	0.597	0.447	1.731	0.754	1.229	0.018	0.316	0.539	0.735	0.964	0.976	0.108	0.444
Glycolysis Krebs																		
87.0092	8.6	Pyruvate	0.256	1.179	0.013	1.450	0.076	1.290	0.150	1.229	0.017	0.565	0.485	0.816	0.288	0.815	0.490	0.874
89.0242	10.2	(R)-Lactate	0.018	2.188	0.106	1.581	0.234	1.347	0.078	1.634	0.867	1.041	0.161	0.572	0.137	0.713	0.708	0.905
Dicarboxylic acids																		
173.082	13.2	Suberic acid	0.039	0.519	0.598	0.804	0.944	0.983	0.386	0.784	0.001	0.474	0.353	0.828	0.889	1.040	0.311	1.342
199.097	11.1	Decenedioic acid	0.007	0.490	0.497	1.132	0.669	0.924	0.034	0.636	0.412	0.959	0.110	1.094	0.805	0.988	0.169	1.079
217.108	13.0	Hydroxysebacicacid	0.066	0.530	0.498	0.816	0.715	0.883	0.649	0.879	0.120	0.535	0.228	0.679	0.983	1.008	0.203	0.643
Neurotransmitters																		
101.024	12.7	2-Oxobutanoate	0.030	1.212	0.250	1.119	0.639	0.967	0.341	1.087	0.690	0.953	0.429	0.930	0.772	0.972	0.519	0.951
104.071	14.9	4-Aminobutanoate	0.000	0.737	0.148	0.901	0.114	0.879	0.042	0.845	0.003	0.801	0.784	0.978	0.502	0.940	0.172	0.900
182.997	17.0	hydroxybutyric acid sulfate	<0.001	2.172	0.000	1.577	0.001	1.652	0.000	2.867	0.519	1.133	0.990	0.998	0.706	0.943	0.069	1.473
198.113	16.8	L-Metanephrine	0.082	3.000	0.130	2.396	0.522	1.433	0.032	5.781	0.074	0.762	0.311	0.807	0.251	0.813	0.206	0.707
246.992	12.8	dihydroxy phenyl acetic acid sulfate o isomer	0.020	1.442	0.005	1.652	0.000	2.339	0.000	1.852	0.513	1.212	0.374	1.292	0.375	1.258	0.785	1.078
261.007	10.5	Homovanillicacidsulfate	0.142	1.397	0.148	1.337	0.022	1.724	0.014	1.833	0.857	0.932	0.529	1.287	0.275	1.654	0.306	1.597
263.023	8.5	3-Methoxy-4-hydroxyphenylethyleneglycolsulfate	0.071	1.385	0.005	1.847	0.005	1.890	0.011	1.685	0.405	0.833	0.724	1.084	0.681	1.087	0.602	1.119
Pyrimidine metabolism																		
111.02	15.3	Uracil	0.013	1.230	0.005	1.222	0.001	1.325	0.048	1.166	0.598	0.942	0.761	0.977	0.292	1.103	0.132	1.144
126.066	13.4	Methylcytosine	0.137	1.221	0.011	1.474	0.001	1.770	0.003	1.604	0.059	0.741	0.517	0.907	0.565	1.070	0.935	1.011
155.01	10.8	Orotate	0.032	1.343	0.618	0.922	0.390	0.884	0.147	1.263	0.061	1.397	0.947	1.011	0.407	1.161	0.016	1.528
Collagen metabolism																		
173.092	13.3	Glycylproline	<0.001	0.540	0.158	0.834	0.002	0.510	0.057	0.700	0.820	1.064	0.265	1.407	0.886	0.958	0.930	na
187.109	13.6	Glycyl-leucine	<0.001	0.708	0.463	0.913	0.305	0.894	0.997	1.000	0.006	0.702	0.079	0.777	0.020	0.733	0.050	0.797

Metabolites			Day 2 (D2)								Day 1 (D1)							
m/z	RT	Name	S3 - S1		S3 - S2		S3 - S4		S3 - S5		S3 - S1		S3 - S2		S3 - S4		S3 - S5	
			P value	Ratio	P value	Ratio	P value	Ratio	P value	Ratio	P value	Ratio	P value	Ratio	P value	Ratio	P value	Ratio
Amino acid metabolites																		
118.051	12.0	Threonine	0.001	0.641	0.714	1.057	0.229	1.199	0.547	1.083	0.685	1.063	0.272	0.852	0.659	0.937	0.617	1.075
128.035	13.1	Pyrralinehydroxycarboxylate	0.071	1.750	0.104	1.669	0.054	1.813	0.027	2.110	0.879	1.054	0.970	1.009	0.285	1.296	0.327	1.296
131.046	15.8	Asparagine	0.003	0.761	0.000	0.645	0.009	0.757	0.158	0.856	0.928	0.989	0.512	0.930	0.397	0.897	0.496	0.910
132.102	11.3	Leucine	0.030	0.593	0.533	0.836	0.267	0.744	0.039	0.552	0.061	0.675	0.361	0.826	0.303	0.811	0.485	0.878
148.043	14.0	Methionine	0.002	0.582	0.917	1.021	0.617	0.923	0.404	0.853	0.011	0.612	0.005	0.655	0.015	0.657	0.010	0.683
176.038	10.4	N-Formyl-L-methionine	0.010	0.504	0.568	1.152	0.945	0.984	0.723	0.911	0.051	0.441	0.132	0.575	0.059	0.496	0.215	0.668
206.082	5.5	N-Acetylphenylalanine	0.096	1.356	0.070	1.416	0.006	1.809	0.007	1.745	0.716	0.929	0.954	0.987	0.909	0.977	0.753	1.074
267.047	11.7	Homocystine	0.031	1.662	0.004	2.248	0.003	2.374	0.002	2.504	na	na	na	na	na	na	na	na
173.057	12.2	N-Formiminoglutamate	0.092	0.781	0.141	0.785	0.343	0.832	0.710	0.937	0.003	0.514	0.842	1.046	0.180	0.768	0.474	0.886
175.108	9.3	N-Acetylnornithine	0.005	0.697	0.893	0.980	0.958	0.991	0.977	1.004	0.000	0.566	0.431	0.902	0.737	0.960	0.020	0.756
187.072	11.4	N-Acetylglutamine	0.001	0.672	0.112	0.802	0.307	0.880	0.293	0.893	0.001	0.628	0.609	0.930	0.410	0.883	0.088	0.799
188.103	14.8	5-guanidino-3-methyl-2-oxo-pentanoate	0.438	1.136	0.094	1.306	0.431	1.103	0.001	1.850	0.002	0.480	0.362	0.807	0.048	0.694	0.045	0.686
188.104	15.9	Homocitrulline	0.028	0.805	0.410	0.892	0.401	0.898	0.113	1.173	0.066	0.727	0.708	1.070	0.956	0.990	0.543	0.904
209.092	11.3	Kynurenine	0.208	0.500	0.813	0.902	0.545	1.390	0.664	1.214	0.017	0.726	0.126	0.777	0.086	0.760	0.170	0.816
216.099	11.8	N-Acetyl-citrulline	0.001	0.604	0.925	1.014	0.999	1.000	0.596	1.086	0.005	0.553	0.928	0.978	0.851	0.958	0.746	0.934
221.092	6.8	5-Hydroxy-L-tryptophan isomer	0.058	2.245	0.111	1.900	0.476	0.775	0.374	1.424	0.530	0.952	0.973	0.998	0.209	0.875	0.383	0.914
221.092	10.7	5-Hydroxy-L-tryptophan	0.017	0.592	0.684	1.111	0.816	0.948	0.733	0.921	0.001	0.523	0.198	0.814	0.167	0.812	0.249	0.852
247.14	15.0	N2-(D-1-Carboxyethyl)-L-arginine	<0.001	2.235	0.000	2.058	0.000	1.822	0.000	3.187	0.323	0.823	0.476	0.823	0.235	0.764	0.300	0.777
245.093	13.0	N-Acetyl-D-tryptophan	0.007	0.676	0.482	0.934	0.695	1.035	0.581	0.942	0.420	0.841	0.919	1.023	0.738	1.076	0.514	1.159
247.073	9.5	5-Hydroxyindoleacetyl glycine	0.109	0.534	0.495	1.420	0.589	0.799	0.551	0.772	0.474	0.823	0.619	1.148	0.984	1.006	0.366	1.300
253.051	11.1	5-L-Glutamyl-taurine	0.001	0.434	0.512	1.235	0.918	1.031	0.626	0.856	0.056	0.778	0.642	0.930	0.548	0.910	0.275	0.855

Metabolites			Day 2 (D2)								Day 1 (D1)							
m/z	RT	Name	S3 - S1		S3 - S2		S3 - S4		S3 - S5		S3 - S1		S3 - S2		S3 - S4		S3 - S5	
			P value	Ratio	P value	Ratio	P value	Ratio	P value	Ratio	P value	Ratio	P value	Ratio	P value	Ratio	P value	Ratio
Sugars																		
119.035	13.4	D-Erythrose	0.001	0.665	0.967	1.005	0.792	0.977	0.558	1.073	0.334	0.865	0.010	0.662	0.329	0.872	0.105	0.764
119.035	10.9	D-Erythrose	0.027	0.725	0.924	1.017	0.259	1.246	0.423	1.158	0.032	0.630	0.017	0.594	0.069	0.684	0.021	0.614
149.046	11.1	D-Ribose	0.003	0.696	0.024	1.333	0.254	1.134	0.121	1.209	0.282	1.134	0.764	1.025	0.186	1.154	0.924	0.989
151.061	13.6	Xylitol	0.016	0.734	0.238	1.207	0.397	1.143	0.442	1.130	0.036	0.617	0.012	0.572	0.035	0.631	0.031	0.637
163.061	9.9	L-Rhamnose	0.025	0.667	0.568	1.115	0.810	0.966	0.445	0.897	0.125	0.715	0.039	0.646	0.022	0.590	0.026	0.610
165.04	8.9	L-Arabinonate	0.023	0.648	0.185	1.365	0.052	1.738	0.923	0.977	0.072	0.600	0.160	0.697	0.029	0.547	0.483	0.824
181.072	14.7	D-Sorbitol	0.050	0.699	0.598	1.075	0.800	1.039	0.172	1.261	0.126	0.653	0.070	0.598	0.047	0.555	0.144	0.666
193.036	15.2	D-Glucuronate	0.018	0.628	0.914	0.986	0.903	0.987	0.391	1.102	0.244	0.846	0.085	0.789	0.165	0.803	0.924	0.978
341.109	13.7	Sucrose	0.028	0.608	0.640	1.111	0.228	0.781	0.036	1.788	0.090	0.705	0.300	0.846	0.189	0.808	0.970	1.011
Vitamins co-factors																		
132.077	15.4	Creatine	0.011	0.538	0.235	1.329	0.904	1.031	0.061	0.558	0.018	0.440	0.674	0.852	0.806	0.925	0.098	0.468
168.066	9.8	Pyridoxal	0.021	5.496	0.019	5.580	0.391	1.441	0.971	1.016	0.875	0.944	0.471	0.784	0.047	0.481	0.152	0.476
175.025	16.9	Ascorbate	0.062	1.274	0.309	0.844	0.399	0.892	0.195	1.233	0.404	0.796	0.954	1.018	0.121	0.665	0.231	0.627
220.118	9.4	Pantothenate	0.008	1.403	0.002	1.575	0.041	1.407	0.019	1.538	0.937	0.987	0.516	0.904	0.214	0.837	0.524	0.889
240.109	13.3	Dihydrobiopterin	0.227	1.195	0.007	1.584	0.004	1.903	0.001	1.634	0.012	0.551	0.451	0.842	0.237	0.807	0.397	0.844
252.074	14.7	Neopterin	0.016	0.608	0.449	1.181	0.341	1.238	0.828	1.056	0.046	0.455	0.801	1.111	0.732	0.884	0.784	0.902
375.13	8.1	Riboflavin	0.013	0.660	0.114	1.315	0.313	1.202	0.529	0.904	0.032	0.500	0.715	0.909	0.708	0.898	0.827	1.058
Microbiome																		
153.02	14.0	2,5-Dihydroxybenzoate	0.078	1.324	0.111	1.319	0.034	1.580	0.016	1.576	0.884	0.964	0.705	1.096	0.271	1.302	0.193	1.415
192.067	6.0	Phenylacetyl glycine	0.004	1.759	0.210	1.295	0.014	1.747	0.001	2.106	0.277	0.756	0.364	0.822	0.424	0.830	0.520	0.825
197.046	9.8	3-(3,4-Dihydroxyphenyl) lactate	0.025	1.426	0.001	1.918	0.004	1.742	0.003	1.760	0.383	0.855	0.895	1.026	0.753	1.057	0.666	1.081
367.104	6.7	O-Feruloylquininate	0.054	1.745	0.366	1.296	0.416	1.245	0.524	0.813	0.018	2.413	0.816	0.922	0.199	0.700	0.423	1.239

There was a very clear separation of D2S1 and D2S3 (Figure 3-5) obtained by using OPLSDA for classifying D2S1/D2S3 samples. The cross validation plot indicated a strong model as can be seen in Figure 3-6 where all the points for the blue squares are below the blue square on the right and the plot intersects the y-axis below 0, and the CV Anova score for the model was 0.0029. However, a clear separation was also found between the D1S1 and D1S3 samples as shown in (Figure 3-7) and the cross validation model for this was also good (figure 3-8) where the CV ANOVA for this model was 0.00097. Thus the composition of the metabolites in urine varies markedly throughout the day whether exercise is used as an intervention or not.

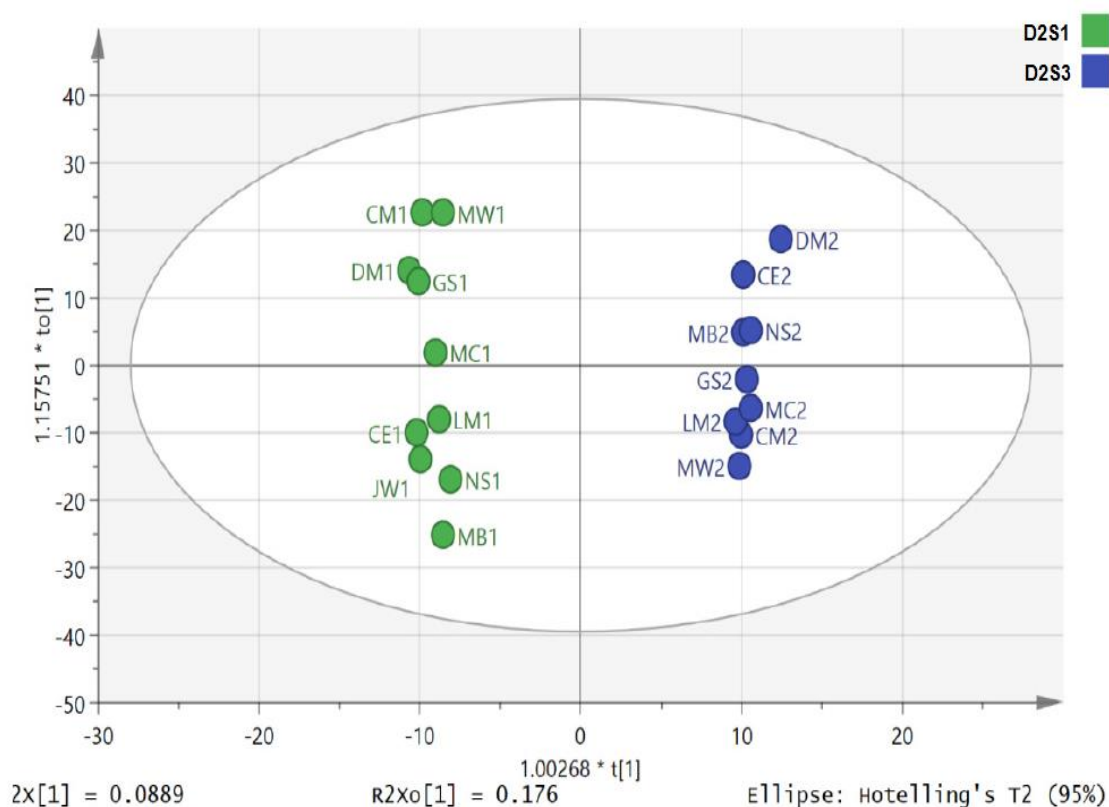


Figure 3-5: Separation of D2S1 (green) and D2S3 (blue) samples by using OPLSDA based on 3078 features. $R2X(cum)=0.35$, $R2Y(cum)=0.99$, $Q2(cum)=0.77$, and three components.

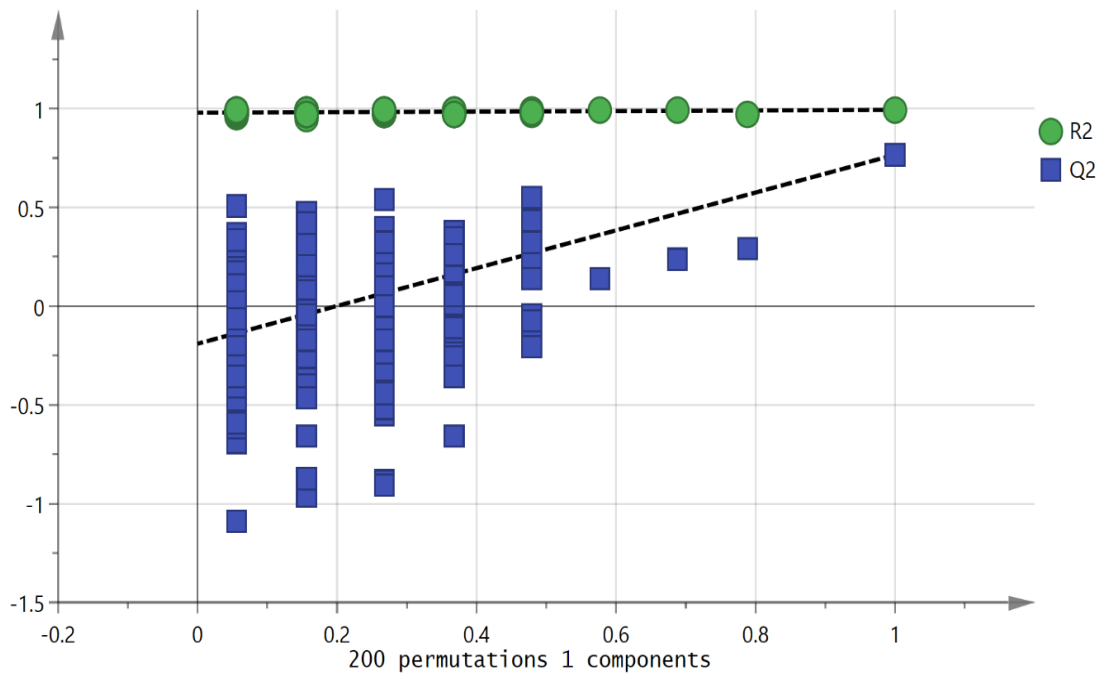


Figure 3-6: Cross validation model for the classification of D2S1 and D2S3 by OPLSDA.

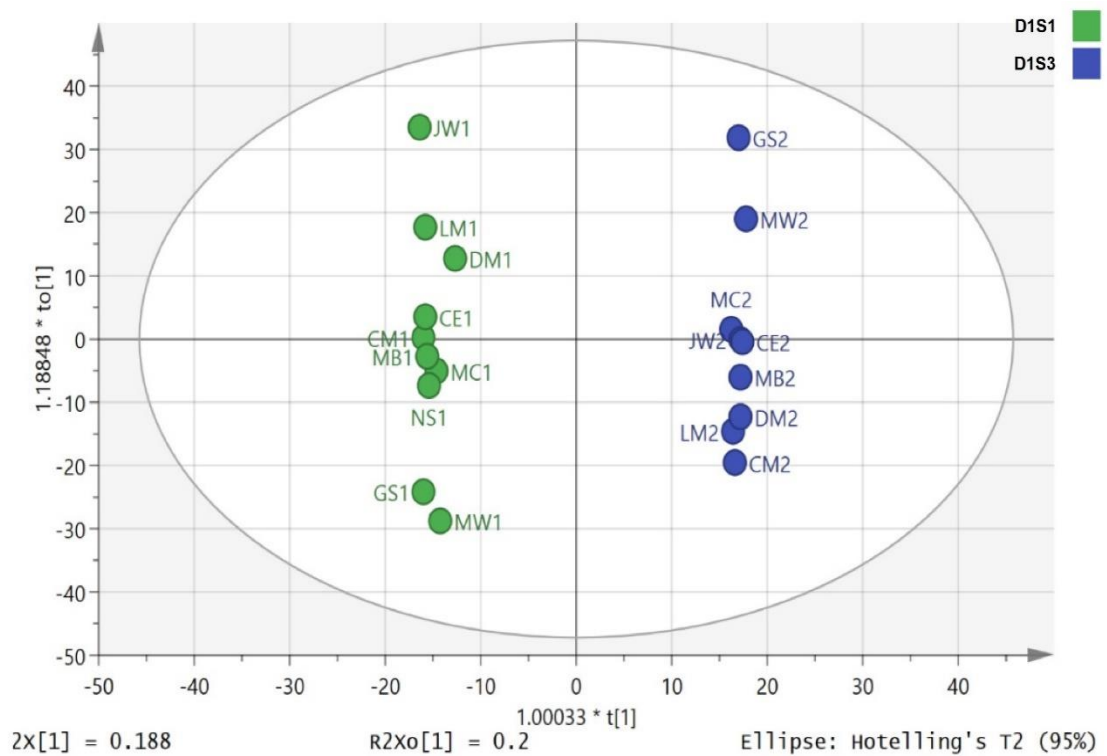


Figure 3-7: Separation of D1S1 (green) and D1S3 (blue) by OPLSDA based on 3540 features. $R2X(cum)=0.56$, $R2Y(cum)=0.997$, $Q2(cum)=0.847$ and four components.

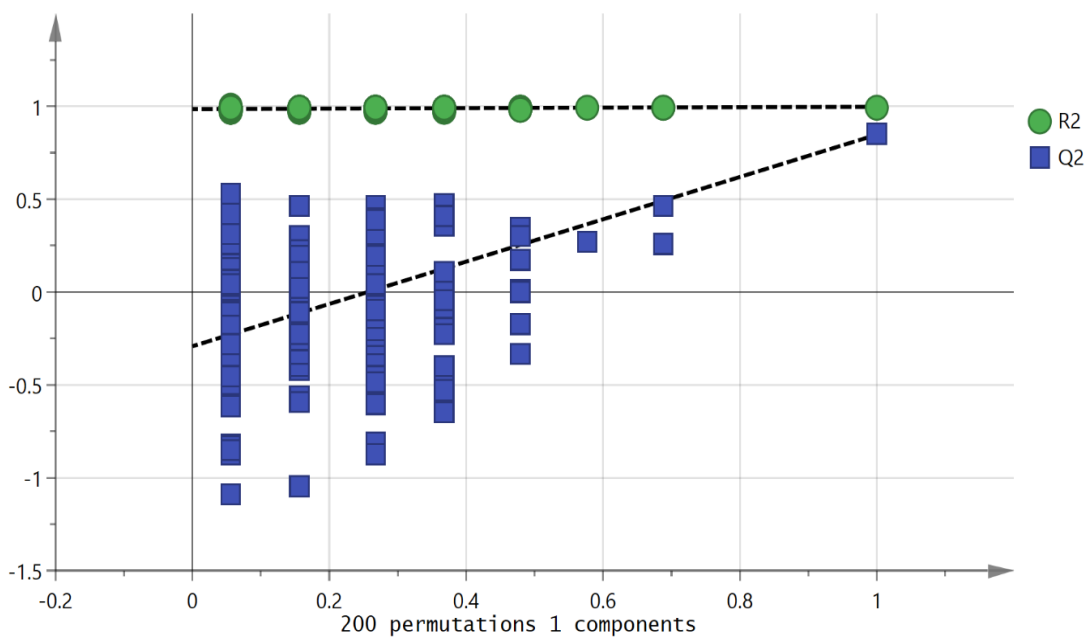


Figure 3-8: Cross validation of the separation of D1S1 and D1S3 by OPLSDA.

Figure 3-9 shows an S-plot highlighting the features with the most impact (largest VIPs), table 3-S2, on the OPLSDA model for the D2S3 and D2S1 samples. In many cases, exact identity of these features is poorly defined. Some of the metabolites match the retention times of analytical standards or are well known urinary metabolites. Figure 3-10 shows an S-plot highlighting the features with the most impact on the OPLSDA model for the D1S1 and D1S3 samples as listed in Table 3-S3. However, some of the important changes in metabolites between the equivalent time points on day 1 and day 2 are similar.

Table 3-4 shows the metabolites which are important in the OPLSDA model for the D2S3 and D2S1 samples shown in Figure 3-5 in comparison with the D1S1 and D1S3 samples shown in Figure 3-6. The highlighted metabolites have been identified with some confidence, the majority have p-values < 0.05. Application of the Benjamini-Hochberg FDR statistical test (Benjamini and Hochberg, 1995, McDonald, 2014) with

$Q = 0.1$ and including 1000 metabolites indicated that all metabolites with a p-value < 0.05 can be regarded as being significantly changed following exercise.

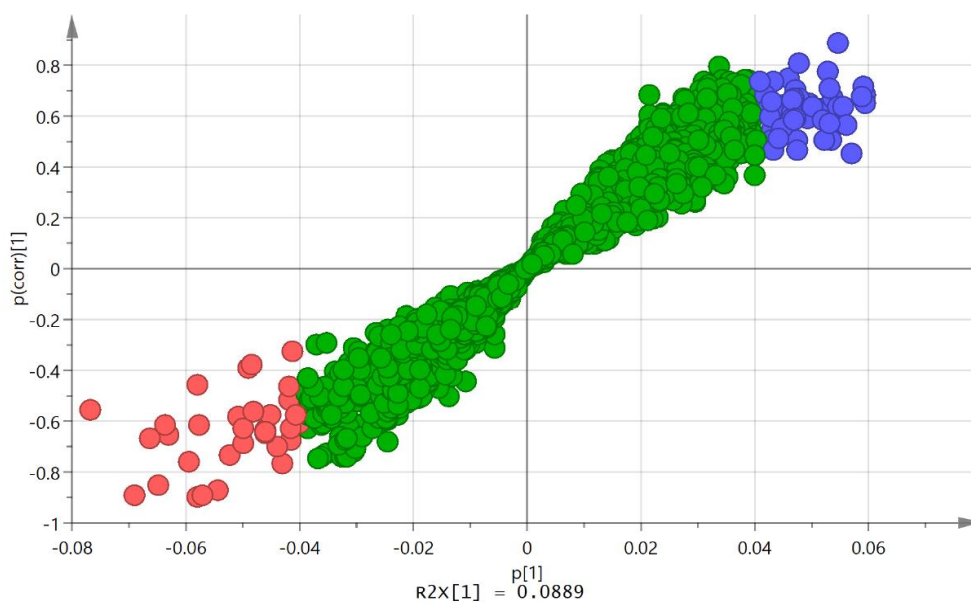


Figure 3-9: S-plot for OPLSDA model of D2S3 vs D2S1 highlighting the metabolites listed in Table 3-S2. The blue colour has a high $p(\text{corr})$ which means a very high reliability while the red has a high model influence partly due to its high variance in the dataset.

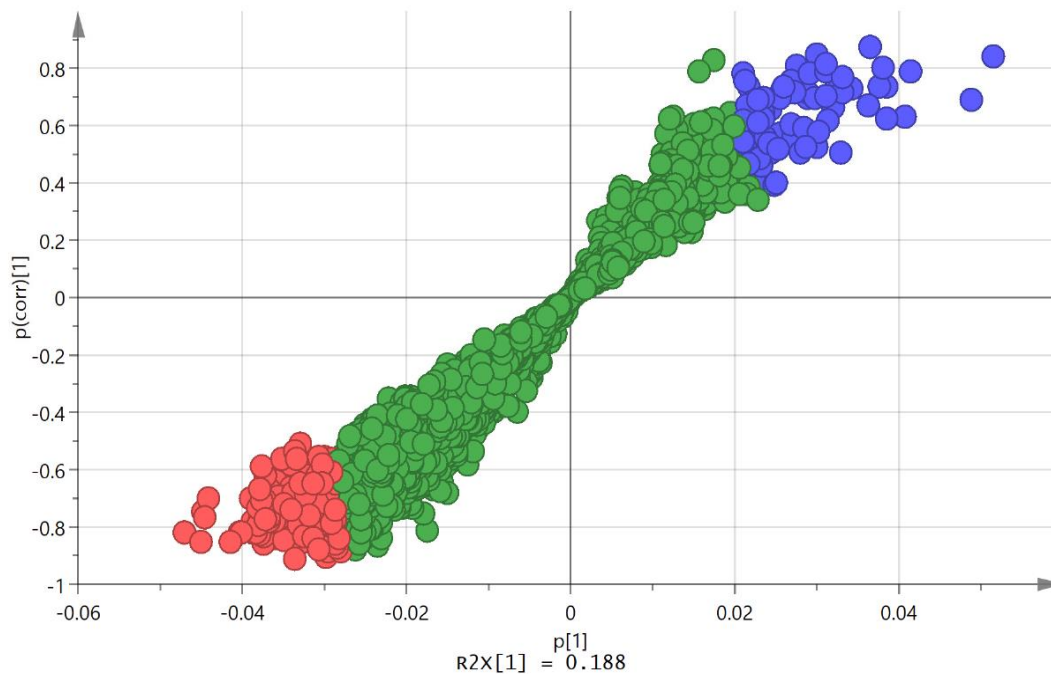


Figure 3-10: S-plot for OPLSDA model of D1S3 vs D1S1 highlighting the metabolites listed in Table 3-S3. The blue colour has a high $p(\text{corr})$ which means a very high reliability while the red has a high model influence partly due to its high variance in the dataset.

Table 3-4: Metabolites differing between D2S1 and D2S3 in comparison with D1S1 and D1S3.

* Matches retention time of standard. ** Same elemental composition as the standard but different retention time. na = not detected in these samples. Matches retention time of standard. na = not detected in these samples. ‡ Same elemental composition as acetyl carnitine but retention time much earlier. *** Application of the Benjamin-Hochberg false discovery rate with $Q = 0.1$ and including 1000 features in the test indicated that all p-values < 0.05 are significant.

Polarity	m/z	Rt	Metabolite	D2S3D2S1		D1S3D1S1	
				P value***	Ratio	P value***	Ratio
Purine Metabolism							
P	137.046	10.8	*Hypoxanthine	<0.001	3.75	0.516	0.832
P	152.057	13.1	*Guanine	0.02	2.56	na	na
N	167.021	13.5	*Urate	0.015	0.748	<0.001	0.534
N	181.037	10.8	1-Methyluric acid	0.01	0.59	0.012	0.561
P	253.093	9.2	Deoxyinosine	0.01	4.97	not	not
P	269.088	11.5	*Inosine	0.02	16.27	0.947	0.967
P	285.083	13.1	*Xanthosine	0.01	2.33	0.012	0.506
P	282.12	13.9	Methyladenosine	0.24	0.856	<0.01	0.516
P	296.136	17.8	Dimethyladenosine	0.20	2.390	<0.01	0.491
P	312.13	9.2	Dimethylguanosine	0.90	0.983	<0.003	0.562
Steroids							
N	367.158	3.9	Testosterone sulfate	0.04	1.57	0.319	1.23
N	539.25	6.7	Tetrahydroaldosterone glucuronide	<0.01	1.62	0.369	1.21
Sugar metabolism							
N	87.0092	8.6	*Pyruvate	0.256	1.179	0.017	0.565
N	89.0242	10.2	*Lactate	0.02	2.19	0.867	1.04
N	151.061	13.6	*Xylitol or isomer	0.016	0.734	0.036	0.617
N	163.061	9.9	* Rhamnose or isomer	0.025	0.667	<0.01	0.629

	165.04	8.9	Arabinonate	0.023	0.648	<0.01	0.520
N	181.072	14.7	*Sorbitol or isomer	0.05	0.70	0.126	0.653
N	193.036	15.2	* Glucuronate or isomer	0.018	0.628	0.024	0.641
Neurotransmitter metabolism							
N	101.024	12.7	Oxobutanoate	0.030	1.212	0.690	0.953
P	104.071	14.9	*4-Aminobutanoate	< 0.001	0.737	0.003	0.801
N	182.997	17.0	Hydroxybutyric acid sulfate	<0.001	2.172	0.519	1.133
P	198.113	16.8	*Metanephrine	0.082	3.000	0.074	0.762
N	246.992	12.8	Dihydroxy phenyl acetic acid sulfate or isomer	0.020	1.442	0.513	1.212
N	261.007	10.5	Homovanillicacid sulfate	0.142	1.397	0.857	0.932
N	263.023	8.5	Methoxyhydroxy phenylethyleneglycol sulfate	0.071	1.385	0.405	0.833
Fatty acid conjugates							
N	202.109	5.8	† Hydroxyhepatonyl glycine	<0.01	1.76	0.238	1.276
P	218.139	6.0	Propanoylcarnitine	0.03	0.360	0.363	1.124
P	288.217	6.4	Octanoylcarnitine	0.5397	1.115	0.002	0.540
P	300.218	6.0	Nonanoyl carnitine	0.015	1.63	0.499	0.850
P	314.234	5.6	Decanoyl carnitine	0.01	1.56	0.391	0.825
P	330.227	6.6	Keto-decanoylcarnitine	0.032	1.61	0.499	0.850
Bile Acids							
N	405.265	5.6	Dihydroxyoxocholanate	<0.01	0.44	0.078	0.512
N	407.281	6.6	Cholic acid	<0.01	0.34	<0.01	0.340
N	583.312	10.3	Cholic acid glucuronide	<0.01	0.27	< 0.01	0.170

N	583.312	11.5	Cholic acid glucuronide	<0.01	0.23	<0.01	0.170
Amino acids and their metabolites							
N	118.051	12.0	*Threonine	<0.01	0.64	0.685	1.06
N	131.046	15.8	*Asparagine	<0.01	0.76	0.879	1.05
P	132.102	11.3	*Leucine	0.030	0.593	0.061	0.675
N	148.043	14.0	*Methionine	<0.01	0.58	0.061	0.675
P	161.128	23.0	Methyllysine	0.114	1.526	0.002	2.669
N	172.098	6.1	N-Acetylleucine	<0.01	0.65	0.010	0.590
P	175.108	9.3	**N-Acetylorithine isomer	<0.01	0.70	< 0.01	0.566
N	187.072	11.4	* N-Acetylglutamine	<0.01	0.67	< 0.01	0.628
P	221.092	6.8	**5-Hydroxytryptophan isomer	0.06	2.24	0.530	0.952
N	214.028	14.0	Chlorotyrosine	0.04	2.09	< 0.01	2.91
N	216.099	11.8	N-Acetylcitrulline	< 0.01	0.60	< 0.01	0.570
P	219.134	13.7	Carboxyethyllysine	<0.01	0.65	<0.01	0.467
P	247.14	15.0	Carboxyethylarginine	< 0.01	2.23	0.022	0.544
Collagen metabolism							
P	173.092	13.3	Glycylproline	<0.001	0.54	0.820	1.064
P	189.123	13.6	Glycylleucine	<0.001	0.72	0.001	0.370
Vitamins and CoNfactors							
P	132.077	15.4	* Creatine	0.011	0.538	0.018	0.440
P	220.118	9.4	*Pantothenate	<0.01	1.40	< 0.01	0.529
N	375.13	8.1	* Riboflavin	0.013	0.66	0.032	0.500
Microbial Metabolites							
N	153.02	14.0	Dihydroxybenzoate	0.078	1.324	0.884	0.964
N	192.067	6.0	Phenylacetyl glycine	<0.01	1.76	0.277	0.756
N	197.046	9.8	Dihydroxyphenyllactate	0.025	1.43	0.383	0.855

Thus, overall, the number of changes observed as a result of exercise were fewer in previous smaller study of laboratory group (Daskalaki *et al.*, 2015a). While some of the changes were consistent with related previous observations particularly with regard to the impact on several purine metabolites and effects on carnitines. In the current study the level of exercise was more carefully controlled than in the previous study and the subjects were in a narrow age range. The additional measure which was made in the current study was the determination of VO_{2max} for each of the subjects.

OPLS modelling was used to predict VO_{2max} from the metabolic pattern in urine post-exercise. A weakly fitted model was built by using the D2S3 and fourth samples of day 2 (D2S4) and then discarding variables of low importance with VIP values < 1 . There seems to be no standard way to build such models and it is easy to be misled with regard to their robustness when several variables are used. It is quite surprising how easy it is for software to fit a model based on even a few variables when the number of samples is low. Eventually, by reducing the number of variables, it was possible to produce a plot of predicted against measure VO_{2max} based on a single putatively identified as being an oxoaminohexanoic acid (OHA) (Figure 3-11). The correlation of predicted VO_{2max} and measured VO_{2max} against normalised level of OHA gave $R^2 = 0.8589$. The formula for the marker compound matched that of 11 compounds in METLIN database (Scripps, 2016) although there are no MS/MS spectra for any of these compounds in the database. Only seven of these compounds have an amine group which would be required for the retention time to be 13.2min on the HILIC column as observed for the current compound. Three of the isomers occur in the lysine degradation pathway. The marker is an abundant compound in urine and

two main isomers of it occur in urine with the marker compound the later running of the pair of isomers (extracted ion trace Figure 3-12).

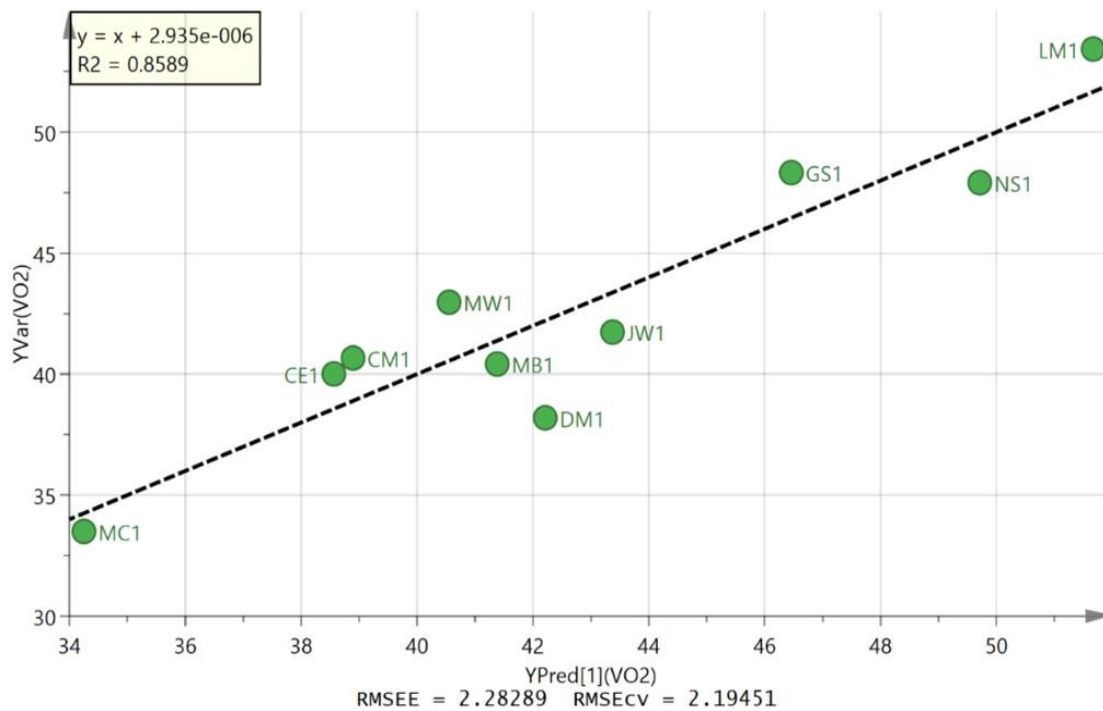


Figure 3-11: Plot of measured against predicted VO2max against normalised levels of OHA.

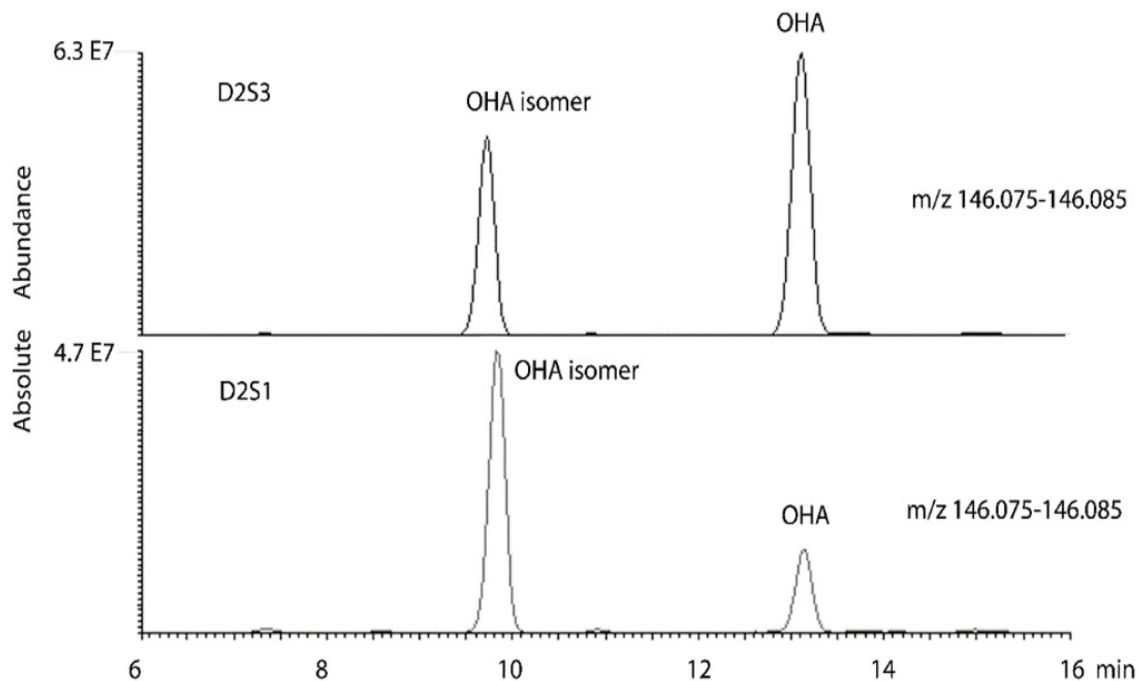


Figure 3-12: Extracted ion trace for OHA isomers in urine comparing a pre- and post-exercise sample for samples D2S1 and D2S3 for a subject with VO2max 53.4.

The MS2 spectrum (Figure 3-13) showed losses of formic acid and water, confirming the presence of a carboxylic acid group followed by loss of a hydroxyl group but not much else. Since it seemed likely that this marker compound was in the lysine degradation pathway, another model was constructed to include all the metabolites present in the samples identified or putatively identified as being in the lysine degradation pathway according to the database search. Although it was possible to fit apparently strong models using several of these variables it was clear from the non-significant CVANOVA scores that using several variables produced over-fitting and the majority of the predictive power belonged to OHA. Table 3-5 shows all the predicted values for VO_{2max} based on a linear plot of the normalised levels for OHA for each individual in each sample collected on day 2. The D2S3 samples have the best predictive power although some of the other data points are predictive and this was generally in the case for the samples that did not have a strong spike in OHA post-exercise and hence are those with lower VO_{2max} values. Thus, clearly, the most important marker of VO_{2max} is the compound putatively identified as OHA. The candidate marker compound was also assessed by using an alternative method of normalisation based on absolute peak areas. It was observed that the OHA isomer remained relatively constant between D2S1 and D2S3 in comparison to OHA. The plot shown in figure 3-14 is plots VO_{2max} against the following ratio:

$$\left(\frac{\text{Area OHA D2S3}}{\text{Area OHA isomer D2S3}} \right) / \left(\frac{\text{Area OHA D2S1}}{\text{Area OHA isomer D2S1}} \right)$$

This simpler treatment produces a plot with R² = 0.654. Although the R² value for this plot is not as good as the peak area normalised to individual metabolic output, this gives some confidence that the observation is not an artefact of the data pre-treatment

which introduces additional smoothing into the data. Thus, OHA shows some promise as a predictor of VO₂max.

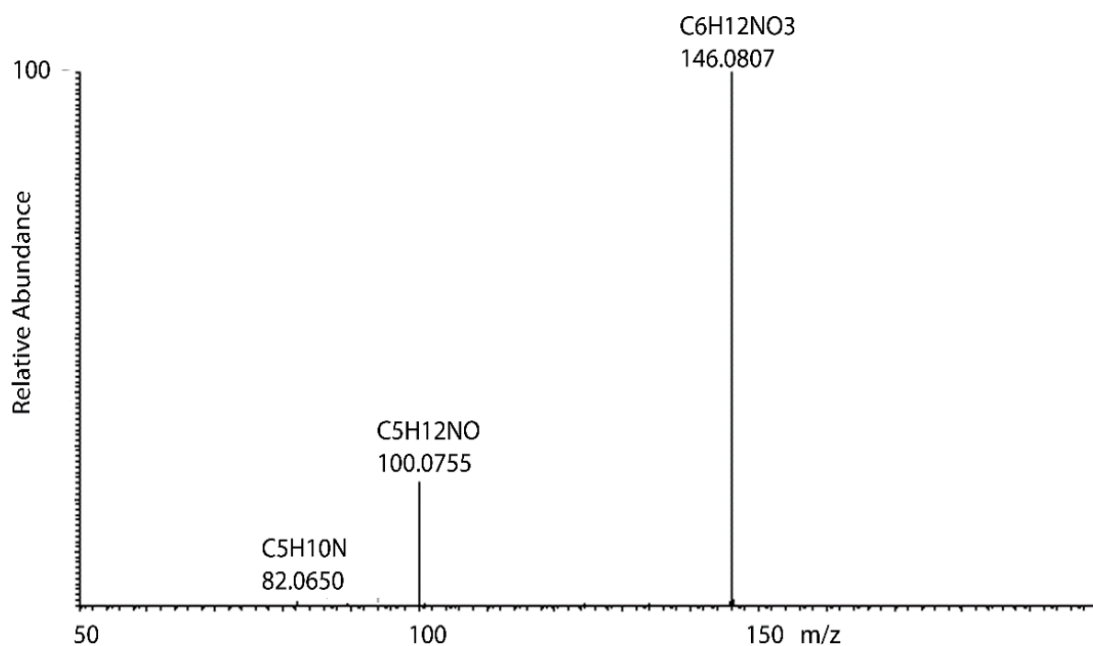


Figure 3-13: MS2 of oxoaminohexanoic acid obtained with a collision energy of 35V.

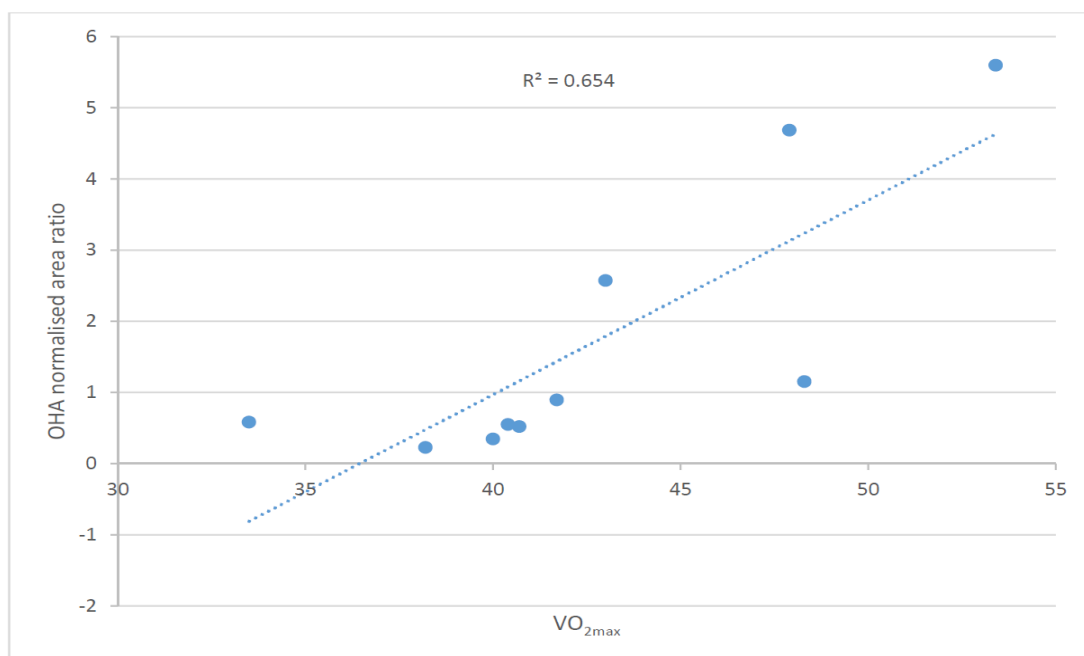


Figure 3-14: Plot of (area OHA D2S3/area OHA isomer D2S3)/(area OHA D2S1/area OHA isomer D2S1).

Table 3-5: Predicted VO_{2max} values for all samples of day-2 based on normalised response for OHA.

Primary ID	Set	OAHA Normalised Level	Measured VO _{2max}	Predicted VO _{2max}
105	CE-D2S3	0.431	40	38.5
65	CM-D2S3	0.464	40.7	38.9
51	DM-D2S3	0.800	38.2	42.2
24	GS-D2S3	1.225	48.3	46.5
91	JW-D2S3	0.917	41.7	43.4
12	LM-D2S3	1.749	53.4	51.7
118	MB-D2S3	0.717	40.4	41.4
78	MC-D2S3	0.000	33.5	34.3
37	MW-D2S3	0.633	43	40.6
128	NS-D2S3	1.554	47.9	49.7
108	CE-D2S1	1.000	40	44.2
68	CM-D2S1	1.069	40.7	44.9
54	DM-D2S1	2.544	38.2	59.6
27	GS-D2S1	1.532	48.3	49.5
94	JW-D2S1	2.152	41.7	55.7
15	LM-D2S1	0.335	53.4	37.6
121	MB-D2S1	1.994	40.4	54.1
81	MC-D2S1	1.989	33.5	54.1
40	MW-D2S1	2.850	43	62.6
133	NS-D2S1	0.399	47.9	38.2
107	CE-D2S2	0.418	40	38.4
67	CM-D2S2	0.812	40.7	42.3
53	DM-D2S2	0.777	38.2	42.0
26	GS-D2S2	0.634	48.3	40.6
93	JW-D2S2	0.318	41.7	37.4
14	LM-D2S2	1.624	53.4	50.4
120	MB-D2S2	1.180	40.4	46.0

Primary ID	Set	OAHA Normalised Level	Measured VO _{2max}	Predicted VO _{2max}
80	MC-D2S2	1.419	33.5	48.4
39	MW-D2S2	0.948	43	43.7
132	NS-D2S2	1.320	47.9	47.4
103	CE-D2S4	1.705	40	51.2
63	CM-D2S4	1.384	40.7	48.0
49	DM-D2S4	0.398	38.2	38.2
22	GS-D2S4	0.867	48.3	42.9
89	JW-D2S4	1.014	41.7	44.4
10	LM-D2S4	0.937	53.4	43.6
116	MB-D2S4	0.706	40.4	41.3
76	MC-D2S4	0.666	33.5	40.9
35	MW-D2S4	0.392	43	38.2
129	NS-D2S4	1.671	47.9	50.9
101	CE-D2S5	1.446	40	48.7
61	CM-D2S5	1.270	40.7	46.9
47	DM-D2S5	0.481	38.2	39.1
20	GS-D2S5	0.743	48.3	41.7
87	JW-D2S5	0.599	41.7	40.2
8	LM-D2S5	0.355	53.4	37.8
114	MB-D2S5	0.403	40.4	38.3
74	MC-D2S5	0.926	33.5	43.5
33	MW-D2S5	0.177	43	36.0
127	NS-D2S5	0.057	47.9	34.8

3.5 Discussion

Collecting samples over a day with no exercise session and over a day where an exercise session was undertaken meant that it was possible to distinguish metabolites which had diurnal variation from those affected by exercise (Figure 3-15). The level of exercise and the age range of the subjects were carefully controlled and this led to fewer metabolic changes which could be ascribed to exercise than were observed in previous pilot study. The samples were run in blocks of 12 samples for each individual with the samples randomised within each block (Table 3-S1). This method of running minimises instrumental drift since the instrument only has to remain stable over each block of 12 samples since the normalisation process for the individual within removes instrumental effects in relation to earlier or later blocks. The bad classification of the samples by PCA in this study (Figure 3-2) was in line with previous results in the pilot study for our group (Daskalaki *et al.*, 2015a) where there was no separation in the PCA model when the raw data normalisation against creatinine was used. In the previous study normalisation against creatinine did not make any difference to the fit of the model and it was concluded as has been observed by others that creatinine normalisation is not always effective (Ryan *et al.*, 2011).

Comparing the compounds responsible for the separation between D2S1 and D2S3, the post-exercise samples have higher levels of the purine metabolites hypoxanthine, guanine, deoxyinosine, inosine and xanthosine. Increases in purine metabolites following exercise have been observed for many years although the focus is usually on hypoxanthine (Dudzinska *et al.*, 2010, Sahlin *et al.*, 1999, Stathis *et al.*, 2006, Zielinski *et al.*, 2013a, Zielinski and Kusy, 2012). In a very recent study conducted by our group, it was observed that the same wider effect on several purine metabolites as is observed

in the current data (Daskalaki *et al.*, 2015a). None of the above purines are significantly changed between D1S1 and D1S3 and uric acid levels decrease between D1S1 and D1S3. Thus the “purine response” obviously requires vigorous physical exercise rather than normal everyday activity to manifest. Methyl adenosine, dimethyl adenosine and dimethyl guanosine all decrease significantly between D1S1 and D1S3 but no significant changes are observed for these metabolites between D2S1 and D2S3. There are other classes of metabolites which typify the response to acute exercise. Nonanoyl carnitine, decanoyl carnitine and ketodecanoyl carnitine all increase between D2S1 and D2S3. In contrast several acylcarnitines are significantly decreased between D1S1 and D1S3. The increase in acyl carnitines between D2S1 and D2S3 may be related to a decreased demand for fatty acids during a short bout of exercise where there is a switch towards glycolysis and in order to maintain ATP levels under conditions of high oxygen demand. Fatty acids are removed from the mitochondria as their carnitine conjugates in order to allow acetyl CoA to enter the Krebs cycle. Pantothenic acid levels have been observed to rise following exercise previously and this is the case in the current study where there is an increase between D2S1 and D2S3 whereas there is a decrease between D1S1 and D1S3. It has been proposed that increased levels of pantothenate might indicate increased requirement for CoA, but it is more likely that this indicates inhibition of CoA biosynthesis which is tightly regulated by pantothenate kinase (PK) activity (Dansie *et al.*, 2014). Acetyl CoA inhibits PK by allosteric binding and an increase in pantothenate indicates a decrease in CoA biosynthesis. Fatty acid oxidation requires an excess of CoA and a decrease in CoA levels would decrease fatty acid oxidation since it is energetically more favourable to rely on oxidation of acetyl CoA generated from glycolysis in the Krebs

cycle. Lactate as the end product of glycolysis increases between D2S1 and D2S3, but there is no change between D1S1 and D1S3 (Table 3-4). Increased lactate indicates that not all the pyruvate produced by glycolysis can be used by the Krebs cycle which mainly produces energy in the form of NADH which has to be oxidised via the terminal respiratory chain to yield ATP and thus requires oxygen. The adrenaline metabolite metanephrine is elevated post-exercise as is methoxyhydroxy phenylethyleneglycol sulfate which is also a metabolite of adrenaline. Increases in adrenaline metabolites post-exercise have been observed previously (Bracken *et al.*, 2009). Gamma-aminobutyric acid (GABA) levels are lower after exercise and the GABA metabolites oxobutanoate and hydroxyl butyrate sulphate are elevated. Dihydroxyphenyl lactate, dihydroxybenzoate and phenacetyl glycine acid are elevated between D2S1 and D2S3 and these are generally regarded as being products of gastrointestinal bacterial action. Elevation of microbial products has previously been reported post-exercise (Daskalaki *et al.*, 2015b, Lustgarten *et al.*, 2014). These metabolites were not changed between D1S1 and D1S3. Testosterone sulphate is elevated between D2S1 and D2S3 which might reflect an increase in testosterone levels post-exercise which has been observed previously and linked to increased anabolic metabolism (Dovio *et al.*, 2010). Similarly the hydrocortisone metabolite tetrahydroaldosterone glucuronide is elevated post-exercise and reflects the fact that hydrocortisone is strongly involved in energy metabolism and it has been proposed that it is directly involved in nitric oxide production (Gatti *et al.*, 2005, Hafezi-Moghadam *et al.*, 2002, Tremblay *et al.*, 2004). There are three bile acids which are important in the separation between D2S1 and D2S3. Two of the bile acids are glucuronide conjugates and such conjugates are used to remove excess bile acids from the body. In the current case the levels of the

conjugates fall thus indicating and possibly an increased demand for bile acids to facilitate uptake of lipids from the gut since post exercise there is an increased requirement for fatty acids. However, the same pattern is observed in the D1S1 and D1S3 comparison thus the demand for bile acids seems to be at its lowest in the early morning since none of the other time points in the S1 differ significantly from time points the S3 in both day 1 and day 2. Several amino acids and amino acid derivatives are lowered between D2S1 and D2S3 but these changes are largely the same between D1S1 and D1S3. Exceptions include an elevation in an isomer of 5-hydroxytryptophan, possibly 3-hydroxy tryptophan which was found to be elevated in previous study (Daskalaki *et al.*, 2015a), and carboxyethyl arginine (CEA). CEA is an advanced glycation end product that has been observed previously to occur in human urine and plasma (Balderas *et al.*, 2013, Lai *et al.*, 2010). This compound forms by reaction between arginine and methylglyoxal which is formed as a side product of glycolysis and it has been shown that CEA is an inhibitor of nitric oxide synthase (Lai *et al.*, 2010) in which case its presence in the body where vasodilation is required may not be desirable. All these changes in metabolites are shown in diagrammatic biochemistry summary (Figure 3-15).

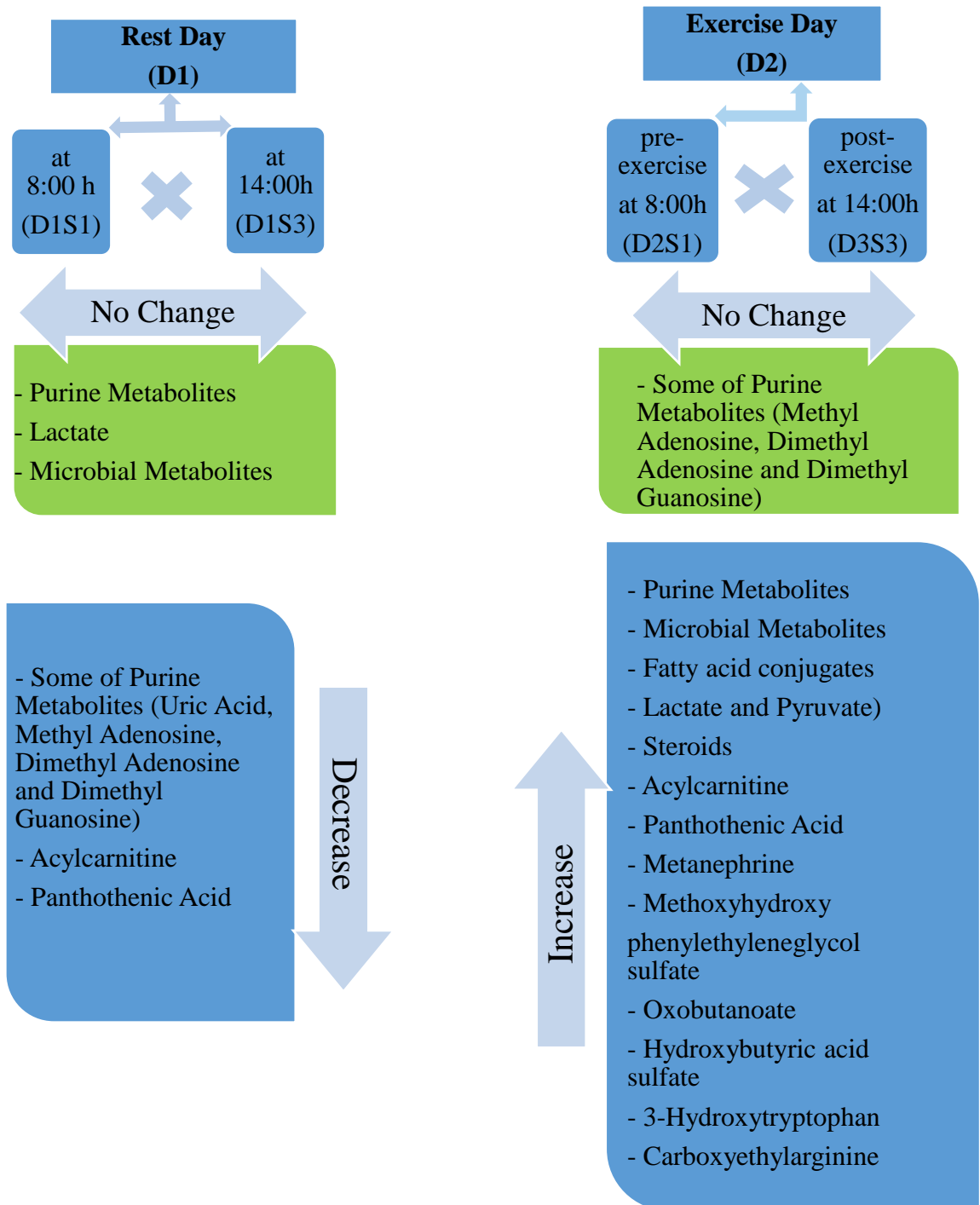


Figure 3- 15: a diagrammatic model of the biochemistry for metabolites differing between D2S1 and D2S3 in comparison with D1S1 and D1S3

3.6 Conclusion

The current study further validates our approach of normalising longitudinally collected urine samples over time and then normalising each individual to their total output for each metabolite over that time. This approach allowed separation of pre- and post-exercise samples based on PCA analysis whereas without using this approach the separation was not possible.

Although many of the changes which can be seen in the current study were observed in related previous study (Daskalaki *et al.*, 2015a), there were also more new changes in microbial metabolites, amino acids metabolites, acyl carnitines, and steroids. The current results clearly revealed the impact of exercise on established markers for exercise such as hypoxanthine and inosine and, in addition, many other compounds were affected by exercise. In order to differentiate metabolites that vary throughout the day and those affected by exercise the metabolites which varied during the non-exercise day were evaluated. Some of these were the same as the metabolites changing on the non-exercise day such as bile acid metabolites but there were many metabolites which were affected only by exercise. The observations of metabolic marker which may be correlated with VO_{2max} was of great interest in present study. Thus, a potential predictive marker for VO_{2max} was identified, but further trials will be required to determine whether or not this is an artefact of the large number of metabolites available as variables. The approach of collecting longitudinal urine samples is simple and non-invasive and the observed output gives a real sense of metabolism in action and could have a role in assessing overall fitness and diagnosing underlying disease which could be related to metabolic differences.

CHAPTER 4

METABOLOMIC PROFILING OF POST-MORTEM BRAIN IN ORDER DETERMINE DIAGNOSTIC MARKERS CLASSIFYING DIFFERENT TYPES OF MENTAL ILLNESS

Abstract

Metabolomic profiling was carried out on 53 post-mortem brain samples from subjects diagnosed with schizophrenia (S), depression (D), bipolar (B) disorder, diabetes (DI) and controls (C). Chromatography on a ZICpHILIC column was used with detection by Orbitrap mass spectrometry. Data extraction was carried out with m/z Mine 2.14 with metabolite searching against an in house metabolites database. There was no clear discrimination between the controls and the SDB samples on the basis of a PCA model of 755 identified or putatively identified metabolites. OPLSDA produced clear separation between 17 of the controls and 19 of the SDB samples (R^2 (cum) 0.976, Q^2 (cum) 0.671, p-value of the cross-validated ANOVA score 0.0024). The most important metabolites producing discrimination were the lipophilic amino acids leucine/isoleucine, proline, methionine, phenylalanine, and tyrosine; the neurotransmitters GABA and NAAG and sugar metabolites sorbitol, gluconic acid, xylitol, ribitol, arabinotol, and erythritol. Eight samples from diabetic brains were analysed, six of which grouped with the SDB samples without compromising the model (R^2 (cum) 0.850, Q^2 (cum) 0.534, p-value for cross-validated ANOVA score 0.00087). There appears on the basis of this small sample set to be some commonality between metabolic perturbations resulting from diabetes and from SDB.

4.1 Introduction

Mental illness, most commonly schizophrenia (S), depression (D), and bipolar (B) disorder (SDB) is common: S has a European prevalence of 0.2–2.6%, D 3.1–10.1%, and B disorder 0.2–1.1% (Wittchen and Jacobi, 2005). These conditions are a major burden on the health-care systems and on the relatives of affected people. Clinically, such illnesses are heterogeneous and present with psychosis or mood state features that vary over time and across individuals. Thus, it would be of great value to have an objective means to assist in diagnosis and categorisation of such illnesses and also give an insight into the best way to manage them (Weickert *et al.*, 2013). Much diagnosis of mental illness remains subjective due to complex and poorly defined mechanisms underlying these diseases; there are no biomarkers and mental illness might be better viewed as a continuum rather than using absolute labelling (Corrigan, 2007). The significance of low-molecular-weight metabolites in driving or reflecting the aetiology of psychiatric disease has been researched for many years using serum samples that are a pragmatic choice for diagnostic testing and, additionally, brain tissue to investigate the central pathologies (Pickard, 2015). In the past 10 years, MS-based metabolomics has evolved as a method for profiling a wide range of low-molecular-weight metabolites (Gika *et al.*, 2014, Zhang and Watson, 2015). Metabolomics is a natural fit with metabolite profiling in mental illness where, for many years, targeted analysis was carried out in order to profile, for instance, biogenic amines in order to determine whether or not abnormalities in their levels might be causative (Burchett and Hicks, 2006). There have been several studies which have carried out metabolomic profiling in mental illness (Koike *et al.*, 2014, Liu *et al.*, 2015, Kaddurah-Daouk and

Krishnan, 2009, Yang *et al.*, 2013, Yao *et al.*, 2010, Orešič *et al.*, 2011, He *et al.*, 2012), but these have not been as extensive as those into other diseases such as cancer.

There have been no untargeted metabolomics studies of human post-mortem brain samples although there was a study which examined disturbed glucose metabolism in post-mortem brains from psychotic patients (Regenold *et al.*, 2004). In the current study, the availability of a unique library of post-mortem brain samples with extensive associated medical information allowed to investigate whether or not these samples might reveal any underlying pathology which could be related to metabolic differences.

4.1.1 Aims of Study

The purpose of this study was to try to better understand disease pathology in mental illness and thus the ideal outcome would be a list of related metabolites corresponding to the disease state in order to develop a hypothesis. Thus, the established LC-MS-based metabolomic profiling methods (Zhang *et al.*, 2013, Zhang *et al.*, 2014) will be applied to determine if it was possible to individually classify healthy C, S, D and B brains. The observation of ‘metabolic syndrome’-like features in those diagnosed with mental illness (Newcomer, 2007) prompted us to determine whether or not there was an overlap between metabolic perturbations in mental illness and diabetes. If such a link between mental illness and diabetes could be established then this might give some rationale for the evaluation of medicines used in the treatment of diabetes in the treatment of mental illness.

4.2 Materials and Methods

4.2.1 Chemicals and Solvents

HPLC-grade ACN was obtained from Fisher Scientific, UK. Ammonium carbonate, ammonium hydroxide solution (28–30%), acetic anhydride, pyridine, and methanol were purchased from Sigma–Aldrich, UK. HPLC grade water was produced by a Direct-Q 3 Ultrapure Water System from Millipore, UK. The mixtures of metabolite authentic standards were prepared from standards obtained from Sigma–Aldrich, UK, as previously described in standard preparation section (2-3).

4.2.2 Post-Mortem Brain Samples:

Post-mortem brain samples were obtained from the Sudden Death Bank collection held in the MRC Edinburgh Brain and Tissue Banks. These samples were stored at -80°C for longer term storage. Psychiatric diagnosis annotations for each sample were made by detailed study of donor case notes by qualified psychiatrists. Full ethics permission has been granted to the Banks for collection of samples and distribution to approved researchers (LREC 2003/8/37). The University of Strathclyde Ethics Committee also approved the local study of this material (UEC101123). Details of the brain samples are given in Table 4-S1 in the Appendix-I. The information regarding the brain samples is summarised in Table 4-1.

Table 4-1: Summary information for the different groups of brain samples.

Group	Number (M+F)	Male (M)	Age range	Mean age \pm RSD	Female (F)	Age range	Mean age \pm RSD
Control	21	18	26–74	47.4 \pm 29.5	3	42–60	50.7 \pm 17.8
Schizophrenic	11	10	25–69	44.4 \pm 34.7	1	40	–
Bipolar	6	1	48	–	5	39–57	45.6 \pm 16.2
Depressive	7	4	24–74	47.5 \pm 49.1	3	20–57	60.3 \pm 33.7
Diabetic	8	8	20–69	44.9 \pm 35.2	0	–	–

4.2.3 Sample Extraction

The brain samples were stored at 4^oC for immediate use or at -80^oC for longer term storage. For extraction, samples of brain tissue were thawed and then 50 mg was homogenised in ice cold methanol/water (1:1, 1.5 ml) using a handheld Lab Gen 7B homogeniser. The samples were then centrifuged at 16,000g, 15 min 4^oC to remove any insoluble material when the supernatant was removed and the pellet reserved for further extraction to remove lipids. Lipids were extracted from the pellet with chloroform/methanol (3:1, 1.6 ml). The methanol/water extract was dried under a stream of nitrogen at 37^oC and re-dissolved in 200 μ l ACN/water (80:20) and then analysed by ZICHILIC and ZICpHILIC chromatography. The chloroform/methanol extract was dried under a stream of nitrogen at 37^oC and re-dissolved in either methanol/water (1:1, 200 μ l) prior to chromatography on a C18 column.

4.2.4 HILIC–HRMS Analysis

Sample analysis was carried out on an Accela 600 HPLC system combined with an Exactive (Orbitrap) mass spectrometer (Thermo Fisher Scientific, UK). An aliquot of each sample solution (10 µl) was injected onto a ZIC-pHILIC column (150 × 4.6 mm, 5µm; HiChrom, Reading UK) with mobile phase A: 20 mM ammonium carbonate in HPLC grade water (pH 9.2), and B: HPLC grade ACN. The LC and the MS conditions were as described previously in the HPLC conditions, section 2-5. Samples were submitted in random order for LC-MS analysis, and pooled quality control samples were injected at the beginning, in the middle and at the end of the experiment to monitor the stability of the instrumentation. Four authentic stock standard mixtures for 220 compounds, see section 2-3, were run in order to calibrate the column. Due to the chromatography of lipids are only weakly retained on the ZICpHILIC column and there is no separation of isomeric species, further analysis of the polar extract and of the lipophilic extracts were carried out on a ZICHILIC column (150 × 4.6 mm, 5 µm), ACE C18 column (150 × 3 mm, 3 µm), and an ACE silica gel column according to previously described methods (*Zhang et al., 2012c, Zheng et al., 2010*).

4.2.5 Analysis of Sugar Acids and Polyols by GC-MS

The individual standards for the polyols (100µg) were treated with acetic anhydride/pyridine (1:1, 100µl) for 30 min at 70°C. The reagent was removed under a stream of nitrogen and the sample was re-dissolved in 1ml of ethyl acetate. The individual standards for the polyol acids were treated with methanol containing 1% HCl for 30 min at 70°C, the reagent was removed under a stream of nitrogen and the

sample was then treated as for the polyols. Brain tissue (200 mg) was extracted with ACN/water (1:1, 1 ml) containing 2µg/ml of pinitol internal standard, centrifuged and the supernatant was removed and evaporated to dryness with a stream of nitrogen at 70°C and treated as for the polyol acids except that the residue was re-dissolved in 0.2 ml of ethyl acetate. GC-MS analysis was carried out on a DSQ GC-MS system (Thermo Fisher Scientific, UK) fitted with a GL Sciences Inert Cap 1 MS column from Hichrom, Reading, UK (30 m × 0.25 mm × 0.25 µm film). The oven was programmed from 100°C to 320°C at 5°C/min. The MS was operated in EI mode at 70 eV. For quantification of the sugars in brains selected, ion monitoring was carried out for ions at m/z 217, 200, 187, 145, 142, and 140, which are typical fragments of alditol acetates (**Ruiz-Matute *et al.*, 2011**).

4.2.6 Data Extraction and Metabolite Identification

MZMine 2.14 (Pluskal *et al.*, 2010) was used for peak extraction and alignment, as previously described in data extraction and processing methods (section 2-6). Putative identification of metabolites was also conducted in MZMine by searching the accurate mass against in-house database or other data bases as mentioned above, section 2-6. Background peaks present in the blank were removed in MZmine before transferring the data to an Excel file. Manual editing of the data was carried out in order to remove idiosyncratic peaks such as metabolites identified as drugs which were presumably from patient treatments and also nicotine metabolites which were particularly abundant in the brains of schizophrenic patients because of their well-established tendency to smoke much more than the general population (Dalack *et al.*, 1998) and ethyl sulphate which is from alcohol metabolism. The GC-MS data were extracted by

using Sieve 1.3 (ThermoFisher Scientific UK), and the ions corresponding to the RT of the sugar standards were extracted in order to build the OPLS-DA model.

4.2.7 Univariate and Multivariate Analysis

All data processing, including data visualisation, biomarker identification, diagnostics, and validation was implemented using SIMCA software v.14 (Umetrics AB, Umeå, Sweden). Prior to univariate and multivariate analysis, data were Pareto scaled where the responses for each variable are centred by subtracting its mean value and then dividing by the square root of its standard deviation (Bartel *et al.*, 2013, Yang *et al.*, 2015). Univariate comparisons were carried out in Excel. All subsequent metabolite responses, paired t-test and fold changes (ratio) were conducted on a new data set. Multivariate analysis were applied by SIMCA-P version 14.0 (Umetrics, Sweden) for data modelling in order to build an unsupervised and supervised models. PCA was used to provide as an unsupervised model in order to explore how variables clustered regardless Y class (Worley and Powers, 2013). OPLS provides a supervised model that can predict Y from X and can separate variation in X that correlates to Y (predictive) and variation in X that is uncorrelated to Y (orthogonal/systemic). OPLS-DA is a discriminant analysis based on OPLS and employed to examine the difference between groups while neglecting the systemic variation (Kirwan *et al.*, 2012). The p-values of the biomarkers were evaluated for their significance applying the false discovery rate statistic (Benjamini and Hochberg, 1995). Variable importance in the projection was employed in order to indicate the contribution of each variable in the in a given model compared to the rest of variables, the average VIP is equal to 1, based

on that a variable larger than 1 has more contribution in explaining y than the average (Chong and Jun, 2005).

4.2.8 Diagnostics and Validation of Models

R^2 and Q^2 are diagnostic tools for supervised and unsupervised models; R^2 represents the percentage of variation explained by the model (the goodness of fit), Q^2 indicates the predictive ability of the model, a large discrepancy between R^2 and Q^2 indicates overfitting of the model (Westerhuis *et al.*, 2008). A permutations test can be applied to evaluate supervised models whether the specific grouping of the observations in the two designated classes is significantly better than any other random grouping in two arbitrary classes. In SIMCA-P, this test indicates the refitted models when all the Q^2 values are lower than the original Q^2 value (Wheelock and Wheelock, 2013). The criteria for validity for OPLSDA models tested via cross-validation are that all blue Q^2 -values to the left are lower than the original points to the right or the blue regression line of the Q^2 -points intersects the vertical axis (on the left) at, or below zero. The R^2 values always show some degree of optimism (Triba *et al.*, 2015). However, when all green R^2 -values to the left are lower than the original point to the right, this is also an indication for the validity of the original model although this is not essential for the model to be valid. Model validity is also assessed using cross-validated ANOVA (CV-ANOVA) which corresponds to H^0 hypothesis of equal cross-validated predictive residuals of the supervised model in comparison with the variation around the mean (Wheelock and Wheelock, 2013, Eriksson *et al.*, 2008).

4.3 Results

4.3.1 The Effect of the HPLC Column Used on the Results

The data produced from the analysis of the polar extracts on the ZICHILIC column (Figure 4.S1) were less satisfactory for producing separation in the sample sets than those produced on ZICpHILIC. There were similar trends in some of the metabolites but the clear-cut differences described below were not observed. This again supports the choice of ZICpHILIC as the best method for analysis of polar metabolites in metabolomics screens (Zhang *et al.*, 2014). The ZICHILIC mobile phase produces a higher background which includes abundant sodium formate cluster ions and thus ion-suppression is potentially more of a problem. In addition, the chromatographic peaks for many metabolites are wider than on ZICpHILIC and the retention times from run to run are less stable which produces a greater challenge for the peak extraction software. This may be due in part to the fact that the initial methanol/water extraction also extracted many of the more polar lipids. The chromatography of lipids on the ZICpHILIC column is satisfactory but they are only weakly retained on this column so there is no separation of isomeric species.

4.3.2 Comparison of Control and Schizophrenic/Depressive/Bipolar/Diabetic Brains Using PCA

Metabolites were identified to MSI levels 2 or 1 (Sumner *et al.*, 2007) according to either exact mass (< 3 ppm deviation) or exact mass plus retention time matching to a standard (Table 2-S1). As a result of data filtering and univariate analysis, 755 metabolites from positive and negative ion modes were combined and used to build multivariate models. The samples set was selected by our collaborators at the sudden death brain and tissue bank to give us the best samples set available from samples in storage for making a comparison between controls, mental illness, and diabetes. Due to the uncontrolled factors are highly variable in both control and affected samples, the expected result might be that variation in the data would preclude statistical separation unless the disease signature was very strong. In order to obtain a reasonable sample size, S, D, B and DI samples were treated as one group to compare against controls. Comparison of the data from SDB and DI samples with controls (C) using PCA did not yield a clear separation of these diagnostic categories (Figure 4-1). In order to rule out variation in level of technical precision across the 55 h required to complete the analysis, a pooled sample: (P1–6) was prepared by combining $5 \times 40\mu\text{l}$ of extract randomly selected from each sample type. Replicates were run as follows: P1 and 2 near the beginning of the sequence after running two blanks and four standard mixtures, P3 after 20 h, P5 after 39 h, P4 and 6 at the end of the run after 55 h. As can be seen in Figure 4-1, the pooled samples all lie towards the centre of the PCA plot and individual sample points are close to each other. This indicates that there is only a small amount of instrumental drift and thus the results reflect biological, rather than technical, differences.

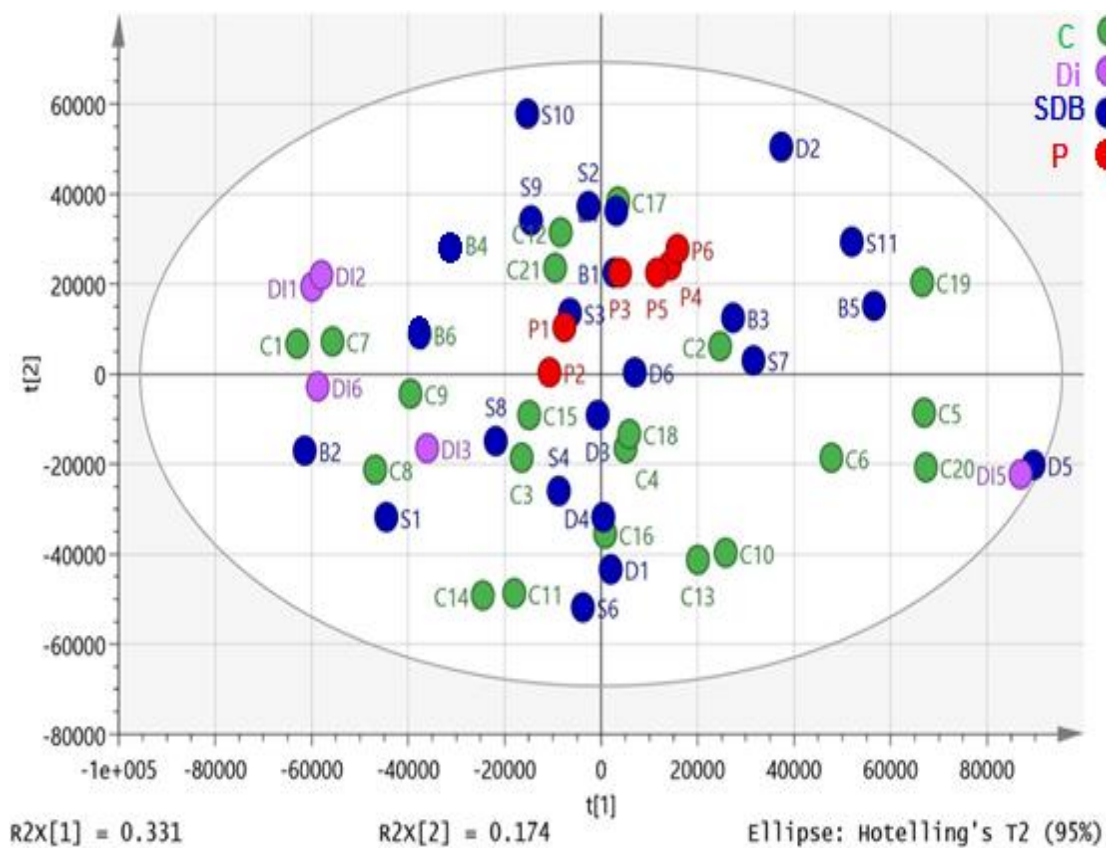


Figure 4-1: PCA plot for control, SDB and DI samples (R2X cum 0.61, Q2 (cum) 0.464, and three components) based on 755 metabolites from positive and negative ion modes. Three of the DI samples (Di4, 7 and 8) lay outside of the ellipse and were omitted from the mod. P = pooled sample used to check instrument stability over time.

4.3.3 Comparison of SDB and SDBDI Samples against Controls Using OPLSDA

When the DI samples were omitted to compare between SDB and C groups, it was found that 36 of the 45 available SDB and control samples (see footnote to Table 4-S1) could be combined where 19 SDB samples were compared against 17 control samples to produce a strong OPLS-DA model (R^2 (cum) 0.976, Q^2 (cum) 0.671) explaining 96.7% of the variation in the samples with six components (Figure 4-2). $Q^2 > 0.5$ is generally accepted as being indicative of a robust model and the model gave a permutations plot where all the permuted Q^2 values on the left are lower than the points on the right (Figure 4-3) and the line plot intercepts the Y-axis below 0 (Westerhuis *et al.*, 2008, Wheelock and Wheelock, 2013, Triba *et al.*, 2015). This preliminary model based on 755 metabolites was used to inform the selection of the samples for univariate statistical comparison by excluding eight samples that did not fit the model, four controls and four SDB samples. Despite variations arising from complex medical histories, length of sample storage and exact cause of death there appeared to be a strong metabolic signature associated with mental illness overriding these confounding factors which apply to both control and affected samples. Thus, Table 4-2 shows the univariate statistical comparisons for the metabolites with VIP scores > 1 in the preliminary OPLSDA model. All of which are significantly different according to a two-tailed t-test and FDR statistics, application of the Benjamini–Hochberg procedure with a Q value of 0.1 (Benjamini and Hochberg, 1995), based on 755 metabolites indicate all P values < 0.05 were significant. A complete list of significantly different metabolites based on univariate comparison of the 17 controls and 19 SDB samples is given in Table 4-2.

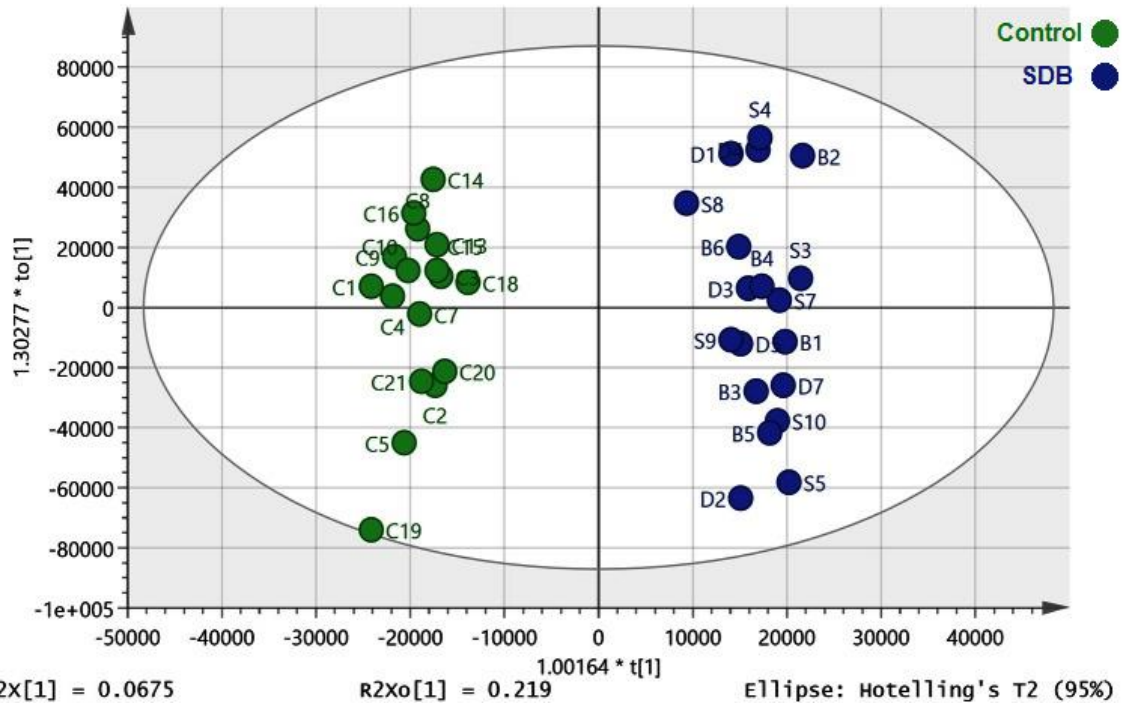


Figure 4-2: OPLS-DA model (R^2 (cum) 0.976, Q^2 (cum) 0.671 and Six components) of control ($n = 17$) compared to SDB ($n = 19$) brain samples based on 755 metabolites from positive and negative ion modes

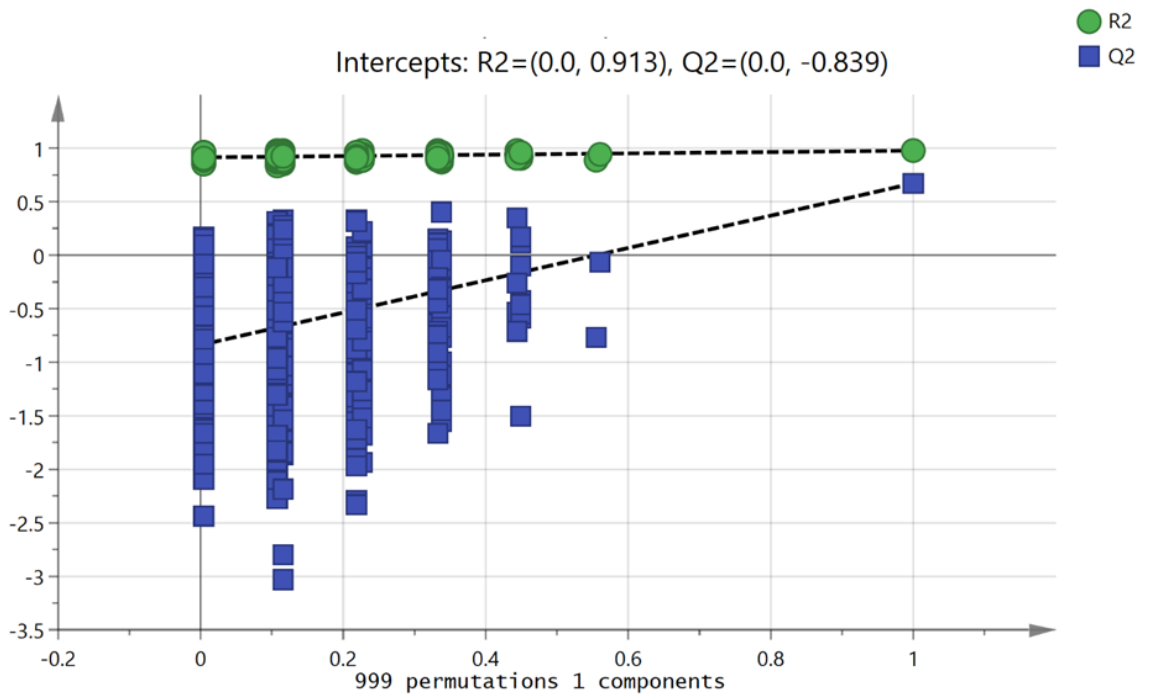


Figure 4-3: Permutation plot for the OPLS-DA model compared to control and SDB brain samples based on 755 metabolites from positive and negative ion modes as shown in Figure 4-2.

Table 4-2: Metabolites with high impact on the LOPS-DA model separating control (17) from SDB (19) samples. * Matches retention time of standard. ** Retention time does not match that of the standard. Application of the Benjamini–Hochberg procedure with a *Q* value of 0.1 indicates that the critical threshold for a regarding a *P* value as being significant is 0.05. *N*=negative ion and *P* = positive ion.

m/z	Rt min.	Metabolite	VIP	P value	Ratio SDB/C
N130.087	11.2	*Leucine/isoleucine	8.3	0.0041	1.34
N 96.9698	13.6	** Orthophosphate (carbonic acid adduct of chloride)	7.5	0.0050	1.17
N116.072	12.9	*Valine	5.1	0.0008	1.36
P 116.071	13.2	*Proline	4.2	0.0021	1.34
N 135.03	10.6	**Threonic acid isomer	4.3	0.0656	1.09
N164.072	10.4	*Phenylalanine	4.0	0.0050	1.31
N102.056	15.9	* 4-Aminobutanoate (GABA)	3.2	0.0050	0.85
N88.0404	15.2	*Sarcosine	3.1	0.0730	1.12
N118.051	14.8	*Homoserine	3.1	0.0140	1.51
N267.074	11.3	*Inosine	3.0	0.0340	0.81
N148.044	11.8	*Methionine	2.8	0.0038	1.30
N181.072	14.3	*Sorbitol/mannitol/iditol/dulcitol	2.6	0.0022	1.99
P 258.11	14.9	*sn-glycero-3-Phosphocholine	2.2	0.0415	1.61
N273.039	15.7	Deoxy sedoheptulose phosphate	1.9	0.0020	0.59
N180.067	13.4	*Tyrosine	1.7	0.0170	1.23
N121.051	12.1	*Erythritol/threitol	1.5	0.0011	1.57
N241.012	17.4	D-myo-Inositol 1,2-cyclic phosphate	1.3	0.0060	0.58
N239.115	16.6	**Homocarnosine isomer (anserine)	1.4	0.0037	0.62
N303.084	17.2	*N-Acetyl-aspartyl-glutamate	1.3	0.0327	0.53
N203.083	12.0	*Tryptophan	1.3	0.0250	1.21
N195.051	14.4	*Gluconic acid	1.3	0.0011	2.20
N215.033	13.7	Hexose (chloride adduct)	1.1	0.0019	2.19
N209.067	14.4	*Sedoheptulose	1.0	0.0006	1.74
P 146.092	15.6	4-Guanidinobutanoate	1.0	0.00021	0.71

4.3.4 SDB Samples Show Differences in Branched Amino Acid, Neurotransmitter and Sugar Metabolism Compared With Controls

Leucine/isoleucine have the highest VIP (8.1) this a very strong variable along with valine which has a VIP of 5.1. Thus, branched chain amino acids are highly correlated in the brains of SDB subjects and are also present in significantly higher levels than in the controls. The other neutral lipophilic amino acids such as proline, phenylalanine, methionine, tyrosine, and tryptophan also have high VIP values of 4.2, 4.0, 2.8, 1.7, and 1.3, respectively. These amino acids are elevated in SDB brains and are important in the model. The important metabolites that are significantly lower in the SDB subjects than in the controls include GABA, its metabolite guanidino amino butyric acid, and the neuromodulator NAAG. In addition, there are higher levels of sugar metabolites, putatively identified according to the LC-MS analysis as sorbitol, gluconic acid, and erythritol, in the SDB samples (Table 4-2).

4.3.5 The Effect of Age on Metabolite Profiles of Brain Tissue

The brains were from subjects with a wide age range and the mean age of the control group at death was 45.9 and mean age for the SDB group was 46.4. An OPLS correlation (R^2X (cum) 0.706, R^2Y (cum) 0.979, Q^2 (cum) 0.476)) gave a very good correlation between age and metabolites (Figure 4-4) and there was no overlap between the metabolites used to discriminate the control and SDB brains and those which discriminated age (Table 4-3). The major changes with age were related to decreases in unsaturated fatty acids in the brain such as eicosatetraenoic, docosahexaenoic, and linoleic acid and increases in glycerol metabolites such as phosphoethanolamine and phosphocholine.

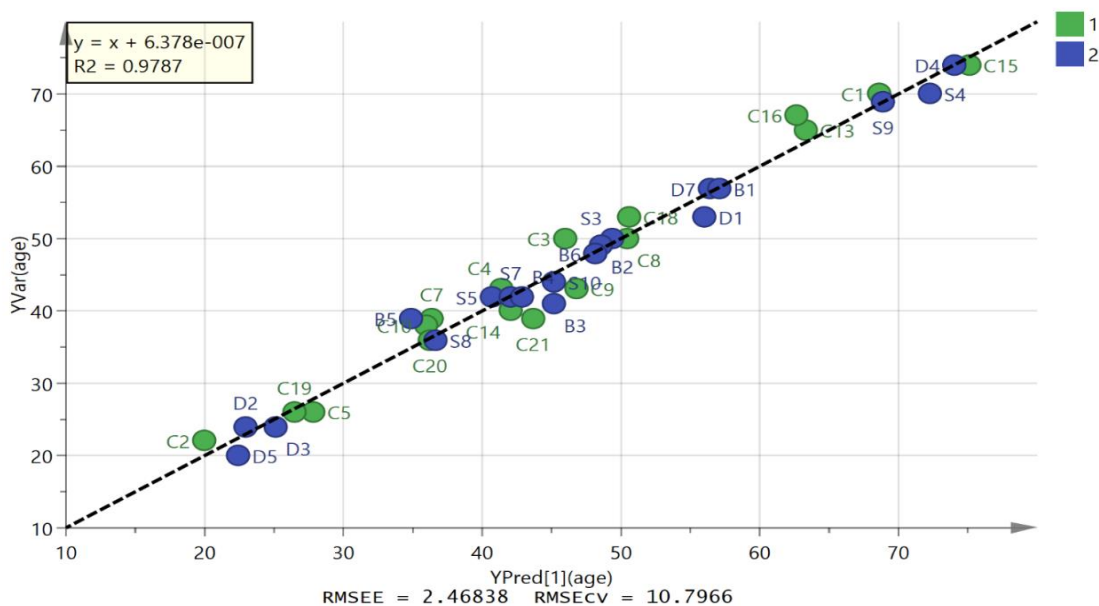


Figure 4-4: OPLS correlation of brain metabolite profiles to the age of the subjects (R2X (cum) 0.706), R2Y (cum) 0.979, Q2 (cum) 0.476).

Table 4-3: Most significant metabolite changes with the age of brain tissue.

m/z	RT min	Metabolite	P corr	VIP
N303.234	3.9	[FA(20:4)] 5Z,8Z,11Z,14Z-eicosatetraenoic	-0.47	10.98
N91.04	10.6	Glycerol	-0.55	8.69
N281.249	4	[FA (18:0)] 9Z-octadecenoic acid	-0.45	7.8
N327.234	3.9	Docosahexaenoic acid	-0.32	6.99
N255.233	4	Hexadecanoic acid	-0.37	6.16
N96.9698	13.6	Orthophosphate	0.38	5.43
N128.035	10.6	L-1-Pyrroline-3-hydroxy-5-carboxylate	-0.51	5.4
P116.071	13.2	L-Proline	-0.41	4.47
N253.218	4	(9Z)-Hexadecenoic acid	-0.44	3.77
N279.233	4	Linoleate	-0.41	2.66
N114.056	13.2	L-Proline	-0.36	2.05
P258.11	14.9	sn-glycero-3-Phosphocholine	0.38	2.02
N111.02	8.8	Uracil	-0.35	1.9
N227.202	4.1	Tetradecanoic acid	-0.37	1.89
N214.049	16	sn-glycero-3-Phosphoethanolamine	0.49	1.81
N175.025	14.6	Ascorbate	0.35	1.56
N180.067	13.4	L-Tyrosine	-0.34	1.39
P178.072	10.5	6-methyl-H2-pterin	-0.54	1.12
N308.099	13.8	N-Acetylneuraminatate	0.37	0.97
N165.041	13.1	L-Arabinonate	-0.48	0.97
N309.281	3.9	[FA (20:0)] 11Z-eicosenoic acid	-0.45	0.8

4.3.6 Inclusion of Diabetic Brains in the OPLSDA Model

There were eight diabetes samples in the set of brain samples and these were subsequently added to the data set used to build the OPLSDA model described in Figure 4-5. Two of the diabetic samples (DI-7 and DI-8) were extreme outliers and were excluded from the initial PCA plot (Figure 4-1) since they were outside of the ellipse. They were also excluded from the combined OPLSDA model along with one of the SDB samples (S5) which was excluded since it did not fit into the new OPLSDA model. Six of the diabetic samples could be classified with the SDB samples (Figure 4-5), R^2 (cum) 0.850, Q^2 (cum) 0.534 and p-value for cross-validated ANOVA score 0.00087, to increase the significance of the ANOVA score. The large decrease in the CV-ANOVA score implies considerable strengthening of the model since the score can be used as a guide to the optimal fitting of a model (Wheelock and Wheelock, 2013). The permutations plot is shown in Figure 4-6 indicates a strong OPLS-DA model to compare between control and SDB-DI brain samples based on 755 metabolites. The addition of the diabetic samples to the model produced some change in the VIP values but basically most of the discriminating metabolites are the same (Table 4-2) which is perhaps not surprising since the model is strengthened by addition of these samples. However, when the univariate comparisons are examined most of the metabolites with high VIP values in the model did not have significant p-values when the DI samples in the model are compared with controls.

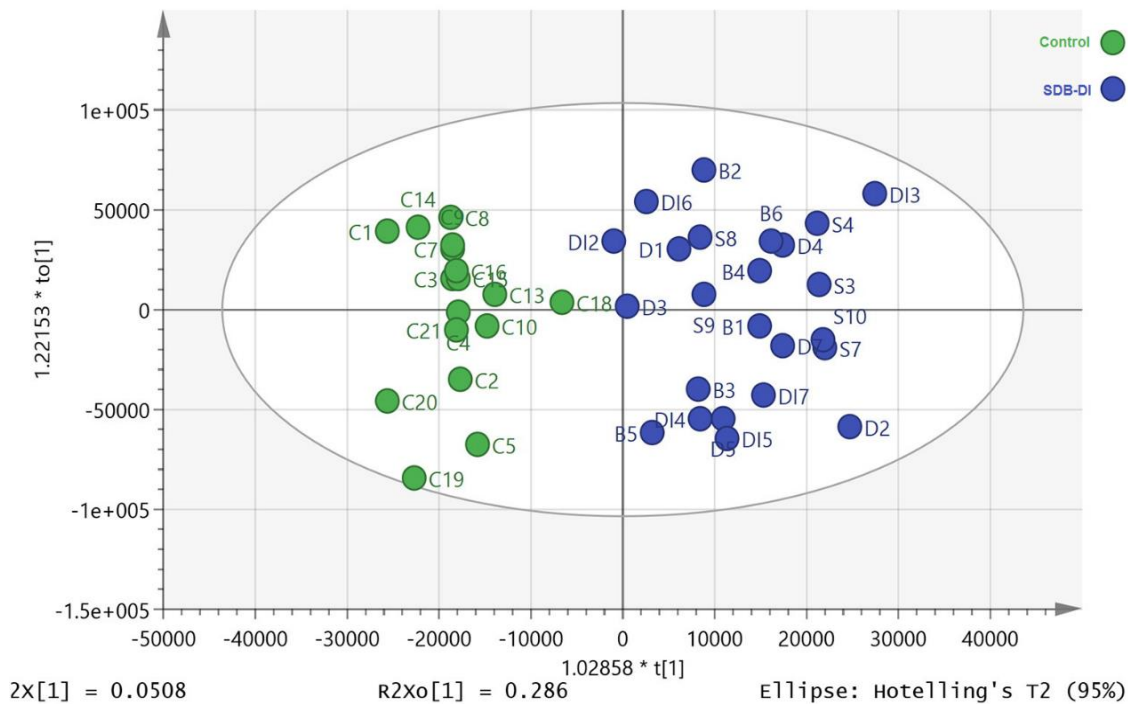


Figure 4-5: OPLS-DA model (R^2 (cum) 0.850, Q^2 (cum) 0.534, four components) including six of the DI samples. Green control and blue SDB + DI brain samples based on 755 metabolites from positive and negative ion modes.

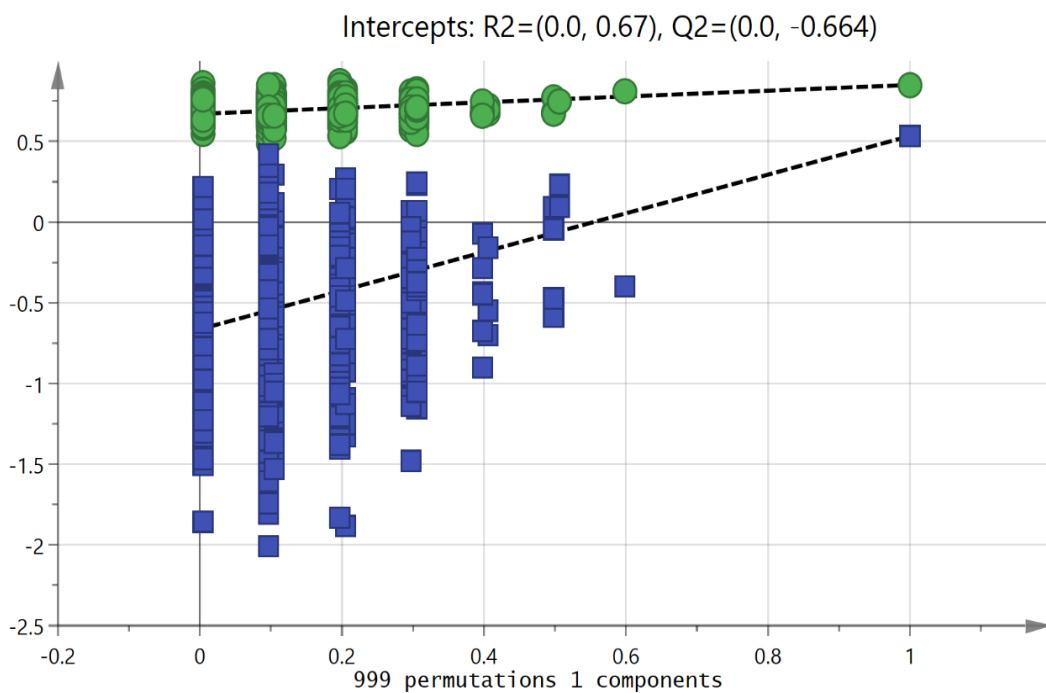


Figure 4-6: Permutations plot for the OPLS-DA model compared to control and SDB-DI brain samples based on 755 metabolites from positive and negative ion modes shown in figure 4-5.

Thus, the similarities between diabetic and the SDB brains compared with controls lie in the covariance of the set of important marker compounds shown in Table 4-4 rather than in the absolute levels. Leaving the DI samples out of the model and using them as a prediction set resulted in four of the samples being classified as SDB samples while two were unclassified, but borderline to the SDB class.

Table 4-4: Metabolites with high impact on the model separating controls from SDB brains combined with diabetic brains. * Matches retention time of standard. ** Retention time does not match that of the standard. N= negative ion and P =positive ion.

m/z	RT min	Metabolite	VIP value
N96.9698	13.6	**Orthophosphate (chloride carbonic acid adduct)	8.4
N130.087	11.2	*L-Leucine/isoleucine	7.2
N174.041	15	*N-Acetyl-L-aspartate	4.9
N116.072	12.9	*L-Valine	4.6
N164.072	10.4	*L-Phenylalanine	3.9
N102.056	15.9	*4-Aminobutanoate	3.1
N118.051	14.8	*L-Threonine	2.8
N181.072	14.3	*D-Sorbitol	2.7
N267.074	11.3	*Inosine	2.6
N114.056	13.2	*L-Proline	2.5
N148.044	11.8	*L-Methionine	2.4
P204.123	11.4	*O-Acetyl carnitine	2.4
N273.039	15.7	Deoxy sedoheptulose phosphate	2
N121.041	7.3	*Nicotinamide	1.8
P241.129	16.6	Anserine	1.5
N121.051	12.1	*Erythritol	1.5
N145.014	13.5	**2-Oxoglutarate	1.5
N241.012	17.4	D-myo-Inositol 1,2-cyclic phosphate	1.4
N195.051	14.4	*D-Gluconic acid	1.3
N209.031	16	*D-Glucarate	1.1
N215.033	13.7	Hexose (chloride adduct)	1.1
P170.081	8.1	*Pyridoxine	1
N209.067	14.4	*Sedoheptulose	0.9
P146.092	15.6	4-Guanidinobutanoate	0.9

4.3.7 Preparation of the PCA Model with a Reduced Metabolite List

The initial application of OPLSDA based on 755 metabolites (Figure 4-2) has been built focusing on more limited list of metabolites than those listed in Table 4-S2. When the reduced list of 120 metabolites with low P-values (Table 4-S2) was used to prepare a PCA model, it was clear that the SDB samples contained subgroups. Hierarchical Cluster Analysis (HCA) was used to define the samples into groups will have similar characteristics, which can give an insight in the situation under investigation, but be different from those in other group. Figure 4-7 shows the PCA model corresponding to the HCA plot, as shown in Figure 4-S2, to define a clear subgroup (green group) containing nine SDB samples, schizophrenic, depressive and bipolar, were quite different from the controls and the rest of the SDB samples. The metabolites defining the subgroup are shown in Table 4-5. This supports the proposal that there are similarities within the SDB group since the sub-group contains all three classes.

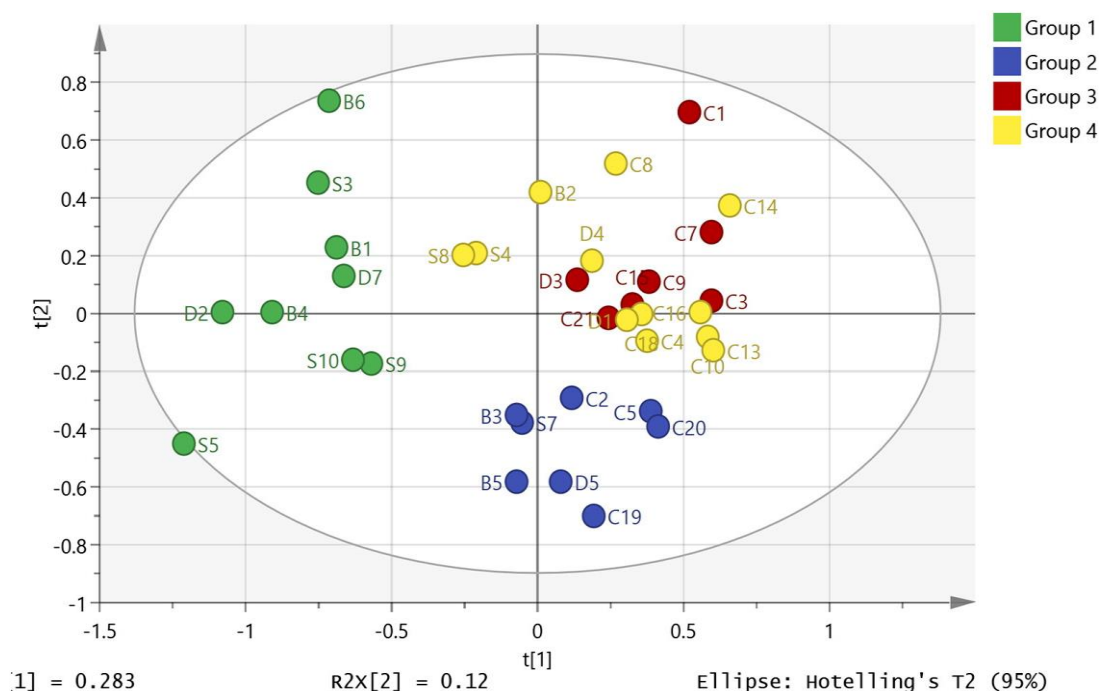


Figure 4-7: PCA model ($R2X=0.68$, $Q2X=0.283$ and five components) based on the metabolites with P -values <0.05 (table 4-S2) when the control and SDB samples are compared and hierarchical cluster analysis (Fig. 4-S2) is used to define subgroups.

Table 4-5: Important metabolites defining the sub-group of nine SDB brains shown in Figure 4-7. *Matches retention time of standard. **Does not match the retention time of the standard therefore is an isomer of the named compound.

m/z	RT min	Metabolite	P value	Ratio SDB/C	VIP
P 305.098	17.2	*N-Acetyl-aspartyl-glutamate	0.003	0.27	2.52
N 195.051	14.4	*Gluconic acid	<0.001	3.3	2.32
N 181.072	14.3	*Sorbitol/mannitol/iditol/dulcitol	<0.001	2.94	2.22
N 209.067	14.4	*Sedoheptulose	<0.001	2.34	2.2
N 252.088	8.1	N-Acetylvanilalanine	<0.001	2.06	2.15
N 202.109	5.5	**O-Acetylcarnitine isomer	<0.001	1.6	2.13
N 231.099	16.8	N2-Succinyl-L-ornithine	0.011	0.36	2.07
N 114.056	13.2	*Proline	0.002	1.52	1.99
N 220.083	12.3	*N-Acetyl-D-glucosamine	<0.001	1.4	1.99
N 180.067	13.4	*Tyrosine	0.001	1.44	1.97
P 277.031	12.6	**Phospho-gluconate isomer	0.003	0.06	1.92
N 171.007	15.4	*Glycerol 3-phosphate	0.004	0.38	1.88
N 164.072	10.4	*Phenylalanine	<0.001	1.88	1.8
P 227.114	10.3	**Carnosine isomer	0.002	8.34	1.7
N 103.004	16.1	*Malonate	0.001	1.56	1.68
N 121.051	12.1	*Erythritol/threitol	<0.001	2	1.65
P 284.099	13	*Guanosine	<0.001	0.58	1.63
P 116.072	12.9	*Valine	<0.001	1.58	1.62
P 230.151	24.2	Gamma-Aminobutyryl-lysine	0.028	1.42	1.62
N 151.061	13.2	*Xylitol/ribitol/arabinotol	<0.001	2.38	1.56
N 130.087	11.2	*Leucine	<0.001	1.66	1.54
N 178.072	12.9	*Glucosamine	0.001	1.88	1.48
P 248.024	10.8	Norepinephrine sulfate	<0.001	0.32	1.48
N 273.039	15.7	1-Deoxy-D-altro-heptulose 7-phosphate	0.002	0.49	1.47
P 104.071	15.9	*4-Aminobutanoate	<0.001	0.78	1.4
P 161.107	10.4	Tryptamine	0.001	1.55	1.39
N 145.014	6.3	**Oxoglutarate isomer	0.031	3.91	1.35
N 159.103	4.9	Ethyl-hydroxyhexanoate	0.002	2.95	1.35
P 169.097	11.3	*Pyridoxamine	0.001	1.53	1.34

4.3.8 Refining the OPLSDA Models

Better understanding of disease pathology in mental illness is the purpose of this study and thus the ideal outcome would be a list of metabolites related to the disease state. With a high number of variables, there is the danger of overfitting and although the OPLSDA models, shown in Figures 4-2 and 4-5, performed well in cross-validation tests, there might still be some doubts with regard to their validity. Thus, the control/SDB OPLSDA model was established based on removing 630 of the lowest priority variables and retaining variables that caused a reduction in the Q2 (cum) score of > 0.05 when removed. Figure 4-8 shows the reduced OPLS-DA model which could accommodate 38 out of the original 45 samples based on the important 120 metabolites shown in Table 4-S2. The cross-validation for this model which had a CV-ANOVA score of 0.0006 and the permutation test is shown in Figure 4-9. In the reduced model, the branched chain amino acid valine and 4-Aminobutanoate, GABA, retain their high importance (Table 4-6).

*Table 4-6: Marker compounds resulted of the OPLSDA model shown in Fig. 4-8. * For the 38 samples used in the model.*

m/z	Rt (min)	Metabolite	P-value*	Ratio* SDB/Control	VIP
116.072	12.9	L-Valine	0.00026	1.39	1.55
104.071	15.9	4-Aminobutanoate	0.0069	0.87	1.43
162.112	13.7	L-Carnitine	0.680	0.96	0.82
204.123	11.4	O-Acetylcarnitine	0.081	1.26	0.75
87.0087	8.3	Pyruvate	0.063	1.26	0.41
175.025	14.6	Ascorbate	0.85	1.03	0.37

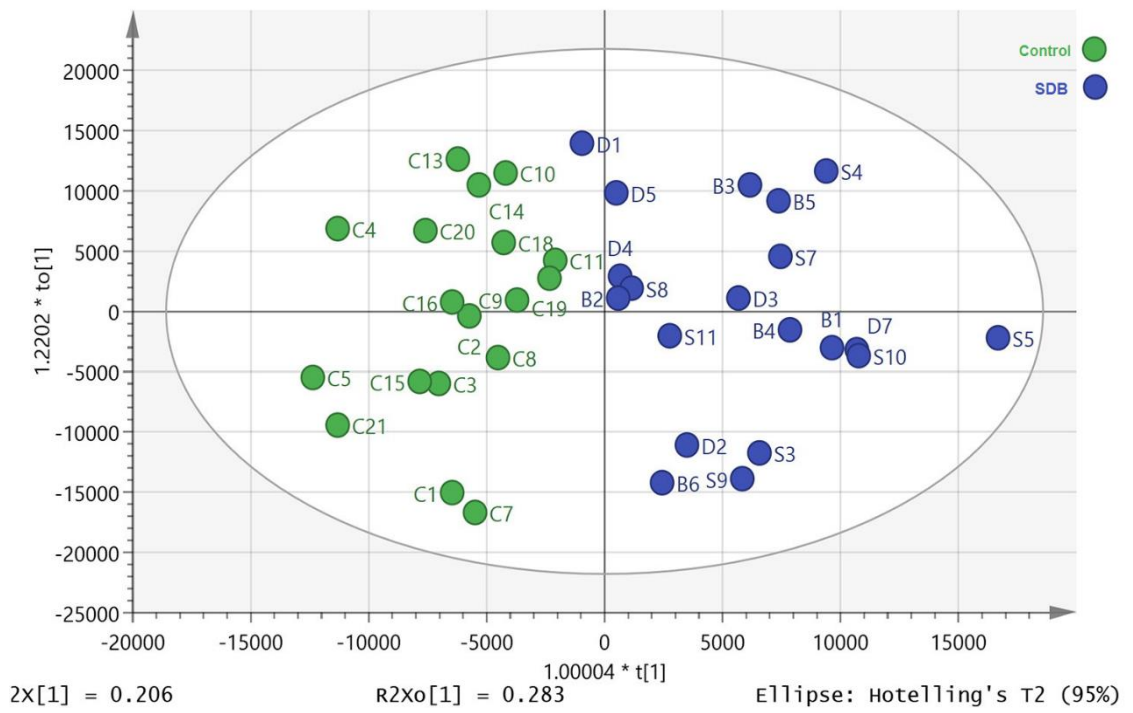


Figure 4-8: OPLSDA model ($R2Y$ (cum) 0.725, $Q2$ (cum) 0.638, and five components) of 18 controls (green) compared to 20 SDB brain samples (blue) based on the filtered 120 metabolites.

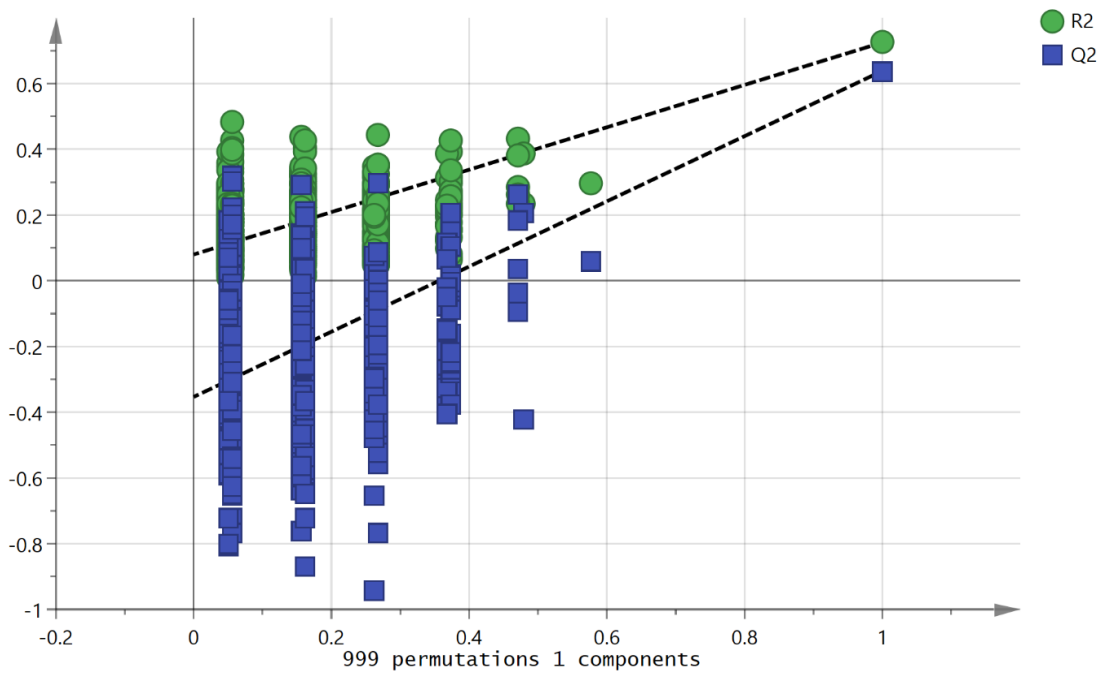


Figure 4-9: Permutations ($n=999$) plot for the OPLS-DA model shown in Figure 4-8.

The same process of variable reduction was applied to the combined DI/SDB model which included seven of the DI samples and resulted in a validated model based on important 120 metabolites into which 45 out of 53 samples could be fitted. This model included six of the diabetic samples, except DI1, shown in Figure 4-10 is validated by a CV-ANOVA score of 0.000013 and permutation test as shown in Figure 4-11. The metabolites obtained from this control/SDB-DI OPLSDA model (Figure 4-10) are the same as those extracted from the previous control/SDB OPLSDA model (Figure 4-8) except that the VIP values for each metabolite were different as show in table 4-7. Removing the 7 DI samples and using them as a prediction set resulted in six of the samples being classified with the SDB group and one of the samples being classified with the controls.

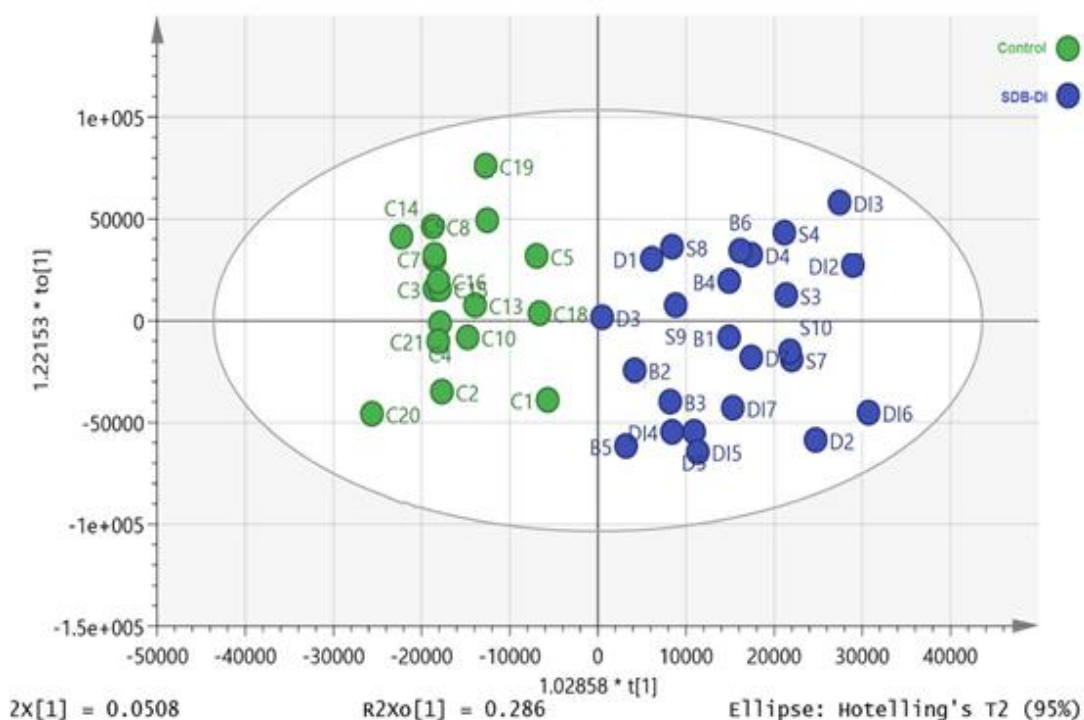


Figure 4-10: OPLSDA model ($R2Y$ (cum) 0.798, $Q2$ (cum) 0.691, and four components) of 18 controls (green) compared to 27 SDBDI brain samples (blue) based on the filtered 120 metabolites.

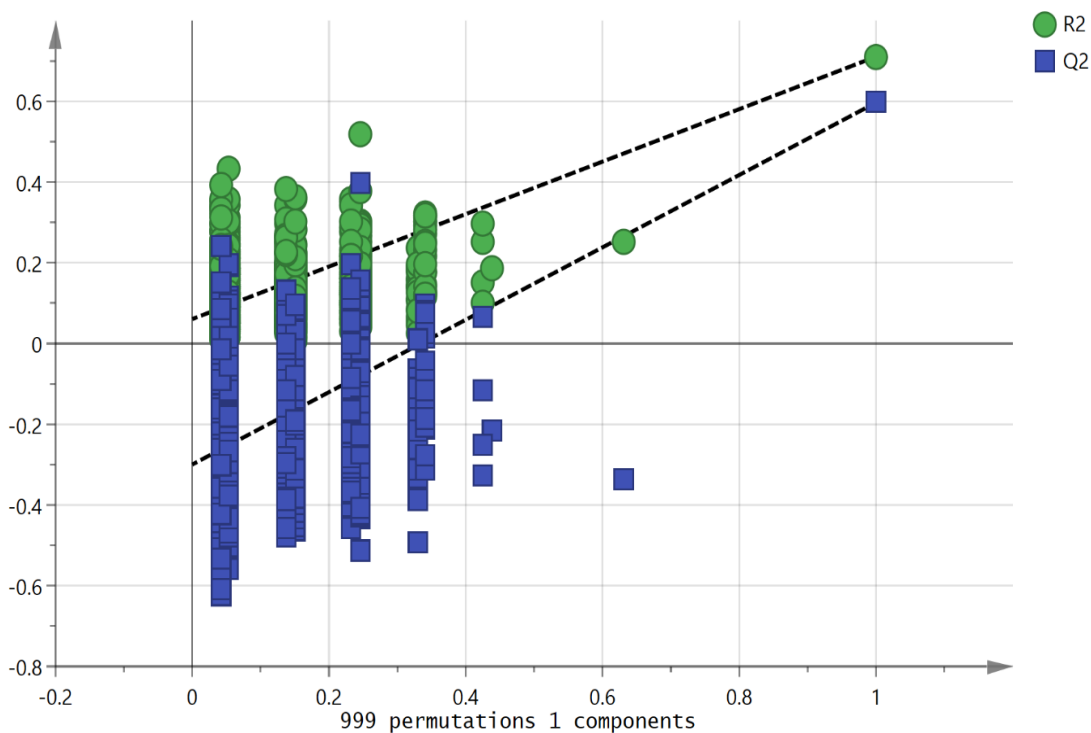


Figure 4-11: Permutations ($n=999$) plot for the OPLS-DA model shown in Figure 4-10.

Table 4-7: Marker compounds resulting from the OPLSDA model shown in Figure 4-10.
* For the 45 samples used in the model.

m/z	Rt (min)	Metabolite	P-value*	Ratio* SDB/Control	VIP
104.071	15.9	4-Aminobutanoate	0.023	0.83	1.64
116.072	12.9	L-Valine	0.0022	1.30	1.32
162.112	13.7	L-Carnitine	0.84	1.01	0.72
204.123	11.4	O-Acetylcarnitine	0.023	1.33	0.71
175.025	14.6	Ascorbate	0.834	1.04	0.50
87.0087	8.3	Pyruvate	0.063	1.26	0.48

4.3.9 GC-MS Analysis to Quantify and Identify Polyols and Polyol

Acids in Brain

In the process of analysing the data, it became apparent that sugar metabolism had an important role in distinguishing the C and SDB brains. The commercially available sugar alcohol standards were run on the ZICpHILIC column and isomeric compounds were found to co-elute or elute closely and thus were not distinguishable from each other. In this study, a GC-MS method was developed for the analysis of the sugar alcohols which were converted into their acetates after initial treatment with methanolic HCl to esterify the acidic groups in gluconic and gulonic acid. The retention times for the available standards are shown in Table 4-8. Figure 4-12 shows the separation of some the polyols present in brain tissue in comparison with a mixture of standards. In this Figure 4-12, the major polyols present were erythritol plus an additional unknown tetritol, ribitol, arabinotol, xylitol, gluconic acid, and sorbitol. Figure 4-13 shows OPLS-DA separation of C and SDB-DI samples based on the ions monitored for the polyol standards; there was not sufficient tissue to repeat analysis of all the samples and the model is based on 21 SDB-DI samples compared to 15 control samples. The cross-validation for the model by permutation test indicates that there was a robust discrimination between groups as shown in Figure 4-14. Calibration curves were prepared in the range 1-16 μ g for all the sugar alcohols against 2 μ g of pinitol which was used as an internal standard (Figure 4-S3 and Table 4-S3). The calibration curves data, Equation of the line and R-squared (R^2) value on chart, extracted from the calibration curves, Figure 4-S3, are detailed in Table 4-9 and have been used to calculate the amounts of sugar alcohols and gluconic acid in brain samples. Table 4-10 shows the quantitative data for the sugar alcohols and gluconic

acid which were calculated based on their intensity in brain samples, Table 4-S4, and the calibration curves data. Clearly, both the diabetic samples and SDB have high levels of sorbitol, gluconic acid, ribitol, and erythritol in comparison to the controls. Elevated levels of sorbitol in schizophrenic and bipolar brains have been reported before (Regenold *et al.*, 2004), but the addition of the other sugar metabolites re-enforces the importance of this pathway in the illness.

Table 4-8: Retention data for polyol isomers and acids analysed by GC-MS in EI mode.

Polyol	MW	Rat GC	MW Derivative	EIMS Main Fragments
Gulonic acid	196	20.66	420	184 (70)145(100)142(97)112(56)103(92)
Gluconic acid	196	20.82	420	217 (25) 173 (56) 157 (38) 155 (69) 115 (100) 103 (51)
Mannitol	182	21.95	434	217 (25) 187 (52) 157 (32) 145 (65) 115 (100) 103 (57)
Sorbitol	182	22.11	434	217 (18) 187 (48) 157 (34) 145 (68) 115 (100)
Dulcitol	182	22.25	434	217 (19) 187(49) 155 (42) 145(50)115(100)
Iditol	182	22.33	434	217 (26) 187 (33) 170 (27) 157 (34) 145 (44) 115(100)
Myoinositol	180	21.99	432	210 (37) 168 (100) 157 (39) 126 (56) 115 (66)
Pinitol	194	20.8	404	182 (74) 140 (100) 87 (62)
Ribitol	152	17.53	362	217 (21) 187 (9) 145(69) 115(100)103(89)
Arabinitol	152	17.67	362	217 (22) 187 (39) 145(65)115(100)103 (72)
Xylitol	152	18.02	362	217 (30) 187 (32) 145(68)115(100)103 (68)
Threitol	122	12.88	290	217(8) 145 (74) 128 (28) 115 (100) 103 (81)
Erythritol	122	12.49	290	217 145 (11) 145 (85) 128 (33) 115(94) 103 (100)

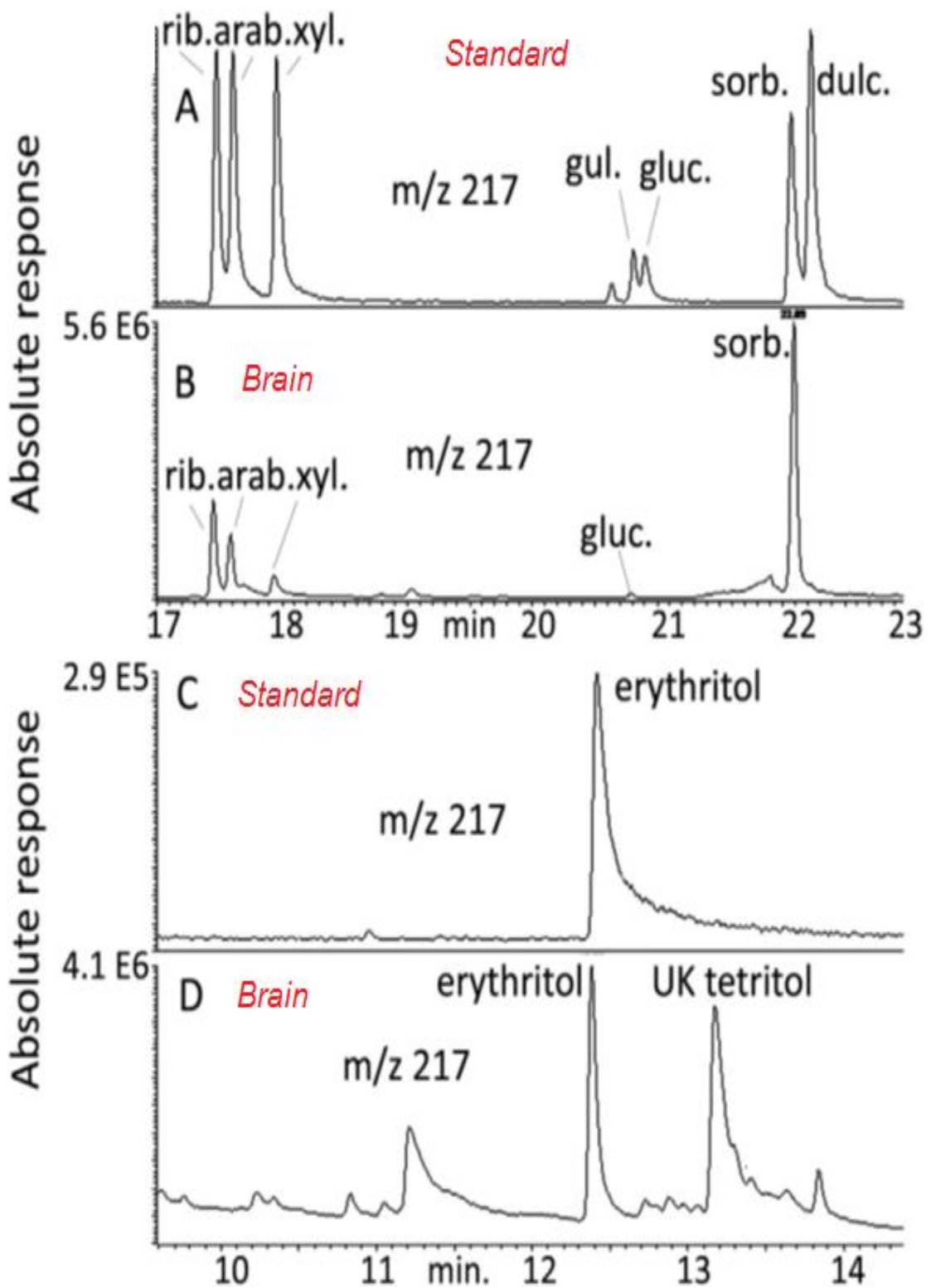


Figure 4-12: GC-MS analysis of polyol standards at 0.8 μ g/0.2ml (A and C) in comparison with polyols in brain (B and D).

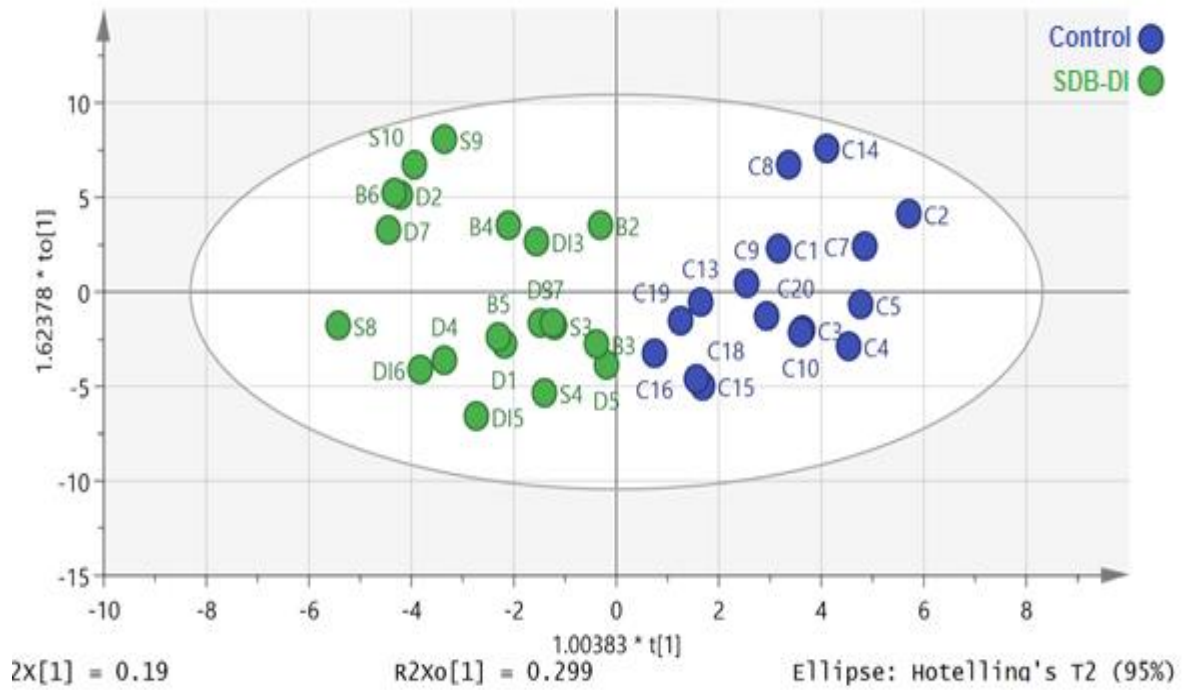


Figure 4-13: Separation of SDB + DI brain samples (green) and controls (blue) on the basis of the GC-MS analysis of sugar alcohols.

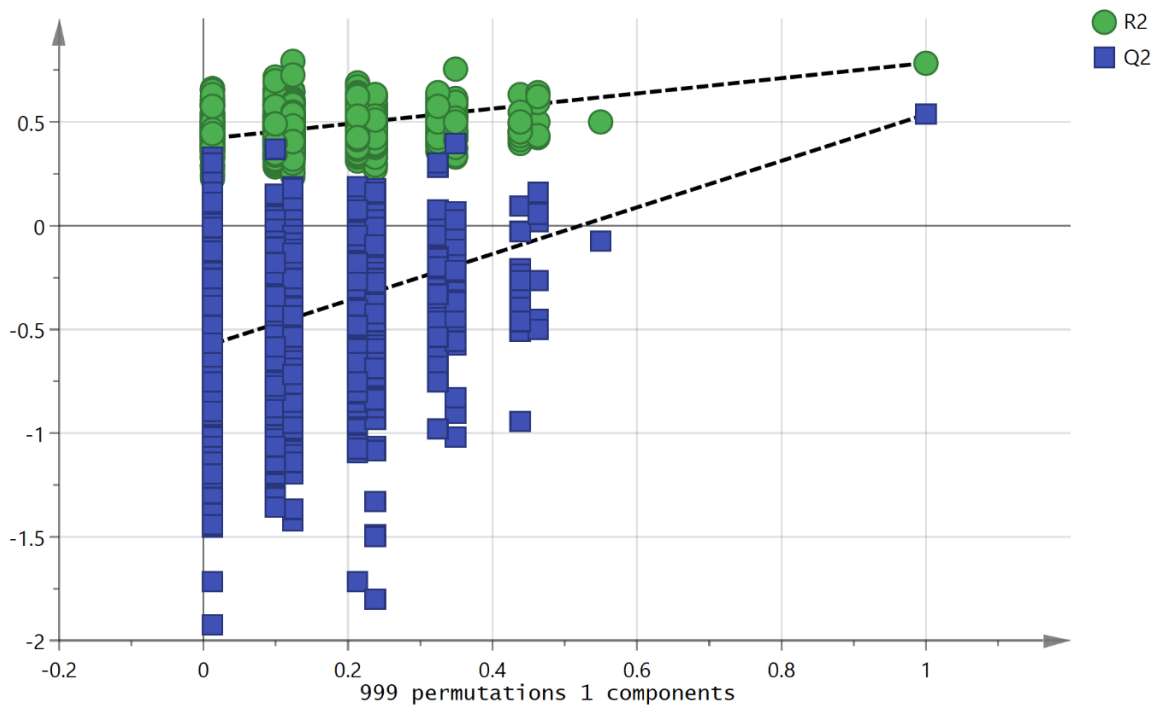


Figure 4-14: Cross validation by permutation plot for Figure 4-13.

Table 4-9: Calibration curve data for sugar alcohols and gluconic acid over the range 1-16µg with pinitol as an internal standard.

Metabolite	Equation of the line	(R ² value)
Sorbitol	Y=0.1093x – 0.5450	0.9994
Gluconic acid	Y=0.0120 x + 0.00113	0.9660
Ribitol	Y=0.1252x – 0.04750	0.9998
Arabinotol	Y=0.1228x – 0.0448	0.9991
Xylitol	Y=0.1277x – 0.0454	0.9996
Erythritol	Y= 0.0450x – 0.0563	0.9918

Table 4-10: The amounts of sugar alcohols and gluconic acid in post-mortem brain samples.

Sugar	SDB+DI µg/g (RSD)	SDB µg/g (RSD)	Control µg/g (RSD)	SDB+DI /C ratio (P.Value)	SDB / C ratio (P.Value)
Sorbitol	22.7 (±56.4)	22.3 (±56.4)	13.5 (±57.0)	1.67 (0.0079)	1.65 (0.0015)
Gluconic acid	3.96 (±55.8)	4.2 (55.6)	1.96 (±40.7)	1.96 (0.0006)	2.06 (0.0012)
Ribitol	9.8 (±21.8)	10.3 (20.2)	9.3 (±25.9)	1.06 (0.18)	1.11 (0.060)
Arabinotol	7.9 (±26.6)	8.0 (26.6)	8.5 (±34.1)	0.93 (0.37)	0.94 (0.490)
Xylitol	4.1 (±28.3)	4.3 (28.3)	7.1 (±57.8)	0.58 (0.0042)	0.61 (0.006)
Erythritol	15.1 (±23.8)	15.4 (±23.8)	12.9 (±34.9)	1.17 (0.028)	1.18 (0.056)

4.4 Discussion

4.4.1 High Levels of BCAs and Other Lipophilic Amino Acids in SDB

Samples

The OPLSDA models based on the larger number of variables (Figures 4-2 and 4-5) and the univariate differences will be used to develop some hypotheses based on the underlying metabolite differences. The highest VIPs in the OPLS-DA model (Figure 4-2) of the SDB samples against the controls are the branched chain amino acids (BCAs) leucine/isoleucine and valine which are elevated above the levels found in the controls. The importance of these metabolites in S and B disorder has recently been highlighted (Burghardt *et al.*, 2015). There have been a number of recent metabolomics studies of obesity and insulin resistance and it has been observed that there is a distinct metabolic signature linked to metabolic syndrome where the plasma levels of BCAs, leucine, isoleucine, and valine, were elevated together with methionine, glutamine, phenylalanine, tyrosine, asparagine, and arginine (Newgard *et al.*, 2009, Huffman *et al.*, 2009). A study which was carried out on a cohort of 1872 individuals who were subdivided in lean, overweight, and obese groups proposed that BCAs levels can provide a better signature of metabolic wellness than BMI (Batch *et al.*, 2013). Another group found that elevated levels of BCAs in plasma could be linked to obesity and potentially to the development of insulin resistance in children and adolescents (McCormack *et al.*, 2013). BCAs are known to promote production of muscle protein (Rennie *et al.*, 2006) and an elevation in their levels may indicate that the uptake of BCAs into muscle tissues is reduced. Metabolomic profiling of plasma from schizophrenics, even before medication, has been found to indicate that they are at risk of developing metabolic syndrome (Paredes *et al.*, 2014). Antipsychotic

medications are known to significantly increase metabolic complications and induce weight gain and although the medication history of the relating to current samples is unknown it unlikely that variations in medication alone would be sufficiently systematic to account for the differences observed. In addition to BCAs, the neutral amino acids including proline, methionine, tyrosine, and tryptophan are all elevated in the SDB/DI group and have high VIP values. There is an early report of marginal differences in the levels of lipophilic amino acids in plasma from schizophrenics with valine, phenylalanine, alanine, leucine, isoleucine, methionine, and tyrosine all being elevated (Bjerkenstedt *et al.*, 1985). However, the current data do not support the theory proposed by that paper, which was that elevation in lipophilic plasma acids might produce competition for lipophilic amino acid transporters into the central nervous system (CNS), resulting in reduced uptake of the amino acids tyrosine and tryptophan which are required for neurotransmitter biosynthesis. Proline is a potential precursor of glutamate which is a neurotransmitter in brain and it has previously been shown to be increased in individuals diagnosed with schizophrenia. There is limited literature indicating that proline dehydrogenase (PRODH) activity may be up-regulated in schizophrenia (Kempf *et al.*, 2008, Tunbridge *et al.*, 2004). However, this would be expected to lead to a fall in proline levels which does not fit with the current observation.

4.4.2 Alterations in Sugar Metabolism

It was not possible to clearly identify the different sugar alcohols using LC-MS since the isomeric compounds have almost identical retention times and their MS/MS spectra are very similar. In order to get a clearer identification of the sugar alcohols in

brain, standards and a brain extracts were derivatised and analysed by GC-MS. The high chromatographic resolving power of a capillary GC column was able to separate the isomers. The levels of glucose in these brains appeared to be very low and the major sugar in the brain was myo-inositol, is a carbocyclic sugar that is abundant in brain and other mammalian tissues. As can be seen in Figure 4-12, there are several sugar alcohols, hexitol, pentitol and tetritols, in the brain. The presence of these compounds has been observed before in human cerebrospinal fluid (CSF) (Shetty *et al.*, 1996). The major hexitol in the brains is sorbitol, but the pentitol peak observed in LC-MS as a single peak is due to the presence of three compounds, ribitol, arabinotol, and xylitol. In addition, there are two tetritols, erythritol and an unknown isomer, which are also elevated. It has been observed that the levels of these polyols in brain are elevated in response to osmotic stress (Lien *et al.*, 1990). In the current case, the levels of sorbitol, gluconic acid, ribitol, and erythritol are higher in the SDB/DI samples in comparison with the controls as judged from both the LC-MS and the GC-MS data (Tables 4-5 and 4-10).

4.4.3 Elevation of Polyols and Oxidative Stress

Hypothesis which suggested that oxidative stress may has a pathophysiological role in mental illness was supported by the increased levels of some indicators of oxidative stress in patients with schizophrenia (Yao *et al.*, 2001). Since the sugar alcohols are not closely linked within a particular pathway and several are elevated, this suggests that the higher levels might be due to an upregulation of aldose reductase which has a wide substrate specificity and is able reduce many different aldoses. Formation of sugar alcohols via aldose reductase activity is responsible for some of the

complications of diabetes and also generates oxidative stress since NADPH is consumed in carrying out the reduction (Yabe-Nishimura, 1998). A previous paper observed that altered glucose metabolism in the brains of those diagnosed with depression and schizophrenia, where sorbitol was increased by a factor of 2.2 (Regenold *et al.*, 2004), similar to the elevations in the SDB brains in the current study. A recent metabolomic study observed altered glucose metabolism in peripheral blood mononuclear cells in schizophrenia with alterations in several glycolysis and Krebs cycle metabolites (Liu *et al.*, 2015). Glucaric acid, which is increased in SDB, also contributes to the model and has a high correlation to the model. Glucaric acid is of interest since it also relates to sorbitol and gluconic acid, being only a single oxidation step away from gluconic acid. Glucaric acid has been frequently monitored in urine as a marker of xenobiotic stress and urinary levels have been observed to rise in response to treatments with phenothiazines (such as the antipsychotic, chlorpromazine) (Wright *et al.*, 1983). Sedoheptulose is considerably elevated in SDB brains while a compound putatively identified as deoxysedoheptulose phosphate is depressed. The published metabolomics study on brain tissue from a mouse model of psychiatric disorder, the *Npas3* knockout, also showed elevated levels of sedoheptulose (2.65-fold increase) (Sha *et al.*, 2012). This suggests that changes in glycolysis or nucleotide metabolism might be altering flux through the pentose phosphate pathway which could correlate with an increased requirement for NADPH as a co-factor for aldose reductase since NADP is converted to NADPH with formation of phosphogluconate at the entry to the pentose phosphate pathway. In addition, there is a deficit in the neuromodulator NAAG in the SDB brains; NAAG has been found to protect against neuronal death

induced by exposure to glucose in a cell-culture model of diabetic neuropathy (Berent - Spillson *et al.*, 2004).

As such, brain tissue accounts for around 20% of the oxygen consumption by the body and thus is a major site of oxidative stress. Carnosine, homocarnosine, and anserine are important antioxidants in brain and skeletal muscle (Kohen *et al.*, 1988). A compound, present in high amount in the brains, putatively identified as anserine which is isomeric with homocarnosine but has a different retention time is an important component in the OPLS-DA model separating control and SDB brains and it is significantly lower in the SDB samples according to the univariate data. Lower levels of anserine might indicate increased oxidative stress in the SDB samples. Of the three commonly occurring histidine dipeptides, anserine has been observed to be the most effective anti-oxidant (Kohen *et al.*, 1988).

4.4.4 Altered Purine Metabolism

From the univariate comparisons, the purines guanine and guanosine were found to be lower in SDB brains and this can be correlated with elevated levels of uric acid in SDB brains. In a recent publication, it was observed that the severity of schizophrenic symptoms could be predicted from a high ratio of uric acid to guanine (Yao *et al.*, 2012, Yao *et al.*, 2001) and the current data indicate that in SDB brains purine oxidation seems to be more active. Also, it has been suggested that the elevated uric acid is indicative of high levels of oxidative stress.

4.4.5 Gamma-aminobutyric acid (GABA) Deficiency

GABA and its metabolite guanidino butyrate, which is formed directly from GABA via arginine–glycine amidinotransferase (Rowland *et al.*, 2012) are important variables in the OPLS-DA model separating control and SDB brains. It is well established that there is a deficit in GABAergic transmission in schizophrenia (Hashimoto *et al.*, 2003, Guidotti *et al.*, 2005). The GABA receptor governs the entry of the chloride ion into cells (Suzdak *et al.*, 1986) and one of the highest VIP values in Table 4-2 is for an adduct formed between chloride and carbonate which is present in the mobile phase which is strongly correlated with the SDB group. Initially, this peak was assigned to orthophosphate according to the library search but it runs earlier than the standard for orthophosphate. Inspection of the peak revealed a chlorine isotope pattern and the elemental composition matches the carbonic acid/chloride adduct. Chloride itself is below the lower mass range cut off for the instrument.

4.4.6 Alterations in Biogenic Amine Metabolism

A number of neurochemically important compounds are significantly changed in the univariate data. Tryptamine has long been associated with mental illness particularly schizophrenia (Burchett and Hicks, 2006) and it is clearly slightly elevated in the SDB brain samples. In the SDB samples, there is a depression of norepinephrine sulphate levels; there are two isomers of this compound in brain both of which are depressed. Glucuronide and sulphate conjugates of dopamine and serotonin have been measured in brain dialysate previously (Suominen *et al.*, 2013); there was no evidence in the current case for the presence norepinephrine glucuronide conjugates in brain. Although not significant in the OPLS-DA model, in the univariate analysis, N-

acetylvanilalanine is significantly elevated in bipolar brains. This metabolite is of great interest since it is a marker for a deficiency of aromatic amino acid decarboxylase (AADC), also known as DOPA decarboxylase deficiency, which can lead to a deficit in the levels of several neurotransmitters (Abdenur *et al.*, 2006). This can be correlated with elevated levels of all the aromatic amino acids in the SDB brains. There are also elevated levels of kynurenine and kynurenamine which are metabolites of tryptophan which have neuropathological effects (Tan *et al.*, 2012).

4.4.7 Differences in a Sub-group of SDB Samples

There are many other differences in the univariate data and it is difficult to rationalise them all. In order to determine if there are subgroups within the samples, a PCA model was fitted to the 36 samples used to produce the OPLS-DA model using only the metabolites shown in Table 4-S2 which were significantly different according to univariate analysis. HCA clearly highlighted a group of 9 SDB samples which were far away from the rest of the samples that did not clearly separate in the PCA plot (Figure 4-7). The metabolites which were most significant in separating this sub-group from the controls in the PCA plot are listed in Table 4-5 along with P-values and ratios derived from univariate comparison of these nine samples with the control samples. The brains in this subgroup contain much lower levels of NAAG in comparison with the rest of the SDB group and sorbitol, gluconic acid, and xylitol/ribitol/arabitol are also higher than in the general cohort. In addition, N-acetylvanilalanine is higher in these samples along with tyrosine and phenylalanine than in the rest of the SDB samples which might indicate a greater degree of aromatic amino acid decarboxylase deficiency. However, tryptophan is not significantly different in this subgroup

compared with the rest of the SDB samples although its metabolite tryptamine is elevated. In addition norepinephrine sulphate and guanosine are significantly lower in this group compared with the rest of the samples.

4.4.8 OPLS-DA Models Based on Reduced Metabolites

Figures 4.S4 – 4.S9 show extracted ion traces for the six marker compounds produced from the OPLS-DA models as listed in Tables 4-6 and 4-10. GABA and valine are important components in the models shown in (Figure 4-8 and Figure 4-10) and have been discussed above. Ascorbic acid does not show up strongly with regard to univariate statistics having a P value of 0.5 when comparing the samples modelled in Figure 4-2. There have been reports of increased ascorbic acid requirements in schizophrenia with reduced urinary excretion being observed (Yao *et al.*, 2001). Carnitine and its acyl derivatives have been reported to have potential in the treatment of neurochemical disorders (Malaguarnera, 2012). Finally, it was observed in a previous study that pyruvate levels were lowered in the thalamus of the post-mortem brains of schizophrenics in comparison with controls (Martins-de-Souza *et al.*, 2010). In the current case, pyruvate is slightly elevated in the SDB group, but the part of the brain analysed in the current case was different.

4.5 Conclusion

In conclusion, many differences were observed in SDB versus control brains which have been observed by previous papers such as lower levels of NAAG and GABA in the SDB brains, elevated levels of sorbitol, and the importance of branched chain amino acids. Current strategy of treating the three psychiatric disorders as a single disease entity (SDB) may reduce the ability to detect specific aetiological biomarkers, but it increased sample size, diluted disease-specific medication effects, and most importantly, allowed the identification of a metabolic profile reflecting a shared pathological state. Since there are no biomarkers for mental illnesses and these diseases are multifaceted, diagnosis is never absolute and indeed this can be seen in scatter plots where each individual is different. However, there is enough in common in the SDB group for them to be classified as more similar to each other than to the controls. Certain key metabolites highlighted as being more important in the pathology and it seems that abnormal sugar and branched chain amino acid metabolism might be a key element in SDB as reflected in the metabolic similarity between SDB and diabetes. There are no previous metabolomics studies of post-mortem brain tissue in mental illness. Although this is only a small study, the findings are in agreement with several previous studies looking at specific markers and in respect of some markers with studies going back many years. In addition it was necessary to develop a GC-MS method in order to separate isomeric sugar polyols which would not separate on HILIC. In future work, the study will be highlighted available markers which could be quantified in physiological fluids for the purpose of diagnosis or the monitoring of treatment. Altered metabolism of sugar polyols in mental illness the reducing sugars (sugar aldehydes) were examined.

CHAPTER 5

THE ANALYSIS OF SUGARS IN POST-MORTEM HUMAN BRAIN IN ORDER TO DETERMINE WHETHER OR NOT PERTURBED SUGAR METABOLISM IS ASSOCIATED WITH MENTAL ILLNESS

Abstract:

Separation of sugar isomers extracted from biological samples is challenging because of their natural occurrence as alpha and beta anomers and, in the case of hexoses, in their pyranose and furanose forms. A reductive amination method was developed for the tagging of sugars with the aim of it becoming part of a metabolomics work flow. The best separation of the common hexoses (glucose, fructose, mannose and galactose) was achieved when $^2\text{H}_5$ -aniline was used as the tagging reagent in combination with separation on a ZICHILIC column. The method was used to tag a range of sugars including pentoses (ribose and xylose) and sugar derivatives (N-acetylneuraminic acid and glucuronic acid). The method was simple to perform and was able to improve both the separation of sugars and their response to electrospray ionisation where a number of hexose and pentose isomers could be observed in biological samples. The method was applied to the profiling of sugars in post-mortem brain samples from six control samples and eighteen samples from individuals who had suffered from schizophrenia, depression and bipolar (SDB) disorder. It was also applied to the quantification of sugars to confirm the important role of sugars metabolism through evaluation of the relation between the changes in sugar levels and psychiatric disorders that proved in this work.

5.1 Introduction

Reducing sugars can exist as α - and β -anomers and also in pyranose (α -anomers) and furanose (β -anomers) ring forms (Figure 5-1). The pyranose form of glucose is a 6-membered hemiacetal, while the furanose form is a 5-membered hemiacetal. In the α -anomers, the hydroxyl group on the anomeric carbon is below the plane of the structure while in the β -anomers the hydroxyl group attached to the anomeric carbon is above the plane of the structure. This configuration is also observed in other hexose sugars such as galactose, fructose, and mannose (Bermejo-Deval *et al.*, 2012).

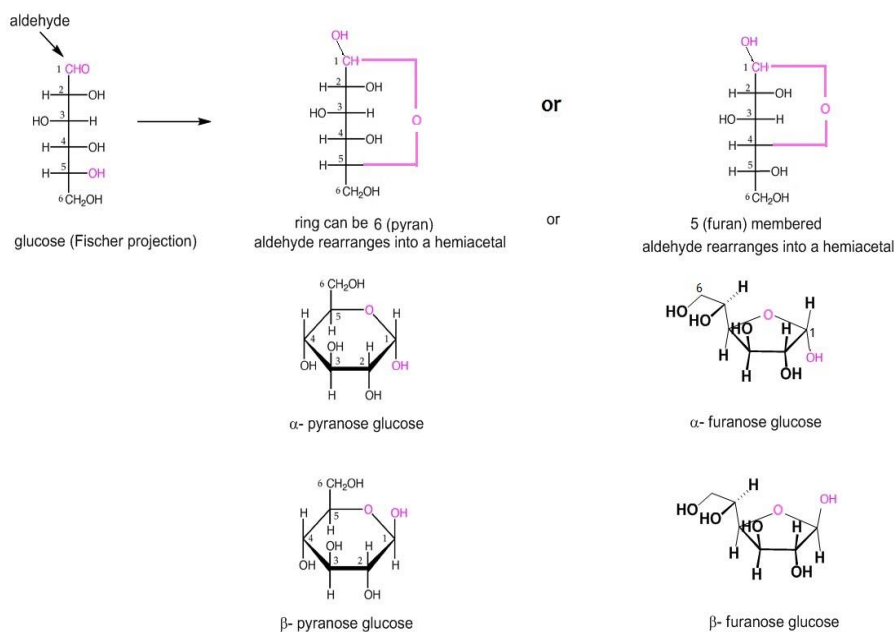


Figure 5-1: The equilibrium forms of glucose where the aldehyde group can react to form 5 (furan) or six membered ring via formation of a hemiacetal. The hydroxyl group generated can be in the α - or β -position.

Neutral sugars are some of the most difficult analytes to characterise during metabolomics analyses by LC-MS and this is for two reasons. Firstly, they do not ionise strongly in negative ion mode given their lack of ionisable groups. Secondly, they tend to give jagged peaks which are broad because they can exist in four different ring forms which are in equilibrium with each other. Raising the pH of the mobile phase can partly overcome these problems since this speeds up the equilibration rate between the four forms so that it becomes more rapid than the chromatographic mass transfer processes. However, additives such as trimethylamine or ammonia which have been used to promote mutarotation are not mass spectrometry friendly and in addition many chromatography columns are not stable to the high pH values required to increase the rate of mutarotation. Complete chromatographic separations of the common monosaccharides using liquid chromatography are rare (Yan *et al.*, 2016, E Young *et al.*, 2016). In previous work, a calcium ligand exchange column was partly able to resolve the problem of sugar separation. Using this column was able to separate glucose and fructose, but was not mass spectrometry compatible because the sugars tended to form a complex mixture of calcium adducts in the MS making spectra hard to interpret (Qian *et al.*, 2008). The separation of the sugar isomers by using GC is achievable although even in this case the elution times of the isomers are close particularly when oximation is used which produces two peaks for each sugar. In GC-MS analysis analytes are subjected to electron impact ionisation and this results in uninformative spectra where there is no molecular ion and the fragments ions are not definitive of a sugar structure (Molnár-Perl and Horváth, 1997, Boldizsar *et al.*, 1998, Medeiros and Simoneit, 2007). In the case of high resolution MS under electrospray conditions, all the ion current is carried by the molecular ion thus giving high

sensitivity and precise identification since the exact molecular weights the sugar isomers are predictable. This allows data from biological samples to be mined for unknown or unexpected sugars.

These major problems, as described above, can be reduced by using of derivatising agents to avoid the formation of several various isoforms. Derivatising agents can be used to introduce ionisable function groups into the sugars thereby both improving separation and the detection of the poorly ionising sugars by electrospray mass spectrometry. A frequently adopted strategy for sugar derivatisation prior the separation by liquid chromatography is to carry out reductive amination of the sugars at low pH (Fischer *et al.*, 2003, Baxter and Reitz, 2004). The aldehyde group of the sugar reacts with the amine to form a Schiff's base, since a Schiff's base can exist in syn- and anti-forms thus potentially producing two chromatographic peaks and it is also not particularly stable. This reaction is pushed to completion by reducing the Schiff's base to produce a single amine product which is stable against hydrolysis. There have been several reviews of the methods used for derivatising sugars (Gao *et al.*, 2003, Harvey, 2011, Fekete *et al.*, 2015). Three basic rules have been established. Firstly, the reaction should be conducted at low pH so that the acyclic form of the sugar is favoured over the cyclic form, since it is the aldehyde form that reacts to form the Schiff base. Thus it is better to carry out the reaction at a fairly low pH (e.g. in dilute acetic acid). The second rule can be determined by having to work at low pH. It is necessary to use a weak base that is not fully protonated at low pH to get a successful reaction because it is the unprotonated form of a base that reacts with the aldehyde. A good example of such a base is aniline which has been used for many years to detect sugars following their separation by thin layer chromatography. The pKa value of

aniline is about 4.5 so even working at around pH 3.5 there is still enough of the unprotonated form of the base to react with the sugar. A base such as aminobenzamide has an even lower pKa value (ca 2.0) and may be even better than aniline for the derivatisation of sugars (Morelle *et al.*, 2005). The presence of the amide group at the para-position to the amino group increased the electron withdrawing effect away from the nitrogen of the basic group, which weakens the latter. Finally, the third rule is that the reducing agent used to reduce the Schiff's base should be stable under acidic conditions. Sodium borohydride is often used in reductive amination reactions but it is of no use in the current case since it is unstable under acidic conditions. Thus it is necessary to use a suitable acid-stable reducing agent such as 2-methylpyridineborane complex which is stable at low pH (Baxter and Reitz, 2004). Other sugar derivatives such as N-acetylneuraminic acid (NANA), N-acetylglucosamine (NAG) which are the saccharide units present in glycosphingolipids occurring in the brain of vertebrates may be strongly correlated with brain disorders (Tettamanti *et al.*, 2003). NANA is the only sialic acid present in human tissues and is essential for appropriate brain development. It is a crucial component of neuronal membranes found in the brain as reported to play an important role in adult brain (YU and LEDEEN, 1970).

The previous project in this thesis, Chapter 4, indicated to the association between sugars metabolism and mental illness. Due to the GC-MS method used in analyse sugars is a less suitable for untargeted profiling, the LC-MS method on the Orbitrap is more suitable for untargeted profiling and gives accurate masses and molecular ions. Therefore, in the current study, LC/MS-based sugars derivatisation method was applied to analysis the sugars in post-mortem human brain in order to determine whether or not perturbed sugar metabolism is associated with mental illness.

5.1.1 Aim of the Study

The aim of the current study was to apply the developed reductive amination method which would allow separation of the common hexoses fructose, glucose, galactose and mannose in the identification of unknown sugars detected in brain samples. Additionally, pentoses, ribose and xylose, and other sugar derivatives including NANA, NAG and glucuronic acid will be quantified in post-mortem brain samples in the present study.

5.2 Materials and Methods

5.2.1 Chemicals and Materials

HPLC grade ACN, formic acid, acetic acid, aniline. HCl, $^2\text{H}_5$ -aniline, picoline borane complex, glucose, fructose, mannose, galactose, ribose, xylose, arabinose, glucuronic acid, galacturonic acid, NAG and NANA were obtained from Sigma Aldrich, Dorset, UK.

5.2.2 Biological Samples

Post-mortem brain samples were also available from a previous study (Zhang *et al.*, 2016) and were provided by from the Sudden Death Bank collection held in the MRC Edinburgh Brain and Tissue Banks. Full ethics permission has been granted to the Banks for collection of samples and distribution to approved researchers, the University of Strathclyde Ethics Committee also approved the local study of this material.

5.2.3 Sugar Derivatisation

Solutions of the sugar standards were prepared at 1 mg/ml in methanol and were then derivatised with deuterated aniline as follows. The tagging agents were prepared at 10 mg/ml in methanol/water containing 10% (v/v) acetic acid (50:50) (solution A) and a solution containing 10mg/ml of picoline-borane in methanol/water (1:1) (solution B) was also prepared. An aliquot of each sugar (50µl) solution was mixed with 40µl of solution A. The mixture was then heated in a heating block at 40°C for 30 min. Then 20µl of solution B was added and the resulting mixture again heated at 30°C for 45 min. The samples were then blown to dryness in a stream of nitrogen gas and re-dissolved in 0.2 ml of water containing 0.1% (v/v) formic acid, before adding 1 ml of ACN. The reaction outline of the reductive amination method to tag sugars and its derivatives by using deuterated-²H₅ aniline is illustrated in Figure 5-2.

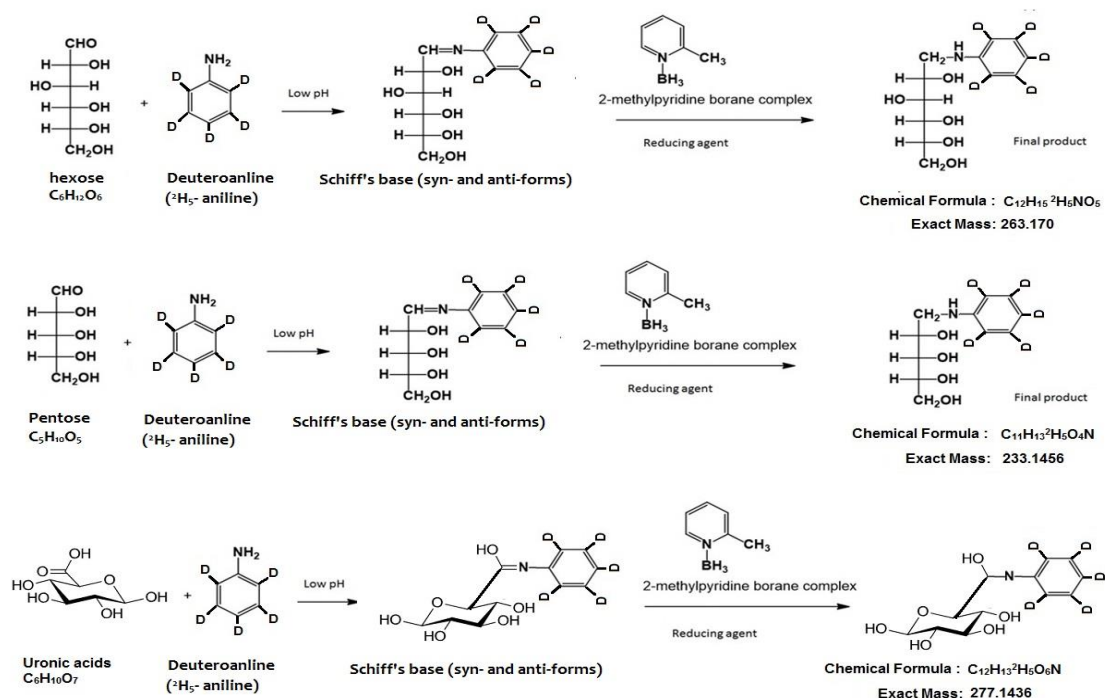


Figure 5-2: Reductive amination of a sugar and its derivatives using deuterio-²H₅ aniline and picoline borane.

5.2.4 Profiling of Biological Samples

Brain tissue (200mg) was extracted by homogenising with 1ml of ACN/water containing 1µg/ml of $^{13}\text{C}_6$ -glucose, a glucose molecule containing six of labelled atoms; where ' ^{13}C ' refers to the atom isotope of glucose (labelled atoms) and '6' refers to the number of atoms labelled in the molecule. The sample was centrifuged at 3000g and then the supernatant was blown to dryness under a stream of nitrogen and the residue was dissolved the 200µl of methanol. Then, this sample was treated for derivatising as described above (section 5-2-3) by using deuterated aniline as the reagent. A calibration curve was prepared by diluting stock solutions of sugar standards and carrying out derivatisation to give solutions containing 1µg of $^{13}\text{C}_6$ -glucose and 0, 0.1, 0.2, 0.4, 0.8, and 1.6µg of fructose, glucose, galactose and mannose.

5.2.5 LC-MS Analysis

LC-MS analysis was carried out using a Surveyor HPLC pump interfaced to an LTQ Orbitrap mass spectrometer operated in positive ion mode with a needle voltage of 4.5 kV, sheath and drying gases flows set a 20 and 50 arbitrary units and a capillary temperature of 250°C. Separation was carried out on a ZICHILIC column (150×4.6mm, 3.5µm particle size, HiChrom Reading, UK) in isocratic mode with an ACN/water (90:10) mobile phase containing 0.01% (v/v) formic acid at a flow rate of 0.6 ml/min.

5.3 Results

5.3.1 Underivatised Sugars

Extracted ion chromatograms obtained for underivatised glucose and galactose on a ZICpHILIC column with standard metabolomics screening conditions (Zhang *et al.*, 2016) are shown in Figure 5-3 which uses hydrophilic interaction chromatography at pH 9.2 with ESI-MS with positive or negative ion detection. There is little chance of getting a good separation as long as all the four forms of the sugars are present since the peaks are broad and misshapen even under the conditions used to produce the chromatograms (Figure 5-3) which were obtained at a pH of 9.2. On the other hand, there was not sufficient resolution to separate the four common hexose sugars by derivatives formed with 4-amino-N,N,N-trimethylbenzenaminium (TMBA). The positive charge on the tag appears to dominate the separation and the stereochemistry of the sugar attached has little impact on the separation (Bawazeer *et al.*, 2017).

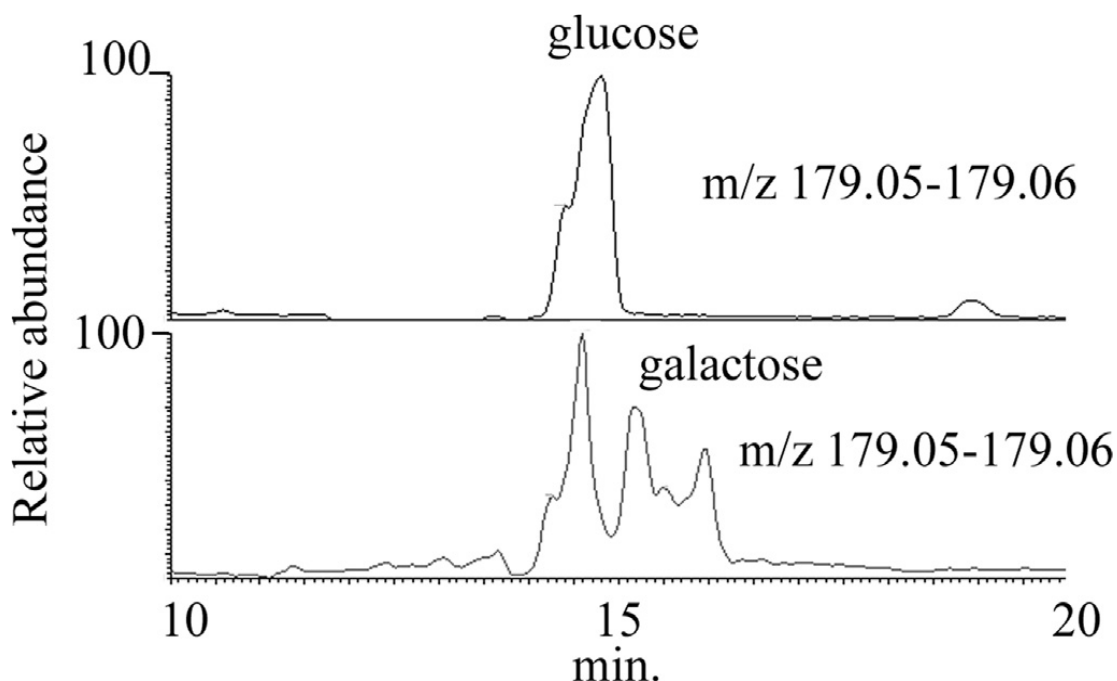


Figure 5-3: Extracted ion chromatograms for glucose and galactose in negative ion mode on a ZICpHILIC column (150×4.6 mm, 5µm) with a gradient between acetonitrile and ammonium carbonate pH 9.2.

5.3.2 Tagging with Deuterated Aniline ($^2\text{H}_5$ -aniline):

Aniline has been used for many years as a tagging agent for sugars and it was found that when used to tag the sugars it produced good separation between glucose and galactose and reasonable separation between galactose and mannose (Figure 5-4A). The original intention had been to use $^2\text{H}_5$ -aniline as a stable isotope tagging agent so that for instance, control and disease samples could be analysed in the same run in the manner pioneered by Guo and Li (Guo and Li, 2009). However, it was found when $^2\text{H}_5$ -aniline was used as a tagging agent there was slightly better separation between mannose and galactose (Figure 5-4B) and better peak shape. Figure 5-5 shows the separation of fructose, glucose, galactose and mannose as their $^2\text{H}_5$ -aniline derivatives on a ZICHILIC column under isocratic conditions in a mobile phase using ACN/water (90:10) containing 0.01% (v/v) formic acid. Mannose and galactose are almost baseline resolved and are well separated from glucose. Fructose produces two peaks since reduction of the Schiff's base introduces an additional stereocentre and thus forms a pair of diastereomers. These derivatives offer both resolution and sensitivity and also the fractional mass increment conferred by the tag is quite distinctive because of the presence of five deuterium atoms giving high confidence in identification of unknown tagged components extracted from a biological matrix.

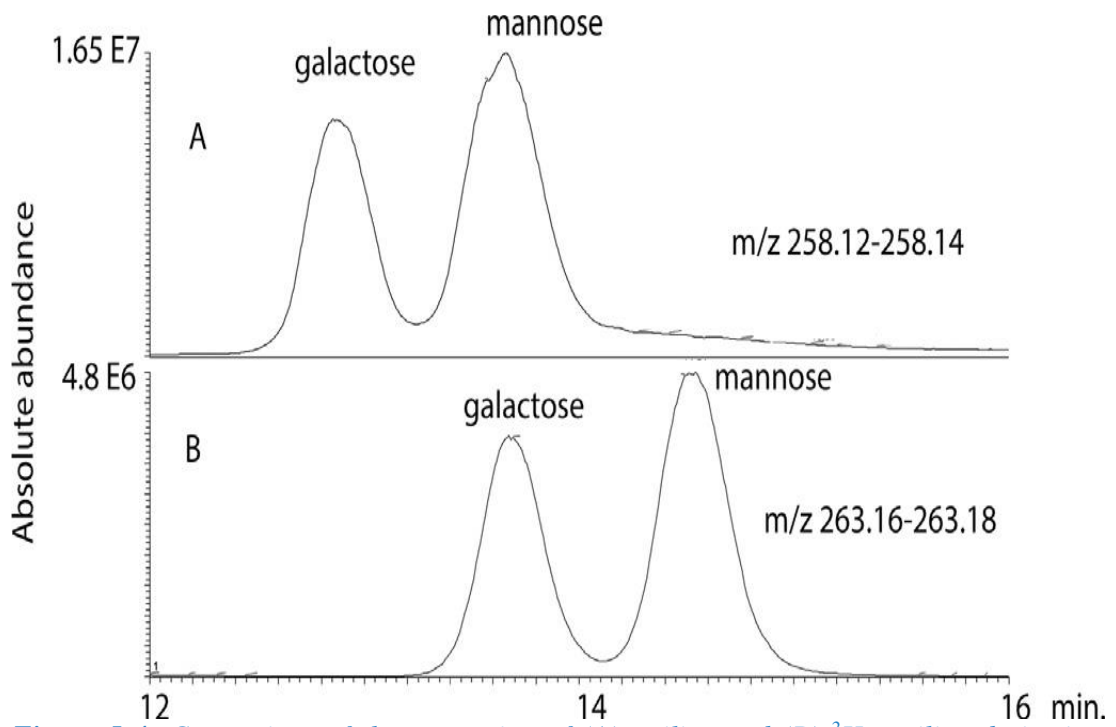


Figure 5-4: Comparison of the separation of (A) aniline and (B) $^2\text{H}_5$ -aniline derivatives galactose and mannose run on a ZICHILIC column in ACN/water containing 0.01% (v/v) formic acid at 0.6 ml/min.

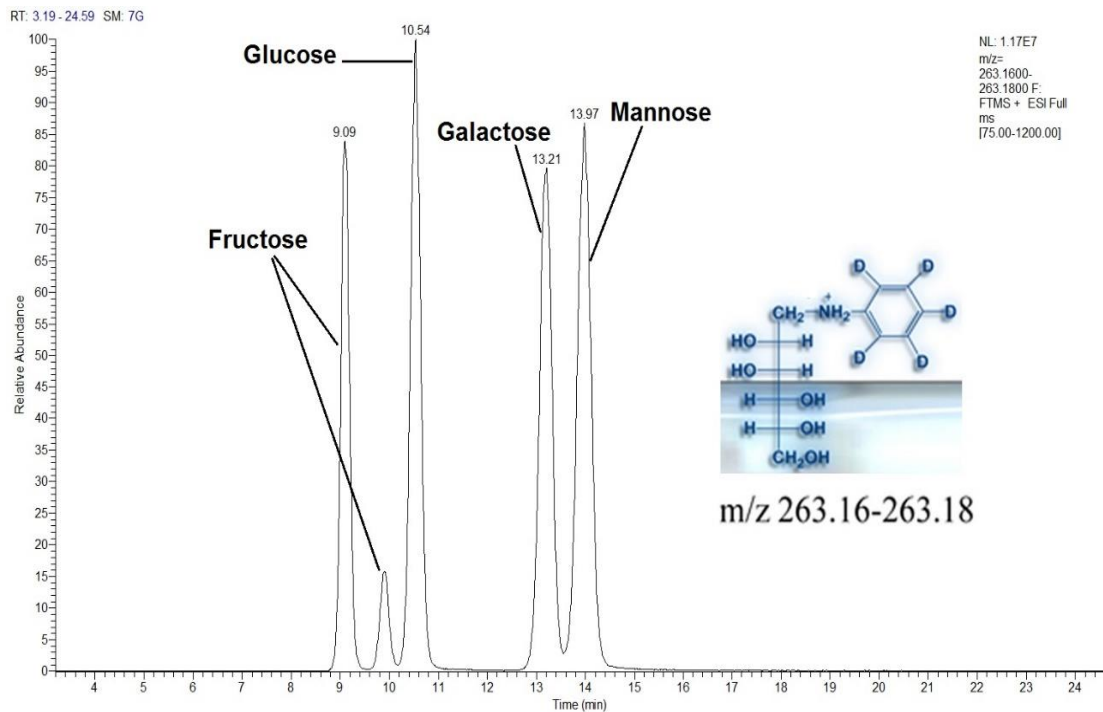


Figure 5-5: $^2\text{H}_5$ -aniline of $1\mu\text{g}$ amounts of hexose standards run on a ZICHILIC column in ACN/water containing 0.01% (v/v) formic acid at 0.6 ml/min.

The derivatisation process can be conducted easily and the formation of the derivatives increases the response for the sugars under ESI conditions. The effect of incorporation deuterium atoms in both reversed phase LC and GC is well known (Wade, 1999). In these chromatographic modes deuterated isotopomers run earlier than their non-deuterated counterparts indicating that deuterated isotopomers are less lipophilic. The reason for this has not been fully explained, but may be related to the lower vibrational energy of the carbon deuterium bond (Wade, 1999) in comparison with the carbon hydrogen bond. Conversely in the case of the HILIC method used in the current study the sugars tagged with the $^2\text{H}_5$ -aniline are more hydrophilic than those tagged with aniline and run circa one minute later. This increased retention is sufficient to produce slightly improved resolution between galactose and mannose in comparison with the aniline derivative. Lowering the water content further did not greatly improve the separation of the aniline tagged derivatives because of increased band broadening with RT. It would seem that the greater the contribution of the tag to the retention properties, the less the sugar stereo chemistry of the sugar contributes to retention. In preliminary work to develop our derivatisation method (Bawazeer *et al.*, 2017), very little separation of the hexose isomers was observed when the amino benzamide used as a tag. It was found that the best separation of the $^2\text{H}_5$ -aniline derivatives was produced by using a low concentration of acid modifier and a relatively high flow rate for a mass spectrometric method of 0.6 ml/min. The tagging method, reductive amination method, was applied to a selection of sugars of biological interest. Table 5-1 summarises the retention times and the molecular ions obtained for $^2\text{H}_5$ - aniline derivatives of some sugars.

Table 5-1: Retention and molecular ion data for some sugar standards tagged with of $^2\text{H}_5$ -aniline and run on a ZICHILIC column in ACN/water containing 0.01% (v/v) formic acid at 0.6 ml/min.

Sugar	Derivatised Chemical Formula	m/z of deuterated-5- aniline derivative	Retention Time (min)
Glucose	$\text{C}_{12}\text{H}_{15}^2\text{H}_5\text{O}_5\text{N}$	263.1646	10.54
Galactose	$\text{C}_{12}\text{H}_{15}^2\text{H}_5\text{O}_5\text{N}$	263.1646	13.20
Mannose	$\text{C}_{12}\text{H}_{15}^2\text{H}_5\text{O}_5\text{N}$	263.1646	13.97
Fructose	$\text{C}_{12}\text{H}_{15}^2\text{H}_5\text{O}_5\text{N}$	263.1646	9.09, 9.90
Glucuronic acid	$\text{C}_{12}\text{H}_{13}^2\text{H}_5\text{O}_6\text{N}$	277.1436	15.3
Galacturonic acid	$\text{C}_{12}\text{H}_{13}^2\text{H}_5\text{O}_6\text{N}$	277.1436	18.5
Ribose	$\text{C}_{11}\text{H}_{13}^2\text{H}_5\text{O}_4\text{N}$	233.1456	8.0
Xylose	$\text{C}_{11}\text{H}_{13}^2\text{H}_5\text{O}_4\text{N}$	233.1456	7.1
N-acetyl glucosamine	$\text{C}_{14}\text{H}_{18}^2\text{H}_5\text{O}_5\text{N}_2$	304.1905	9.4
N-acetylneuraminic	$\text{C}_{17}\text{H}_{22}^2\text{H}_5\text{O}_8\text{N}_2$	392.2063	27.7

5.3.3 Quantification and Profiling of Sugars in Post-Mortem Human

Brain:

In related earlier paper (Zhang *et al.*, 2016), it was showed that post-mortem brains from subjects who had S, D and B disorder had elevated levels of polyols in comparison to controls, also the details of the samples and results are given in Chapter 4 of this thesis. In order to illustrate the potential applying of this method for uncovering unusual patterns in quantification of sugars, the derivatisation procedure was applied to the analysis of a sample of mental illness brains followed by quantification using the extracted ion traces for the sugar derivatives. Several hexoses and pentoses (Table 5-1) were observed in the mental illness samples when these samples were treated by the reductive amination method for the analysis of sugars. The

calibration curves were prepared in five concentrations (0.0, 0.1, 0.2, 0.4, 0.8 and 1.6µg) for a mixture of some sugar standards tagged with of ²H₅- aniline (Table 5-1). ¹³C₆-glucose was added as internal standard (InS) and was also added to the standard sample mixtures at a fixed concentration of 1µg. Table 5-2 summarises the peak areas of each of the sugars and the peak-area ratio of analyte to the internal standard (¹³C₆-glucose) at each of the above five concentrations prepared for the sugar standards. The Figures 5-6 - 5-15 show the calibration curves for the sugar derivatives detailed in Table 5-1. These calibration curves were established based on the ratio of sugar standards to internal standard (Table 5-2) in order to calculate the linearity, slope and intercept values, to be used in quantification of the amount of sugars in the biological samples.

Table 5-2: Summary table showing peaks areas and peak-area ratios of A: glucose with (0.5-8µg) and B: other sugar standards with (0.1-1.6µg) to ¹³C₆- glucose as internal standard (InS)

A					
Con. µg	0.5	1	2	4	8
¹³ C_Glucose Area (InS)	220090409	214776002	206314371	185003622	164523924
Glucose Area	22432995	44185542	78797603	137959396	224337688
Glucose/ InS Ratio	0.1	0.21	0.38	0.75	1.36
B					
Con. µg	0.1	0.2	0.4	0.8	1.6
¹³ C_Glucose Area	220090409	214776002	206314371	185003622	164523924
Galactose Area	9761883	21962177	40551615	82164045	154706883
Galactose/ InS Ratio	0.04	0.1	0.2	0.44	0.94
Mannose	6789431	15770765	28103931	64373819	122387981
Mann/ InS Ratio	0.03	0.07	0.14	0.35	0.74
Fructose	78200	148439	556143	1574602	3037843
Fructose/ InS Ratio	0.01	0.03	0.08	0.25	0.46
Glucuronic acid Area	437040	561991	5220146	8223444	25450593
Glucuronic acid/ InS Ratio	0.002	0.003	0.025	0.044	0.155
Galacturonic acid Area	17409	66152	49725	98251	87177
Galacturonic acid/ InS Ratio	0.0001	0.0003	0.0002	0.0005	0.0005
Ribose Area	5712241	14419857	25310665	50270603	103399224
Ribose/ InS Ratio	0.03	0.07	0.12	0.27	0.63
Xylose Area	11663019	22091847	36244008	74047574	114615603
Xylose/ InS Ratio	0.05	0.1	0.18	0.4	0.7
NAG Area	90608	504509	868177	1287085	1217663
NAG / InS Ratio	0.0004	0.0023	0.0042	0.007	0.0074
NANA Area	21990	201407	854165	657111	3604511
NANA/ InS Ratio	0.0001	0.0009	0.0041	0.0036	0.0219

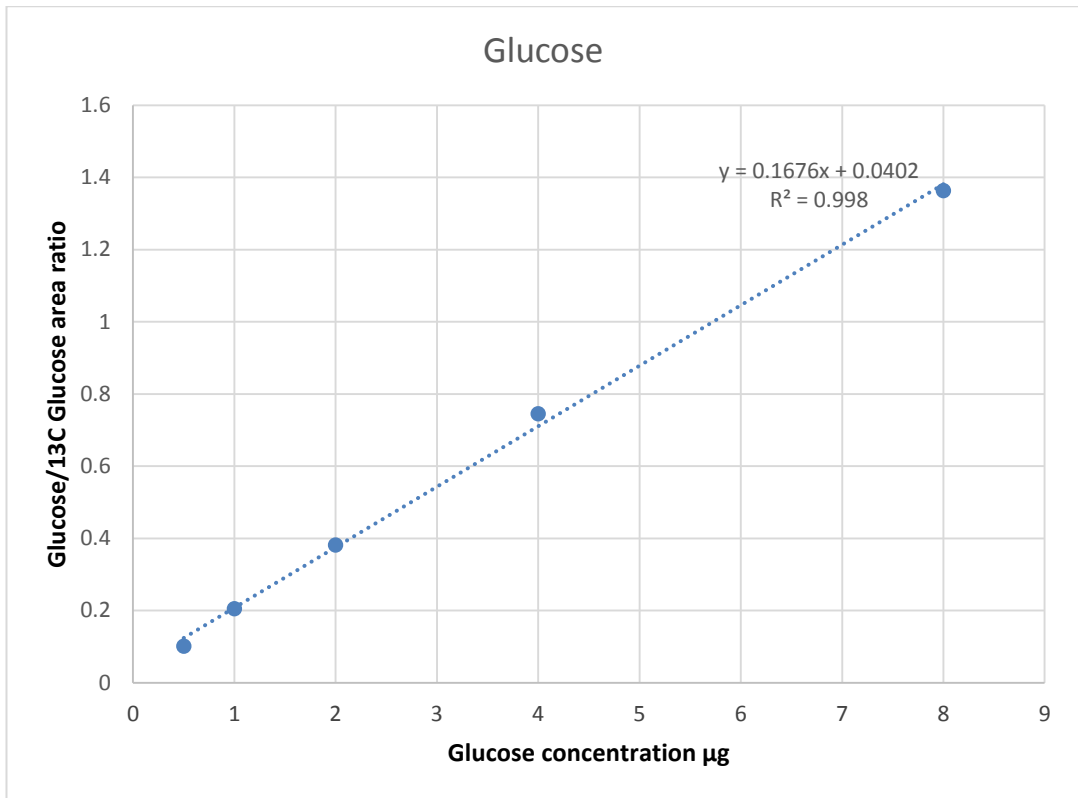


Figure 5-6: Calibration curve for glucose (0.5-8.0μg).

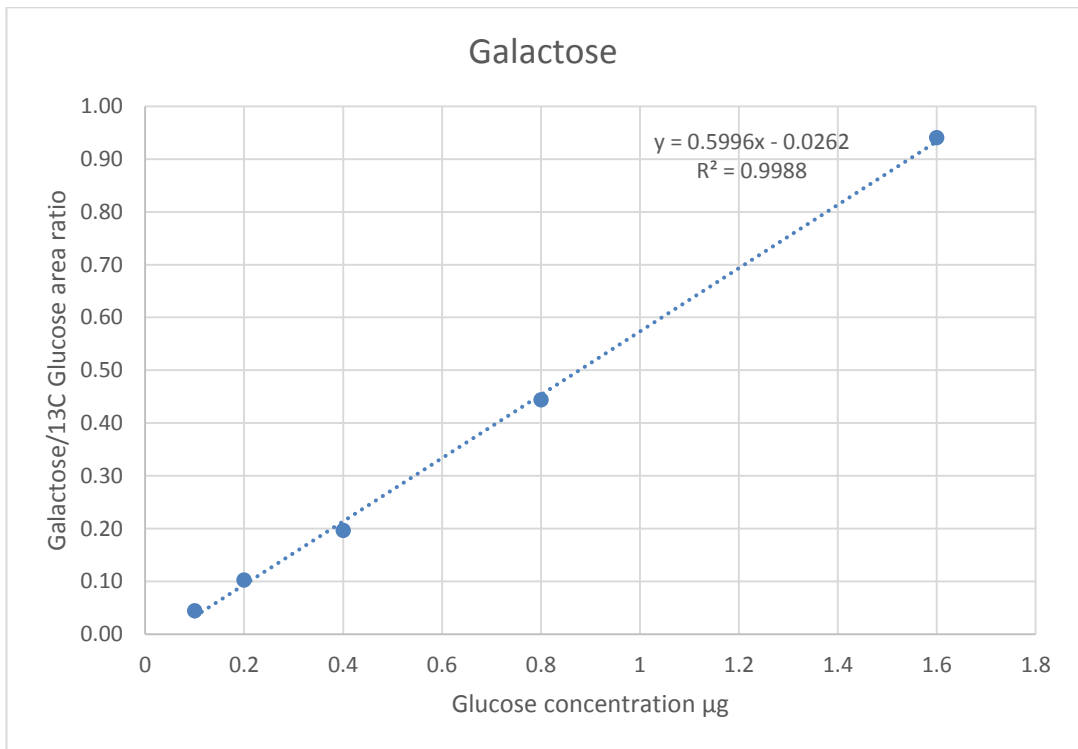


Figure 5-7: Calibration curve for galactose (0.1-1.6μg).

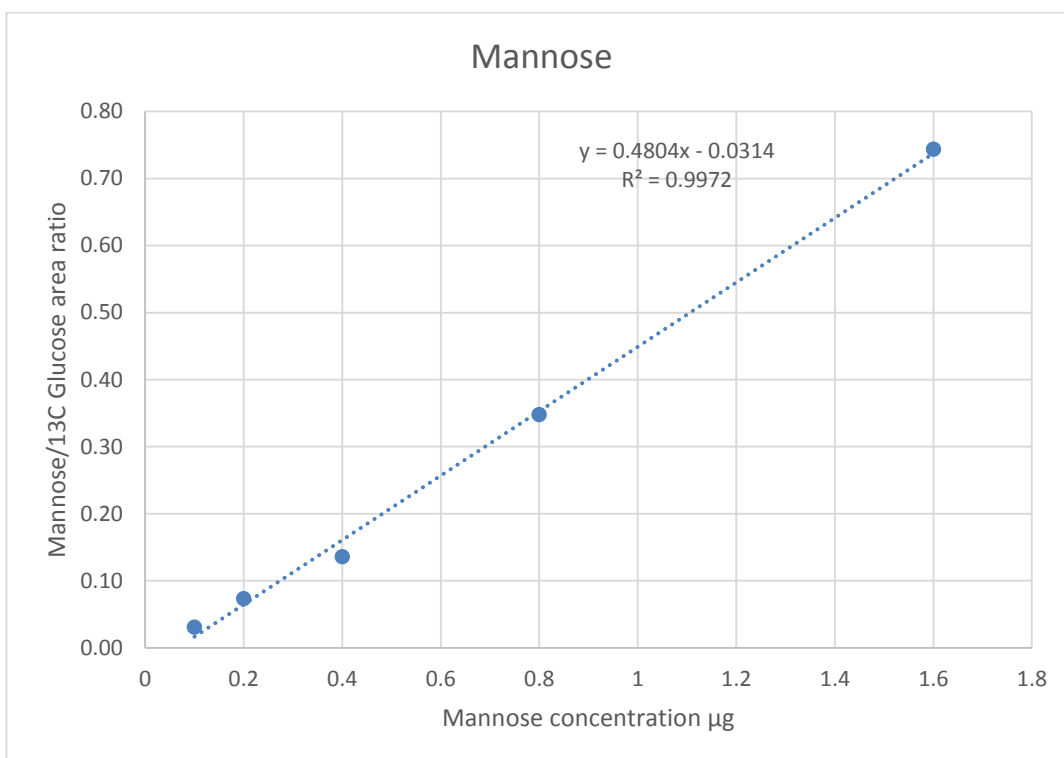


Figure 5-8: Calibration curve for mannose (0.1-1.6μg).

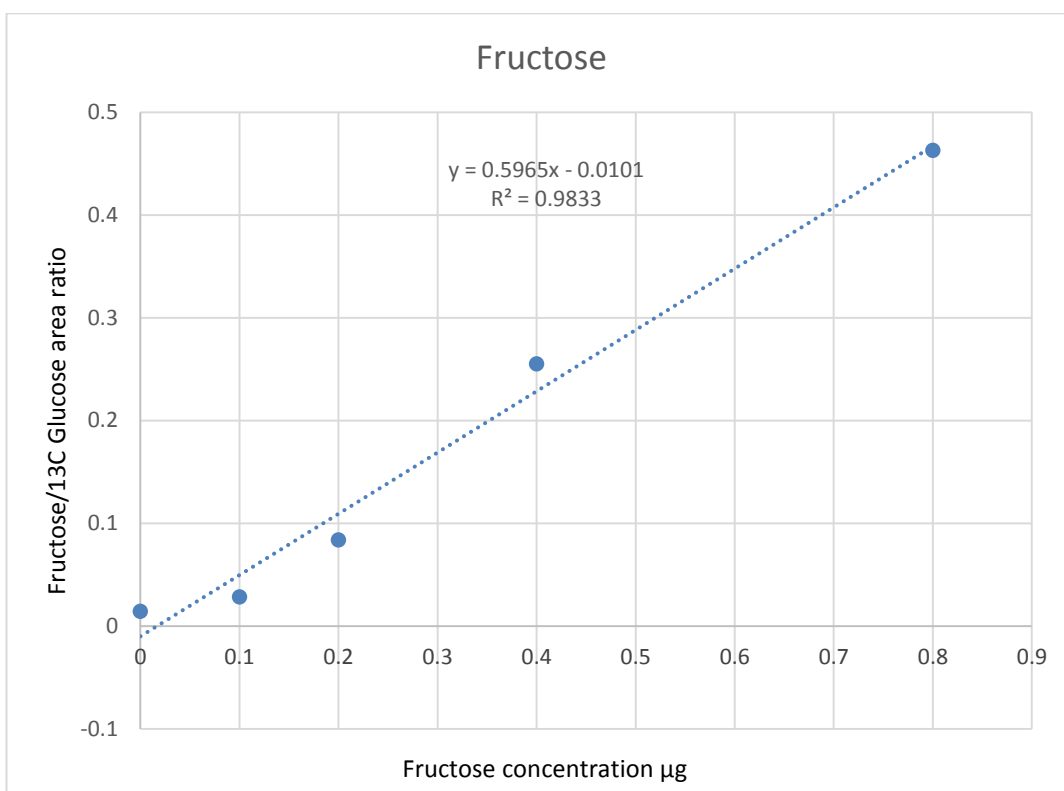


Figure 5-9: Calibration curve for fructose (0.1-1.6μg).

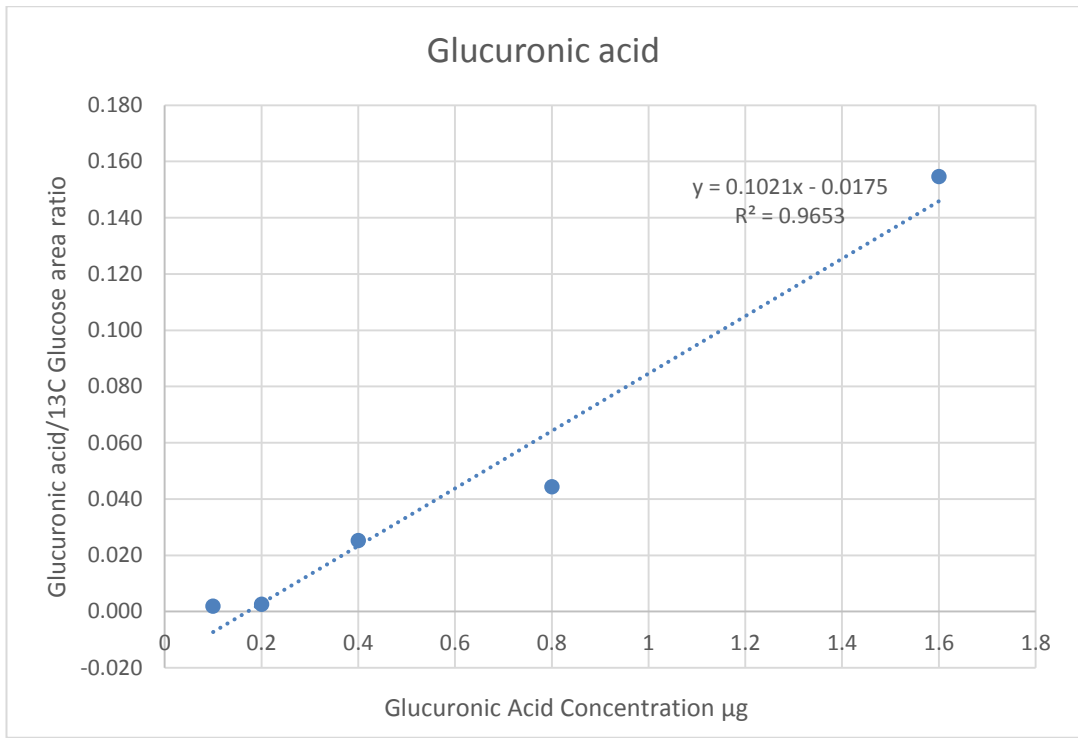


Figure 5-10: Calibration curve for glucuronic acid (0.1-1.6μg).

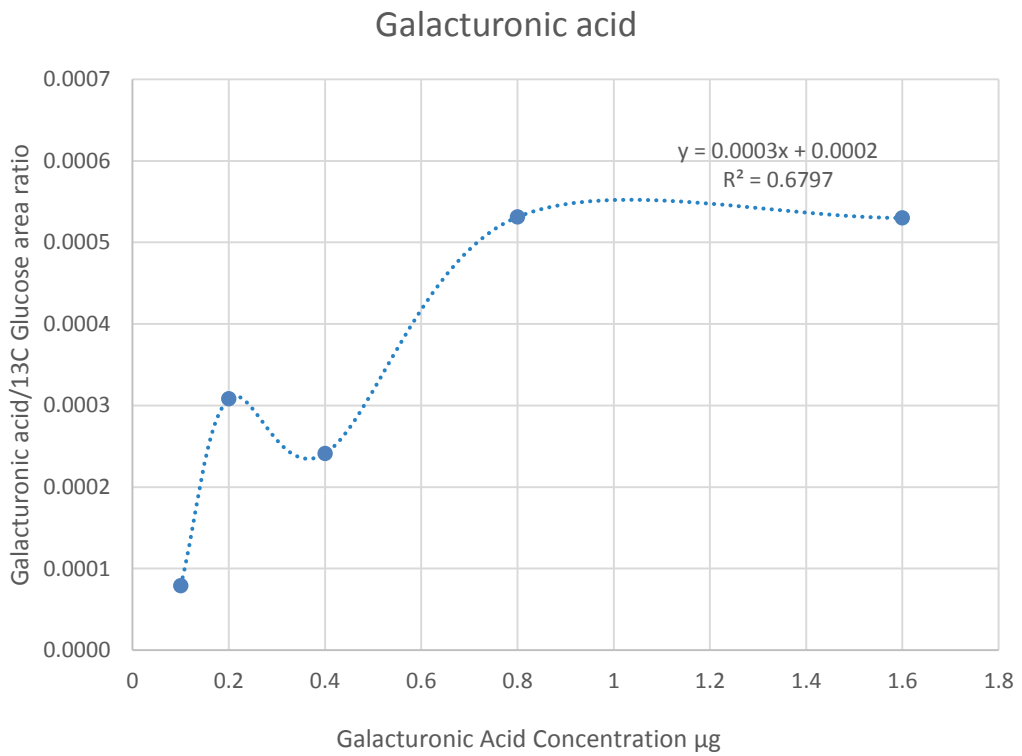


Figure 5-11: Calibration curve for galacturonic acid (0.1-1.6μg)

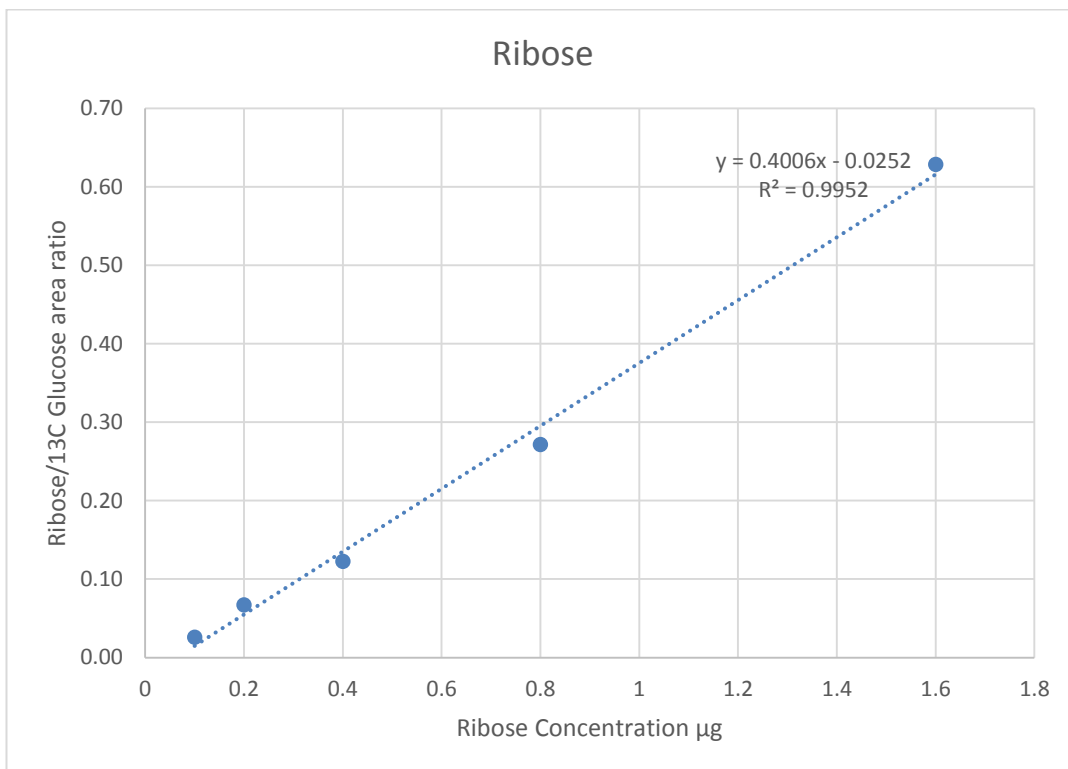


Figure 5-12: Calibration curve for ribose (0.1-1.6 μg).

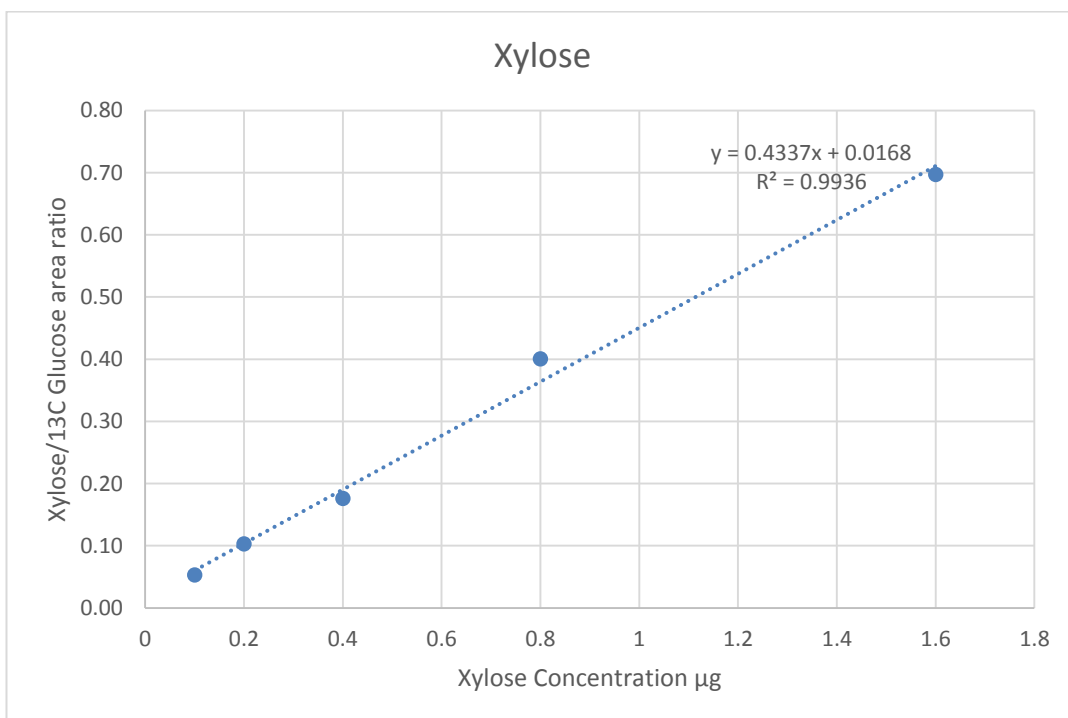


Figure 5-13: Calibration curve for xylose (0.1-1.6 μg).

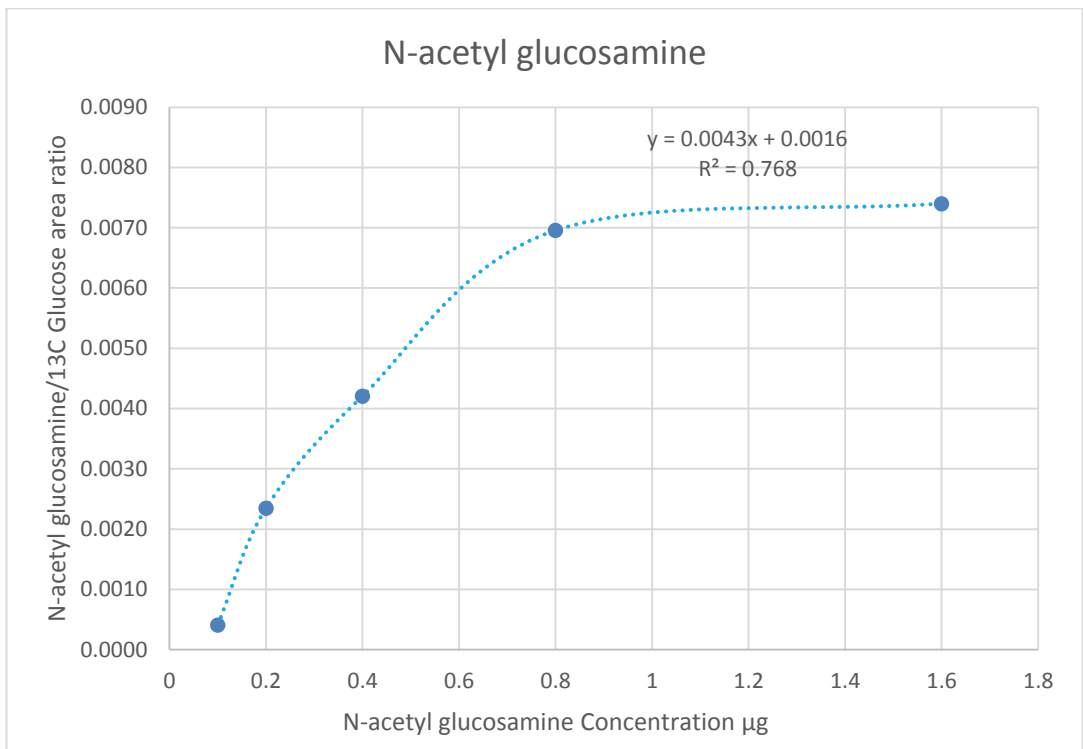


Figure 5-14: Calibration curve for N-acetyl glucosamine (0.1-1.6μg).

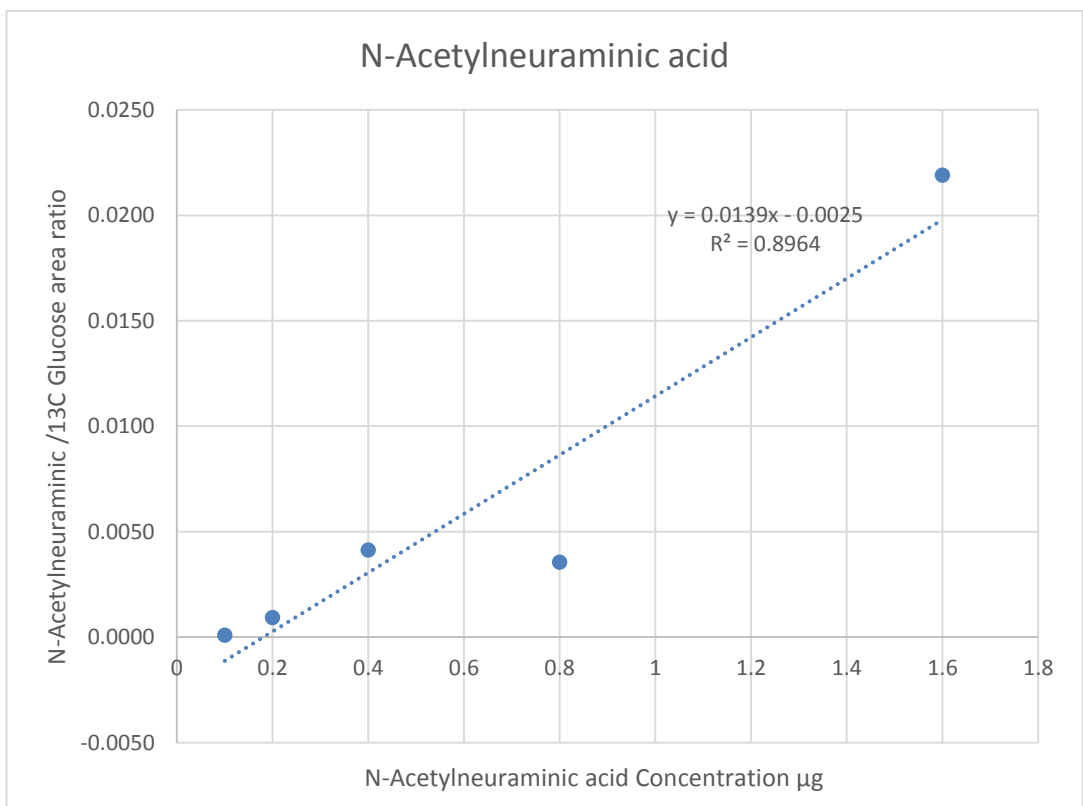


Figure 5-15: Calibration curve for N-acetylneuraminic (0.1-1.6μg).

Table 5-3 shows the calibration data for some sugar derivatives obtained by plotting the ratio of the peak-area ratio for each hexose against the $^{13}\text{C}_6$ -glucose (analyte to InS) in the range 0.1–1.6 μg . These data, the coefficient of regression (R^2 on chart) and the regression equation on chart (slope and intercept values), were extracted from the calibration curves for examined sugars as shown in Figures 5-6 – 5-15 to evaluate the linearity of method. It is clear that the hexoses and pentoses react much more efficiently with the tag than the sugar acids and amino sugars. The LC/MS-based developed reductive amination method was applied to measure the amount of sugars tagged with deuterated aniline in mental illness brain (SDB) samples. The derivatised sugar levels in 200 mg of control and SDB brain tissue which are summarised in Table 5-4 were quantified based on slope and intercept values obtained from calibration (standard) curves.

Table 5-3: Calibration data based on ratio of response of derivatised sugars to response for derivatised internal standard (^{13}C -glucose) over the range 0.1-1.6 μg .

Sugars	Equation of the line	(R^2)
Glucose	$y = 0.1676x + 0.0402$	0.998
Galactose	$y = 0.5996x - 0.0262$	0.9988
Mannose	$y = 0.4804x - 0.0314$	0.9972
Fructose	$y = 0.5965x - 0.0101$	0.9833
Glucuronic acid	$y = 0.1021x - 0.0175$	0.9653
Galacturonic acid	$y = 0.0003x + 0.0002$	0.6797
Ribose	$y = 0.4006x - 0.0252$	0.9952
Xylose	$y = 0.4337x + 0.0168$	0.9936
N-acetyl glucosamine	$y = 0.0043x + 0.0016$	0.768
N-acetyl neuraminic	$y = 0.0139x - 0.0025$	0.8964

Table 5-4: Summary table showing amount of the major sugars tagged with of ²H₅- aniline in 200mg of control, and SDB brain tissue.

Samples	Glucose μg/200mg	Galactose μg/200mg	Mannose μg/200mg	Glucuronic acid μg/200mg	Ribose μg/200mg	N-acetyl neuraminic μg/200mg
B1	18.93	4.12	234.6	7.77	11.86	8.52
B2	97.16	1.18	417.75	43.13	35.14	50.83
B3	170.34	3.97	52.48	2.62	18.02	51.8
B4	481.85	4.29	322.7	12.61	35.4	69.89
B5	297.33	10.42	116.76	8.45	43.22	120.37
B6	161.44	1.46	316.35	11.8	15.32	43.3
D1	115.08	2.48	43.75	2.88	18.15	29.64
D2	501.26	2.05	548.25	10.15	33.22	60.78
D3	243.27	12.08	207.07	53.01	72.05	127.11
D4	199.6	0.78	192.14	25.86	19.18	26.4
D5	50.08	0.69	34.21	9.27	10.75	42.36
D7	197.81	1.55	478.66	24.35	33.72	205.47
S3	107.89	0.58	446.45	46.01	18.63	60.77
S4	97.67	0.48	89.85	5.28	12.67	30.76
S7	245.12	2.06	90.41	8.58	29.09	432.48
S8	238.36	1.48	340.83	5.26	31.88	123.29
S9	71.88	0.47	187.23	16.79	9.62	19.1
S10	307.64	1.05	564.03	6.02	22.73	225.42
C1	25.54	0.75	32.02	3.37	20.71	68.47
C2	10.18	3.61	81.72	6.55	24.84	56.73
C3	27.56	5.93	37.95	17.69	42.08	83.47
C4	8.39	1.74	15.86	3.81	18.22	62.14
C16	7.31	0.66	74.73	6.21	12.15	41.47
C20	12.76	2.54	72.06	8.69	26.74	42.27

Table 5-5 shows the average of the concentrations of major sugars in C and brain sample groups (SDB). The p-value (t-test) and the peak-area ratio of each analyte in SDB to C are also summarised in Table 5-5. The major hexoses which could be observed in the brain samples were glucose, galactose, mannose and ribose. Figures 5-16 and 5-17, respectively, show extracted ion traces for hexoses (glucose, galactose and mannose) and pentose (ribose) extracted from post-mortem human brain. The level of glucose in the three groups of brain samples (SDB) in all cases is higher than the C brains, where the bipolar brains contained a huge amount (up to 217.85 $\mu\text{g}/200\text{mg}$, Table 5-5) which was far above the range of calibration curve and it was unfortunately not possible to re-calibrate because of lack of further samples of tissue. The glucose levels in the bipolar brain samples fluctuate widely and a larger sample number would be required to achieve a statistically significant comparison. Mannose and galactose levels are much more consistent in the C samples in comparison with the SDB brain samples (Table 5-5). The pentose sugar, ribose, also was elevated in depression (31.18 $\mu\text{g}/200\text{mg}$) and bipolar (26.49 $\mu\text{g}/200\text{mg}$) brain samples in comparison with control samples (24.12 $\mu\text{g}/200\text{mg}$). In addition, it was possible to observe several other sugars in the brain samples including NANA and glucuronic acid, which matched the retention times of their derivatised standards (Table 5-1), three isomers of NAG one of which matched the standard for this compound, an abundant deoxy hexose and two isomers corresponding to reductive amination products probably derived from the ketone sedoheptulose (Figure 5-18).

Table 5-5: Summarises the average of the amounts of hexose, pentose, NANA and gluconic acid in post-mortem brain samples with schizophrenia, depression, bipolar and control.

Sugars	Glucose	Galactose	Mannose	Glucuronic acid	Ribose	Xylose	NANA
Average C µg/200mg	15.29	1.02	52.39	7.72	20.77	50.28	51.45
Average B µg/200mg	217.85	4.24	243.44	14.40	26.49	66.56	59.09
B/C Ratio	14.248	4.157	4.647	1.865	1.276	1.459	1.148
P-Value	0.0240	0.0639	0.0184	0.3284	0.3962	0.4536	0.9232
Average D µg/200mg	204.51	3.27	250.68	20.92	31.18	66.83	81.96
D/C Ratio	13.375	3.208	4.785	2.710	1.501	1.465	1.387
P-Value	0.0368	0.2650	0.0754	0.1389	0.3195	0.4881	0.4727
Average S µg/200mg	178.09	2.54	286.47	14.66	24.12	48.26	148.64
S/C Ratio	11.648	2.488	5.468	1.899	1.161	1.058	2.515
P-Value	0.0093	0.1270	0.0325	0.3508	0.5566	0.9149	0.2257

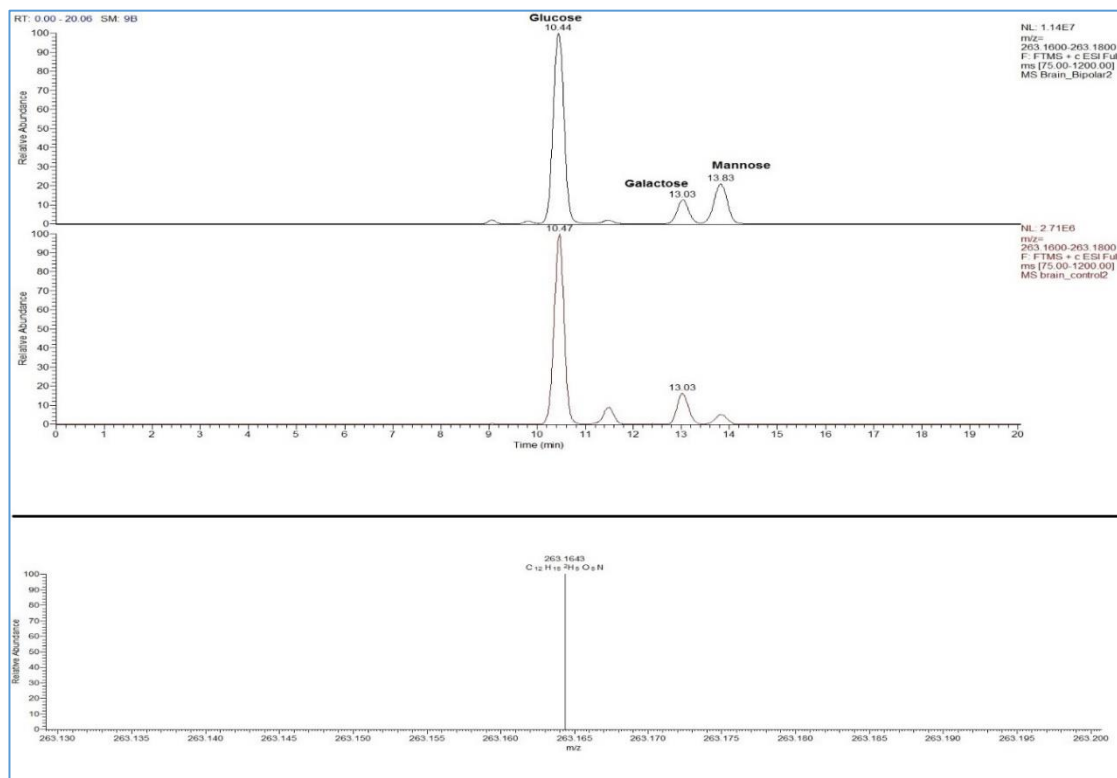


Figure 5-16: Hexoses extracted from brain tissue obtained from an individual with bipolar disorder and a control sample.

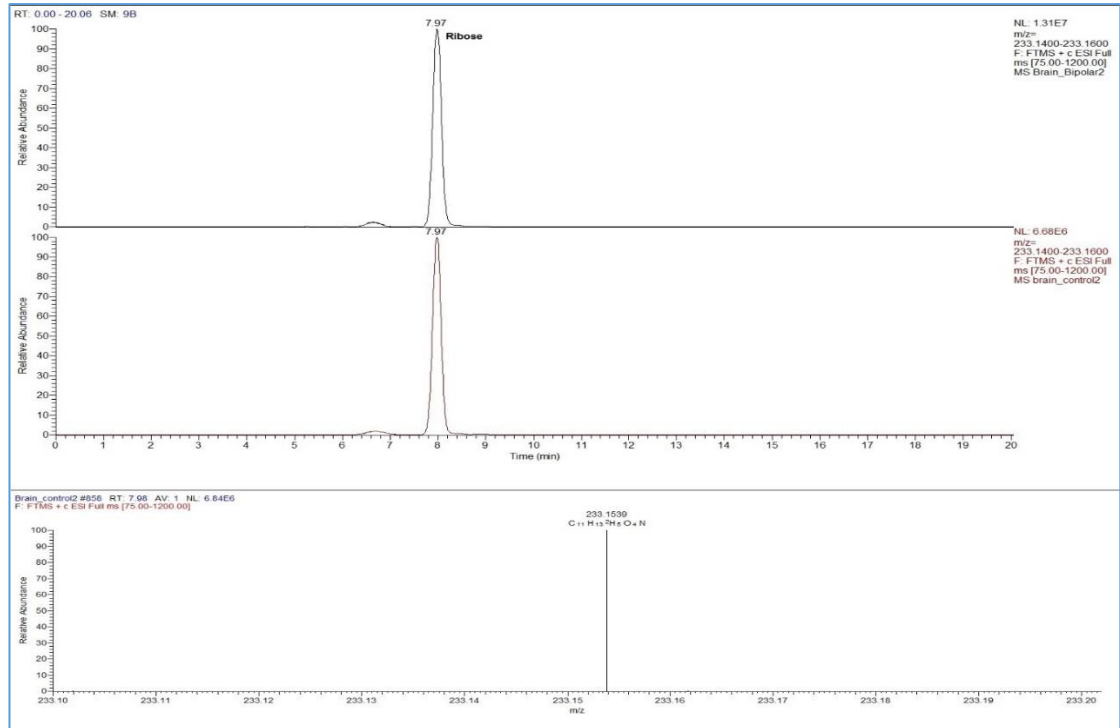


Figure 5-17: Pentose extracted from brain tissue obtained from an individual with bipolar disorder and a control sample.

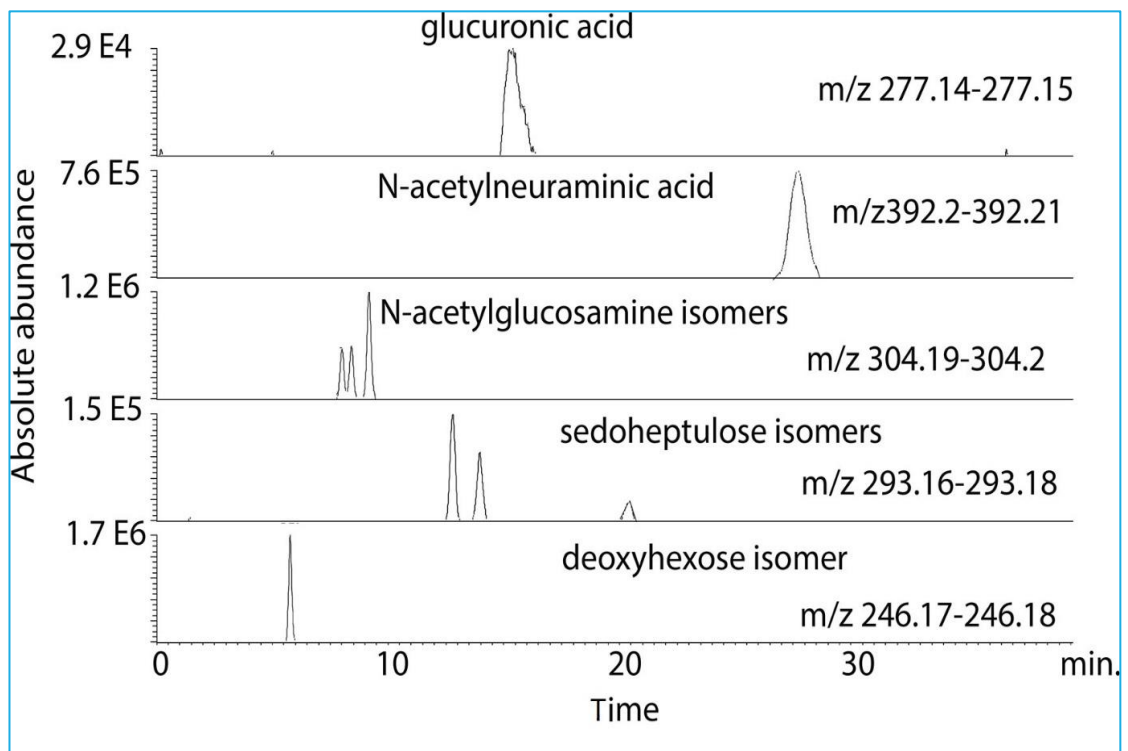


Figure 5-18: Additional sugar isomers extracted from brain tissue obtained from an individual with bipolar disorder

5.4 Discussion:

Separation of sugar isomers by LC methods is difficult and has not often been achieved for even a small set of isomers like the four common hexoses. Capillary GC-MS methods have higher chromatographic resolving power than LC-MS methods and can be applied to separation of sugar isomers. However, even when using capillary GC separation sugar isomers elute closely and this is complicated by the fact that the commonly used oximation procedures produce two peaks for each aldose (Molnár-Perl and Horváth, 1997, Boldizsar *et al.*, 1998, Medeiros and Simoneit, 2007). The electron impact fragmentation patterns for derivatised sugars obtained from GC-MS analysis are not very informative and are thus not conducive to uncovering the presence of new sugars whereas under positive ion ESI conditions most of the ion current is associated with the molecular ion giving better specificity and sensitivity. The precision of the method for the four common hexoses was determined by carrying out the analysis of five aliquots taken from control and bipolar brain samples as described recently in our paper (Bawazeer *et al.*, 2017). It reported that the best precision was obtained for glucose, where the concentrations were higher and the internal standard closely matched the properties of the analyte, compared with another sugar, galactose, which gave poorer precisions as specified by Food and Drug Administration (FDA) guidelines for bioanalysis (Health and Services, 2001). According to this precisions, the high levels of glucose and mannose and the slight elevations of galactose level in the present results, based on 18 SDB brain samples support the ability of the tagging method to quantify sugar concentrations in biological samples. It also has ability to uncover further unknown patterns, there is at least one additional unknown hexose, as illustrated in the human brain extracts shown in Figures

5-16 and 5-17. Fructose is a ketone, ketonic monosaccharide, and thus is reduced less readily than the other sugar aldehydes, aldohexoses, and this probably accounts for the poorer precision obtained for this analyte. Thus, if accurate quantification of fructose were required, it would be better to employ a stable isotope labelled form of fructose as an internal standard. Therefore, although it was one of the four common hexoses separated by this method and has good linearity ($R^2= 0.9833$), fructose was not quantified in this work.

In addition, elevated levels of a pentose, ribose and xylose, were observed in some the SDB post-mortem brain samples, but did not achieve statistical significance. The elevated level of the pentose mirrored the elevation in the levels pentitols observed in our earlier paper (Zhang *et al.*, 2016) as described in Chapter four in this thesis. Since high-resolution mass spectrometry is used in combination with a tag containing the five deuterium atoms, it is possible to be very sure of the identity of such unknowns although without a standard the exact isomer remains unknown. The results also indicated an increase in level of other sugars including NANA and glucuronic acid in three mental illness groups (SDB). The level of NANA in S and D brain samples was far higher than B samples in comparison with C although again wide fluctuations meant the differences were not statistically significant. Due to its essential role in appropriate adult brain development, NANA biosynthesis and more subtle mutations in its metabolism may be associated with psychiatric disorders including S and B disorder (Schnaar *et al.*, 2014). A current results are similar to other studies which reported that the elevation of NANA levels were found in CSF and post-mortem brain samples of schizophrenic patients and other psychiatric disorders such as D and B (Sullivan *et al.*, 2007, Schnaar *et al.*, 2014, Vawter, 2000).

Based on the goodness of linearity for eight from ten calibration curves of sugars as described in Table 5-3, only two sugar derivatives were excluded from the quantification; galacturonic acid ($R^2=0.6797$) and NAG ($R^2=0.768$).

5.5 Conclusion

The present study confirms that the reductive amination method provides a sensitive and specific mechanism for probing sugar metabolism as part of a metabolomics workflow for uncovering biomarkers in clinical and biological samples. The deuterated tag as well as offering the best chromatographic separation was also useful in the characterisation of sugars and succeeded in providing a quantitative estimate to quantify the changes of sugar levels in post-mortem brain samples. This method is able to achieve separation of the three common hexoses which is rare in the literature and has very good potential for monitoring sugar metabolism since the masses of the tagged sugars are very characteristic. Due to the importance of sugar metabolism, the present results have highlighted the relationship between the rises in the levels of sugars and their derivatives and psychiatric disorders including schizophrenia, depression and bipolar. This relation which matched with other studies once again supported our previous results. For future work, altered metabolism of sugar polyols in post-mortem mental illness brain can be examined in non-post mortem samples to explore whether anti-diabetic treatments may have a role in the management of SDB.

CHAPTER 6

DEVELOPMENT OF AN LC-MS METHOD FOR THE ENHANCED DETECTION OF OXIDISED FATTY ACIDS IN PLASMA AND ITS APPLICATION TO DETERMINE THE EFFECTS OF THE INGESTION OF THE ANTI-OXIDANT BEETROOT JUICE

Abstract

Fatty acids and other metabolites containing a carboxyl group are of high interest in biomedicine because of their major role in metabolic pathways. Tagging of carboxylic acid compounds with a permanent positive charge such as with a quaternary ammonium compound will increase the LC-MS detection sensitivity and selectivity. This study pursued a new strategy for analysing carboxyl-containing compounds in biological samples by LC-MS by coupling them to choline. Carboxylic acids were coupled to choline using 2-fluoro-methyl-pyridinium p- toluene sulfonate (FMP) coupling reagent. The analysis of the derivatised oxidised fatty acids was performed by using ACE-HPLC (C18) column coupled with an Orbitrap Exactive mass spectrometer. Twenty-eight plasma samples which were collected from seven participants before and after taking of beetroot juice, which is a potential antioxidant, were examined by the developed method to quantify the oxidised fatty acids. The results showed that choline coupling reactions were successful in determining oxidised fatty acid metabolites in biological samples. In conclusion, a new and easy method was developed to enhance detection of carboxylic acid derivatives in plasma samples following consumption of beetroot juice. The method proved to be precise and reproducible and can quantify oxidised fatty acids compounds up to below ng/ml levels.

6.1 Introduction

Carboxylic acids are one of the most common organic compounds that present in living organisms, human, animals and plant. Fatty acids (FAs) mainly refer to the metabolites that possess single or multiple carboxyl groups (-COOH) and serve important functions in many biochemical processes inside the body and cells. In biomedicine, fatty acids and other carboxylic metabolites are of high interest because of their major role in metabolic pathways. Monitoring of carboxylic compounds, particularly fatty acids, has been contributed in understanding the aetiology of many diseases and prevention of chronic disease such as atherosclerosis, obesity induced insulin resistance and for promoting cardiovascular health (Joffe *et al.*, 2013, Soardo *et al.*, 2011, Morgan *et al.*, 2016). Although many lipids are produced in the body by simple precursors, some essential fatty acids (EFAs) cannot be synthesised and should therefore be consumed with the diet. Oxylipins or oxidised fatty acids are a group of metabolites derived from polyunsaturated fatty acids (PUFA), and include arachidonic acid (ArA) and linoleic acid (LA). They can be formed by the reactions depending on mono- or dioxygen and occur as hydroxy, dihydroxy, epoxy and oxo species. One of the challenges of nutrition studies is the determination of subtle shifts in the fatty acids or bioactive lipids, especially the oxylipins, because they are unstable and/or rapidly inactivated by metabolic degradation and have a low concentrations and similar structures, resulting in isomers (Yang *et al.*, 2009).

Due to the important role of fatty acids in human metabolic changes, investigation of their physiological and clinical implications in human health is necessary in pathological and healthy conditions. Many instrumental techniques included GC (Eder, 1995) and HPLC (Chen and Chuang, 2002) have been applied in the analysis

of carboxylic acid and related compounds. The most common separation techniques, GC and LC, have been improved based by combination with tandem mass spectrometry (MS). In the field of bioinformatics, LC-MS and GC-MS approaches have been developed to be a simple and fast analytical methods for low molecular weight carboxylic acids and have provided rapid progress for omics research (Gamoh *et al.*, 2003, Hernández-Pérez *et al.*, 2002).

However, these methods lack sensitivity and selectivity in analysis of fatty acids. Sample derivatisation is widely used in analytical chemistry and instrumental analysis to improve analytical capabilities. The chemical structure of the sample can be modified to new chemical form that provides an enhanced response in terms of either improved selectivity or sensitivity. This modification is required because the response factors for the positively tagged fatty acids were more 100 times than those for the untagged compounds in negative ion (Ko and Brodbelt, 2012).

6.1.1 Derivatisation in Mass Spectrometric Analysis

The separation and quantification of important compounds, such as carboxylic acids, which are present in small amounts in biological samples is a major problem in different metabolomics studies. Due to their important functions in many biochemical processes inside the body and cells, carboxyl-containing metabolites, mainly fatty acids and their oxidation products, are the most common organic compounds in living organisms. Therefore, enhancing of accurate and sensitive liquid chromatography methods is necessary in determination of very small quantities of these compounds in biological specimens. For enhancing of the sensitivity of chromatography

performance, chemical derivatisation has been found to be a powerful technique in making these metabolites more ionisable in the LC-MS approach.

Derivatisation reactions used in MS are designed to enhance ionisation or introduce a specific mass shift to the sample ions that becomes evident in the mass spectrum. Many MS derivatisation reports are present in the literature (Zaikin and Halket, 2006, Qi *et al.*, 2014, Halket *et al.*, 2005). Traditional derivatisation by silylation or methylation in GC-MS methods was employed in the analysis of fatty acids (Brooks *et al.*, 1978). Recently, with the invention of soft ionisation techniques such as electrospray ionisation HPLC/ESI-MS, derivatisation has become a powerful technique in the analysis of such compounds. The negative ionisation of carboxylic acid in LC-MS is only achieved in basic mobile phase. However, chromatographic resolution with reversed-phase columns is best achieved at acidic pH mobile phases where the ionisation of carboxyl group is suppressed. The alternative way is to tag carboxylic acid with a permanent positive charge such using a quaternary ammonium compound. This will cause targeted carboxylic acid compounds to have a positive charge in both acidic and alkaline mobile phases. This strategy has been very successfully applied in the HPLC/ESI-MS analysis of amino acids and peptides (Ko and Brodbelt, 2012, Frey *et al.*, 2008).

The technique of chemical derivatisation for LC-MS seen a continuous growth and progress in the technique for the analysis of a variety of compounds that were difficult to analyse without chemical derivatisation. The aim of derivatisation is to introduce a moiety into the structure resulting in the modification of the structure of the target compound changing their physical and chemical properties so that they are more ionisable in the LC-MS system. Derivatisation is a specific type of chemical reaction

which for its completion needs a functional group present on the target compound and a reactive group in the derivatisation reagent. In addition to the reagent should be effective and selective, the derivatisation reaction should not be very long and the resultant product should be stable.

Choline is chemically known as 2-hydroxyethyl-azanium (2-hydroxyethyl-trimethylamin) and it is a quaternary ammonium salt containing the N,N,N-trimethylethanolammonium cation. It was recently found that a choline chloride-based catalyst was employed as green approach for the amidation of methyl esters of fatty acids under solvent free system (Patil and Pratap, 2016).

Due to the roles of lipids such as oxylipins that are formed by oxidation is still poorly understood, a lot of research deals with the development of suitable methods for profiling oxylipins in order to better understand their influence on the regulation of various biological processes. It would be useful to develop LC-MS method for the enhanced detection of these compounds in plasma and its application to determine the effects of the ingestion of the anti-oxidant beetroot juice. Thus, the quaternary ammonium part of the coupled choline is the alternative way to negative ion ESI mass spectrometry to tag carboxylic acid and makes the derivatised compound permanently ionised in both acid and basic mobile phases.

6.1.2 Aim of the Study

The overall aim of this work was to develop strategy for analysing carboxyl-containing compounds, particularly oxidised fatty acids, in biological samples by soft ionisation (ESI) LC-MS after being coupled to choline. The advantage of this strategy is the

efficacy of chemical derivatisation applied utilising choline to quantify the oxylipin metabolites related to nutrition in human plasma samples.

6.2 Materials and Methods

6.2.1 Chemical and Materials

HPLC grade ACN, tetrahydrofuran (THF) and formic acid were purchased from Sigma Aldrich, Dorset UK. Also, the reagents including 2-fluoro-1-methyl-pyridinium p-toluene sulfonate (FMP), triethyl amine (TEA), and choline chloride were obtained from Sigma Aldrich, Dorset UK. The native standard mixtures of oxidised fatty acids included the linoleic acid oxylipins mixture (LAO) and arachidonic acid oxylipins (ArAO) mixture. The native standard mixture of LOA contains oxylipin metabolites derived from linoleic acid including (\pm)12(13)-DiHOME, (\pm)9(10)-DiHOME, 9(s)-HODE, 13(s)-HODE, 13-OxoODE, 9-OxoODE, (\pm)12(13)-EpOME, and (\pm)9(10)-EpOME. The native standard mixture of ArAO contains oxylipin metabolites derived from arachidonic acid including 5-OxoETE, 12-OxoETE, 15-OxoETE, 15(S)-HETE, 12(S)-HETE, 11(S)-HETE, 9(R)-HETE, 8(S)-HETE, and 5(S)-HETE. Internal standards mixture included deuterated linoleic acid oxylipins (DLAO), contains deuterated (^2H) versions of oxylipin metabolites derived from linoleic acid included (\pm)12(13)-DiHOME-d4, 13(s)-HODE-d4, 13-OxoODE-d4, and (\pm)12(13)-EpOME-d4. LAO, ArAO and DLAO compounds were purchased from Cayman Chemical Company. Their product information are described on company website [<https://www.caymanchem.com>] in products Item № 20794, Item № 20666 and Item № 20795, respectively. HPLC grade water was produced by Direct-Q 3 Ultrapure Water System from Millipore, UK

6.2.2 Plasma Samples Collection:

Human plasma samples were collected from seven males healthy individuals (age 28 ± 4 years, stature: 181 ± 8 cm, body mass: 83.4 ± 10.4 kg) at four different time points (baseline, 60min, 120min and 360min) in the same day after beetroot ingestion as shown in Figure 6-1. After it was separated from collected blood and centrifuged at 5000rpm for 10min, plasma samples were stored at -25°C to be used in preparation of plasma solution which will be transferred later to oxidised acids derivatives procedure. The written informed consent and a medical questionnaire to all participants was approved by the ethics committee of at the School of Science and Sport, University of the West of Scotland. Before the study began, participants were excluded if they were currently taking dietary supplements or any medication, regularly used mouthwash, smokers, had a current illness or virus within the previous month, had a known disorder or history of disorders of the hematopoietic system, and were hypertensive ($\geq 140/90$ mmHg) or had a family history of premature cardiovascular disease.

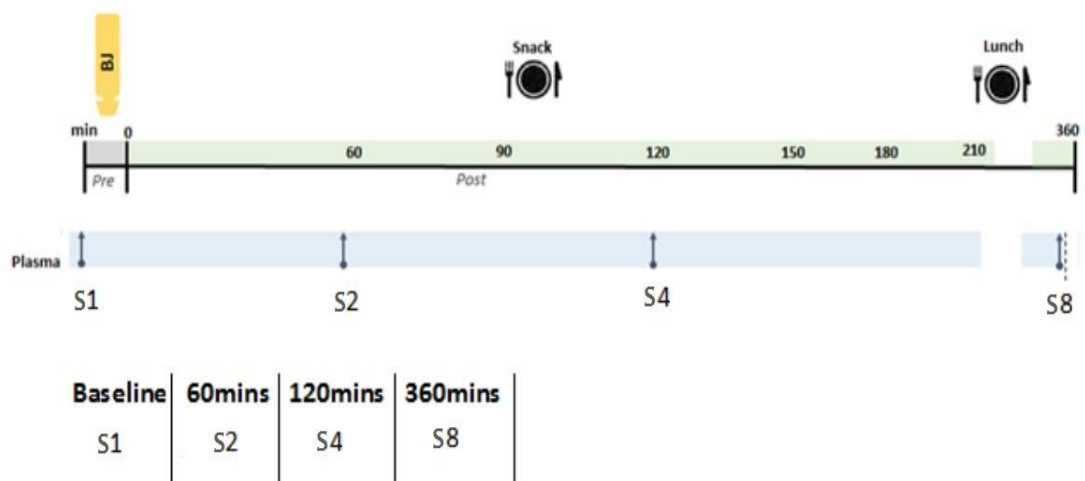


Figure 6-1: Scheme for the time-points of plasma collection.

6.2.3 Preparation of Plasma Solutions and Reagents

Plasma solutions were prepared by transferring 100µl of the separated plasma sample to an Eppendorf tube and adding 1ml of ACN to perform a protein precipitation (PPT) process. Then the sample was vortexed for two minutes and centrifuged at 9000 rpm for 10min. After centrifuging, the supernatant of plasma solution was taken for coupling reactions (Chambers *et al.*, 2007).

Also, the stock solutions were prepared for all the reagents of coupling reaction which included choline chloride and FMP. Choline chloride solution was prepared in ACN at original concentration of 1mg/ml. Stock solution of FMP coupling reagent were prepared at concentration of 1mg/ml with ACN as solvent.

6.2.4 Native and Internal Standards

Fatty acid standards included myristic acid, 1-tetradecanoic acid, and palmitic acid, hexadecanoic acid, were used in this study. The standard stock solutions were prepared at concentration of 10µg/ml in THF and stored at room temperature.

To increase the number of oxidised fatty acids measured simultaneously in a single analytical run, seventeen oxylipins in two different mixtures of the oxidised compounds, LAO and ArAO, were used as native standard (Table 6-S1). Also, internal standard mixture (DLAO) consisted of deuterated (2H) versions of four oxylipins metabolites derived from linoleic acid was added for distinguish among the isomers. LAO, ArAO and DLAO mixtures have been designed by Cayman Chemical Company at concentration of 10µg/ml in ethanol to be used directly as native standards and internal standards. All standard mixtures were kept in glass screw cap vials and stored at -80°C to prevent solvent evaporation.

6.2.5 Standard Curve Preparation

A calibration curve was made by diluting the stock solutions of oxidised fatty acids standards (10µg/ml) to prepare seven different batches (0.0, 2.5, 5.0, 10.0, 20.0, 40.0, 80.0, and 160.0 ng/100µl) as the native standard mixture of LAO and ArAO. For the purpose of quantification, 50ng/100µl of HODE-d4 was added to each batch as internal standard instead of DLAO mixture to avoid intervention between derivatised mass for other compounds.

These calibration solutions treated by using the choline coupling derivatisation reaction as described in section 7.2.6 in order to quantify the oxylipin metabolites of oxidised fatty acids.

6.2.6 Fatty Acids and its Oxidised Derivatisation

Choline esterification to the fatty acids was performed using the FMP coupling agent (Yang *et al.*, 2007). The reaction outline of the coupling of choline to acids and its oxidised by using FMP coupling reagent is illustrated in Figure 6-2. Oxidised acids standards mixture (100µL) and plasma solutions, as prepared in section 7.2.3, were derivatised with 100µL of choline chloride solution (1mg/ml in ACN) and 100µL of the stock coupling agent FMP (1mg/ml in ACN). Then 6µL of TEA is added to this mixture with shaking for 2min and heated by using the vortex water bath at 50°C for 30min. The combined mixture was then blown to dryness in a stream of nitrogen gas and re-dissolved in 1ml ACN prior to injection into the LC-MS.

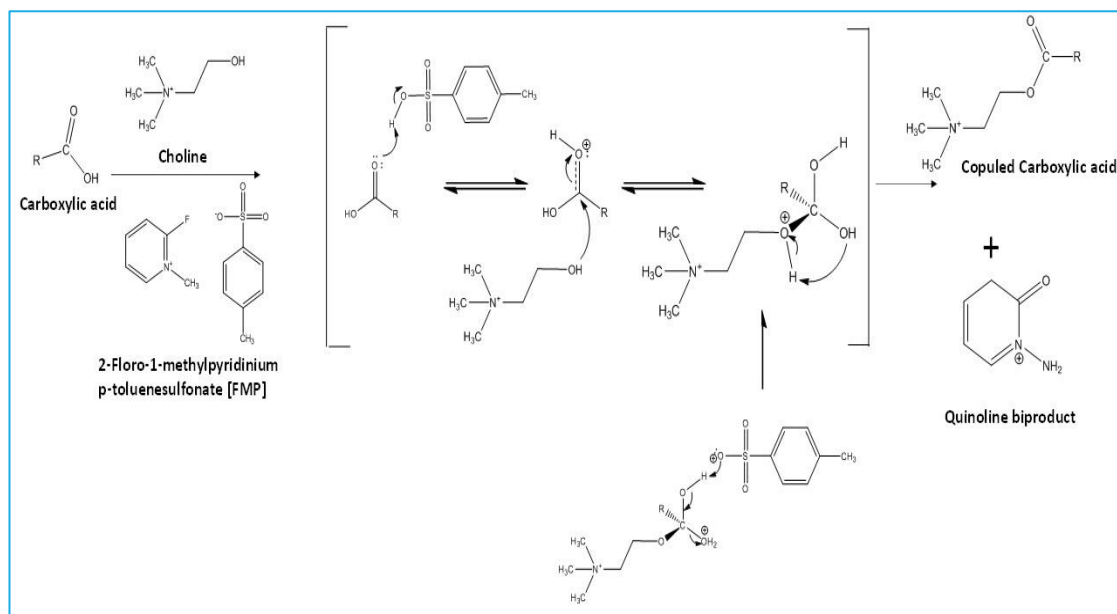


Figure 6-2: Choline coupling of carboxylic acids scheme.

6.2.7 LC-MS Analysis

Measurements of samples and standards was carried out on the Surveyor HPLC system combined with LTQ Orbitrap mass spectrometer (Thermo Fisher Scientific, Hemel Hempstead, UK). An aliquot of each sample solution (10 μ l) was injected onto an ACE 3 C18 column (150 x 3.0mm, 5 μ m Hichrom, Reading, UK) and the flow rate was 300 μ l/min. Mobile phase A consisted of 0.1% (v/v) formic acid in water and mobile phase B consisted of 0.1% (v/v) formic acid in ACN. The gradient used was as follows: 0 min 10% B, 10 min 90% B, 15 min 90% B, 16 min 10% B, 21min 10% B, the last 5min were for column re-equilibration before the next injection. The ESI interface was operated in positive ion mode with spray voltage of 4.5kv. The temperature in ion transfer capillary was 275 and the flow rate of the sheath and auxiliary gases were 50 and 17 arbitrary units. Some of the samples were also run on the LTQ Orbitrap to produce MS/MS spectra using a collision energy of 35 V. The full scan range was 75 to 1200m/z. The acquired data was processed by using Xcalibur™.

6.3 Results

6.3.1 Underivatised Oxidised Fatty Acids

A group of oxidised metabolites that are derived from various FAs, oxidised fatty acids, perform a variety of different functions in the human body. As a part of the lipidome, oxylipins as oxidised FAs were extracted and quantified in human plasma samples in previous studies (Gouveia-Figueira *et al.*, 2015, Yang *et al.*, 2009, Strassburg *et al.*, 2012). These studies have used UPLC-ESI-MS/MS techniques with only negative ion detection to examine the metabolites of regulatory lipids related to nutrition.

Under non-derivatisation conditions, the oxylipin metabolites derived from LAO and ArAO which are detailed in Table 6-S1 were examined. Table 6-S1 shows the name, molar mass and chemical formula and structure for these underivatised oxylipins.

Figure 6-3 illustrates extracted ion chromatograms obtained for the standard mixture of linoleic acid oxylipins by run without derivatisation on a C18 column. In the same way, the ion chromatograms of arachidonic acid oxylipins were extracted and are shown in Figure 6-4. In this method reversed phase liquid chromatography (RPLC) was used with ESI-MS with positive ion detection.

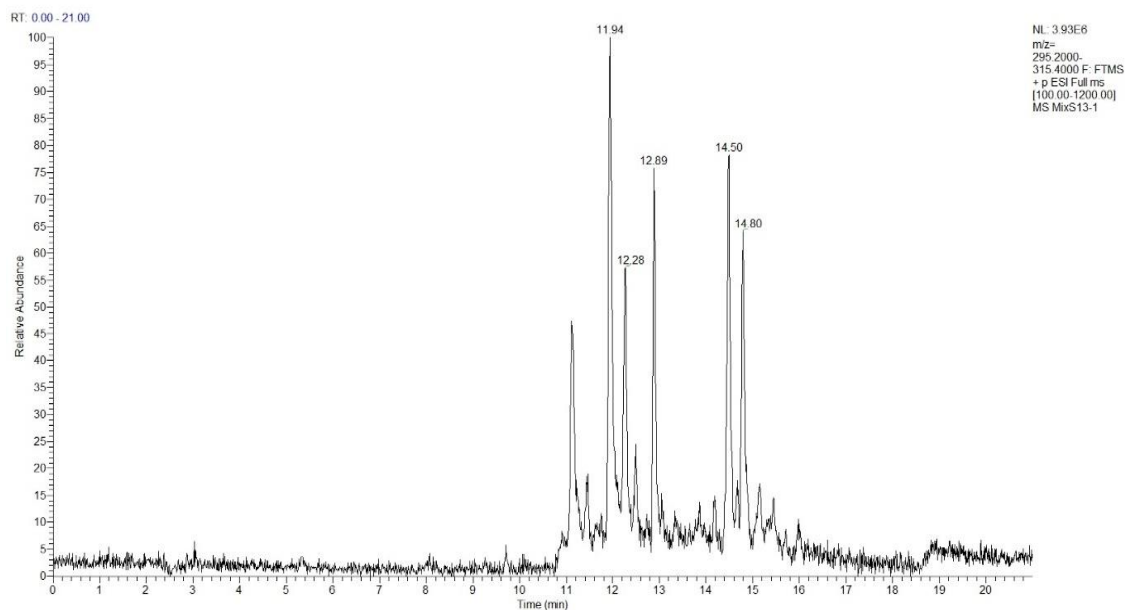


Figure 6-3: Extracted ion chromatograms for the standard mixture of LAO in positive ion mode by non-derivatisation LC-MS method on a ACE 3 C18 column (150 x 3.0mm, 5 μ m) with a gradient mobile phase between 0.1% (v/v) formic acid in water and 0.1% v/v formic acid in acetonitrile.

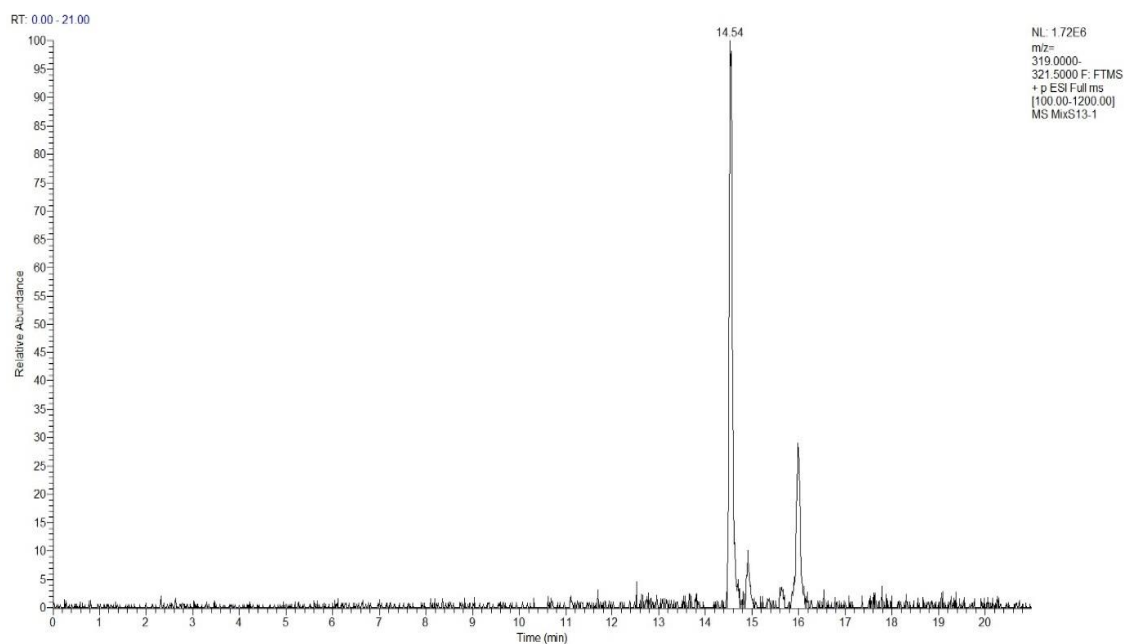


Figure 6-4: Extracted ion chromatograms for the standard mixture of ArAO in positive ion mode by non-derivatisation LC-MS method on a ACE 3 C18 column (150 x 3.0mm, 5 μ m) with a gradient mobile phase between 0.1% (v/v) formic acid in water and 0.1% v/v formic acid in acetonitrile.

6.3.2 Fatty Acids Derivatisation

The derivatisation approach was developed in order to enhance the detection of the oxidised fatty acids. In order to develop the method, hexadecanoic acid and tetradecanoic acid were coupled with choline by using the FMP coupling reagents procedure. The results showed that both saturated long-chain fatty acids (SLCFA) were successfully coupled with choline and were detected based on the exact mass of the coupling and the reaction outline as shown in Figure 6-5. It was found that the method worked best when a large excess of choline (100 μ g) was used. The results of carboxylic acid derivatisation method showed that the peak area and shape of FAs were better when the coupling was performed using the FMP. Extracted ion chromatograms and the mass spectral analysis for derivatives of FAs are illustrated in Figure 6-6 for palmitic acid, and Figure 6-7 for myristic acid.

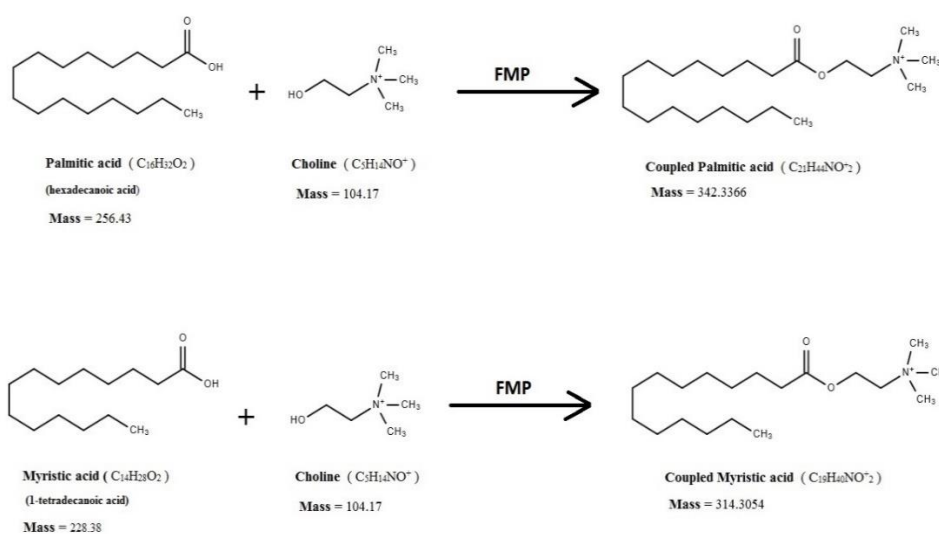


Figure 6-5: The coupling reaction outline and the exact mass of the coupled fatty acids, palmitic acid and myrestic acid after derivatisation method.

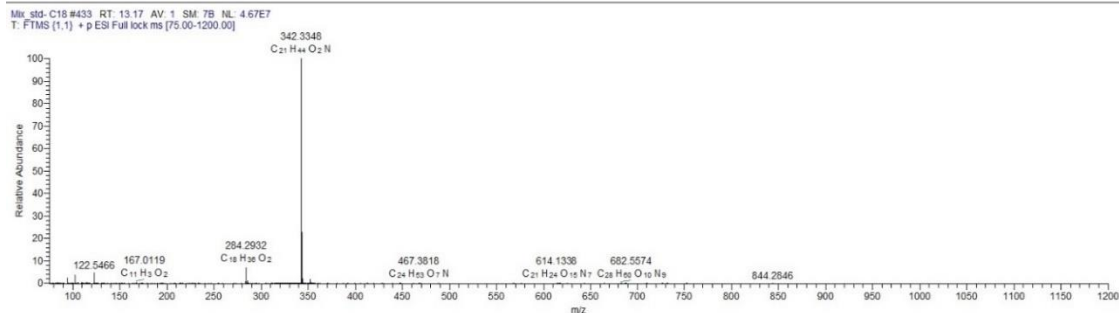
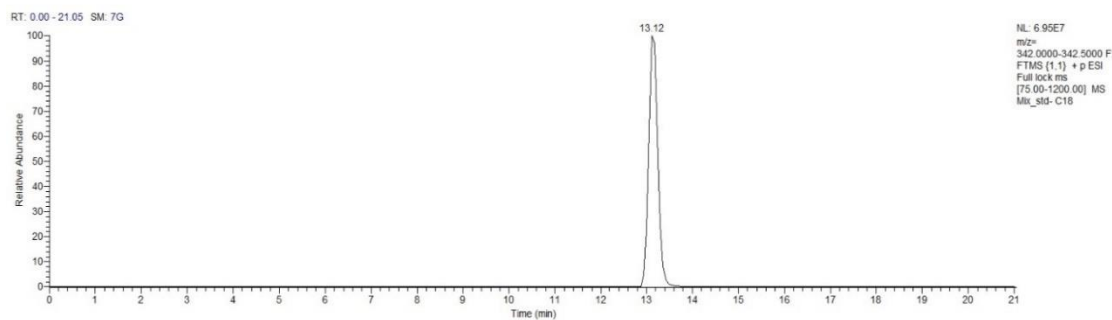


Figure 6-6: Extracted ion chromatograms and the mass spectral analysis for derivatives of palmitic acid by coupling with choline using FMP reagent on a C18 column with mobile phase (A) 0.1% (v/v) formic acid in water and mobile phase (B) 0.1% (v/v) formic acid in ACN.

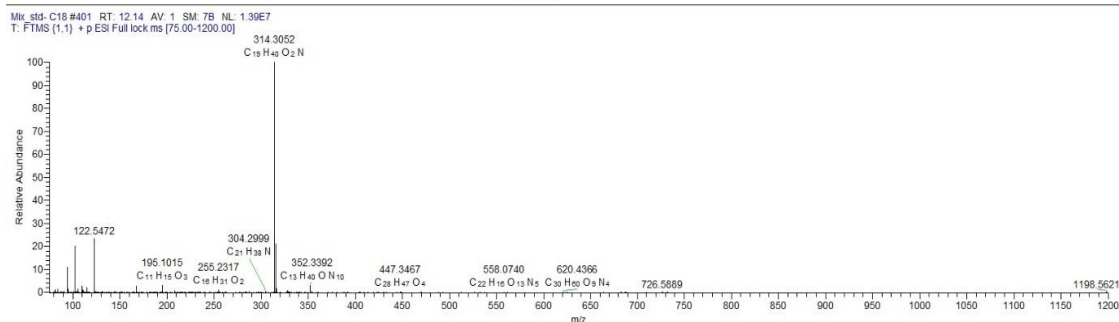
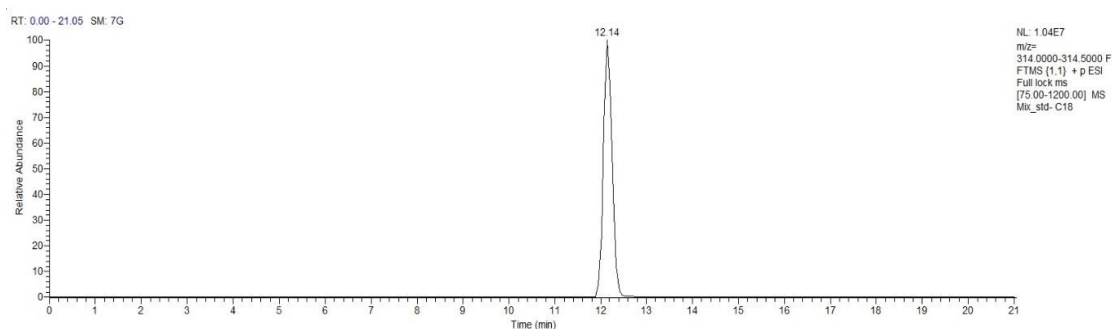


Figure 6-7: Extracted ion chromatograms and the mass spectral analysis for derivatives of myristic acid by coupling with choline using FMP reagent on a C18 column with mobile phase (A) 0.1% (v/v) formic acid in water and mobile phase (B) 0.1% (v/v) formic acid in ACN.

Serial dilution of palmitic acid in the range 0.01-1 μ g/ml was tested in order to gain some impression of the LOQ, the area of the peak was plotted against its concentration and the calibration curve was constructed. The calibration curve showed linearity with $R^2 = 0.995$ and the regression equation was $Y = 58517 X + 7887.60$ as show in Figure 6-8.

Thus all further couplings of this research project, choline coupling of carboxylic acid derivatives, were performed using FMP coupling agent to identify and quantify oxidised fatty acids, oxylipin metabolites derived from linoleic acid and arachidonic acid, in human plasma.

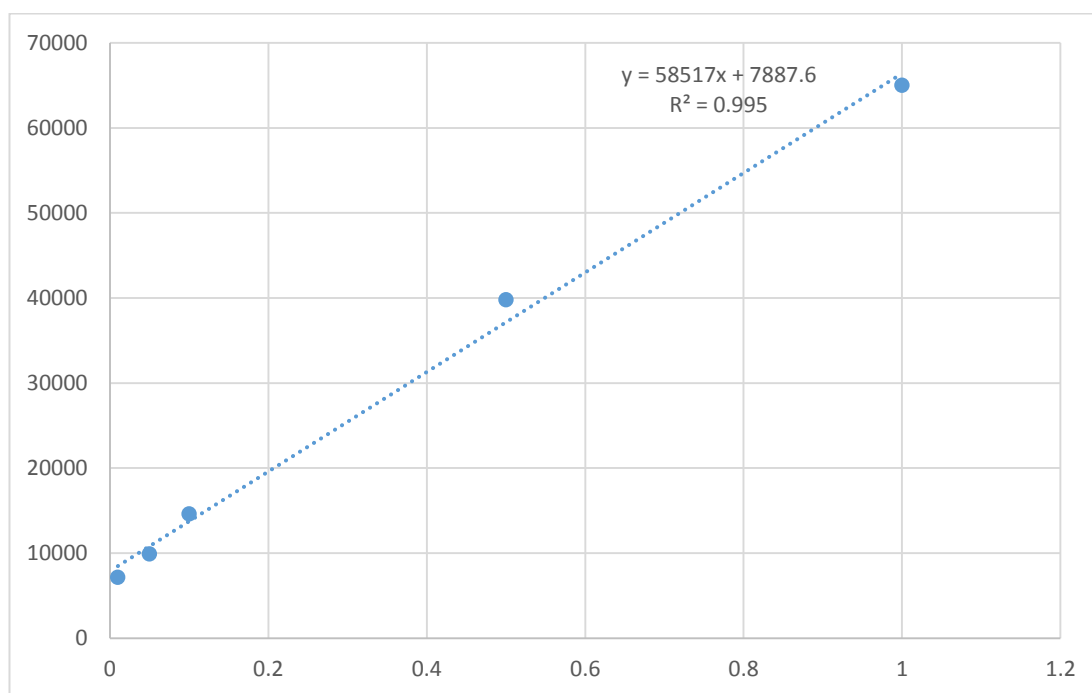


Figure 6-8: Calibration curve of palmitic acid in the range of 0.01-1 μ g/ml

6.3.3 Oxidised Fatty Acids Derivatisation

The standard mixtures of LAO and ArAO were used to examine the ability of this method for the identification and quantification of oxylipin metabolites in biological samples. The standard mixture of LAO which contains sets of isomers, including 1. 9-OxoODE and 13-OxoODE 2. (\pm)9(10)-DiHOME and (\pm)12(13)-DiHOME 3. 9(S)-HODE, 13(S)-HODE, (\pm)9(10)-EpOME and (\pm)12(13)-EpOME. Generally, there are four linoleic acid derivatives (OxoODE, DiHOME, HODE and EpOME) that have three different chemical formulas and molar masses as listed in Table 6-S1 for which there were no standards. A deuterated linoleic acid oxylipins (DLAO) mixture was utilised to discriminate between isomers in the LAO mixture through comparison of the retention times of the labelled and unlabelled LAOs. The discrimination between of the oxylipin isomers in the LAO mixture is shown in Figure 6-9 (A, B and C). Using this information in combination with the differentiation among these isomers, under underivatised conditions according to product information provided by company Figure 6-S1 (Caymanchem, Item № 20794) as well as studies reporting that elution of HODE is faster than EpOME (Gouveia-Figueira *et al.*, 2015, Strassburg *et al.*, 2012) it was possible to be fairly confident of the assignment. Thus, perhaps not surprisingly the order of elution for the derivatised compounds under RP conditions appeared to be the same as for the underivatised compounds. In the same way, the differentiation among ArAO isomers was based on the product information of ArAO mixture provided by company Figure 6-S2 (Caymanchem, Item № 20666) for the elution order of the underivatised compounds under RP conditions.

Separation of all the standard mixture components of LAO and ArAO is shown in Figure 6-10 and Figure 6-11, respectively.

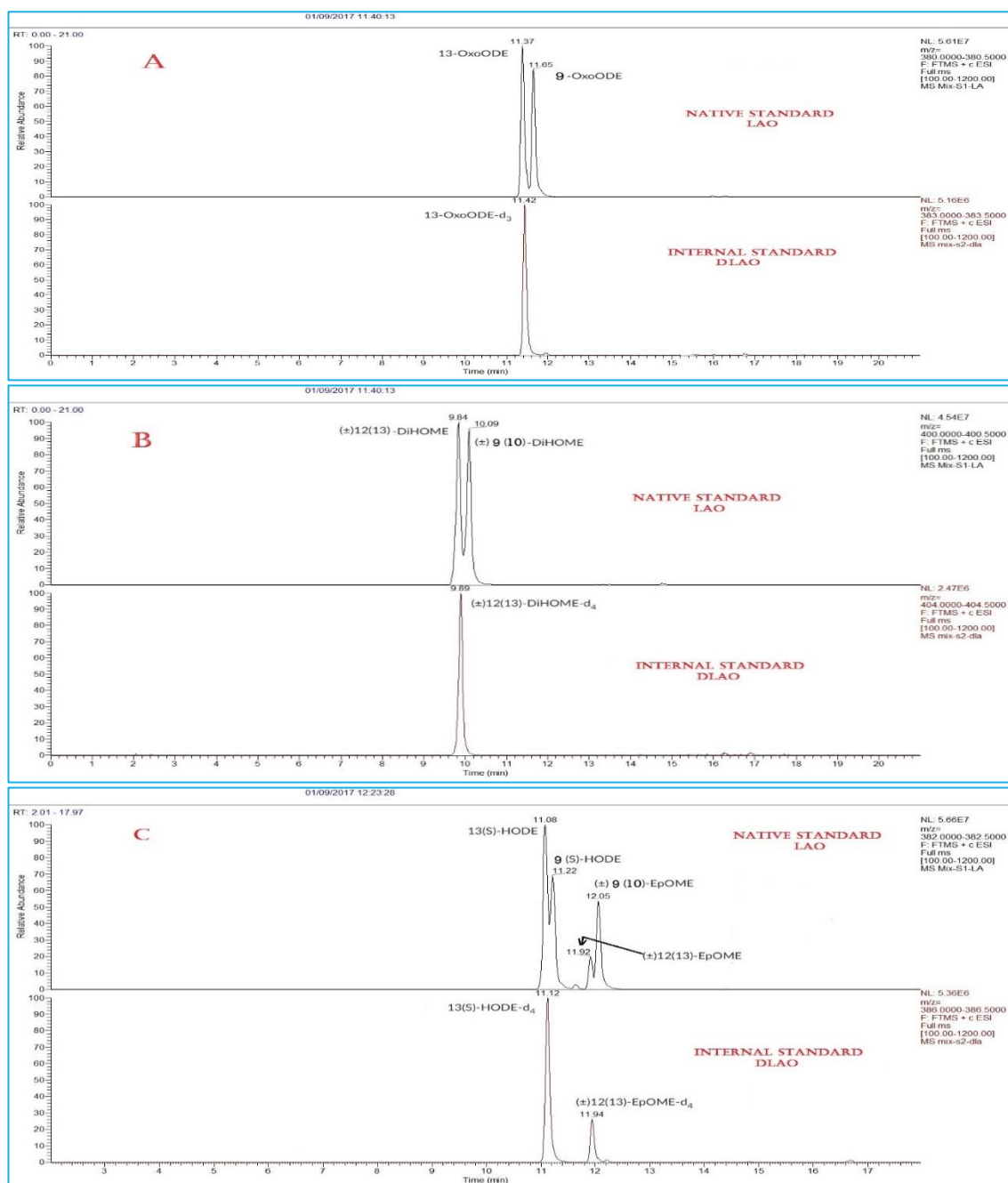


Figure 6-9: The discrimination between LAO isomers: (A) 9-OxoODE and 13-OxoODE, (B) (±)9(10)-DiHOME and (±)12(13)-DiHOME; and (C) 9(S)-HODE, 13(S)-HODE, (±)9(10)-EpOME and (±)12(13)-EpOME.

The comprehensive details of the oxylipin metabolites of LAO and ArAO as well as internal standard mixture components analysed by derivatisation procedure in this work are summarised in Table 6-1. The overview of extracted ion chromatography in

Figures 6-10 and 6-11 indicates that oxidised fatty acids derivatisation method with choline coupling is a suitable method to achieve a good chromatographic separation and has the ability to identify and quantify oxylipins in biological samples.

Table 6-1: The chemical formula, molar mass and retention time for the oxylipin metabolites after carrying out derivatisation procedure.

Oxylipins name	Abbreviation	Derivatised Chemical Formula	Derivatised Molar Mass	Retention Time (RT)
(±)12,13-dihydroxy-9Z-octadecenoic acid	(±)12(13)-DiHOME	C ₂₃ H ₄₆ O ₄ N	400.34	9.84
(±)9,10-dihydroxy-12Z-octadecenoic acid	(±)9(10)-DiHOME	C ₂₃ H ₄₆ O ₄ N	400.34	10.09
9S-hydroxy-10E,12Z-octadecadienoic acid	9(s)-HODE	C ₂₃ H ₄₄ O ₃ N	382.33	11.08
13S-hydroxy-9Z,11E-octadecadienoic acid	13(s)-HODE	C ₂₃ H ₄₄ O ₃ N	382.33	11.22
13-oxo-9Z,11E-octadecadienoic acid	13-OxoODE	C ₂₃ H ₄₂ O ₃ N	380.32	11.37
9-oxo-10E,12Z-octadecadienoic acid	9-OxoODE	C ₂₃ H ₄₂ O ₃ N	380.32	11.65
(±)12(13)epoxy-9Z-octadecenoic acid	(±)12(13)-EpOME	C ₂₃ H ₄₄ O ₃ N	382.33	11.92
(±)9,10-epoxy-12Z-octadecenoic acid	(±)9(10)-EpOME	C ₂₃ H ₄₄ O ₃ N	382.33	12.05
5-oxo-6E,8Z,11Z,14Z-eicosatetraenoic acid	5-OxoETE	C ₂₅ H ₄₂ O ₃ N	404.33	12.62
12-oxo-5Z,8Z,10E,14Z-eicosatetraenoic acid	12-OxoETE	C ₂₅ H ₄₂ O ₃ N	404.33	12.42
15-oxo-5Z,8Z,11Z,13E-eicosatetraenoic acid	15-OxoETE	C ₂₅ H ₄₂ O ₃ N	404.33	11.60
15S-hydroxy-5Z,8Z,11Z,13E-eicosatetraenoic acid	15(S)-HETE	C ₂₅ H ₄₄ O ₃ N	406.33	11.28
12S-hydroxy-5Z,8Z,10E,14Z-eicosatetraenoic acid	12(S)-HETE	C ₂₅ H ₄₄ O ₃ N	406.33	11.58
11S-hydroxy-5Z,8Z,12E,14Z-eicosatetraenoic acid	11(S)-HETE	C ₂₅ H ₄₄ O ₃ N	406.33	11.55
9R-hydroxy-5Z,7E,11Z,14Z-eicosatetraenoic acid	9(R)-HETE	C ₂₅ H ₄₄ O ₃ N	406.33	11.73
8S-hydroxy-5Z,9E,11Z,14Z-eicosatetraenoic acid	8(S)-HETE	C ₂₅ H ₄₄ O ₃ N	406.33	11.55
5S-hydroxy-6E,8Z,11Z,14Z-eicosatetraenoic acid	5(S)-HETE	C ₂₅ H ₄₄ O ₃ N	406.33	11.85

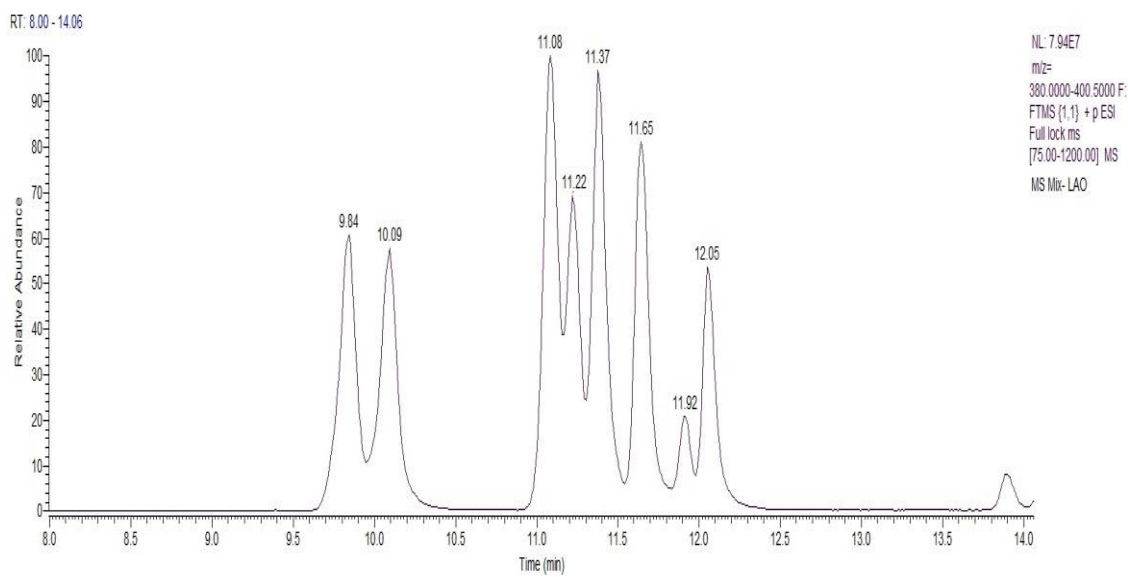


Figure 6-10: The chromatographic separation among the standard mixture components of LAO under derivatisation conditions.

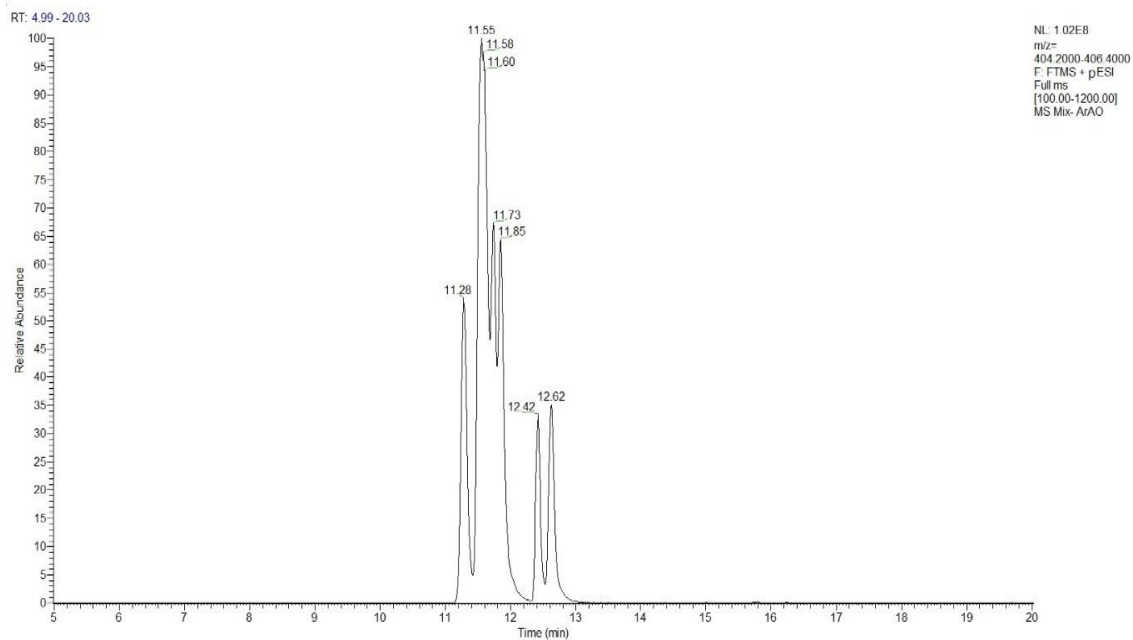


Figure 6-11: The chromatographic separation among the standard mixture components of ArAO under derivatisation conditions.

6.3.4 Oxylipin Quantification and Profiling of Plasma Samples from Healthy Human

Human plasma samples were extracted and analysed by HPLC-ESI-MS according to the current derivatisation method. Figure 6-12 shows an extracted ion for the oxylipins obtained from the human plasma samples following consumption of beetroot juice. An eight point (0.0, 2.5, 5.0, 10.0, 20.0, 40.0, 80.0 and 160.0 ng) calibration curve was prepared for a mix of native LAO and ArAO standards in ACN. The internal standard (13(S)-HODE-d4) was added in the native standard and sample mixtures at a fixed concentration of 50.0 ng. Table 6-2 summarises the calibration data for the fourteen oxylipin derivatives obtained by plotting the ratio of the peak area for each the oxylipin against the 13(S)-HODE-d4 as an internal standard. Calibration data were obtained from the standard curves as shown in Figures 6-13–6-26 and are used to evaluate linearity, the slope and R^2 , for all the oxylipins in the range (2.5-160.0 ng). The LC-MS method was applied to measure the amount of oxylipin in different biological samples. The plasma oxylipin levels before and after ingestion of beetroot juice were quantified based on the calibration (standard) curves. Table 6-3 shows the concentrations of oxylipins detected in plasma of healthy subjects at two time-points are baseline (0 min) and after 120min of ingestion of beetroot juice. The comparison between the concentrations of oxylipins at these time-points indicates that there were only weakly significant changes being observed for 9 and 12 EpOME which were slightly elevated post ingestion of beetroot juice. This method was able to achieve the requirements and provided good sensitivity to evaluate oxylipin profiles and quantify their levels at low concentrations down ng/ml.

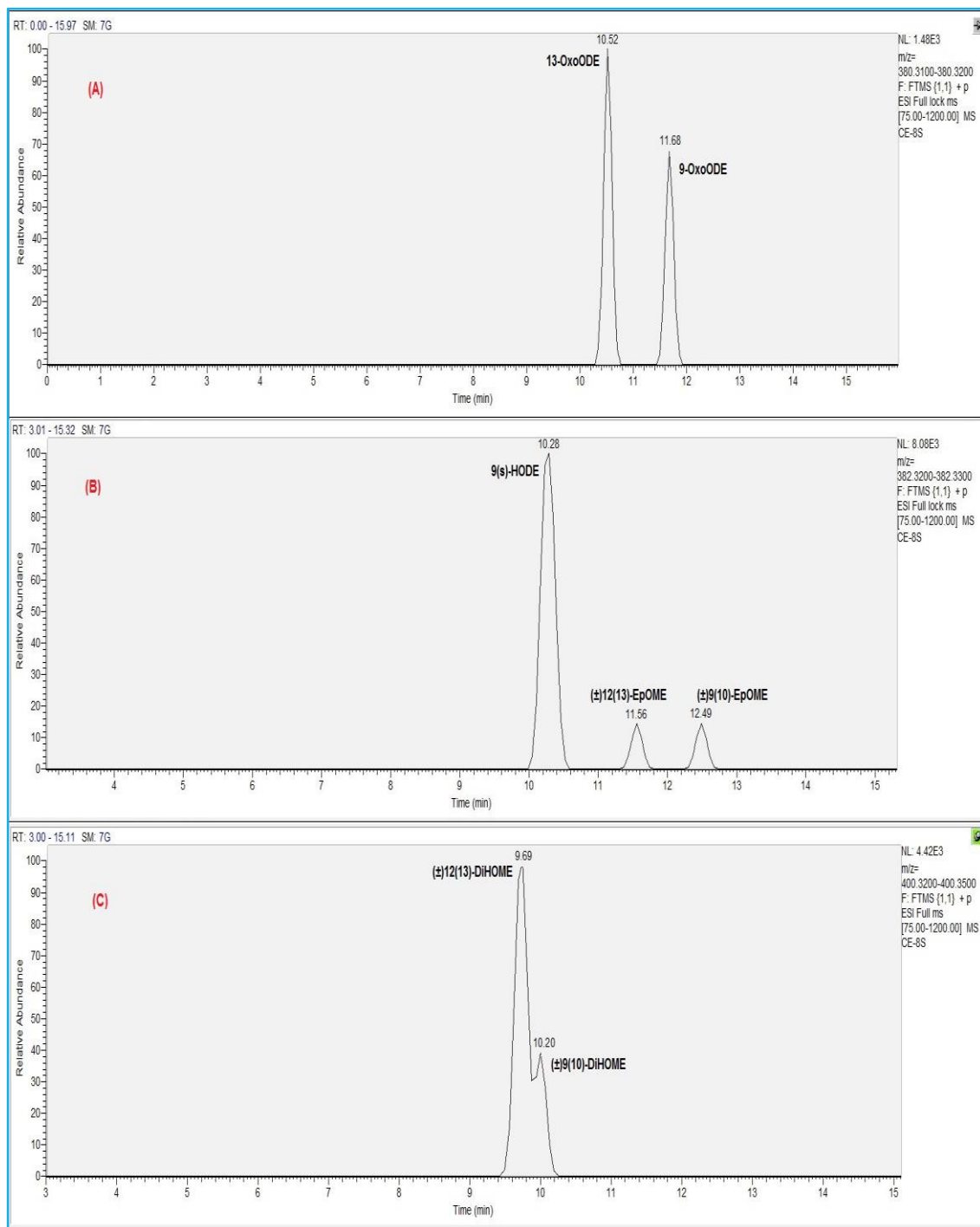


Figure 6-12: LAO isomers extracted from plasma samples: (A) 9-OxoODE and 13-OxoODE, (B) 9(S)-HODE, 13(S)-HODE, (±)9(10)-EpOME and (±)12(13)-EpOME; and (C) (±)9(10)-DiHOME and (±)12(13)-DiHOME

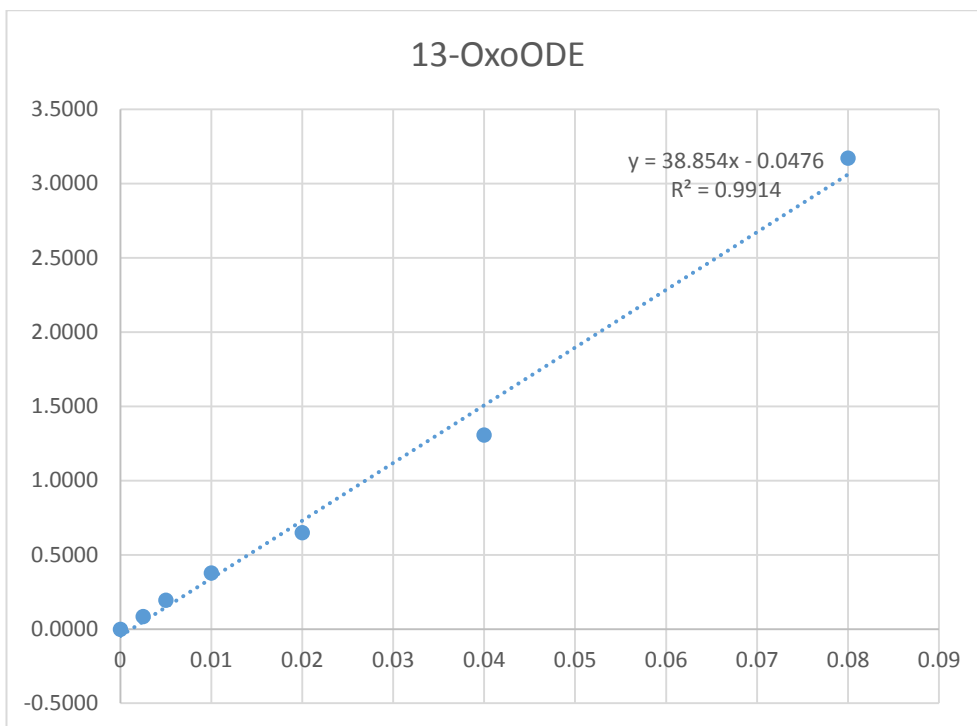


Figure 6- 13: the calibration curves of 13-oxo-9Z,11E-octadecadienoic acid in the range (2.5-160.0 ng).

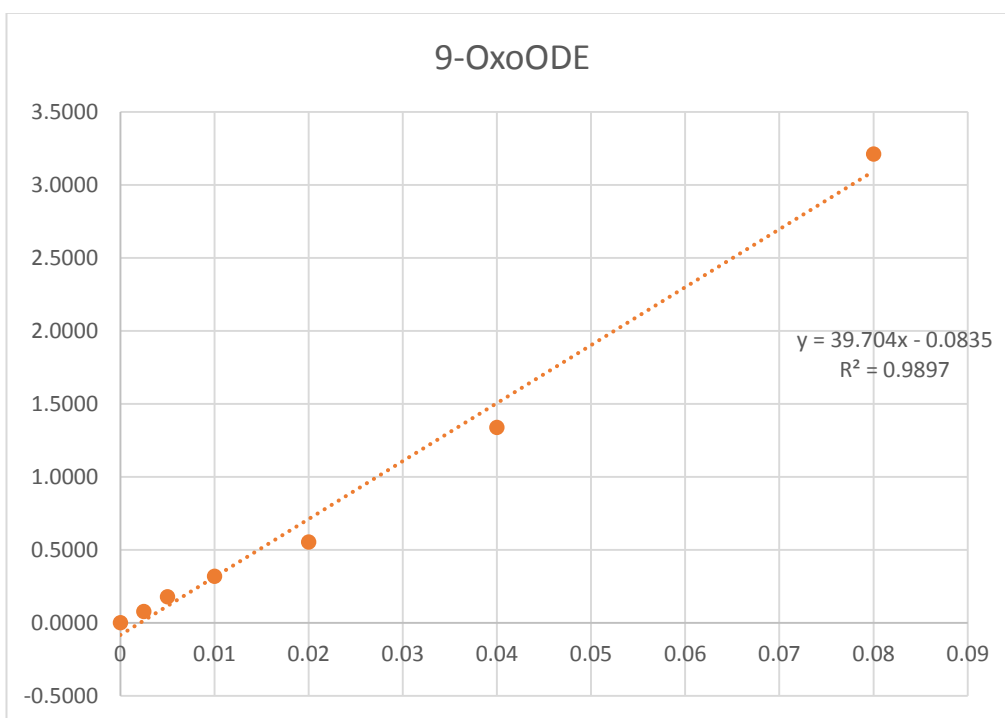


Figure 6- 14: The calibration curves of 9-oxo-10E,12Z-octadecadienoic acid in the range (2.5-160.0 ng).

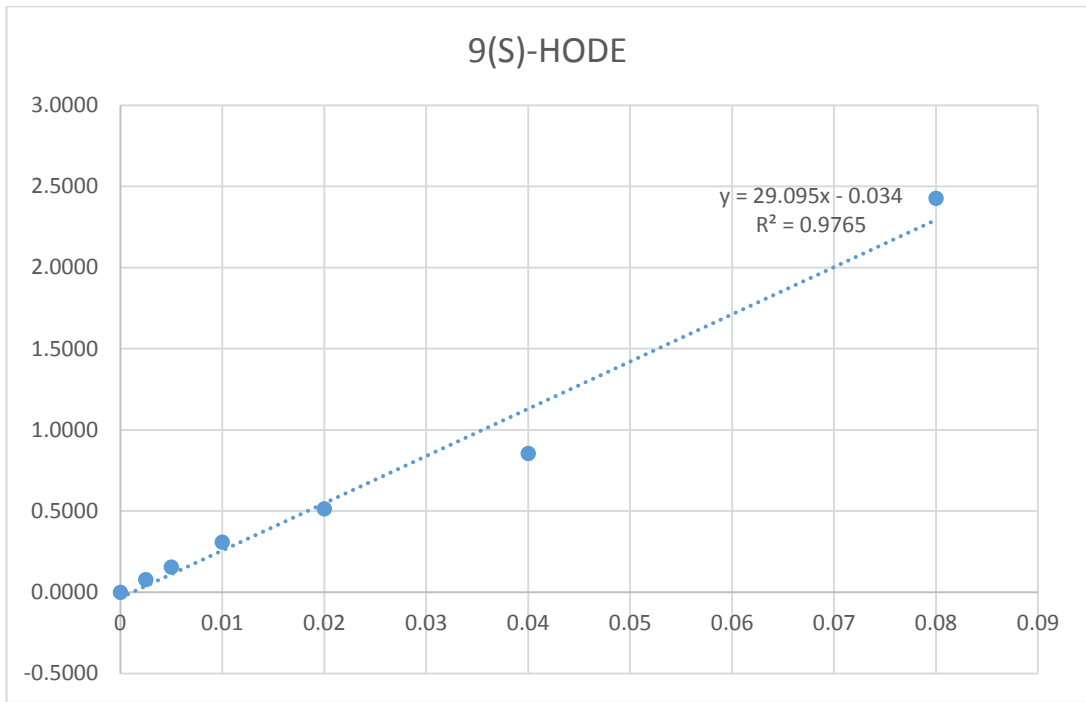


Figure 6- 15: the calibration curves of 9S-hydroxy-10E,12Z-octadecadienoic acid in the range (2.5-160.0 ng).

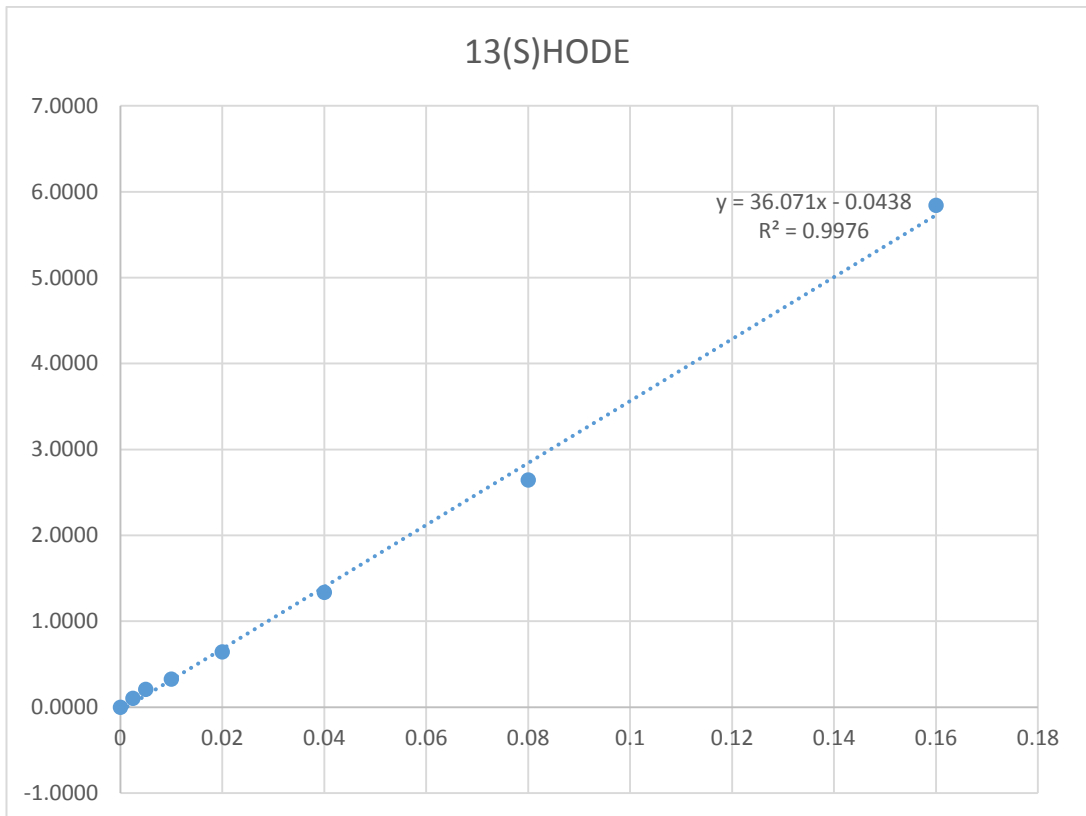


Figure 6- 16: the calibration curves of 13S-hydroxy-9Z, 11E-octadecadienoic acid in the range (2.5-160.0 ng).

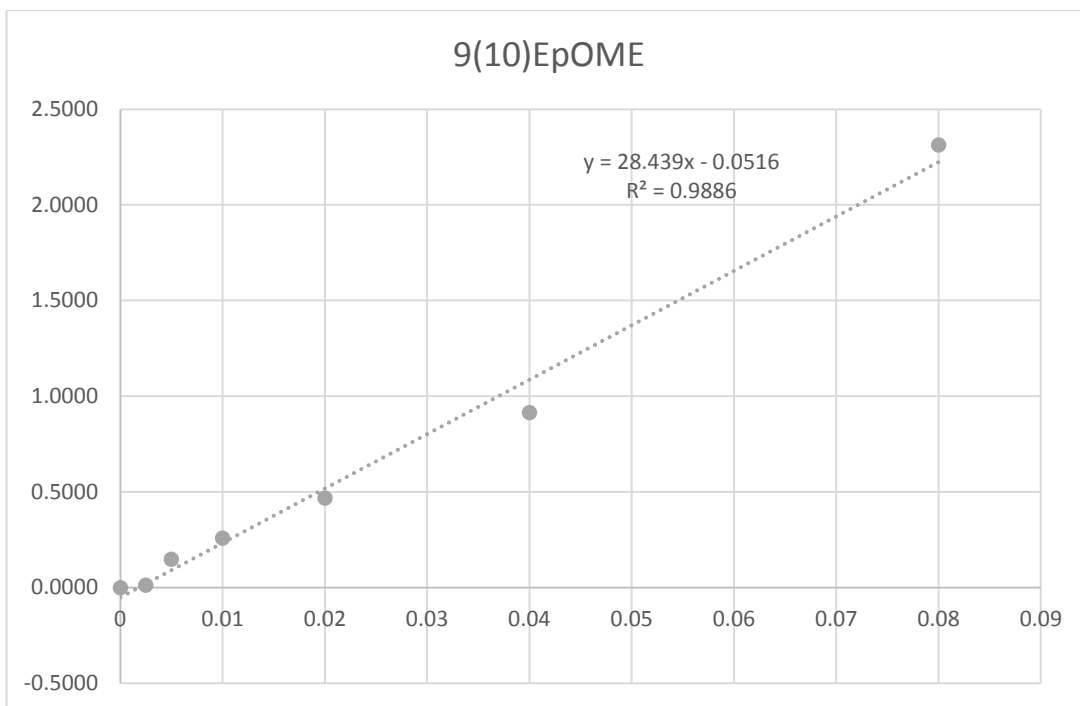


Figure 6- 17: the calibration curves of (\pm) 9, 10-epoxy-12Z-octadecenoic acid in the range (2.5-160.0 ng).

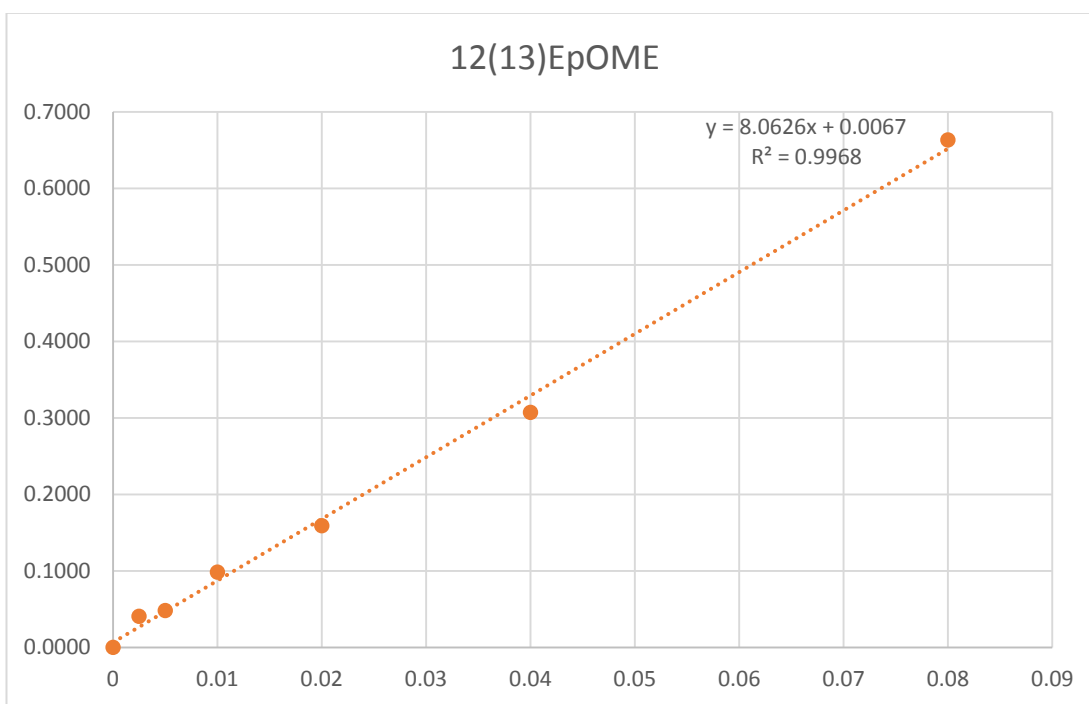


Figure 6- 18: the calibration curves of (\pm) 12, (13) epoxy-9Z-octadecenoic acid in the range (2.5-160.0 ng).

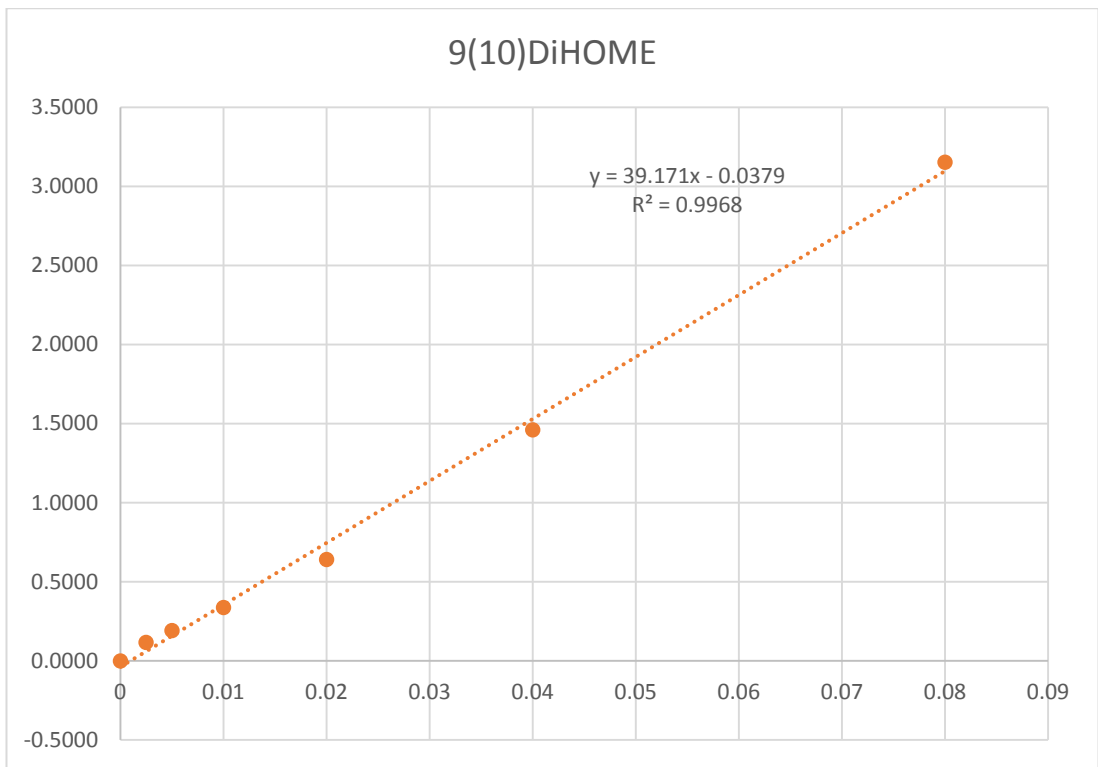


Figure 6- 19: the calibration curves of (\pm) 9, 10-dihydroxy-12Z-octadecenoic acid in the range (2.5-160.0 ng).

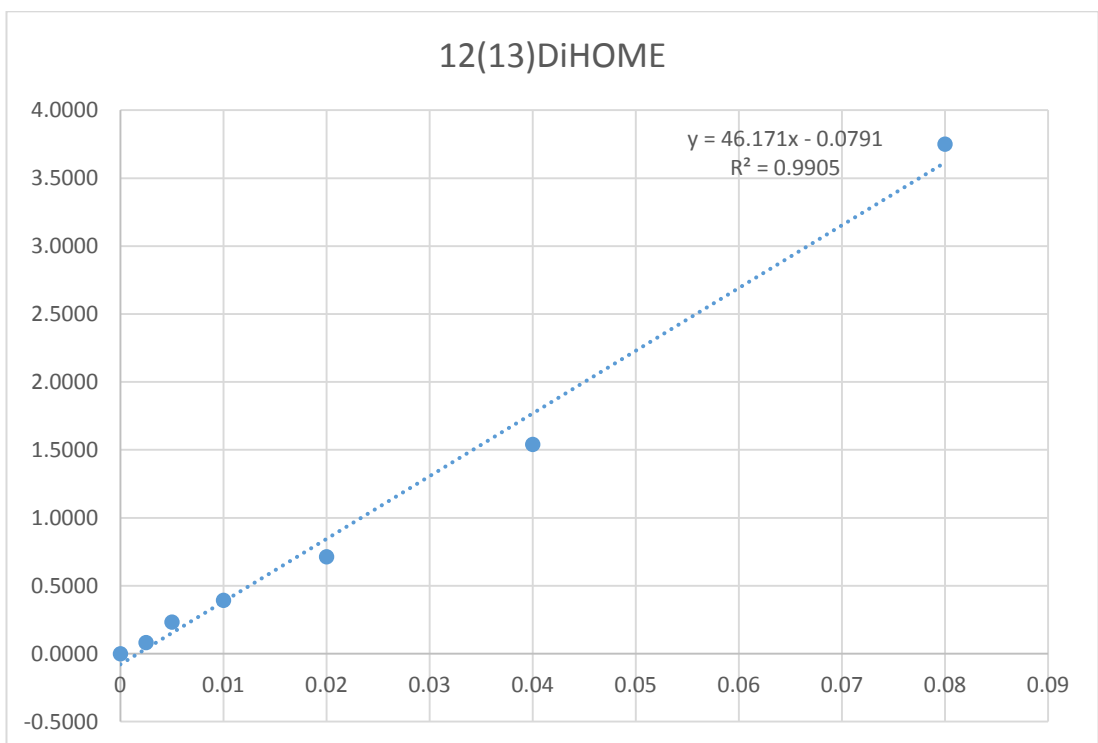


Figure 6- 20: the calibration curves of (\pm) 12, 13-dihydroxy-9Z-octadecenoic acid in the range (2.5-160.0 ng).

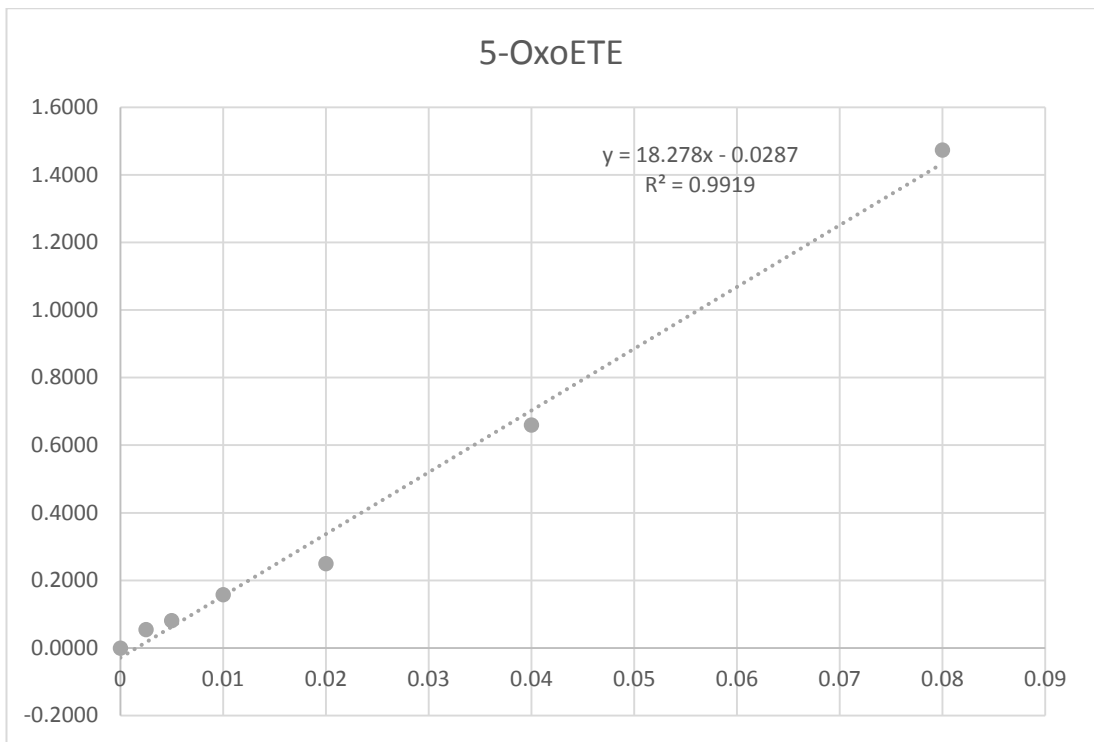


Figure 6- 21: the calibration curves of 5-oxo-6E, 8Z, 11Z, 14Z-eicosatetraenoic acid in the range (2.5-160.0 ng).

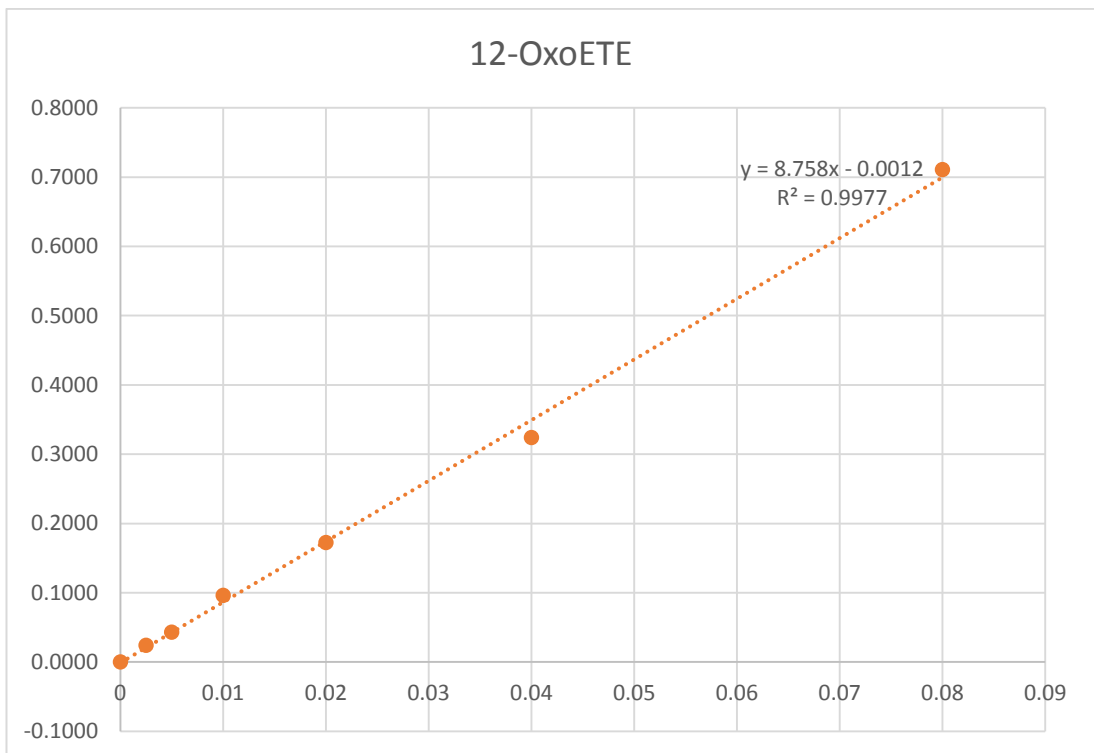


Figure 6- 22: the calibration curves of 12-oxo-5Z, 8Z, 10E, 14Z-eicosatetraenoic acid in the range (2.5-160.0 ng).

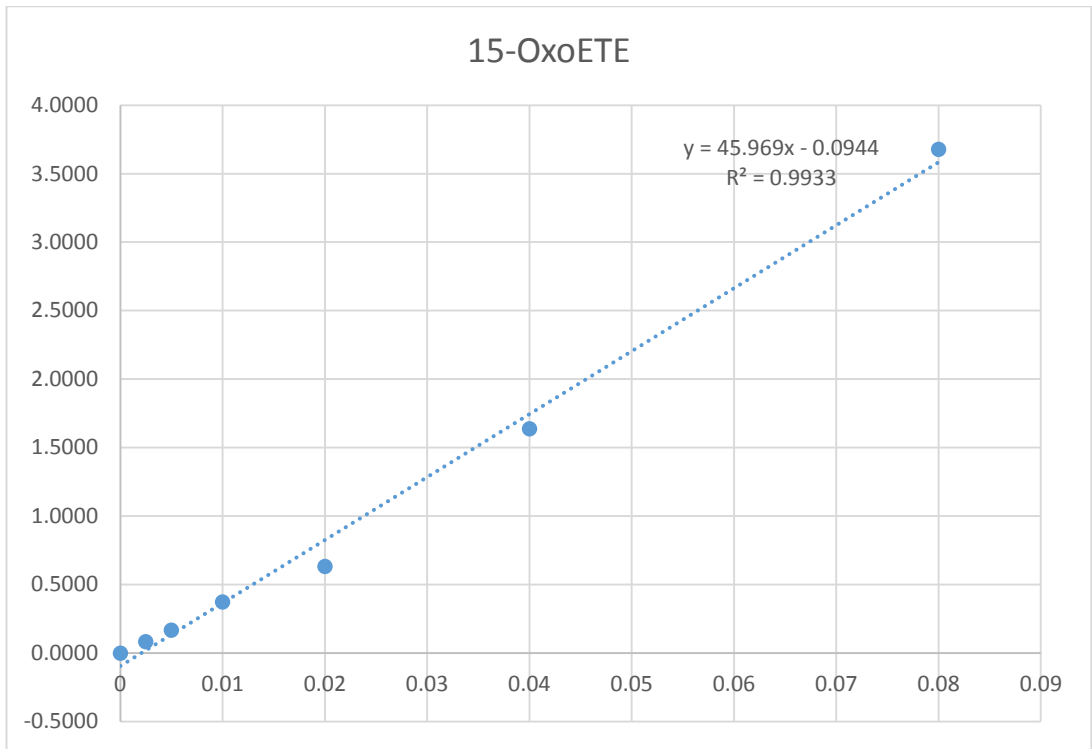


Figure 6- 23: the calibration curves of 15-oxo-5Z, 8Z, 11Z, 13E-eicosatetraenoic acid in the range (2.5-160.0 ng).

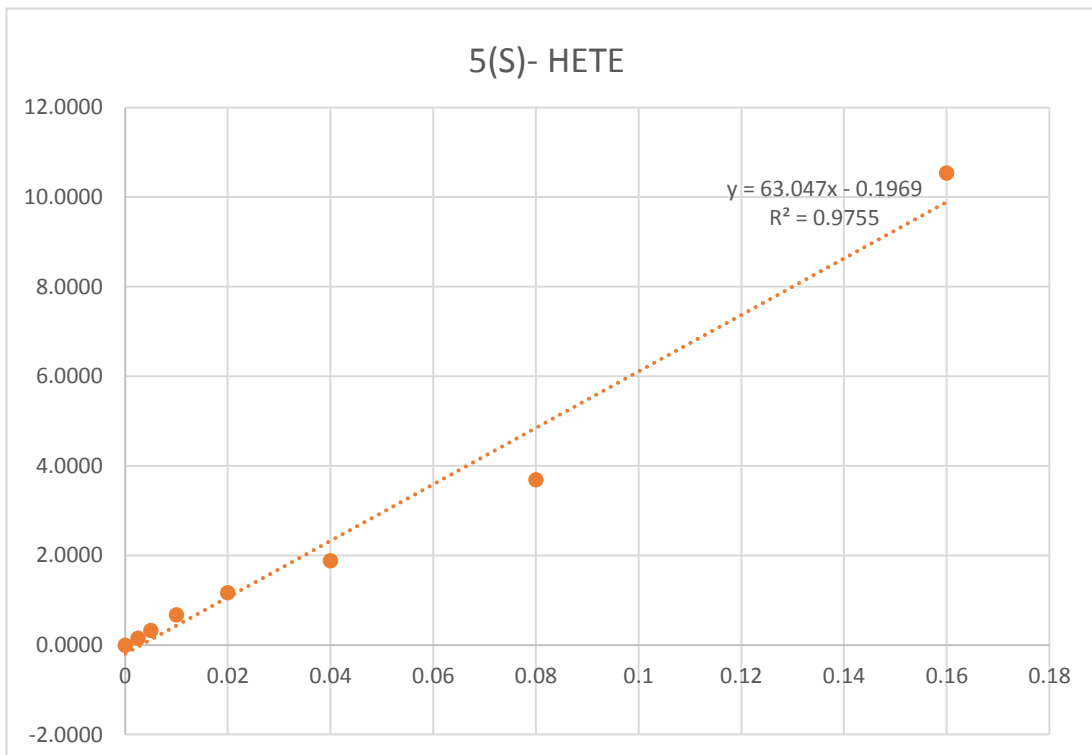


Figure 6- 24: the calibration curves of 5S-hydroxy-6E, 8Z, 11Z, 14Z-eicosatetraenoic acid in the range (2.5-160.0 ng).

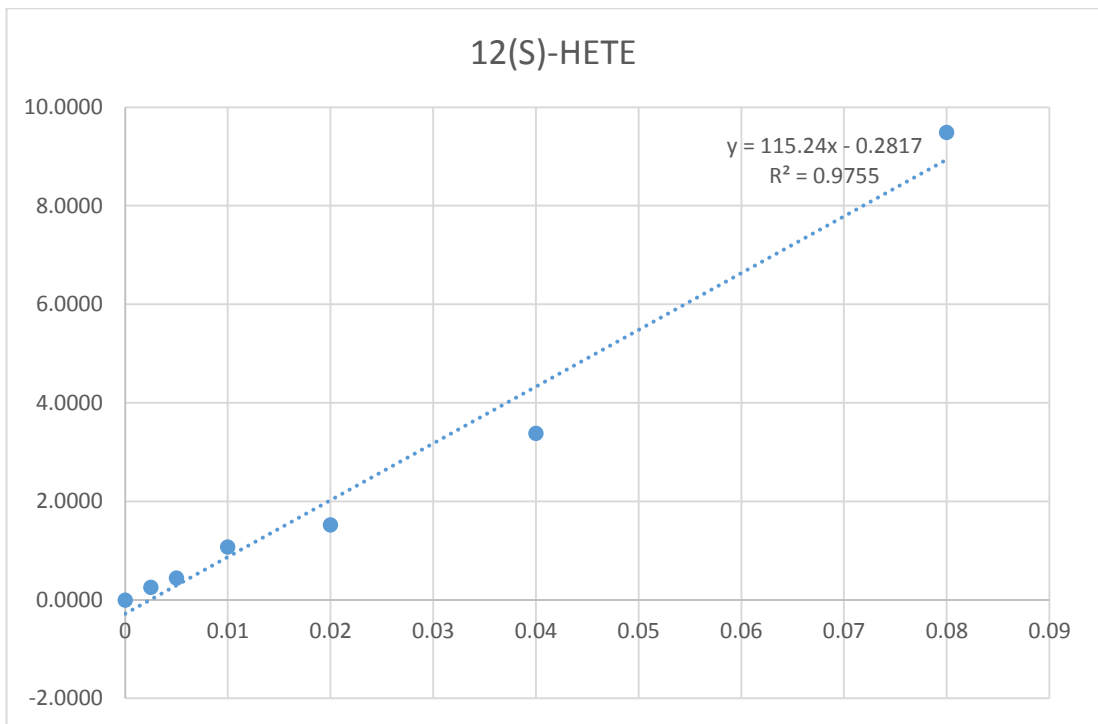


Figure 6- 25: the calibration curves of 12S-hydroxy-5Z, 8Z, 10E, 14Z-eicosatetraenoic acid in the range (2.5-160.0 ng).

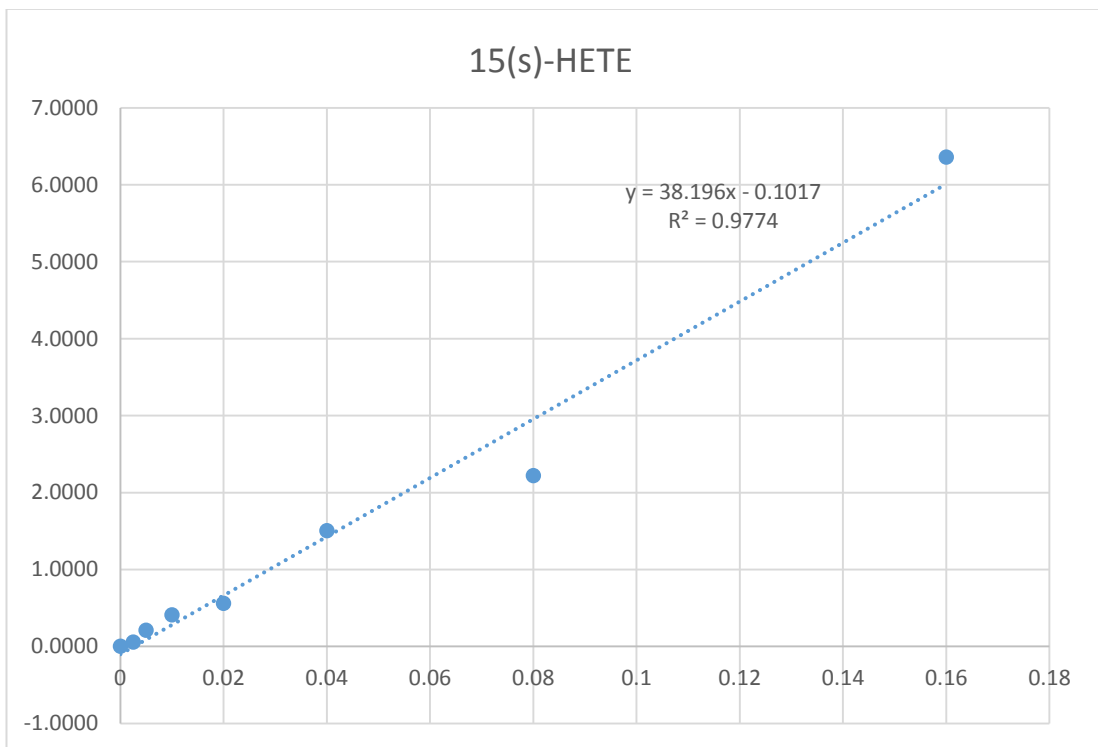


Figure 6- 26: the calibration curves of 15S-hydroxy-5Z, 8Z, 11Z, 13E-eicosatetraenoic acid in the range (2.5-160.0 ng).

Table 6-2: Calibration data based on ratio of response of derivatised oxylipins to response for derivatised internal standard (13(S)-HODE-d4) over the range 2.5-160.0 ng

LAO Mixture	Equation of the line	(R ²)
13-OxoODE	Y=38.854X-0.0476	0.9914
9-OxoODE	Y=39.704X-0.0835	0.9897
13 (S)-HODE	Y=36.071X-0.0438	0.9976
9 (S)-HODE	Y=29.095X-0.034	0.9765
(±)12 (13)-EpOME	Y=8.0626X+0.0067	0.9968
(±)9 (10)-EpOME	Y=28.439X-0.0516	0.9968
(±)12 (13)-DiHOME	Y=46.171X-0.0791	0.9905
(±)9 (10)-DiHOME	Y=39.171X-0.0379	0.9968
ArAO Mixture		
15-OxoETE	Y=45.969X-0.0944	0.9933
12-OxoETE	Y=8.758X-0.0012	0.9977
5-OxoETE	Y=18.278X-0.0287	0.9919
15(S)-HETE	Y=38.196X-0.1017	0.9774
12(S)-HETE	Y=115.24X-0.2817	0.9755
5(S)-HETE	Y=63.047X-0.1969	0.9755

Table 6-3: Concentrations (ng/100ul) for oxylipin metabolites derived from LAO and ArAO in plasma samples at pre- and post-ingested beetroot.

Sample	Linoleic Acid Oxylipins (ng/100ul)							Arachidonic Acid Oxylipins (ng/100ul)				
	13-Oxo ODE	9-Oxo ODE	13(S)-HODE	9(S)-HODE	9(10)-EpOME	12(13)-EpOME	12(13)-DiHOME	15-Oxo ETE	12-Oxo ETE	15(S)-HETE	12(S)-HETE	5(S)-HETE
CE-S1	36.8	38.6	43.6	79.8	97.2	270.6	11.4	26.6	24.9	40	41.2	46.3
CM-S1	29.7	28.8	66.9	105.5	84.9	227.2	10.6	23.1	33.1	59	48.2	60.4
DR-S1	17	24.4	50	74.3	44.5	84.5	10.3	22.6	38	47.6	36.3	40.6
GS-S1	21.8	27.5	34.2	56.1	66.6	162.4	10.7	20.9	10.9	40.4	31	37.8
LM-S1	23.5	25.4	50	86.6	70.8	177.4	10.4	24.2	9	62.4	44.5	51.6
CE-S4	26.8	25.5	56.5	131.9	65.5	158.8	9.7	23.3	82.2	63.8	47	59.8
CM-S4	25.2	22.7	55	80.8	53.4	116	9.7	22.4	19.4	60.4	39.7	57.9
DR-S4	21.5	25.7	41.7	71.3	39.5	67.1	9.7	22.8	11.2	44.6	35.8	48.5
GS-S4	24.6	25.9	45.2	71.7	48.3	97.9	9.7	22.4	24.5	53.5	42.1	49
LM-S4	24.3	28.4	49.9	90.9	55.3	122.6	9.7	22.8	38.3	53.3	45.6	58.4
P Val.	0.734	0.275	0.909	0.541	0.086	0.087	0.007	0.481	0.424	0.388	0.636	0.165
Ratio	1.052	1.129	0.986	0.901	1.389	1.640	1.101	1.033	0.660	0.905	0.957	0.865

6.4 Discussion

It is noted in metabolomics research that the LC-MS-based profiling of FAs has three major challenges in achieving quantification and identification of oxylipins. Firstly, the structures of most oxidised fatty acids, especially isomers, are similar. Secondly, oxylipins are present at low endogenous concentrations. In the studies carried out by LC-MS analysis for bioactive lipids without prior derivatisation, samples undergo a process of extraction by solid phase extraction (SPE) and are analysed with negative ion detection (Gouveia-Figueira *et al.*, 2015, Yang *et al.*, 2009, Strassburg *et al.*, 2012). This method is effective for targeted analysis of lipids by using MS/MS but for untargeted analysis improved sensitivity afforded by using positive ion mode.

Several derivatisation-based studies report methods for tagging carboxylic acids with a permanent positive charge such as a quaternary ammonium ion or alternatively an electron-capturing pentafluorobenzyl moiety (Johnson, 2000, Yang *et al.*, 2007, Li and Franke, 2011, Johnson *et al.*, 2003, Lee *et al.*, 2003, Pettinella *et al.*, 2007) for improved detection by negative ion chemical ionisation.

The limited application of the derivatisation method developed by Johnson *et al.* and modified by Xingnan and Adrian for the detection of FAs may be because of the use of harmful reagents and multiple derivatisation steps (Li and Franke, 2011, Johnson *et al.*, 2003). The long analysis run is a major challenge in Yang's method (Yang *et al.*, 2007). Additionally, there are other problems such as incomplete separation for oxidised fatty acids and dicarboxylic acids and the failure in tagging of saturated FAs that may limit the application of some methods of carboxylic acid derivatisation (Johnson, 2000, Lee *et al.*, 2003, Pettinella *et al.*, 2007).

After the investigation of strengths and weakness points in previous studies, many requirements must be available in developed derivatisation methods for them to provide an optimal method to identify and quantify the carboxylic acids and its derivatives. The first requirement is that the derivatisation reaction must be simple and carry out in short time with a few steps. Secondly, it is preferred that these methods do not use harmful and expensive reagents. Thirdly, the products of the derivatisation reaction should be stable compounds and contain readily protonated group, such as an amine group, which can be easily ionised to provide an increase in sensitivity for detection by positive ion ESI. Finally, the accurate and sensitive derivatisation approach should provide good chromatographic separation and good discrimination among the isomers of oxidised fatty acids.

One of the most common quaternary ammonium salts which can be combined with carboxylic acids is choline, trimethylaminoethyl (TMAE). The choice of choline was due to its characteristics such as low toxicity, high stability, non-reactivity with water, biodegradability and the wide commercial availability (Crespo *et al.*, 2017, Pontes *et al.*, 2017). Chemically, TMAE or choline is more sensitive for the analysis different types of carboxylic acids by ESI-MS/MS in comparison with dimethylaminoethyl (DMAE). The TMAE derivatives of long chain fatty acids (FA-TMAE), choline ester salt, can provide compounds selectivity and stability because of they have a positive charge in both acidic and mobile phases (Johnson, 2000). Moreover, choline coupling procedure using FMP coupling reagent was chosen as it consumes less time and has uncomplicated handling compared to other procedures which require at least three hours for the reaction to complete (Li and Franke, 2011, Johnson *et al.*, 2003). Yang *et al.* derivatised carboxylic acids by the coupling reaction of 2-bromo-1-

methylpyridinium iodide and 3-carbinol-1-methylpyridinium iodide, forming 3-acyloxymethyl-1-methylpyridinium iodide (AMMP). This method used a separation and detection systems performed on HPLC/ESI-MS with a long analysis run, 40 min, and it was not applied for quantification of oxidised fatty acids (Yang *et al.*, 2007). This derivatising method is fast and quantitative, without a complicated handling procedure. Higashi and his team have investigated the coupling reaction of 2-picolylamine with carboxylic acid using triphenylphosphine (TPP) and 2, 2-dipyridyl disulphide (DPDS) via a one-pot synthesis step. However, it is found that the TPP/DPDS catalysed reaction products interfere with late eluting FAs as well as the reaction time is longer compared to the total reaction time under current LC conditions (Higashi *et al.*, 2010). The ease ionization of analytes and ionization efficiency are the main challenges in LC/MS applications in the case of carboxyl-containing compounds. Ionization efficiency of fatty acids in the negative ion mode of ionization is impacted by the concentration of organic solvent, in the range of 50-95% acetonitrile. Dissociation of fatty acids in acetonitrile can be suppressed through increases detection sensitivity in the positive ion mode. Thus, derivatization of fatty acids affords the opportunity to incorporate features that can substantially enhance their detection and quantification by HPLC/ESI-MS (Yang *et al.*, 2007). A simple method was developed for this objective by first tagging and sorting fatty acids through derivatization to overcome the complexity of plasma samples in quantification of fatty acids. In the current case choline esterification to the carboxylic acids and their oxidation products resulted in formation of derivatives containing a quaternary ammonium group (OFA-TMAE) with short and uncomplicated steps (Figure 6-2) and the isomeric species in the mixtures could be separated with a short run time.

6.5 Conclusion

A simple, fast and sensitive derivatisation method was developed to detect and quantify carboxylic acid derivatives in biological by HPLC/ESI-MS. The new derivatisation approach was performed by the coupling of fatty acids to choline using 2-fluoro-1-methylpyridinium p-toluene sulfonate (FMP) and formed stable derivatives. The quaternary ammonium part of the coupled choline made the derivatised compound permanently ionised in both acid and basic mobile phases. The choline-derivatisation was successfully applied to determine oxidised carboxylic acid metabolites in biological samples. A developed HPLC/ESI-MS method was tested by simultaneously quantifying 14 oxylipins in human plasma samples. Separation and detection of all oxylipins in plasma samples was achieved and it was able to separate isomeric species and quantify oxylipins to the low ng/ml level. The use of tandem MS would allow determination at much lower levels. The method was successfully applied for the analysis of oxylipins in human plasma samples to determine significant differences in baseline levels as well as significant differences in other time points (60min, 120min and 360min). In future, the developed method in the current study must be validated according to guidelines given by different organizations such as the laboratory of the government chemists (LGC) and the food and drug administration (FDA). The validation process should be performed to assure the suitability for its intended use and to be widely applied in future studies that require the analysis of carboxylic acid metabolites in complex biological samples.

CHAPTER 7
GENERAL DISCUSSION

7.1 Discussion

The successful study and application of metabolomics involves various fields in different disciplines, including organic chemistry, analytical chemistry, chemometrics, bioinformatics and bioscience (Fukusaki and Kobayashi, 2005).

Over the past two decades, the efforts have been devoted to using metabolomics studies in biomedical area for prediction of the suitability of metabolites as molecular biomarkers which can be used in clinical investigation. Due to the fact that the early biomarkers of a disease may be different from those in its advanced stages or that many biomarkers are indicative of more than one disease, many studies have reported that exploring reliable specific biomarkers increases the sensitivity and specificity of disease prognosis. Thus, one of the most common aims of metabolomic studies is biomarker detection because of correlations between different biomarkers may give clues to pathogenic mechanisms (Bartel *et al.*, 2013, Denoroy *et al.*, 2013). Metabolomics studies have been found to address most of the challenges associated with MS/MS data interpretation, database content, and isomer resolution and identification confidence. Metabolome research has had tremendous successes in biomedical sciences through providing a better understanding of the mechanisms underlying health and disease.

The current study has added new evidence to support the usefulness of the metabolomics approach in biomedical research through using LC-MS techniques for metabolomic profiling of biological fluids, human urine and plasma, and brain tissue. In this thesis, metabolomics based on LC-MS was used as analytical technique in both untargeted metabolic profiling, i.e. measuring many metabolites as possible, and targeted metabolic profiling, i.e. targeting of sugars and carboxylic acid compounds.

Untargeted metabolomics was performed by using chromatography on a ZICpHILIC and C18-AR columns with detection by Orbitrap mass spectrometry to obtain broader coverage for polar and non-polar metabolites. These metabolites were profiled in urine samples after submaximal exercise at a standardised relative intensity in healthy adults (Chapter 3) and post-mortem brain samples from subject with mental illness (Chapter 4). The choice of these columns as the best method for analysis of metabolites in metabolomic screens is supported by previous related study (Zhang *et al.*, 2014).

Metabolomics can be applied not only to monitor the metabolic changes in many pathological conditions and diseases, but can also be used to follow and investigate the effects of physiological factors relevant to metabolic phenotype.

Although things such as diet might be controlled relative in metabolomic comparison studies between health and disease, the levels of exercise are not generally controlled and could have a big impact on the results. Also, it is important to know which metabolites are very sensitive to change as a result of exercise. The first question in this study sought to determine the effects of submaximal exercise at standardised relative intensity on urinary metabolome for healthy adults. The results of the impact of exercise, are those exhibited in the purine metabolism and acyl carnitine, were fully discussed in Chapter 3 of this thesis. Maximal oxygen consumption (VO_{2max}) is among a number of mechanisms which may cause free radical production during exercise and it has been used as a useful tool for predicting cardiovascular and other mortality causes (Sousa *et al.*, 2015). Therefore, it was of interest to determine if there was a metabolite or metabolites which could be correlated to VO_{2max} . The most interesting clinically relevant finding was the observation of a single metabolic marker which is apparently correlated to VO_{2max} . A previous study aimed to find markers which could

predict VO_{2max} and found that a model based on a combination of 4-ethylphenylsulfate, tryptophan, γ -tocopherol, and α -hydroxyisovalerate was predictive of VO_{2max} in a cohort of 77 subjects with $R^2 = 0.66$ (Lustgarten *et al.*, 2013). Although the current study is small the single OHA marker in the current case gave $R^2 = 0.8589$ and thus a greater degree of correlation to VO_{2max} than the previous study and based on a single marker. The current study can only be considered to have made a preliminary observation and a follow up trial with an independent cohort of subjects would be required to definitely prove this association. The trial could be reduced in terms of sample collection since it is the difference between the first void sample and the first post-exercise sample which is most predictive of VO_{2max} and with a high ratio of first post-exercise to first void sample indicating a high VO_{2max} as indicated by the plot shown in Figure 3-14. Although the MW of the marker compound is small, further work is required in order to make a definitive identification since several isomers of it are known. A notable strength of the current study is that we were able to obtain valid determinations of VO_{2max} in all participants which is of vital importance in terms of assessing the predictive of any metabolic markers. This is likely due to the fact that participants had completed several previous maximal exercise tests prior to participation in the present study. This is an important point to consider for future larger scale research work in this area.

In Chapter 4, a full discussion of the metabolomic profiling of post-mortem brain samples that revealed changes in amino acid and glucose metabolism in mental illness disorders compared with controls was presented. This project was designed according to evidences that indicated historically a clinical relationship between diabetes and mental illness in addition there were no previous metabolomics studies of post-mortem

brain tissue in mental illness (Regenold *et al.*, 2004). The importance of this study came across highlighted key elements in SDB metabolism which could reflect the metabolic similarity between SDB and diabetes. Thus, this finding is clinically important and further supports the idea that anti-diabetic treatments might have a role in the management of SDB.

In Chapter 5 targeted metabolomics was performed in order to tag the sugars which otherwise give only weak responses and are difficult distinguish since sugar isomers usually overlap in most HPLC methods. Considering negative ion LC-ESI-MS is less sensitive than positive ion, the derivatisation methods with a permanent positive charge provide response factors of the tagged compounds more 100 times than those for the untagged compounds in negative ion. The work in chapter 5 further re-enforced the view that sugar metabolism is perturbed in mental illness.

In Chapter 6 a novel method was developed for tagging fatty acids which gave relatively low responses in negative ion mode. Attachment of choline as a tag enabled enhancement of detection limits in comparison to the untagged acids by *ca* x 100. This enables the detection of biologically active oxidised fatty acids in human plasma and the method was applied to assess the effect of the ingestion of beetroot juice on the profile of oxidised fatty acids in human plasma.

In overview the studies also underlined the reliability of the current results ensuring analytical confidence in the used methods. These activities are further divided into validation of instrumental and method identification limits. The removal of instrumental variation can be corrected by making a pooled sample of all the samples in the run or by a QC sample. Although it time consuming, making a pooled sample

from all the examined samples is practically better than buying a QC sample, because a QC sample contains compounds which are likely to be different than those in the examined samples. Therefore, with high precision, pooled samples were prepared from all actual samples and were injected at intervals during the analytical run to exclude instrumental drift that would impact on the results.

Along these lines, data modelling validation was employed in this thesis to check the accuracy and quality of source data and to determine the importance of the model with the goodness of fit. Data modelling validation is an important approach to validate the applied methods and to obtain reliable results because, without validation, there are always associated risks of over-fitting the data. Such over-fitted data stands out to be unreliable if considered for any clinical situations.

In the present untargeted metabolomic applications, the internal validation tools include a variance explained (R^2) and predicted values (Q^2) which are used to evaluate the quality and goodness of models. The R^2 represents a quantitative measure of the goodness of fit and the best its value is close to 1. The goodness of model has been inferred through increasing the R^2 value to be close to the maximal value of one, whilst reduction of this value to zero indicates a poor model. Despite a high R^2 value (close to 1) the goodness of these models can be evaluated as poor models, models that cannot predict, by reason of a large discrepancy of R^2 and Q^2 values (Westerhuis *et al.*, 2008).

After internal validation, the accepted modelling was also validated by two external methods including CV-ANOVA, where the returned P-value is indicative of the statistical significance of difference in the investigated samples, and the permutation test. The permutation test gives a reliable assessment for the spurious nature or

credibility of the model through the comparison of the goodness of fit then provides reference distributions of the R^2/Q^2 -value (Worley and Powers, 2013). The criteria for validity are: All blue Q^2 -values to the left are lower than the original points to the right or regression line of the Q^2 -points intersects the vertical axis (on the left) at, or below zero. Note that the R^2 -values always show some degree of optimism, when all green R^2 -values to the left are lower than the original point to the right, this is also an indication for the validity of the original model, for example Figures 4.9 and 4.11. Model validity was also assessed using CV-ANOVA which corresponds to H_0 hypothesis of equal cross validated predictive residual of the supervised model in comparison with the variation around the mean (Eriksson *et al.*, 2008).

References:

- ABDENUR, J. E., ABELING, N., SPECOLA, N., JORGE, L., SCHENONE, A. B., VAN CRUCHTEN, A. C. & CHAMOLES, N. A. 2006. Aromatic l-aminoacid decarboxylase deficiency: unusual neonatal presentation and additional findings in organic acid analysis. *Molecular genetics and metabolism*, 87, 48-53.
- ABDI, H. & WILLIAMS, L. J. 2010. Principal component analysis. *Wiley interdisciplinary reviews: computational statistics*, 2, 433-459.
- ALLENDER, S., FOSTER, C., SCARBOROUGH, P. & RAYNER, M. 2007. The burden of physical activity-related ill health in the UK. *J Epidemiol Community Health*, 61, 344-8.
- ARKIN, A., SHEN, P. & ROSS, J. 1997. A test case of correlation metric construction of a reaction pathway from measurements. *Science*, 277, 1275-1279.
- BALDERAS, C., RUPEREZ, F. J., IBANEZ, E., SENORANS, J., GUERRERO-FERNANDEZ, J., CASADO, I. G., GRACIA-BOUTHELIER, R., GARCIA, A. & BARBAS, C. 2013. Plasma and urine metabolic fingerprinting of type 1 diabetic children. *Electrophoresis*, 34, 2882-90.
- BARTEL, J., KRUMSIEK, J. & THEIS, F. J. 2013. STATISTICAL METHODS FOR THE ANALYSIS OF HIGH-THROUGHPUT METABOLOMICS DATA. *Computational and Structural Biotechnology Journal*, 4, e201301009.
- BATCH, B. C., SHAH, S. H., NEWGARD, C. B., TURER, C. B., HAYNES, C., BAIN, J. R., MUEHLBAUER, M., PATEL, M. J., STEVENS, R. D. & APPEL, L. J. 2013. Branched chain amino acids are novel biomarkers for discrimination of metabolic wellness. *Metabolism-Clinical and Experimental*, 62, 961-969.
- BAWAZEER, S., ALI, A. M., ALHAWITI, A., KHALAF, A., GIBSON, C., TUSIIMIRE, J. & WATSON, D. G. 2017. A method for the analysis of sugars in biological systems using reductive amination in combination with hydrophilic interaction chromatography and high resolution mass spectrometry. *Talanta*, 166, 75-80.
- BAXTER, E. W. & REITZ, A. B. 2004. Reductive aminations of carbonyl compounds with borohydride and borane reducing agents. *Organic reactions*, 59, 1-714.
- BEECHER, C. W. 2003. The human metabolome. *Metabolic profiling: Its role in biomarker discovery and gene function analysis*. Springer.
- BENJAMINI, Y. & HOCHBERG, Y. 1995. Controlling the false discovery rate: a practical and powerful approach to multiple testing. *Journal of the royal statistical society. Series B (Methodological)*, 289-300.
- BERENT-SPILLSON, A., ROBINSON, A. M., GOLOVOY, D., SLUSHER, B., ROJAS, C. & RUSSELL, J. W. 2004. Protection against glucose-induced neuronal death by NAAG and GCP II inhibition is regulated by mGluR3. *Journal of neurochemistry*, 89, 90-99.
- BERMEJO-DEVAL, R., ASSARY, R. S., NIKOLLA, E., MOLINER, M., ROMÁN-LESHKOV, Y., HWANG, S.-J., PALSDOTTIR, A., SILVERMAN, D., LOBO, R. F. & CURTISS, L. A. 2012. Metalloenzyme-like catalyzed isomerizations of sugars by Lewis acid zeolites. *Proceedings of the National Academy of Sciences*, 109, 9727-9732.
- BHARTI, S. K. & ROY, R. 2014. Metabolite Identification in NMR-based Metabolomics. *Current Metabolomics*, 2, 163-173.

- BHATTACHARYA, M., FUHRMAN, L., INGRAM, A., NICKERSON, K. W. & CONWAY, T. 1995. Single-Run Separation and Detection of Multiple Metabolic Intermediates by Anion-Exchange High-Performance Liquid Chromatography and Application to Cell Pool Extracts Prepared from *Escherichia coli*. *Analytical biochemistry*, 232, 98-106.
- BIOMARKERS DEFINITIONS WORKING, G. 2001. Biomarkers and surrogate endpoints: preferred definitions and conceptual framework. *Clin Pharmacol Ther*, 69, 89-95.
- BJERKENSTEDT, L., EDMAN, G., HAGENFELDT, L., SEDVALL, G. & WIESEL, F.-A. 1985. Plasma amino acids in relation to cerebrospinal fluid monoamine metabolites in schizophrenic patients and healthy controls. *The British Journal of Psychiatry*, 147, 276-282.
- BOLDIZSAR, I., HORVATH, K., SZEDLAY, G. & MOLNAR-PERL, I. 1998. Simultaneous GC-MS quantitation of acids and sugars in the hydrolyzates of immunostimulant, water-soluble polysaccharides of basidiomycetes. *Chromatographia*, 47, 413.
- BOUATRA, S., AZIAT, F., MANDAL, R., GUO, A. C., WILSON, M. R., KNOX, C., BJORNDahl, T. C., KRISHNAMURTHY, R., SALEEM, F., LIU, P., DAME, Z. T., POELZER, J., HUYNH, J., YALLOU, F. S., PSYCHOGIOS, N., DONG, E., BOGUMIL, R., ROEHRING, C. & WISHART, D. S. 2013. The human urine metabolome. *PLoS One*, 8, e73076.
- BRACKEN, R. M., LINNANE, D. M. & BROOKS, S. 2009. Plasma catecholamine and nehrine responses to brief intermittent maximal intensity exercise. *Amino Acids*, 36, 209-17.
- BRIDI, R., ARALDI, J., SGARBI, M. B., TESTA, C. G., DURIGON, K., WAJNER, M. & DUTRA-FILHO, C. S. 2003. Induction of oxidative stress in rat brain by the metabolites accumulating in maple syrup urine disease. *Int J Dev Neurosci*, 21, 327-32.
- BROOKS, C., EDMONDS, C., GASKELL, S. & SMITH, A. 1978. Derivatives suitable for GC-MS. *Chemistry and Physics of Lipids*, 21, 403-416.
- BURCHETT, S. A. & HICKS, T. P. 2006. The mysterious trace amines: protean neuromodulators of synaptic transmission in mammalian brain. *Progress in neurobiology*, 79, 223-246.
- BURGHARDT, K. J., EVANS, S. J., WIESE, K. M. & ELLINGROD, V. L. 2015. An untargeted metabolomics analysis of antipsychotic use in bipolar disorder. *Clinical and translational science*, 8, 432-440.
- CARNETHON, M. R., GULATI, M. & GREENLAND, P. 2005. Prevalence and cardiovascular disease correlates of low cardiorespiratory fitness in adolescents and adults. *JAMA*, 294, 2981-8.
- CAYMANCHEM. Item № 20666. *Caymanchem.com, Arachidonic Acid Oxylipins LC-MS Mixture, Item № 20666*. [Online]. Available: <https://www.caymanchem.com/pdfs/20666.pdf>.
- CAYMANCHEM. Item № 20794. *Caymanchem.com, Linoleic Acid Oxylipins LC-MS Mixture, Item № 20794* [Online]. Available: <https://www.caymanchem.com/pdfs/20794.pdf>.
- CELI, P. & GABAI, G. 2015. Oxidant/Antioxidant Balance in Animal Nutrition and Health: The Role of Protein Oxidation. *Frontiers in Veterinary Science*, 2, 48.

- CHAMBERS, E., WAGROWSKI-DIEHL, D. M., LU, Z. & MAZZEO, J. R. 2007. Systematic and comprehensive strategy for reducing matrix effects in LC/MS/MS analyses. *Journal of Chromatography B*, 852, 22-34.
- CHEN, S.-H. & CHUANG, Y.-J. 2002. Analysis of fatty acids by column liquid chromatography. *Analytica Chimica Acta*, 465, 145-155.
- CHONG, I.-G. & JUN, C.-H. 2005. Performance of some variable selection methods when multicollinearity is present. *Chemometrics and intelligent laboratory systems*, 78, 103-112.
- CORRIGAN, P. W. 2007. How clinical diagnosis might exacerbate the stigma of mental illness. *Social Work*, 52, 31-39.
- CRESPO, E. A., SILVA, L. P., MARTINS, M. N. A., FERNANDEZ, L., ORTEGA, J., FERREIRA, O., SADOWSKI, G., HELD, C., PINHO, S. O. P. & COUTINHO, J. O. A. 2017. Characterization and Modeling of the Liquid Phase of Deep Eutectic Solvents Based on Fatty Acids/Alcohols and Choline Chloride. *Industrial & Engineering Chemistry Research*, 56, 12192-12202.
- CUBBON, S., ANTONIO, C., WILSON, J. & THOMAS-OATES, J. 2010. Metabolomic applications of HILIC–LC–MS. *Mass Spectrometry Reviews*, 29, 671-684.
- DALACK, G. W., HEALY, D. J. & MEADOR-WOODRUFF, J. H. 1998. Nicotine dependence in schizophrenia: clinical phenomena and laboratory findings. *American Journal of Psychiatry*, 155, 1490-1501.
- DANSIE, L. E., REEVES, S., MILLER, K., ZANO, S. P., FRANK, M., PATE, C., WANG, J. & JACKOWSKI, S. 2014. Physiological roles of the pantothenate kinases. *Biochem Soc Trans*, 42, 1033-6.
- DASKALAKI, E., BLACKBURN, G., KALNA, G., ZHANG, T., ANTHONY, N. & WATSON, D. G. 2015a. A study of the effects of exercise on the urinary metabolome using normalisation to individual metabolic output. *Metabolites*, 5, 119-39.
- DASKALAKI, E., EASTON, C. & WATSON, D. 2015b. The Application of Metabolomic Profiling to the Effects of Physical Activity. *Current Metabolomics*, 2, 233-263.
- DE PAIVA, M. J. N., MENEZES, H. C. & DE LOURDES CARDEAL, Z. 2014. Sampling and analysis of metabolomes in biological fluids. *Analyst*, 139, 3683-3694.
- DENOROY, L., ZIMMER, L., RENAUD, B. & PARROT, S. 2013. Ultra high performance liquid chromatography as a tool for the discovery and the analysis of biomarkers of diseases: a review. *J Chromatogr B Analyt Technol Biomed Life Sci*, 927, 37-53.
- DETTMER, K., ARONOV, P. A. & HAMMOCK, B. D. 2007. Mass spectrometry-based metabolomics. *Mass Spectrom Rev*, 26, 51-78.
- DI MARZO, V., FONTANA, A., CADAS, H., SCHINELLI, S., CIMINO, G., SCHWARTZ, J.-C. & PIOMELLI, D. 1994. Formation and inactivation of endogenous cannabinoid anandamide in central neurons. *Nature*, 372, 686.
- DJOUMBOU-FEUNANG, Y., FIAMONCINI, J., GIL-DE-LA-FUENTE, A., GREINER, R., MANACH, C. & WISHART, D. S. 2019. BioTransformer: a comprehensive computational tool for small molecule metabolism prediction and metabolite identification. *Journal of Cheminformatics*, 11, 2.

- DOVIO, A., ROVEDA, E., SCIOLLA, C., MONTARULI, A., RAFFAELLI, A., SABA, A., CALOGIURI, G., DE FRANCIA, S., BORRIONE, P., SALVADORI, P., CARANDENTE, F. & ANGELI, A. 2010. Intense physical exercise increases systemic 11beta-hydroxysteroid dehydrogenase type 1 activity in healthy adult subjects. *Eur J Appl Physiol*, 108, 681-7.
- DUDZINSKA, W., LUBKOWSKA, A., DOLEGOWSKA, B., SAFRANOW, K. & JAKUBOWSKA, K. 2010. Adenine, guanine and pyridine nucleotides in blood during physical exercise and restitution in healthy subjects. *Eur J Appl Physiol*, 110, 1155-62.
- DUNN, W. B., BROADHURST, D., BEGLEY, P., ZELENA, E., FRANCIS-MCINTYRE, S., ANDERSON, N., BROWN, M., KNOWLES, J. D., HALSALL, A., HASELDEN, J. N., NICHOLLS, A. W., WILSON, I. D., KELL, D. B. & GOODACRE, R. 2011. Procedures for large-scale metabolic profiling of serum and plasma using gas chromatography and liquid chromatography coupled to mass spectrometry. *Nat. Protocols*, 6, 1060-1083.
- E YOUNG, J., J PESEK, J. & T MATYSKA, M. 2016. Robust HPLC-Refractive Index Analysis of Simple Sugars in Beverages Using Silica Hydride Columns. *Current Nutrition & Food Science*, 12, 125-131.
- EDER, K. 1995. Gas chromatographic analysis of fatty acid methyl esters. *Journal of Chromatography B: Biomedical Sciences and Applications*, 671, 113-131.
- EDMANDS, W. M., FERRARI, P. & SCALBERT, A. 2014. Normalization to specific gravity prior to analysis improves information recovery from high resolution mass spectrometry metabolomic profiles of human urine. *Anal Chem*, 86, 10925-31.
- EJIGU, B. A., VALKENBORG, D., BAGGERMAN, G., VANAERSCHOT, M., WITTERS, E., DUJARDIN, J.-C., BURZYKOWSKI, T. & BERG, M. 2013. Evaluation of normalization methods to pave the way towards large-scale LC-MS-based metabolomics profiling experiments. *Omics: a journal of integrative biology*, 17, 473-485.
- ELLIS, D. I., DUNN, W. B., GRIFFIN, J. L., ALLWOOD, J. W. & GOODACRE, R. 2007. Metabolic fingerprinting as a diagnostic tool. *Pharmacogenomics*, 8, 1243-66.
- ENOT, D. P., HAAS, B. & WEINBERGER, K. M. 2011. Bioinformatics for mass spectrometry-based metabolomics. *Methods Mol Biol*, 719, 351-75.
- ERIKSSON, L., TRYGG, J. & WOLD, S. 2008. CV-ANOVA for significance testing of PLS and OPLS® models. *Journal of Chemometrics*, 22, 594-600.
- FEKETE, S., GUILLARME, D., SANDRA, P. & SANDRA, K. 2015. Chromatographic, electrophoretic, and mass spectrometric methods for the analytical characterization of protein biopharmaceuticals. *Analytical chemistry*, 88, 480-507.
- FELIZOLA, S. J. 2015. Ursolic acid in experimental models and human subjects: Potential as an anti-obesity/overweight treatment? *cancer*, 1, 2.
- FELL, D. & CORNISH-BOWDEN, A. 1997. *Understanding the control of metabolism*, Portland press London.
- FIEHN, O. 2002. Metabolomics--the link between genotypes and phenotypes. *Plant Mol Biol*, 48, 155-71.
- FISCHER, K., WACHT, M. & MEYER, A. 2003. Simultaneous and Sensitive HPLC Determination of Mono- and Disaccharides, Uronic Acids, and Amino Sugars

- after Derivatization by Reductive Amination. *Acta hydrochimica et hydrobiologica*, 31, 134-144.
- FREY, B. L., KRUSEMARK, C. J., LEDVINA, A. R., COON, J. J., BELSHAW, P. J. & SMITH, L. M. 2008. Ion-ion reactions with fixed-charge modified proteins to produce ions in a single, very high charge state. *International journal of mass spectrometry*, 276, 136-143.
- FUKUCHI, S., HAMAGUCHI, K., SEIKE, M., HIMENO, K., SAKATA, T. & YOSHIMATSU, H. 2004. Role of fatty acid composition in the development of metabolic disorders in sucrose-induced obese rats. *Experimental Biology and Medicine*, 229, 486-493.
- FUKUSAKI, E. & KOBAYASHI, A. 2005. Plant metabolomics: potential for practical operation. *Journal of Bioscience and Bioengineering*, 100, 347-354.
- FUKUSHIMA, A. & KUSANO, M. 2013. Recent Progress in the Development of Metabolome Databases for Plant Systems Biology. *Frontiers in Plant Science*, 4.
- GAMA, M. R., DA COSTA SILVA, R. G., COLLINS, C. H. & BOTTOLI, C. B. G. 2012. Hydrophilic interaction chromatography. *TrAC Trends in Analytical Chemistry*, 37, 48-60.
- GAMOH, K., SAITOH, H. & WADA, H. 2003. Improved liquid chromatography/mass spectrometric analysis of low molecular weight carboxylic acids by ion exclusion separation with electrospray ionization. *Rapid communications in mass spectrometry*, 17, 685-689.
- GAO, X., YANG, J., HUANG, F., WU, X., LI, L. & SUN, C. 2003. Progresses of derivatization techniques for analyses of carbohydrates. *Analytical letters*, 36, 1281-1310.
- GATTI, R., CAPPELLIN, E., ZECCHIN, B., ANTONELLI, G., SPINELLA, P., MANTERO, F. & DE PALO, E. F. 2005. Urinary high performance reverse phase chromatography cortisol and cortisone analyses before and at the end of a race in elite cyclists. *Journal of Chromatography B*, 824, 51-56.
- GIKA, H. G., THEODORIDIS, G. A., PLUMB, R. S. & WILSON, I. D. 2014. Current practice of liquid chromatography-mass spectrometry in metabolomics and metabonomics. *Journal of Pharmaceutical and Biomedical Analysis*, 87, 12-25.
- GOUVEIA-FIGUEIRA, S., SPÄTH, J., ZIVKOVIC, A. M. & NORDING, M. L. 2015. Profiling the oxylipin and endocannabinoid metabolome by UPLC-ESI-MS/MS in human plasma to monitor postprandial inflammation. *PLoS One*, 10, e0132042.
- GROMSKI, P. S., XU, Y., KOTZE, H. L., CORREA, E., ELLIS, D. I., ARMITAGE, E. G., TURNER, M. L. & GOODACRE, R. 2014. Influence of missing values substitutes on multivariate analysis of metabolomics data. *Metabolites*, 4, 433-452.
- GU, H., DU, J., CARNEVALE NETO, F., CARROLL, P. A., TURNER, S. J., CHIOREAN, E. G., EISENMAN, R. N. & RAFTERY, D. 2015. Metabolomics method to comprehensively analyze amino acids in different domains. *Analyst*, 140, 2726-34.
- GUIDOTTI, A., AUTA, J., DAVIS, J. M., DONG, E., GRAYSON, D. R., VELDIC, M., ZHANG, X. & COSTA, E. 2005. GABAergic dysfunction in schizophrenia: new treatment strategies on the horizon. *Psychopharmacology*, 180, 191-205.

- GUO, K. & LI, L. 2009. Differential ^{12}C -/ ^{13}C -isotope dansylation labeling and fast liquid chromatography/mass spectrometry for absolute and relative quantification of the metabolome. *Analytical chemistry*, 81, 3919-3932.
- HAFEZI-MOGHADAM, A., SIMONCINI, T., YANG, Z., LIMBOURG, F. P., PLUMIER, J. C., REBSAMEN, M. C., HSIEH, C. M., CHUI, D. S., THOMAS, K. L., PROROCK, A. J., LAUBACH, V. E., MOSKOWITZ, M. A., FRENCH, B. A., LEY, K. & LIAO, J. K. 2002. Acute cardiovascular protective effects of corticosteroids are mediated by non-transcriptional activation of endothelial nitric oxide synthase. *Nat Med*, 8, 473-9.
- HALKET, J. M., WATERMAN, D., PRZYBOROWSKA, A. M., PATEL, R. K. P., FRASER, P. D. & BRAMLEY, P. M. 2005. Chemical derivatization and mass spectral libraries in metabolic profiling by GC/MS and LC/MS/MS. *Journal of Experimental Botany*, 56, 219-243.
- HARVEY, D. J. 2011. Derivatization of carbohydrates for analysis by chromatography; electrophoresis and mass spectrometry. *Journal of Chromatography B*, 879, 1196-1225.
- HASHIMOTO, T., VOLK, D. W., EGGAN, S. M., MIRNICS, K., PIERRI, J. N., SUN, Z., SAMPSON, A. R. & LEWIS, D. A. 2003. Gene expression deficits in a subclass of GABA neurons in the prefrontal cortex of subjects with schizophrenia. *Journal of Neuroscience*, 23, 6315-6326.
- HE, Y., YU, Z., GIEGLING, I., XIE, L., HARTMANN, A., PREHN, C., ADAMSKI, J., KAHN, R., LI, Y. & ILLIG, T. 2012. Schizophrenia shows a unique metabolomics signature in plasma. *Translational psychiatry*, 2, e149.
- HEALTH, U. D. O. & SERVICES, H. 2001. Bioanalytical Method Validation, Guidance for Industry. <http://www.fda.gov/cder/guidance/4252fnl.htm>.
- HERNÁNDEZ-PÉREZ, J. M., CABRÉ, E., FLUVIÀ, L., MOTOS, Á., PASTOR, C., COROMINAS, A. & GASSULL, M. A. 2002. Improved Method for Gas Chromatographic–Mass Spectrometric Analysis of ^{13}C -labeled Long-Chain Fatty Acids in Plasma Samples. *Clinical chemistry*, 48, 906-912.
- HIGASHI, T., ICHIKAWA, T., INAGAKI, S., MIN, J. Z., FUKUSHIMA, T. & TOYO'OKA, T. 2010. Simple and practical derivatization procedure for enhanced detection of carboxylic acids in liquid chromatography–electrospray ionization–tandem mass spectrometry. *Journal of pharmaceutical and biomedical analysis*, 52, 809-818.
- HRYDZIUSZKO, O. & VIANT, M. R. 2012. Missing values in mass spectrometry based metabolomics: an undervalued step in the data processing pipeline. *Metabolomics*, 8, 161-174.
- HUFFMAN, K. M., SHAH, S. H., STEVENS, R. D., BAIN, J. R., MUEHLBAUER, M., SLENTZ, C. A., TANNER, C. J., KUCHIBHATLA, M., HOUMARD, J. A. & NEWGARD, C. B. 2009. Relationships between circulating metabolic intermediates and insulin action in overweight to obese, inactive men and women. *Diabetes care*, 32, 1678-1683.
- ISSAQ, H. J., VAN, Q. N., WAYBRIGHT, T. J., MUSCHIK, G. M. & VEENSTRA, T. D. 2009. Analytical and statistical approaches to metabolomics research. *J Sep Sci*, 32, 2183-99.
- IWASAKI, Y., ISHII, Y., ITO, R., SAITO, K. & NAKAZAWA, H. 2007. New approaches for analysis of metabolism compounds in hydrophilic interaction

- chromatography. *Journal of liquid chromatography & related technologies*, 30, 2117-2126.
- IWASAKI, Y., SAWADA, T., HATAYAMA, K., OHYAGI, A., TSUKUDA, Y., NAMEKAWA, K., ITO, R., SAITO, K. & NAKAZAWA, H. 2012. Separation technique for the determination of highly polar metabolites in biological samples. *Metabolites*, 2, 496-515.
- JACKA, F. N., MYKLETUN, A. & BERK, M. 2012. Moving towards a population health approach to the primary prevention of common mental disorders. *BMC Med*, 10, 149.
- JANDERA, P. 2008. Stationary phases for hydrophilic interaction chromatography, their characterization and implementation into multidimensional chromatography concepts. *Journal of separation science*, 31, 1421-1437.
- JOFFE, Y. T., COLLINS, M. & GOEDECKE, J. H. 2013. The relationship between dietary fatty acids and inflammatory genes on the obese phenotype and serum lipids. *Nutrients*, 5, 1672-1705.
- JOHNSON, D. W. 2000. Alkyldimethylaminoethyl ester iodides for improved analysis of fatty acids by electrospray ionization tandem mass spectrometry. *Rapid Communications in Mass Spectrometry*, 14, 2019-2024.
- JOHNSON, D. W., TRINH, M.-U. & OE, T. 2003. Measurement of plasma pristanic, phytanic and very long chain fatty acids by liquid chromatography-electrospray tandem mass spectrometry for the diagnosis of peroxisomal disorders. *Journal of Chromatography B*, 798, 159-162.
- JOYNER, M. J. & COYLE, E. F. 2008. Endurance exercise performance: the physiology of champions. *J Physiol*, 586, 35-44.
- KADDURAH-DAOUK, R. & KRISHNAN, K. R. R. 2009. Metabolomics: a global biochemical approach to the study of central nervous system diseases. *Neuropsychopharmacology*, 34, 173.
- KATAJAMAA, M. & OREŠIČ, M. 2005. Processing methods for differential analysis of LC/MS profile data. *BMC Bioinformatics*, 6, 1-12.
- KAUR, J. 2014. A comprehensive review on metabolic syndrome. *Cardiology research and practice*, 2014.
- KELL, D. B. & OLIVER, S. G. 2016. The metabolome 18 years on: a concept comes of age. *Metabolomics : Official journal of the Metabolomic Society*, 12, 148-148.
- KELLEY, E. E., PAES, A. M. D. A., YADAV, H., QUIJANO, C., CASSINA, A. & TROSTCHANSKY, A. 2017. Interplay between Oxidative Stress and Metabolism in Signalling and Disease 2016. *Oxidative medicine and cellular longevity*, 2017.
- KEMPF, L., NICODEMUS, K. K., KOLACHANA, B., VAKKALANKA, R., VERCHINSKI, B. A., EGAN, M. F., STRAUB, R. E., MATTAY, V. A., CALLICOTT, J. H. & WEINBERGER, D. R. 2008. Functional polymorphisms in PRODH are associated with risk and protection for schizophrenia and fronto-striatal structure and function. *PLoS genetics*, 4, e1000252.
- KIRWAN, G. M., JOHANSSON, E., KLEEMANN, R., VERHEIJ, E. R., WHEELOCK, Å. M., GOTO, S., TRYGG, J. & WHEELOCK, C. E. 2012. Building multivariate systems biology models. *Analytical chemistry*, 84, 7064-7071.

- KO, B. J. & BRODBELT, J. S. 2012. Enhanced electron transfer dissociation of peptides modified at C-terminus with fixed charges. *Journal of the American Society for Mass Spectrometry*, 23, 1991-2000.
- KOHEN, R., YAMAMOTO, Y., CUNDY, K. C. & AMES, B. N. 1988. Antioxidant activity of carnosine, homocarnosine, and anserine present in muscle and brain. *Proceedings of the National Academy of Sciences*, 85, 3175-3179.
- KOIKE, S., BUNDO, M., IWAMOTO, K., SUGA, M., KUWABARA, H., OHASHI, Y., SHINODA, K., TAKANO, Y., IWASHIRO, N. & SATOMURA, Y. 2014. A snapshot of plasma metabolites in first-episode schizophrenia: a capillary electrophoresis time-of-flight mass spectrometry study. *Translational psychiatry*, 4, e379.
- KUJALA, U. M., MAKINEN, V. P., HEINONEN, I., SOININEN, P., KANGAS, A. J., LESKINEN, T. H., RAHKILA, P., WURTZ, P., KOVANEN, V., CHENG, S., SIPILA, S., HIRVENSALO, M., TELAMA, R., TAMMELIN, T., SAVOLAINEN, M. J., POUTA, A., O'REILLY, P. F., MANTYSELKA, P., VIIKARI, J., KAHONEN, M., LEHTIMAKI, T., ELLIOTT, P., VANHALA, M. J., RAITAKARI, O. T., JARVELIN, M. R., KAPRIO, J., KAINULAINEN, H. & ALA-KORPELA, M. 2013. Long-term leisure-time physical activity and serum metabolome. *Circulation*, 127, 340-8.
- LAI, Y.-L., AOYAMA, S., NAGAI, R., MIYOSHI, N. & OHSHIMA, H. 2010. Inhibition of L-Arginine Metabolizing Enzymes by L-Arginine-Derived Advanced Glycation End Products. *Journal of Clinical Biochemistry and Nutrition*, 46, 177-185.
- LEE, S. H., WILLIAMS, M. V., DUBOIS, R. N. & BLAIR, I. A. 2003. Targeted lipidomics using electron capture atmospheric pressure chemical ionization mass spectrometry. *Rapid Communications in Mass Spectrometry*, 17, 2168-2176.
- LENZ, E. M., BRIGHT, J., WILSON, I. D., HUGHES, A., MORRISSON, J., LINDBERG, H. & LOCKTON, A. 2004. Metabonomics, dietary influences and cultural differences: a ¹H NMR-based study of urine samples obtained from healthy British and Swedish subjects. *Journal of Pharmaceutical and Biomedical Analysis*, 36, 841-849.
- LI, X. & FRANKE, A. A. 2011. Improved LC- MS method for the determination of fatty acids in red blood cells by LC- orbitrap MS. *Analytical chemistry*, 83, 3192-3198.
- LIEN, Y., SHAPIRO, J. & CHAN, L. 1990. Effects of hypernatremia on organic brain osmoles. *The Journal of clinical investigation*, 85, 1427-1435.
- LIU, J., LITT, L., SEGAL, M. R., KELLY, M. J., PELTON, J. G. & KIM, M. 2011. Metabolomics of oxidative stress in recent studies of endogenous and exogenously administered intermediate metabolites. *Int J Mol Sci*, 12, 6469-501.
- LIU, M.-L., ZHANG, X.-T., DU, X.-Y., FANG, Z., LIU, Z., XU, Y., ZHENG, P., XU, X.-J., CHENG, P.-F. & HUANG, T. 2015. Severe disturbance of glucose metabolism in peripheral blood mononuclear cells of schizophrenia patients: a targeted metabolomic study. *Journal of translational medicine*, 13, 226.
- LOBO, V., PATIL, A., PHATAK, A. & CHANDRA, N. 2010. Free radicals, antioxidants and functional foods: Impact on human health. *Pharmacognosy Reviews*, 4, 118-126.

- LOMMEN, A. 2009. MetAlign: interface-driven, versatile metabolomics tool for hyphenated full-scan mass spectrometry data preprocessing. *Anal Chem*, 81, 3079-86.
- LUNDIN, U., MODRE-OSPRIAN, R. & WEINBERGER, K. M. 2011. Targeted Metabolomics for Clinical Biomarker Discovery in Multifactorial Diseases. In: IKEHARA, D. K. (ed.) *Advances in the Study of Genetic Disorders*. InTech.
- LUSTGARTEN, M. S., PRICE, L. L., CHALE, A. & FIELDING, R. A. 2014. Metabolites related to gut bacterial metabolism, peroxisome proliferator-activated receptor-alpha activation, and insulin sensitivity are associated with physical function in functionally-limited older adults. *Aging Cell*, 13, 918-25.
- LUSTGARTEN, M. S., PRICE, L. L., LOGVINENKO, T., HATZIS, C., PADUKONE, N., REO, N. V., PHILLIPS, E. M., KIRN, D., MILLS, J. & FIELDING, R. A. 2013. Identification of serum analytes and metabolites associated with aerobic capacity. *Eur J Appl Physiol*, 113, 1311-20.
- MAJORS, R. E. & PRZYBYCIEL, M. 2002. Columns for reversed-phase LC separations in highly aqueous mobile phases. *LC GC NORTH AMERICA*, 20, 584-593.
- MAKAROV, A., DENISOV, E., LANGE, O. & HORNING, S. 2006. Dynamic range of mass accuracy in LTQ Orbitrap hybrid mass spectrometer. *Journal of the American Society for Mass Spectrometry*, 17, 977-982.
- MAKAROV, A. & SCIGELOVA, M. 2010. Coupling liquid chromatography to Orbitrap mass spectrometry. *Journal of Chromatography A*, 1217, 3938-3945.
- MALAGUARNERA, M. 2012. Carnitine derivatives: clinical usefulness. *Current opinion in gastroenterology*, 28, 166-176.
- MALIK, V. S., POPKIN, B. M., BRAY, G. A., DESPRÉS, J.-P., WILLETT, W. C. & HU, F. B. 2010. Sugar-sweetened beverages and risk of metabolic syndrome and type 2 diabetes: a meta-analysis. *Diabetes care*, 33, 2477-2483.
- MARTIN, A. & SYNGE, R. 1977. A new form of chromatogram employing two liquid phases: 1. A theory of chromatography 2. Application to the micro-determination of the higher monoamino-acids in proteins. *Trends in Biochemical Sciences*, 2, N245.
- MARTINS-DE-SOUZA, D., MACCARRONE, G., WOBROCK, T., ZERR, I., GORMANNS, P., RECKOW, S., FALKAI, P., SCHMITT, A. & TURCK, C. W. 2010. Proteome analysis of the thalamus and cerebrospinal fluid reveals glycolysis dysfunction and potential biomarkers candidates for schizophrenia. *Journal of psychiatric research*, 44, 1176-1189.
- MASHEGO, M. R., RUMBOLD, K., DE MEY, M., VANDAMME, E., SOETAERT, W. & HEIJNEN, J. J. 2007. Microbial metabolomics: past, present and future methodologies. *Biotechnol Lett*, 29, 1-16.
- MATUS, J. T. 2016. Transcriptomic and Metabolomic Networks in the Grape Berry Illustrate That it Takes More Than Flavonoids to Fight Against Ultraviolet Radiation. *Frontiers in Plant Science*, 7.
- MCCORMACK, S. E., SHAHAM, O., MCCARTHY, M. A., DEIK, A. A., WANG, T. J., GERSZTEN, R. E., CLISH, C. B., MOOTHA, V. K., GRINSPOON, S. K. & FLEISCHMAN, A. 2013. Circulating branched-chain amino acid concentrations are associated with obesity and future insulin resistance in children and adolescents. *Pediatric obesity*, 8, 52-61.

- MCDONALD, J. H. 2014. *Handbook of biological statistics*, Sparky House Publishing Baltimore, MD.
- MEDEIROS, P. M. & SIMONEIT, B. R. 2007. Analysis of sugars in environmental samples by gas chromatography–mass spectrometry. *Journal of Chromatography A*, 1141, 271-278.
- MOCO, S., VERVOORT, J., MOCO, S., BINO, R. J., DE VOS, R. C. H. & BINO, R. 2007. Metabolomics technologies and metabolite identification. *TrAC Trends in Analytical Chemistry*, 26, 855-866.
- MOLNÁR-PERL, I. & HORVÁTH, K. 1997. Simultaneous quantitation of mono-, di- and trisaccharides as their TMS ether oxime derivatives by GC-MS: I. In model solutions. *Chromatographia*, 45, 321-327.
- MORELLE, W., SLOMIANNY, M. C., DIEMER, H., SCHAEFFER, C., DORSSELAER, A. V. & MICHALSKI, J. C. 2005. Structural characterization of 2-aminobenzamide-derivatized oligosaccharides using a matrix-assisted laser desorption/ionization two-stage time-of-flight tandem mass spectrometer. *Rapid Communications in Mass Spectrometry: An International Journal Devoted to the Rapid Dissemination of Up-to-the-Minute Research in Mass Spectrometry*, 19, 2075-2084.
- MORGAN, A., MOONEY, K. & MC AULEY, M. 2016. Obesity and the dysregulation of fatty acid metabolism: implications for healthy aging. *Expert Review of Endocrinology & Metabolism*, 11, 501-510.
- MOSS, G. P., SMITH, P. A. S. & TAVERNIER, D. 1995. Glossary of class names of organic compounds and reactivity intermediates based on structure (IUPAC Recommendations 1995). *Pure and Applied Chemistry*.
- NASRALLAH, S. & AL-KHALIDI, U. 1964. NATURE OF PURINES EXCRETED IN URINE DURING MUSCULAR EXERCISE. *J Appl Physiol*, 19, 246-8.
- NEAL, C. M., HUNTER, A. M., BRENNAN, L., O'SULLIVAN, A., HAMILTON, D. L., DE VITO, G. & GALLOWAY, S. D. 2013. Six weeks of a polarized training-intensity distribution leads to greater physiological and performance adaptations than a threshold model in trained cyclists. *J Appl Physiol (1985)*, 114, 461-71.
- NEWCOMER, J. W. 2007. Metabolic syndrome and mental illness. *The American journal of managed care*, 13, S170-7.
- NEWGARD, C. B., AN, J., BAIN, J. R., MUEHLBAUER, M. J., STEVENS, R. D., LIEN, L. F., HAQQ, A. M., SHAH, S. H., ARLOTTO, M. & SLENTZ, C. A. 2009. A branched-chain amino acid-related metabolic signature that differentiates obese and lean humans and contributes to insulin resistance. *Cell metabolism*, 9, 311-326.
- NICHOLSON, J. K., LINDON, J. C. & HOLMES, E. 1999. 'Metabonomics': understanding the metabolic responses of living systems to pathophysiological stimuli via multivariate statistical analysis of biological NMR spectroscopic data. *Xenobiotica*, 29, 1181-9.
- NORDSTROM, A., WANT, E., NORTHEN, T., LEHTIO, J. & SIUZDAK, G. 2008. Multiple ionization mass spectrometry strategy used to reveal the complexity of metabolomics. *Anal Chem*, 80, 421-9.
- NYAMUNDANDA, G., BRENNAN, L. & GORMLEY, I. C. 2010. Probabilistic principal component analysis for metabolomic data. *BMC Bioinformatics*, 11, 571.

- OREŠIČ, M., TANG, J., SEPPÄNEN-LAAKSO, T., MATTILA, I., SAARNI, S. E., SAARNI, S. I., LÖNNQVIST, J., SYSI-AHO, M., HYÖTYLÄINEN, T. & PERÄLÄ, J. 2011. Metabolome in schizophrenia and other psychotic disorders: a general population-based study. *Genome medicine*, 3, 19.
- OSL, M., DREISEITL, S., PFEIFER, B., WEINBERGER, K., KLOCKER, H., BARTSCH, G., SCHÄFER, G., TILG, B., GRABER, A. & BAUMGARTNER, C. 2008. A new rule-based algorithm for identifying metabolic markers in prostate cancer using tandem mass spectrometry. *Bioinformatics*, 24, 2908-2914.
- PAREDES, R. M., QUINONES, M., MARBALLI, K., GAO, X., VALDEZ, C., AHUJA, S. S., VELLIGAN, D. & WALSS-BASS, C. 2014. Metabolomic profiling of schizophrenia patients at risk for metabolic syndrome. *International Journal of Neuropsychopharmacology*, 17, 1139-1148.
- PARK, H. M., SHON, J. C., LEE, M. Y., LIU, K.-H., KIM, J. K., LEE, S. J. & LEE, C. H. 2014. Mass spectrometry-based metabolite profiling in the mouse liver following exposure to ultraviolet B radiation. *PLoS one*, 9, e109479.
- PASIKANTI, K. K., HO, P. C. & CHAN, E. C. 2008. Gas chromatography/mass spectrometry in metabolic profiling of biological fluids. *J Chromatogr B Analyt Technol Biomed Life Sci*, 871, 202-11.
- PATIL, P. & PRATAP, A. 2016. Choline Chloride Catalyzed Amidation of Fatty Acid Ester to Monoethanolamide: A Green Approach. *Journal of oleo science*, 65, 75-79.
- PATTI, G. J. 2011. Separation strategies for untargeted metabolomics. *J Sep Sci*, 34, 3460-9.
- PATTI, G. J., YANES, O. & SIUZDAK, G. 2012. Innovation: Metabolomics: the apogee of the omics trilogy. *Nat Rev Mol Cell Biol*, 13, 263-9.
- PECHLIVANIS, A., KOSTIDIS, S., SARASLANIDIS, P., PETRIDOU, A., TSALIS, G., MOUGIOS, V., GIKA, H. G., MIKROS, E. & THEODORIDIS, G. A. 2010. (1)H NMR-based metabonomic investigation of the effect of two different exercise sessions on the metabolic fingerprint of human urine. *J Proteome Res*, 9, 6405-16.
- PECHLIVANIS, A., KOSTIDIS, S., SARASLANIDIS, P., PETRIDOU, A., TSALIS, G., VESELKOV, K., MIKROS, E., MOUGIOS, V. & THEODORIDIS, G. A. 2013. 1H NMR study on the short- and long-term impact of two training programs of sprint running on the metabolic fingerprint of human serum. *J Proteome Res*, 12, 470-80.
- PETTINELLA, C., LEE, S. H., CIPOLLONE, F. & BLAIR, I. A. 2007. Targeted quantitative analysis of fatty acids in atherosclerotic plaques by high sensitivity liquid chromatography/tandem mass spectrometry. *Journal of Chromatography B*, 850, 168-176.
- PHAM-TUAN, H., KASKAVELIS, L., DAYKIN, C. A. & JANSSEN, H.-G. 2003. Method development in high-performance liquid chromatography for high-throughput profiling and metabonomic studies of biofluid samples. *Journal of Chromatography B*, 789, 283-301.
- PICKARD, B. S. 2015. Schizophrenia biomarkers: translating the descriptive into the diagnostic. *Journal of Psychopharmacology*, 29, 138-143.
- PITSAVOS, C., PANAGIOTAKOS, D., WEINEM, M. & STEFANADIS, C. 2006. Diet, exercise and the metabolic syndrome. *The Review of Diabetic Studies*, 3, 118.

- PLUMB, R. S., STUMPF, C. L., GORENSTEIN, M. V., CASTRO-PEREZ, J. M., DEAR, G. J., ANTHONY, M., SWEATMAN, B. C., CONNOR, S. C. & HASELDEN, J. N. 2002. Metabonomics: the use of electrospray mass spectrometry coupled to reversed-phase liquid chromatography shows potential for the screening of rat urine in drug development. *Rapid Commun Mass Spectrom*, 16, 1991-6.
- PLUSKAL, T., CASTILLO, S., VILLAR-BRIONES, A. & OREŠIČ, M. 2010. MZmine 2: Modular framework for processing, visualizing, and analyzing mass spectrometry-based molecular profile data. *BMC Bioinformatics*, 11, 1-11.
- PONTES, P. V., CRESPO, E. A., MARTINS, M. A., SILVA, L. P., NEVES, C. M., MAXIMO, G. J., HUBINGER, M. D., BATISTA, E. A., PINHO, S. P. & COUTINHO, J. A. 2017. Measurement and PC-SAFT modeling of solid-liquid equilibrium of deep eutectic solvents of quaternary ammonium chlorides and carboxylic acids. *Fluid Phase Equilibria*, 448, 69-80.
- QI, B.-L., LIU, P., WANG, Q.-Y., CAI, W.-J., YUAN, B.-F. & FENG, Y.-Q. 2014. Derivatization for liquid chromatography-mass spectrometry. *TrAC Trends in Analytical Chemistry*, 59, 121-132.
- QIAN, W. L., KHAN, Z., WATSON, D. G. & FEARNLEY, J. 2008. Analysis of sugars in bee pollen and propolis by ligand exchange chromatography in combination with pulsed amperometric detection and mass spectrometry. *Journal of Food Composition and Analysis*, 21, 78-83.
- RAMEL, A., WAGNER, K. H. & ELMADFA, I. 2004. Plasma antioxidants and lipid oxidation after submaximal resistance exercise in men. *Eur J Nutr*, 43, 2-6.
- REGENOLD, W., PHATAK, P., KLING, M. & HAUSER, P. 2004. Post-mortem evidence from human brain tissue of disturbed glucose metabolism in mood and psychotic disorders. *Molecular psychiatry*, 9, 731.
- REILLY, J. J., DICK, S., MCNEILL, G. & TREMBLAY, M. S. 2014. Results from Scotland's 2013 Report Card on Physical Activity for Children and Youth. *J Phys Act Health*, 11 Suppl 1, S93-7.
- RENNIE, M. J., BOHÉ, J., SMITH, K., WACKERHAGE, H. & GREENHAFF, P. 2006. Branched-chain amino acids as fuels and anabolic signals in human muscle. *The Journal of nutrition*, 136, 264S-268S.
- ROWLAND, L. M., KONTSON, K., WEST, J., EDDEN, R. A., ZHU, H., WIJTENBURG, S. A., HOLCOMB, H. H. & BARKER, P. B. 2012. In vivo measurements of glutamate, GABA, and NAAG in schizophrenia. *Schizophrenia bulletin*, 39, 1096-1104.
- RUIZ-MATUTE, A. I., HERNÁNDEZ-HERNÁNDEZ, O., RODRÍGUEZ-SÁNCHEZ, S., SANZ, M. L. & MARTÍNEZ-CASTRO, I. 2011. Derivatization of carbohydrates for GC and GC-MS analyses. *Journal of Chromatography B*, 879, 1226-1240.
- RYAN, D., ROBARDS, K., PRENZLER, P. D. & KENDALL, M. 2011. Recent and potential developments in the analysis of urine: a review. *Analytica Chimica Acta*, 684, 17-29.
- SAHLIN, K., TONKONOGLI, M. & SODERLUND, K. 1999. Plasma hypoxanthine and ammonia in humans during prolonged exercise. *Eur J Appl Physiol Occup Physiol*, 80, 417-22.
- SARRIS, J., O'NEIL, A., COULSON, C. E., SCHWEITZER, I. & BERK, M. 2014. Lifestyle medicine for depression. *BMC Psychiatry*, 14, 107.

- SCARBOROUGH, P., BHATNAGAR, P., WICKRAMASINGHE, K. K., ALLENDER, S., FOSTER, C. & RAYNER, M. 2011. The economic burden of ill health due to diet, physical inactivity, smoking, alcohol and obesity in the UK: an update to 2006-07 NHS costs. *J Public Health (Oxf)*, 33, 527-35.
- SCHNAAR, R. L., GERARDY-SCHAHN, R. & HILDEBRANDT, H. 2014. Sialic acids in the brain: gangliosides and polysialic acid in nervous system development, stability, disease, and regeneration. *Physiological Reviews*, 94, 461-518.
- SCHOLZ, M., GATZEK, S., STERLING, A., FIEHN, O. & SELBIG, J. 2004. Metabolite fingerprinting: detecting biological features by independent component analysis. *Bioinformatics*, 20, 2447-54.
- SCHÖNFELD, P. & WOJTCZAK, L. 2016. Short- and medium-chain fatty acids in energy metabolism: the cellular perspective. *Journal of Lipid Research*, 57, 943-954.
- SCIGELOVA, M. & MAKAROV, A. 2006. Orbitrap mass analyzer—overview and applications in proteomics. *Proteomics*, 6, 16-21.
- SCRIPPS. 2016. *Scripps Center for Metabolomics. METLIN* [Online]. Available: <https://metlin.scripps.edu/index.php>. (accessed on 22 February 2016).
- SERKOVA, N. J., STANDIFORD, T. J. & STRINGER, K. A. 2011. The emerging field of quantitative blood metabolomics for biomarker discovery in critical illnesses. *American journal of respiratory and critical care medicine*, 184, 647-655.
- SHA, L., MACINTYRE, L., MACHELL, J., KELLY, M., PORTEOUS, D., BRANDON, N., MUIR, W. J., BLACKWOOD, D., WATSON, D. & CLAPCOTE, S. 2012. Transcriptional regulation of neurodevelopmental and metabolic pathways by NPAS3. *Molecular psychiatry*, 17, 267.
- SHEEDY, J. R., GOOLEY, P. R., NAHID, A., TULL, D. L., MCCONVILLE, M. J., KUKULJAN, S., NOWSON, C. A., DALY, R. M. & EBELING, P. R. 2014. (1)H-NMR analysis of the human urinary metabolome in response to an 18-month multi-component exercise program and calcium-vitamin-D3 supplementation in older men. *Appl Physiol Nutr Metab*, 39, 1294-304.
- SHETTY, H., HOLLOWAY, H. & SCHAPIRO, M. 1996. Cerebrospinal fluid and plasma distribution of myo-inositol and other polyols in Alzheimer disease. *Clinical chemistry*, 42, 298-302.
- SHURUBOR, Y. I., PAOLUCCI, U., KRASNIKOV, B. F., MATSON, W. R. & KRISTAL, B. S. 2005. Analytical precision, biological variation, and mathematical normalization in high data density metabolomics. *Metabolomics*, 1, 75-85.
- SIES, H. 1997. Oxidative stress: oxidants and antioxidants. *Exp Physiol*, 82, 291-5.
- SIMES, R. J. 1986. An improved Bonferroni procedure for multiple tests of significance. *Biometrika*, 73, 751-754.
- SMITH, C. A., WANT, E. J., O'MAILLE, G., ABAGYAN, R. & SIUZDAK, G. 2006. XCMS: processing mass spectrometry data for metabolite profiling using nonlinear peak alignment, matching, and identification. *Anal Chem*, 78, 779-87.
- SOARDO, G., DONNINI, D., DOMENIS, L., CATENA, C., DE SILVESTRI, D., CAPPELLO, D., DIBENEDETTO, A., CARNELUTTI, A., BONASIA, V. & PAGANO, C. 2011. Oxidative stress is activated by free fatty acids in cultured human hepatocytes. *Metabolic syndrome and related disorders*, 9, 397-401.

- SOUSA, A., FIGUEIREDO, P., ZAMPARO, P., PYNE, D. B., VILAS-BOAS, J. P. & FERNANDES, R. J. 2015. Exercise Modality Effect on Bioenergetical Performance at V O₂max Intensity. *Med Sci Sports Exerc*, 47, 1705-13.
- STATHIS, C. G., CAREY, M. F., HAYES, A., GARNHAM, A. P. & SNOW, R. J. 2006. Sprint training reduces urinary purine loss following intense exercise in humans. *Appl Physiol Nutr Metab*, 31, 702-8.
- STAUFFER, E., DOLAN, J. A. & NEWMAN, R. 2008. CHAPTER 8 - Gas Chromatography and Gas Chromatography—Mass Spectrometry. *Fire Debris Analysis*. Burlington: Academic Press.
- STEUER, R. 2006. On the analysis and interpretation of correlations in metabolomic data. *Briefings in bioinformatics*, 7, 151-158.
- STRASSBURG, K., HUIJBRECHTS, A. M., KORTEKAAS, K. A., LINDEMAN, J. H., PEDERSEN, T. L., DANE, A., BERGER, R., BRENKMAN, A., HANKEMEIER, T. & VAN DUYNHOVEN, J. 2012. Quantitative profiling of oxylipins through comprehensive LC-MS/MS analysis: application in cardiac surgery. *Analytical and bioanalytical chemistry*, 404, 1413-1426.
- SUBUDHI, A. W., DAVIS, S. L., KIPP, R. W. & ASKEW, E. W. 2001. Antioxidant status and oxidative stress in elite alpine ski racers. *Int J Sport Nutr Exerc Metab*, 11, 32-41.
- SUGIMOTO, M., KAWAKAMI, M., ROBERT, M., SOGA, T. & TOMITA, M. 2012. Bioinformatics Tools for Mass Spectroscopy-Based Metabolomic Data Processing and Analysis. *Current Bioinformatics*, 7, 96-108.
- SULLIVAN, P. F., KEEFE, R. S., LANGE, L. A., LANGE, E. M., STROUP, T. S., LIEBERMAN, J. & MANESS, P. F. 2007. NCAM1 and neurocognition in schizophrenia. *Biological psychiatry*, 61, 902-910.
- SUMNER, L. W., AMBERG, A., BARRETT, D., BEALE, M. H., BEGER, R., DAYKIN, C. A., FAN, T. W., FIEHN, O., GOODACRE, R., GRIFFIN, J. L., HANKEMEIER, T., HARDY, N., HARNLY, J., HIGASHI, R., KOPKA, J., LANE, A. N., LINDON, J. C., MARRIOTT, P., NICHOLLS, A. W., REILY, M. D., THADEN, J. J. & VIANT, M. R. 2007. Proposed minimum reporting standards for chemical analysis Chemical Analysis Working Group (CAWG) Metabolomics Standards Initiative (MSI). *Metabolomics*, 3, 211-221.
- SUMNER, L. W., MENDES, P. & DIXON, R. A. 2003. Plant metabolomics: large-scale phytochemistry in the functional genomics era. *Phytochemistry*, 62, 817-836.
- SUOMINEN, T., UUTELA, P., KETOLA, R. A., BERGQUIST, J., HILLERED, L., FINEL, M., ZHANG, H., LAAKSO, A. & KOSTIAINEN, R. 2013. Determination of serotonin and dopamine metabolites in human brain microdialysis and cerebrospinal fluid samples by UPLC-MS/MS: discovery of intact glucuronide and sulfate conjugates. *PLoS One*, 8, e68007.
- SUZDAK, P. D., SCHWARTZ, R. D., SKOLNICK, P. & PAUL, S. M. 1986. Ethanol stimulates gamma-aminobutyric acid receptor-mediated chloride transport in rat brain synaptoneurosome. *Proceedings of the National Academy of Sciences*, 83, 4071-4075.
- TAN, L., YU, J.-T. & TAN, L. 2012. The kynurenine pathway in neurodegenerative diseases: mechanistic and therapeutic considerations. *Journal of the neurological sciences*, 323, 1-8.

- TETTAMANTI, G., BASSI, R., VIANI, P. & RIBONI, L. 2003. Salvage pathways in glycosphingolipid metabolism. *Biochimie*, 85, 423-437.
- THEODORIDIS, G. A., GIKA, H. G., WANT, E. J. & WILSON, I. D. 2012. Liquid chromatography–mass spectrometry based global metabolite profiling: A review. *Analytica Chimica Acta*, 711, 7-16.
- TREMBLAY, M. S., COPELAND, J. L. & VAN HELDER, W. 2004. Effect of training status and exercise mode on endogenous steroid hormones in men. *J Appl Physiol (1985)*, 96, 531-9.
- TRIBA, M. N., LE MOYEC, L., AMATHIEU, R., GOOSSENS, C., BOUCHEMAL, N., NAHON, P., RUTLEDGE, D. N. & SAVARIN, P. 2015. PLS/OPLS models in metabolomics: the impact of permutation of dataset rows on the K-fold cross-validation quality parameters. *Molecular BioSystems*, 11, 13-19.
- TRIVEDI, D. K. & ILES, R. K. 2012. The application of SIMCA P+ in shotgun metabolomics analysis of ZIC® HILIC-MS spectra of human urine-experience with the Shimadzu IT-TOF and profiling solutions data extraction software. *J Chromatogr Sep Tech*, 3, 1-5.
- TUNBRIDGE, E., BURNET, P. W., SODHI, M. S. & HARRISON, P. J. 2004. Catechol-o-methyltransferase (COMT) and proline dehydrogenase (PRODH) mRNAs in the dorsolateral prefrontal cortex in schizophrenia, bipolar disorder, and major depression. *Synapse*, 51, 112-118.
- TWEEDDALE, H., NOTLEY-MCROBB, L. & FERENCI, T. 1998. Effect of slow growth on metabolism of Escherichia coli, as revealed by global metabolite pool (“metabolome”) analysis. *Journal of bacteriology*, 180, 5109-5116.
- URBAN, M., ENOT, D. P., DALLMANN, G., KÖRNER, L., FORCHER, V., ENOH, P., KOAL, T., KELLER, M. & DEIGNER, H.-P. 2010. Complexity and pitfalls of mass spectrometry-based targeted metabolomics in brain research. *Analytical biochemistry*, 406, 124-131.
- VAN DER KLOET, F. M., BOBELDIJK, I., VERHEIJ, E. R. & JELLEMA, R. H. 2009. Analytical error reduction using single point calibration for accurate and precise metabolomic phenotyping. *J Proteome Res*, 8, 5132-41.
- VAN VELZEN, E. J., WESTERHUIS, J. A., VAN DUYNHOVEN, J. P., VAN DORSTEN, F. A., GRUN, C. H., JACOBS, D. M., DUCHATEAU, G. S., VIS, D. J. & SMILDE, A. K. 2009. Phenotyping tea consumers by nutrikinetic analysis of polyphenolic end-metabolites. *J Proteome Res*, 8, 3317-30.
- VAWTER, M. P. 2000. Dysregulation of the neural cell adhesion molecule and neuropsychiatric disorders. *European journal of pharmacology*, 405, 385-395.
- VICKERY, H. B. & SCHMIDT, C. L. 1931. The history of the discovery of the amino acids. *Chemical Reviews*, 9, 169-318.
- VINAIXA, M., SAMINO, S., SAEZ, I., DURAN, J., GUINOVART, J. J. & YANES, O. 2012. A Guideline to Univariate Statistical Analysis for LC/MS-Based Untargeted Metabolomics-Derived Data. *Metabolites*, 2, 775-95.
- VOLLAARD, N. B., SHEARMAN, J. P. & COOPER, C. E. 2005. Exercise-induced oxidative stress. *Sports medicine*, 35, 1045-1062.
- WADE, D. 1999. Deuterium isotope effects on noncovalent interactions between molecules. *Chemico-biological interactions*, 117, 191-217.
- WAJNER, M. & AMARAL, A. U. 2016. Mitochondrial dysfunction in fatty acid oxidation disorders: insights from human and animal studies. *Bioscience reports*, 36, e00281.

- WARRACK, B. M., HNATYSHYN, S., OTT, K.-H., REILY, M. D., SANDERS, M., ZHANG, H. & DREXLER, D. M. 2009. Normalization strategies for metabonomic analysis of urine samples. *Journal of Chromatography B*, 877, 547-552.
- WATSON, D. G. 2015. *Pharmaceutical Analysis E-Book: A Textbook for Pharmacy Students and Pharmaceutical Chemists*, Elsevier Health Sciences.
- WEBER, G., VON WIRÉN, N. & HAYEN, H. 2008. Hydrophilic interaction chromatography of small metal species in plants using sulfobetaine-and phosphorylcholine-type zwitterionic stationary phases. *Journal of separation science*, 31, 1615-1622.
- WEICKERT, C. S., WEICKERT, T. W., PILLAI, A. & BUCKLEY, P. F. 2013. Biomarkers in schizophrenia: a brief conceptual consideration. *Disease markers*, 35, 3-9.
- WEINBERGER, K. & GRABER, A. 2005. Using comprehensive metabolomics to identify novel biomarkers. *Screening Trends in Drug Discovery*, 6, 42-45.
- WESTERHUIS, J. A., HOEFSLOOT, H. C., SMIT, S., VIS, D. J., SMILDE, A. K., VAN VELZEN, E. J., VAN DUIJNHOFEN, J. P. & VAN DORSTEN, F. A. 2008. Assessment of PLS-DA cross validation. *Metabolomics*, 4, 81-89.
- WHEELOCK, Å. M. & WHEELOCK, C. E. 2013. Trials and tribulations of 'omics data analysis: assessing quality of SIMCA-based multivariate models using examples from pulmonary medicine. *Molecular bioSystems*, 9, 2589-2596.
- WHO. 2014. *Deaths from Cardiovascular Diseases and Diabetes*. [Online]. Available: from http://www.who.int/gho/ncd/mortality_morbidity/cvd/en/.
- WHO. 1993. *Biomarkers and Risk Assessment: Concepts and Principles* [Online]. Available: <http://apps.who.int/iris/handle/10665/39037>.
- WHO. 2009. Global Health Risks: Mortality and Burden of Disease Attributable to Selected Major Risks.
- WIKLUND, S., JOHANSSON, E., SJÖSTRÖM, L., MELLEROWICZ, E. J., EDLUND, U., SHOCKCOR, J. P., GOTTFRIES, J., MORITZ, T. & TRYGG, J. 2008. Visualization of GC/TOF-MS-based metabolomics data for identification of biochemically interesting compounds using OPLS class models. *Analytical chemistry*, 80, 115-122.
- WITTCHEN, H.-U. & JACOBI, F. 2005. Size and burden of mental disorders in Europe—a critical review and appraisal of 27 studies. *European neuropsychopharmacology*, 15, 357-376.
- WOLD, S., SJÖSTRÖM, M. & ERIKSSON, L. 2001. PLS-regression: a basic tool of chemometrics. *Chemometrics and intelligent laboratory systems*, 58, 109-130.
- WORLEY, B. & POWERS, R. 2013. Multivariate Analysis in Metabolomics. *Curr Metabolomics*, 1, 92-107.
- WORLEY, B. & POWERS, R. 2016. PCA as a practical indicator of OPLS-DA model reliability. *Current metabolomics*, 4, 97-103.
- WRIGHT, J. H., WHITAKER, S. B., WELCH, C. B. & TELLER, D. N. 1983. Hepatic enzyme induction patterns and phenothiazine side effects. *Clinical Pharmacology & Therapeutics*, 34, 533-538.
- WU, Y. & LI, L. 2016. Sample normalization methods in quantitative metabolomics. *Journal of Chromatography A*, 1430, 80-95.
- XIA, J., SINELNIKOV, I. V., HAN, B. & WISHART, D. S. 2015. MetaboAnalyst 3.0--making metabolomics more meaningful. *Nucleic Acids Res*, 43, W251-7.

- YABE-NISHIMURA, C. 1998. Aldose reductase in glucose toxicity: a potential target for the prevention of diabetic complications. *Pharmacological reviews*, 50, 21-34.
- YAN, J., SHI, S., WANG, H., LIU, R., LI, N., CHEN, Y. & WANG, S. 2016. Neutral monosaccharide composition analysis of plant-derived oligo- and polysaccharides by high performance liquid chromatography. *Carbohydrate polymers*, 136, 1273-1280.
- YANG, J., CHEN, T., SUN, L., ZHAO, Z., QI, X., ZHOU, K., CAO, Y., WANG, X., QIU, Y. & SU, M. 2013. Potential metabolite markers of schizophrenia. *Molecular psychiatry*, 18, 67.
- YANG, J., SCHMELZER, K., GEORGI, K. & HAMMOCK, B. D. 2009. Quantitative profiling method for oxylipin metabolome by liquid chromatography electrospray ionization tandem mass spectrometry. *Anal Chem*, 81, 8085-93.
- YANG, J., ZHAO, X., LU, X., LIN, X. & XU, G. 2015. A data preprocessing strategy for metabolomics to reduce the mask effect in data analysis. *Frontiers in molecular biosciences*, 2, 4.
- YANG, W.-C., ADAMEC, J. & REGNIER, F. E. 2007. Enhancement of the LC/MS analysis of fatty acids through derivatization and stable isotope coding. *Analytical chemistry*, 79, 5150-5157.
- YAO, J., DOUGHERTY JR, G., REDDY, R., KESHAVAN, M., MONTROSE, D., MATSON, W., ROZEN, S., KRISHNAN, R., MCEVOY, J. & KADDURAH-DAOUK, R. 2010. Altered interactions of tryptophan metabolites in first-episode neuroleptic-naive patients with schizophrenia. *Molecular psychiatry*, 15, 938.
- YAO, J. K., CONDRAY, R., DOUGHERTY JR, G. G., KESHAVAN, M. S., MONTROSE, D. M., MATSON, W. R., MCEVOY, J., KADDURAH-DAOUK, R. & REDDY, R. D. 2012. Associations between purine metabolites and clinical symptoms in schizophrenia. *PLoS One*, 7, e42165.
- YAO, J. K., REDDY, R. D. & VAN KAMMEN, D. P. 2001. Oxidative damage and schizophrenia. *CNS drugs*, 15, 287-310.
- YU, R. K. & LEDEEN, R. W. 1970. Gas-liquid chromatographic assay of lipid-bound sialic acids: measurement of gangliosides in brain of several species. *Journal of lipid research*, 11, 506-516.
- ZAIKIN, V. G. & HALKET, J. M. 2006. Derivatization in mass spectrometry—8. Soft ionization mass spectrometry of small molecules. *European Journal of Mass Spectrometry*, 12, 79-115.
- ZHANG, A., SUN, H., WU, X. & WANG, X. 2012a. Urine metabolomics. *Clin Chim Acta*, 414, 65-9.
- ZHANG, H. M., LI, S. L., ZHANG, H., WANG, Y., ZHAO, Z. L., CHEN, S. L. & XU, H. X. 2012b. Holistic quality evaluation of commercial white and red ginseng using a UPLC-QTOF-MS/MS-based metabolomics approach. *J Pharm Biomed Anal*, 62, 258-73.
- ZHANG, R., WATSON, D. G., WANG, L., WESTROP, G. D., COOMBS, G. H. & ZHANG, T. 2014. Evaluation of mobile phase characteristics on three zwitterionic columns in hydrophilic interaction liquid chromatography mode for liquid chromatography-high resolution mass spectrometry based untargeted metabolite profiling of Leishmania parasites. *J Chromatogr A*, 1362, 168-79.

- ZHANG, R., ZHANG, T., ALI, A. M., AL WASHIH, M., PICKARD, B. & WATSON, D. G. 2016. Metabolomic Profiling of Post-Mortem Brain Reveals Changes in Amino Acid and Glucose Metabolism in Mental Illness Compared with Controls. *Computational and structural biotechnology journal*, 14, 106-116.
- ZHANG, T., CREEK, D. J., BARRETT, M. P., BLACKBURN, G. & WATSON, D. G. 2012c. Evaluation of coupling reversed phase, aqueous normal phase, and hydrophilic interaction liquid chromatography with Orbitrap mass spectrometry for metabolomic studies of human urine. *Anal Chem*, 84, 1994-2001.
- ZHANG, T. & WATSON, D. G. 2015. A short review of applications of liquid chromatography mass spectrometry based metabolomics techniques to the analysis of human urine. *Analyst*, 140, 2907-2915.
- ZHANG, T., WATSON, D. G., WANG, L., ABBAS, M., MURDOCH, L., BASHFORD, L., AHMAD, I., LAM, N. Y., NG, A. C. & LEUNG, H. Y. 2013. Application of Holistic Liquid Chromatography-High Resolution Mass Spectrometry Based Urinary Metabolomics for Prostate Cancer Detection and Biomarker Discovery. *PLoS One*, 8, e65880.
- ZHENG, L., T'KIND, R., DECUYPERE, S., VON FREYEND, S. J., COOMBS, G. H. & WATSON, D. G. 2010. Profiling of lipids in *Leishmania donovani* using hydrophilic interaction chromatography in combination with Fourier transform mass spectrometry. *Rapid Communications in Mass Spectrometry*, 24, 2074-2082.
- ZIELINSKI, J., KRASINSKA, B. & KUSY, K. 2013a. Hypoxanthine as a predictor of performance in highly trained athletes. *Int J Sports Med*, 34, 1079-86.
- ZIELINSKI, J. & KUSY, K. 2012. Training-induced adaptation in purine metabolism in high-level sprinters vs. triathletes. *J Appl Physiol (1985)*, 112, 542-51.
- ZIELINSKI, J., KUSY, K. & RYCHLEWSKI, T. 2011. Effect of training load structure on purine metabolism in middle-distance runners. *Med Sci Sports Exerc*, 43, 1798-807.
- ZIELINSKI, J., KUSY, K. & SLOMINSKA, E. 2013b. Alterations in purine metabolism in middle-aged elite, amateur, and recreational runners across a 1-year training cycle. *Eur J Appl Physiol*, 113, 763-73.
- ZIELINSKI, J., RYCHLEWSKI, T., KUSY, K., DOMASZEWSKA, K. & LAURENTOWSKA, M. 2009. The effect of endurance training on changes in purine metabolism: a longitudinal study of competitive long-distance runners. *Eur J Appl Physiol*, 106, 867-76.
- ZUBAREV, R. A. & MAKAROV, A. 2013. Orbitrap mass spectrometry. ACS Publications.

Appendix-I: Supplementary Data

Table 2-S1: the details of 440 positive and negative ions for 220 standards prepared in four standard mixtures (Std. mix) used to determine the matched metabolites in biological samples

No.	Polarity	Std. mix	Compound Name	Formula	m/z	Pathway map	ZIC-HILIC		ZIC-pHILIC		C18	
							RT	peak	RT	peak	RT	peak
1	N	1	Inosine	C10H12N4O5	268.080771	Purine Metabolism	11.43	1.28E+07	11.4	7.33E+06	7.52	1.01E+07
2	P	1	Inosine	C10H12N4O5	268.080771	Purine Metabolism	11.46	8.66E+06	11.34	5.51E+06	7.53	3.83E+06
3	N	1	Xanthosine	C10H12N4O6	284.075686	Purine Metabolism	11.52	4.20E+06	13.08	1.89E+06	10.82	3.65E+06
4	P	1	Xanthosine	C10H12N4O6	284.075686	Purine Metabolism	11.55	1.83E+06	13.02	7.17E+05	10.81	5.76E+05
5	N	1	IMP	C10H13N4O8P	348.047103	Purine Metabolism	15.84	4.00E+06	16.28	2.27E+06	6.22	1.22E+07
6	P	1	IMP	C10H13N4O8P	348.047103	Purine Metabolism	15.85	3.86E+05	16.27	2.38E+05	6.21	1.19E+06
7	N	1	Adenosine	C10H13N5O4	267.096755	Purine Metabolism	12.8	4.15E+06	9.44	1.50E+06	-	N
8	P	1	Adenosine	C10H13N5O4	267.096755	Purine Metabolism	14.92	1.04E+07	9.47	1.41E+07	7.49	1.42E+07
9	N	1	Maltose	C12H22O11	342.116215	Starch and Sucrose Metabolism	14.89	2.00E+05	16.56	5.39E+05	-	N
10	P	1	Maltose	C12H22O11	342.116215	Starch and Sucrose Metabolism	16.44	1.37E+05	-	N	-	N
11	N	1	Uridine 5'-diphosphoglucose	C15H24N2O17P2	566.055027	Starch and Sucrose Metabolism; Galactose Metabolism	21.39	1.26E+05	17.24	3.31E+06	8.89	3.29E+05
12	P	1	Uridine 5'-diphosphoglucose	C15H24N2O17P2	566.055027	Starch and Sucrose Metabolism; Galactose Metabolism	-	N	17.23	1.63E+03	-	N
13	N	1	Riboflavin	C17H20N4O6	376.138286	Riboflavin Metabolism	8.89	3.94E+06	8.99	2.14E+06	15.32	1.19E+07
14	P	1	Riboflavin	C17H20N4O6	376.138286	Riboflavin Metabolism	8.9	7.80E+06	9	8.98E+06	15.31	1.10E+07
15	N	1	UDP-N-acetyl-D-glucosamine	C17H27N3O17P2	607.081576	Amino Sugar Metabolism	19.08	1.24E+05	16.01	3.16E+06	9.12	3.48E+05
16	P	1	UDP-N-acetyl-D-glucosamine	C17H27N3O17P2	607.081576	Amino Sugar Metabolism	-	N	16	3.10E+04	-	N

No.	Polarity	Std. mix	Compound Name	Formula	MW	Pathway map	ZIC-HILIC		ZIC-pHILIC		C18	
							RT	peak	RT	peak	RT	peak
17	N	1	CoA	C21H36N7O16P3S	767.115215	Phenylacetate Metabolism; Butyrate Metabolism	-	N	14.54	1.18E+06	-	N
18	P	1	CoA	C21H36N7O16P3S	767.115215	Phenylacetate Metabolism; Butyrate Metabolism	-	N	14.56	2.31E+05	-	N
19	N	1	FAD	C27H33N9O15P2	785.15714	Citric Acid Cycle; Riboflavin Metabolism	30.23	5.52E+04	12.45	1.54E+06	13.64	3.89E+05
20	P	1	FAD	C27H33N9O15P2	785.15714	Citric Acid Cycle; Riboflavin Metabolism	-	N	12.47	4.23E+05	-	N
21	N	1	Taurine	C2H7NO3S	125.014665	Taurine and Hypotaurine Metabolism; Bile Acid Biosynthesis	16.93	1.73E+07	15.64	4.76E+06	5.48	1.37E+07
22	P	1	Taurine	C2H7NO3S	125.014665	Taurine and Hypotaurine Metabolism; Bile Acid Biosynthesis	16.94	2.25E+06	15.68	3.06E+05	5.49	8.14E+05
23	N	1	Malonate	C3H4O4	104.01096	Aspartate Metabolism/Fatty acid Biosynthesis	8.24	5.29E+06	16.64	1.61E+07	7.16	3.01E+06
24	P	1	Malonate	C3H4O4	104.01096	Aspartate Metabolism/Fatty acid Biosynthesis	-	N	-	N	-	N
25	N	1	L-Alanine	C3H7NO2	89.047679	Transcription/Translation; Urea Cycle	18.83	5.00E+04	15.34	1.09E+06	-	N
26	P	1	L-Alanine	C3H7NO2	89.047679	Transcription/Translation; Urea Cycle	18.93	1.21E+07	15.3	8.33E+06	5.45	2.35E+07
27	N	1	L-Serine	C3H7NO3	105.042594	Ammonia Recycling; Sphingolipid Metabolism	19.9	2.87E+06	16.39	2.96E+05	5.37	1.76E+06
28	P	1	L-Serine	C3H7NO3	105.042594	Ammonia Recycling; Sphingolipid Metabolism	19.93	2.40E+06	16.35	4.00E+05	5.36	1.54E+06
29	N	1	DL-Glyceraldehyde 3-phosphate	C3H7O6P	169.998027	Fructose and Mannose Degradation; Pentose Phosphate Pathway	17.22	8.25E+05	17.07	7.95E+04	5.41	4.37E+05
30	P	1	DL-Glyceraldehyde 3-phosphate	C3H7O6P	169.998027	Fructose and Mannose Degradation; Pentose Phosphate Pathway	-	N	-	N	-	N
31	N	1	D(+)-2-Phosphoglyceric acid	C3H7O7P	185.992942	no	19.99	3.24E+05	17.68	2.91E+06	6.13	1.14E+06
32	P	1	D(+)-2-Phosphoglyceric acid	C3H7O7P	185.992942	no	-	N	-	N	-	N
33	N	1	Putrescine	C4H12N2	88.100048	Spermidine and Spermine Biosynthesis/Methionine Metabolism	-	N	-	N	-	N
34	P	1	Putrescine	C4H12N2	88.100048	Spermidine and Spermine Biosynthesis/Methionine Metabolism	35.52	5.72E+06	19.97	4.65E+04	4.75	1.39E+07
35	N	1	Fumarate	C4H4O4	116.01096	Phenylalanine and Tyrosine Metabolism; Arginine and Proline Metabolism	7.44	1.30E+07	17.04	1.68E+07	9.41	1.13E+07

No.	Polarity	Std. mix	Compound Name	Formula	MW	Pathway map	ZIC-HILIC		ZIC-pHILIC		C18	
							RT	peak	RT	peak	RT	peak
36	P	1	Fumarate	C4H4O4	116.01096	Phenylalanine and Tyrosine Metabolism; Arginine and Proline Metabolism	-	N	-	N	-	N
37	N	1	Cytosine	C4H5N3O	111.043262	no	20.89	2.66E+04	11.68	3.43E+05	-	N
38	P	1	Cytosine	C4H5N3O	111.043262	no	20.86	1.95E+07	11.53	1.10E+07	5.67	2.08E+07
39	N	1	Acetoacetate	C4H6O3	102.031695	Ketone Body Metabolism; Tyrosine Metabolism	6.2	1.44E+05	7.74	7.82E+05	-	N
40	P	1	Acetoacetate	C4H6O3	102.031695	Ketone Body Metabolism; Tyrosine Metabolism	-	N	-	N	-	N
41	N	1	Methylmalonate	C4H6O4	118.02661	Valine, Leucine and Isoleucine Degradation; Propanoate Metabolism	7.7	1.99E+07	15.81	3.68E+07	10.62	1.72E+07
42	P	1	Methylmalonate	C4H6O4	118.02661	Valine, Leucine and Isoleucine Degradation; Propanoate Metabolism	-	N	-	N	-	N
43	N	1	L-Aspartate	C4H7NO4	133.037509	Transcription/Translation; Arginine and Proline Metabolism	18.83	2.01E+06	15.88	1.44E+05	5.44	8.45E+05
44	P	1	L-Aspartate	C4H7NO4	133.037509	Transcription/Translation; Arginine and Proline Metabolism	18.82	3.29E+05	15.84	3.34E+04	5.45	1.77E+05
45	N	1	L-Threonic acid	C4H8O5	136.037175	no	13.42	7.10E+06	13.63	3.59E+07	5.77	2.83E+07
46	P	1	L-Threonic acid	C4H8O5	136.037175	no	-	N	-	N	-	N
47	N	1	creatine	C4H9N3O2	131.069477	Glycine and Serine Metabolism; Arginine and Proline Metabolism	18.24	9.76E+05	15.18	6.21E+05	5.88	1.27E+05
48	P	1	creatine	C4H9N3O2	131.069477	Glycine and Serine Metabolism; Arginine and Proline Metabolism	18.25	3.50E+06	15.16	3.02E+07	5.87	4.23E+06
49	N	1	L-Homoserine	C4H9NO3	119.058244	Methionine Metabolism	19.24	1.88E+07	15.57	3.09E+06	5.41	9.71E+06
50	P	1	L-Homoserine	C4H9NO3	119.058244	Methionine Metabolism	19.25	2.60E+07	15.61	1.62E+07	5.42	2.33E+07
51	N	1	L-Glutamine	C5H10N2O3	146.069143	Pyrimidine Metabolism; Glutamate Metabolism	19.44	1.42E+07	15.64	1.38E+06	5.41	6.48E+06
52	P	1	L-Glutamine	C5H10N2O3	146.069143	Pyrimidine Metabolism; Glutamate Metabolism	19.43	9.03E+06	15.68	8.52E+06	5.45	7.01E+06
53	N	1	L-Arabinose	C5H10O5	150.052825	no	14.55	3.97E+05	13.82	2.00E+05	-	N
54	P	1	L-Arabinose	C5H10O5	150.052825	no	-	N	-	N	-	N

No.	Polarity	Std. mix	Compound Name	Formula	MW	Pathway map	ZIC-HILIC		ZIC-pHILIC		C18	
							RT	peak	RT	peak	RT	peak
55	N	1	Betaine	C5H11NO2	117.078979	Glycine and Serine Metabolism; Betaine Metabolism	-	N	-	N	-	N
56	P	1	Betaine	C5H11NO2	117.078979	Glycine and Serine Metabolism; Betaine Metabolism	16.92	2.99E+07	11.69	1.19E+08	5.76	4.23E+07
57	N	1	L-Methionine	C5H11NO2S	149.05105	Betaine Metabolism; Methionine Metabolism	15.18	1.05E+06	12.17	4.60E+06	7.46	2.52E+06
58	P	1	L-Methionine	C5H11NO2S	149.05105	Betaine Metabolism; Methionine Metabolism	15.2	2.56E+07	12.16	2.52E+07	7.47	3.61E+07
59	N	1	D-Ribose 5-phosphate	C5H11O8P	230.019157	Purine Metabolism; Pentose Phosphate Pathway	16.14	1.24E+05	14.1	1.97E+04	5.61	2.59E+06
60	P	1	D-Ribose 5-phosphate	C5H11O8P	230.019157	Purine Metabolism; Pentose Phosphate Pathway	-	N	14.42	1.85E+03	-	N
61	N	1	Xylitol	C5H12O5	152.068475	no	13.67	9.63E+05	13.34	4.03E+06	-	N
62	P	1	Xylitol	C5H12O5	152.068475	no	13.68	2.97E+05	-	N	5.58	5.66E+05
63	N	1	Choline(+)	C5H14NO	104.107539	Betaine Metabolism; Methionine Metabolism	-	N	-	N	-	N
64	P	1	Choline(+)	C5H14NO	104.107539	Betaine Metabolism; Methionine Metabolism	20.29	3.67E+07	20.18	1.45E+08	5.58	3.42E+07
65	N	1	Xanthine	C5H4N4O2	152.033426	Purine Metabolism	9.93	9.43E+06	12.05	5.43E+06	7.48	2.48E+07
66	P	1	Xanthine	C5H4N4O2	152.033426	Purine Metabolism	9.92	3.22E+06	-	N	7.47	4.84E+05
67	N	1	Citraconate	C5H6O4	130.02661	no	6.27	1.33E+06	7.71	9.64E+06	15.43	5.29E+06
68	P	1	Citraconate	C5H6O4	130.02661	no	-	N	-	N	-	N
69	N	1	2-Oxoglutarate	C5H6O5	146.021525	Citric Acid Cycle; Gluconeogenesis	8.56	5.04E+04	16.58	1.85E+06	7.32	2.21E+05
70	P	1	2-Oxoglutarate	C5H6O5	146.021525	Citric Acid Cycle; Gluconeogenesis	-	N	-	N	-	N
71	N	1	Citramalate	C5H8O5	148.037175	no	10.23	1.39E+07	15.73	1.62E+08	7.59	5.96E+07
72	P	1	Citramalate	C5H8O5	148.037175	no	-	N	-	N	-	N
73	N	1	L-Proline	C5H9NO2	115.063329	Arginine and Proline Metabolism	-	N	13.31	1.24E+06	-	N
74	P	1	L-Proline	C5H9NO2	115.063329	Arginine and Proline Metabolism	16.8	2.27E+07	13.28	6.59E+07	5.83	3.89E+07

No.	Polarity	Std. mix	Compound Name	Formula	MW	Pathway map	ZIC-HILIC		ZIC-pHILIC		C18	
							RT	peak	RT	peak	RT	Peak
75	N	1	Cis-4-Hydroxy-D-Proline	C5H9NO3	131.058244	no	18.72	1.56E+07	15.53	2.53E+06	5.46	1.78E+06
76	P	1	Cis-4-Hydroxy-D-Proline	C5H9NO3	131.058244	no	18.71	1.72E+07	15.54	1.78E+07	5.47	1.19E+07
77	N	1	L-Glutamate	C5H9NO4	147.053159	Alanine Metabolism; Histidine Metabolism	15.77	3.00E+05	11.82	1.82E+06	5.57	4.49E+05
78	P	1	L-Glutamate	C5H9NO4	147.053159	Alanine Metabolism; Histidine Metabolism	15.81	9.14E+06	11.92	5.75E+06	5.9	1.15E+07
79	N	1	Ectoine	C6H10N2O2	142.074228	Glycine, serine and threonine metabolism	17.2	5.02E+06	13.56	1.15E+07	6.04	3.71E+06
80	P	1	Ectoine	C6H10N2O2	142.074228	Glycine, serine and threonine metabolism	17.14	3.39E+07	13.62	1.73E+08	6.03	6.58E+07
81	N	1	D-Galacturonate	C6H10O7	194.042655	no	16.25	5.15E+06	17.07	2.29E+06	5.64	5.71E+06
82	P	1	D-Galacturonate	C6H10O7	194.042655	no	-	N	-	N	-	N
83	N	1	L-Cystine	C6H12N2O4S2	240.02385	no	23.58	1.24E+06	17.07	3.70E+05	5.32	9.10E+05
84	P	1	L-Cystine	C6H12N2O4S2	240.02385	no	23.62	5.06E+05	17.03	1.50E+05	5.31	3.93E+05
85	N	1	rhamnose	C6H12O5	164.068475	no	12.18	7.44E+05	11.47	6.53E+05	5.88	2.04E+05
86	P	1	rhamnose	C6H12O5	164.068475	no	-	N	-	N	-	N
87	N	1	glucose	C6H12O6	180.06339	Glycolysis; Galactose Metabolism	15.48	8.72E+06	15.22	1.48E+06	-	N
88	P	1	glucose	C6H12O6	180.06339	Glycolysis; Galactose Metabolism	-	N	-	N	-	N
89	N	1	L-isoleucine	C6H13NO2	131.094629	Valine, Leucine and Isoleucine Degradation	14.75	3.54E+04	11.82	4.28E+06	7.52	6.95E+04
90	P	1	L-isoleucine	C6H13NO2	131.094629	Valine, Leucine and Isoleucine Degradation	14.65	3.42E+07	11.9	1.40E+07	7.51	6.69E+07
91	N	1	glucose 1 phosphate	C6H13O9P	260.029722	Starch and Sucrose Metabolism; Glycolysis	16.7	6.61E+06	16.72	2.68E+06	5.39	8.85E+06
92	P	1	glucose 1 phosphate	C6H13O9P	260.029722	Starch and Sucrose Metabolism; Glycolysis	16.74	1.75E+05	16.77	3.78E+04	5.38	5.28E+04
93	N	1	D-Sorbitol	C6H14O6	182.07904	Fructose and Mannose Degradation; Galactose Metabolism	14.73	1.56E+07	14.38	4.46E+06	5.53	3.65E+05
94	P	1	D-Sorbitol	C6H14O6	182.07904	Fructose and Mannose Degradation; Galactose Metabolism	14.72	5.28E+05	14.34	1.44E+04	5.54	9.41E+05
95	N	1	Isonicotinic acid	C6H5NO2	123.032029	no	10.23	1.07E+07	8.44	1.74E+07	6.15	1.74E+07

No.	Polarity	Std. mix	Compound Name	Formula	MW	Pathway map	ZIC-HILIC		ZIC-pHILIC		C18	
							RT	peak	RT	peak	RT	Peak
96	P	1	Isonicotinic acid	C6H5NO2	123.032029	no	10.22	2.09E+07	8.22	1.37E+07	6.16	1.73E+07
97	N	1	Ascorbate	C6H8O6	176.03209	Catecholamine Biosynthesis	11.34	2.76E+05	11.12	6.73E+04	15.46	3.33E+05
98	P	1	Ascorbate	C6H8O6	176.03209	Catecholamine Biosynthesis	-	N	-	N	-	N
99	N	1	Isocitrate	C6H8O7	192.027005	Citric Acid Cycle	11.96	7.88E+06	19.56	1.59E+07	6.53	1.07E+07
100	P	1	Isocitrate	C6H8O7	192.027005	Citric Acid Cycle	-	N	-	N	-	N
101	N	1	Theophylline	C7H8N4O2	180.064726	Caffeine Metabolism	-	N	-	N	-	N
102	P	1	Theophylline	C7H8N4O2	180.064726	Caffeine Metabolism	-	N	-	N	-	N
103	N	1	N-Acetyl-D-Glucosamine	C8H15NO6	221.089939	Amino Sugar Metabolism	12.8	1.45E+06	12.21	2.04E+06	5.82	3.09E+05
104	P	1	N-Acetyl-D-Glucosamine	C8H15NO6	221.089939	Amino Sugar Metabolism	12.81	6.60E+06	12.27	5.21E+06	5.83	4.32E+06
105	N	1	2-Phenylglycine	C8H9NO2	151.063329	no	14.62	4.97E+05	11.87	3.01E+06	7.48	1.03E+06
106	P	1	2-Phenylglycine	C8H9NO2	151.063329	no	14.65	1.71E+07	11.92	7.01E+06	7.49	2.20E+07
107	N	1	Sepiapterin	C9H11N5O3	237.08619	Pterine Biosynthesis	-	N	-	N	-	N
108	P	1	Sepiapterin	C9H11N5O3	237.08619	Pterine Biosynthesis	-	N	-	N	-	N
109	N	1	Pantothenate	C9H17NO5	219.110674	Beta-alanine Metabolism and Pantothenate and CoA Biosynthesis	8.14	2.44E+07	9.44	3.26E+07	11.59	3.12E+07
110	P	1	Pantothenate	C9H17NO5	219.110674	Beta-alanine Metabolism and Pantothenate and CoA Biosynthesis	8.18	1.89E+07	9.4	2.58E+07	11.71	1.25E+07
111	N	1	N6-Trimethyl-L-lysine	C9H20N2O2	188.152478	Carnitine Synthesis	-	N	22.55	1.31E+04	-	N
112	P	1	N6-Trimethyl-L-lysine	C9H20N2O2	188.152478	Carnitine Synthesis	29.86	1.45E+07	22.49	4.21E+07	5.27	2.49E+07
113	N	1	2-phenyl imidazole	C9H8N2	144.068748		13.82	5.90E+04	6.26	2.55E+06	12.59	4.72E+05
114	P	1	2-phenyl imidazole	C9H8N2	144.068748		13.79	7.81E+07	5.83	5.43E+07	12.65	9.25E+07
115	N	1	4-Coumarate	C9H8O3	164.047345	no	6.29	9.83E+06	8.92	1.64E+07	18.72	4.02E+07
116	P	1	4-Coumarate	C9H8O3	164.047345	no	6.31	2.15E+05	8.91	5.62E+04	18.71	2.15E+05

No.	Polarity	Std. mix	Compound Name	Formula	MW	Pathway map	ZIC-HILIC		ZIC-pHILIC		C18	
							RT	peak	RT	peak	RT	peak
117	N	1	Hippuric acid	C9H9NO3	179.058244	no	6.53	3.51E+07	7.74	1.30E+08	16.55	8.71E+07
118	P	1	Hippuric acid	C9H9NO3	179.058244	no	6.54	3.96E+06	7.77	4.45E+05	16.54	6.89E+06
119	N	2	Sucrose	C12H22O11	342.116215	Starch and sucrose/Galactose Metabolism	16.09	3.37E+06	15.6	1.66E+06	-	N
120	P	2	Sucrose	C12H22O11	342.116215	Starch and sucrose/Galactose Metabolism	-	N	15.61	7.67E+03	-	N
121	N	2	B-Alanine	C3H7NO2	89.047679	Propanoate Metabolism; Aspartate Metabolism	-	N	15.86	6.98E+05	-	N
122	P	2	B-Alanine	C3H7NO2	89.047679	Propanoate Metabolism; Aspartate Metabolism	20.6	2.56E+07	15.8	1.88E+07	5.43	3.01E+07
123	N	2	Dihydroxyacetone phosphate	C3H7O6P	169.998027	Fructose and Mannose Degradation; Glycerol Phosphate Shuttle	15.66	1.15E+07	16.21	6.41E+06	5.44	2.74E+06
124	P	2	Dihydroxyacetone phosphate	C3H7O6P	169.998027	Fructose and Mannose Degradation; Glycerol Phosphate Shuttle	15.58	1.43E+05	16.17	3.59E+03	5.57	3.94E+04
125	N	2	3-Phosphoglycerate	C3H7O7P	185.992942	Glycine and Serine/Glycerolipid Metabolism and Glycolysis Gluconeogenesis	27.1	4.25E+05	17.82	5.16E+06	5.6	4.06E+06
126	P	2	3-Phosphoglycerate	C3H7O7P	185.992942	Glycine and Serine/Glycerolipid Metabolism and Glycolysis Gluconeogenesis	-	N	17.81	1.72E+04	5.68	4.60E+04
127	N	2	Maleic acid	C4H4O4	116.01096		6.37	2.53E+07	12.2	4.79E+07	8.45	7.79E+06
128	P	2	Maleic acid	C4H4O4	116.01096		-	N	-	N	5.55	1.49E+04
129	N	2	Ketobutyric acid	C4H6O3	102.031695	Methionine Metabolism; Glycine and Serine Metabolism	6.62	3.96E+07	7.8	1.88E+08	9.14	3.34E+07
130	P	2	Ketobutyric acid	C4H6O3	102.031695	Methionine Metabolism; Glycine and Serine Metabolism	-	N	-	N	-	N
131	N	2	Succinate	C4H6O4	118.02661	Citric Acid Cycle; Glutamate Metabolism	8.15	1.46E+07	16.09	8.67E+06	10.02	1.46E+07
132	P	2	Succinate	C4H6O4	118.02661	Citric Acid Cycle; Glutamate Metabolism	-	N	-	N	-	N
133	N	2	L-Threonine	C4H9NO3	119.058244	Transcription/Translation; Glycine and Serine Metabolism	18.79	1.13E+07	15.03	4.75E+06	5.44	2.64E+06
134	P	2	L-Threonine	C4H9NO3	119.058244	Transcription/Translation; Glycine and Serine Metabolism	18.8	1.97E+07	15.06	1.01E+07	5.48	7.95E+06

No.	Polarity	Std. mix	Compound Name	Formula	MW	Pathway map	ZIC-HILIC		ZIC-pHILIC		C18	
							RT	peak	RT	peak	RT	Peak
135	N	2	ribose	C5H10O5	150.052825	Pentose Phosphate Pathway	12.18	2.68E+06	12.09	7.71E+05	9.28	3.78E+05
136	P	2	ribose	C5H10O5	150.052825	Pentose Phosphate Pathway	-	N	-	N	-	N
137	N	2	L-Valine	C5H11NO2	117.078979	Valine, Leucine and Isoleucine Degradation; Propanoate Metabolism	15.75	4.81E+04	13.03	5.50E+06	-	N
138	P	2	L-Valine	C5H11NO2	117.078979	Valine, Leucine and Isoleucine Degradation; Propanoate Metabolism	15.79	4.60E+07	12.99	3.47E+07	6.31	3.48E+07
139	N	2	D-Ribulose 5-phosphate	C5H11O8P	230.019157	Pentose Phosphate Pathway	15.96	2.88E+06	16.39	2.52E+06	5.47	1.08E+06
140	P	2	D-Ribulose 5-phosphate	C5H11O8P	230.019157	Pentose Phosphate Pathway	16.62	9.64E+04	16.37	1.20E+04	-	N
141	N	2	Oxypurinol	C5H4N4O2	152.033426	no	9.42	1.94E+07	11.02	1.48E+07	9.48	1.11E+07
142	P	2	Oxypurinol	C5H4N4O2	152.033426	no	9.39	2.40E+04	-	N	-	N
143	N	2	Mesaconate	C5H6O4	130.02661	no	6.53	6.65E+06	16.41	8.43E+06	12.1	3.94E+07
144	P	2	Mesaconate	C5H6O4	130.02661	no	6.49	7.01E+04	-	N	12.58	1.34E+06
145	N	2	D-2-Hydroxyglutaric acid	C5H8O5	148.037175	no	8.74	3.38E+07	16.11	5.58E+07	7.64	2.45E+07
146	P	2	D-2-Hydroxyglutaric acid	C5H8O5	148.037175	no	-	N	-	N	-	N
147	N	2	5-Aminolevulinate	C5H9NO3	131.058244	Glycine and Serine/Prophyrin Metabolism	20.37	2.46E+06	14.46	1.67E+07	-	N
148	P	2	5-Aminolevulinate	C5H9NO3	131.058244	Glycine and Serine/Prophyrin Metabolism	19.88	3.24E+07	14.42	6.17E+07	5.75	5.97E+07
149	N	2	O-Acetyl-L-serine	C5H9NO4	147.053159	no	15.41	1.40E+06	11.48	1.47E+07	6.39	1.77E+06
150	P	2	O-Acetyl-L-serine	C5H9NO4	147.053159	no	15.42	6.34E+06	11.58	1.87E+06	5.81	3.12E+06
151	N	2	D-Glucuronate	C6H10O7	194.042655	Inositol Metabolism; Starch and Sucrose Metabolism	16.34	2.90E+05	16.79	3.58E+05	5.51	3.21E+05
152	P	2	D-Glucuronate	C6H10O7	194.042655	Inositol Metabolism; Starch and Sucrose Metabolism	-	N	-	N	-	N
153	N	2	fructose	C6H12O5	164.068475	Fructose and Mannose Degradation	11.86	3.71E+05	12.59	1.92E+05	-	N
154	P	2	fructose	C6H12O5	164.068475	Fructose and Mannose Degradation	-	N	-	N	-	N

No.	Polarity	Std. mix	Compound Name	Formula	MW	Pathway map	ZIC-HILIC		ZIC-pHILIC		C18	
							RT	peak	RT	peak	RT	peak
155	N	2	galactose	C6H12O6	180.06339	Galactose Metabolism; Nucleotide Sugars Metabolism	15.89	6.05E+06	10.31	3.12E+06	6.07	7.49E+05
156	P	2	galactose	C6H12O6	180.06339	Galactose Metabolism; Nucleotide Sugars Metabolism	-	N	-	N	-	N
157	N	2	L-Leucine	C6H13NO2	131.094629	Valine, Leucine and Isoleucine Degradation	-	N	11.27	2.98E+06	-	N
158	P	2	L-Leucine	C6H13NO2	131.094629	Valine, Leucine and Isoleucine Degradation	14.27	2.18E+07	11.24	1.25E+07	9.33	1.13E+07
159	N	2	glucose 6 phosphate	C6H13O9P	260.029722	Gluconeogenesis; Pentose Phosphate Pathway	18.38	8.20E+06	17.68	3.25E+06	5.21	3.91E+06
160	P	2	glucose 6 phosphate	C6H13O9P	260.029722	Gluconeogenesis; Pentose Phosphate Pathway	18.41	3.25E+05	17.67	5.15E+04	5.2	3.96E+04
161	N	2	Mannitol	C6H14O6	182.07904	no	14.94	2.50E+06	14.46	1.03E+07	5.53	3.62E+05
162	P	2	Mannitol	C6H14O6	182.07904	no	14.74	8.90E+05	-	N	5.55	4.53E+05
163	N	2	Nicotinate	C6H5NO2	123.032029	Nicotinate and Nicotinamide Metabolism	8.92	2.93E+06	8.37	1.13E+07	6.83	2.76E+06
164	P	2	Nicotinate	C6H5NO2	123.032029	Nicotinate and Nicotinamide Metabolism	8.91	2.01E+07	8.41	1.01E+07	7.16	4.52E+06
165	N	2	D-Isoascorbic acid	C6H8O6	176.03209		10.39	9.67E+06	10.68	2.37E+06	12.1	6.73E+06
166	N	2	Citrate	C6H8O7	192.027005	Citric Acid Cycle	20.71	2.87E+06	19.04	1.02E+07	7.71	7.30E+06
167	P	2	Citrate	C6H8O7	192.027005	Citric Acid Cycle	-	N	-	N	-	N
168	N	2	Theobromine	C7H8N4O2	180.064726	Caffeine Metabolism	-	N	7.78	1.42E+05	-	N
169	P	2	Theobromine	C7H8N4O2	180.064726	Caffeine Metabolism	8.16	1.40E+06	-	N	12.58	5.12E+06
170	N	2	N-Acetyl-D-mannosamine	C8H15NO6	221.089939	Amino Sugar Metabolism	12.96	1.23E+06	12.59	1.46E+06	5.85	3.64E+05
171	P	2	N-Acetyl-D-mannosamine	C8H15NO6	221.089939	Amino Sugar Metabolism	12.99	3.38E+06	12.74	1.44E+06	5.84	1.89E+06
172	N	2	4-Hydroxyphenylacetaldoxime	C8H9NO2	151.063329		-	N	7.78	2.92E+07	12.88	1.45E+06
173	P	2	4-Hydroxyphenylacetaldoxime	C8H9NO2	151.063329		8.11	5.53E+06	-	N	12.87	7.06E+06
174	N	2	Biopterin	C9H11N5O3	237.08619	no	13.28	8.71E+06	12.09	8.71E+06	7.75	4.22E+06
175	P	2	Biopterin	C9H11N5O3	237.08619	no	13.31	5.63E+06	12.03	2.50E+06	7.74	1.92E+06

No.	Polarity	Std. mix	Compound Name	Formula	MW	Pathway map	ZIC-HILIC		ZIC-pHILIC		C18	
							RT	peak	RT	peak	RT	Peak
176	N	2	Serotonin	C10H12N2O	176.094963	Tryptophan Metabolism	-	N	-	N	-	N
177	P	2	Serotonin	C10H12N2O	176.094963	Tryptophan Metabolism	17.58	7.08E+06	36.4	5.58E+05	11.82	1.41E+07
178	N	2	ADP	C10H15N5O10P2	427.029419		28.93	2.18E+05	15.98	2.74E+06	6.14	1.44E+06
179	P	2	ADP	C10H15N5O10P2	427.029419		-	N	15.96	2.36E+05	-	N
180	N	2	Biotin	C10H16N2O3S	244.088164	Biotin Metabolism	8.24	2.49E+05	9.51	8.26E+05	16.08	5.51E+06
181	P	2	Biotin	C10H16N2O3S	244.088164	Biotin Metabolism	8.25	5.06E+05	9.54	1.07E+06	16.09	2.06E+06
182	N	2	Glutathione	C10H17N3O6S	307.083808	Glutamate Metabolism; Glutathione Metabolism	17.22	7.33E+06	15.08	2.04E+06	7.68	2.04E+06
183	P	2	Glutathione	C10H17N3O6S	307.083808	Glutamate Metabolism; Glutathione Metabolism	17.21	2.61E+06	15.09	5.63E+05	6.46	7.17E+05
184	N	2	Lactoylglutathione	C13H21N3O8S	379.104938	Pyruvate Metabolism	16.5	1.34E+07	14.11	1.01E+07	10.13	9.18E+06
185	P	2	Lactoylglutathione	C13H21N3O8S	379.104938	Pyruvate Metabolism	16.51	5.94E+06	14.12	2.78E+06	10.12	3.06E+06
186	N	2	S-Adenosyl-L-methionine(easy degradation)	C15H22N6O5S	398.13724	Betaine Metabolism; Methionine Metabolism	-	N	17.09	1.83E+04	18.81	N
187	P	2	S-Adenosyl-L-methionine(easy degradation)	C15H22N6O5S	398.13724	Betaine Metabolism; Methionine Metabolism	33.27	3.03E+05	17.08	8.45E+05	5.39	5.71E+05
188	N	2	Folate	C19H19N7O6	441.139683	Pterine Biosynthesis; Folate Metabolism	11.49	1.28E+07	17.49	3.23E+06	13.69	3.68E+07
189	P	2	Folate	C19H19N7O6	441.139683	Pterine Biosynthesis; Folate Metabolism	11.53	2.47E+06	17.51	4.52E+05	13.7	3.28E+06
190	N	2	NADP(+)	C21H29N7O17P3	744.083284	Glucose-Alanine Cycle; Nicotinate and Nicotinamide Metabolism	-	N	-	N	-	N
191	P	2	NADP(+)	C21H29N7O17P3	744.083284	Glucose-Alanine Cycle; Nicotinate and Nicotinamide Metabolism	-	N	-	N	-	N
192	N	2	Oxalate	C2H2O4	89.99531	no	43.7	1.26E+05	18.61	5.15E+06	4.99	3.79E+05
193	P	2	Oxalate	C2H2O4	89.99531	no	-	N	-	N	-	N
194	N	2	Bilirubin	C33H36N4O6	584.263486	Porphyrin Metabolism	-	N	4.03	1.98E+04	-	N
195	P	2	Bilirubin	C33H36N4O6	584.263486	Porphyrin Metabolism	-	N	3.99	1.82E+04	-	N

No.	Polarity	Std. mix	Compound Name	Formula	MW	Pathway map	ZIC-HILIC		ZIC-pHILIC		C18	
							RT	peak	RT	peak	RT	peak
196	N	2	Phosphoenolpyruvate	C3H5O6P	167.982377	Glycolysis; Gluconeogenesis	14.8	1.32E+07	18.43	9.65E+06	6.14	3.05E+06
197	P	2	Phosphoenolpyruvate	C3H5O6P	167.982377	Glycolysis; Gluconeogenesis	14.81	1.86E+05	18.42	6.83E+03	-	N
198	N	2	sn-Glycerol 3-phosphate	C3H9O6P	172.013677	Glycerol Phosphate Shuttle/Glycerolipid Metabolism	13.64	7.03E+04	-	N	5.65	5.36E+05
199	P	2	sn-Glycerol 3-phosphate	C3H9O6P	172.013677	Glycerol Phosphate Shuttle/Glycerolipid Metabolism	-	N	-	N	-	N
200	N	2	Uracil	C4H4N2O2	112.027278	Pyrimidine Metabolism; Beta-Alanine Metabolism	8.74	6.17E+06	8.9	1.58E+07	6.83	3.41E+06
201	P	2	Uracil	C4H4N2O2	112.027278	Pyrimidine Metabolism; Beta-Alanine Metabolism	8.71	6.80E+05	8.94	3.39E+04	7.4	1.42E+05
202	N	2	Allantoin	C4H6N4O3	158.043991	no	13.82	1.37E+07	14.25	3.19E+06	5.94	7.03E+06
203	P	2	Allantoin	C4H6N4O3	158.043991	no	13.81	2.94E+06	9.81	4.81E+03	5.93	4.15E+05
204	N	2	Creatinine	C4H7N3O	113.058912	no	19.08	3.85E+05	10.08	4.46E+06	6.03	1.31E+05
205	P	2	Creatinine	C4H7N3O	113.058912	no	18.95	3.12E+07	10.04	6.73E+07	5.99	6.33E+07
206	N	2	D-3-hydroxy-butyrates	C4H8O3	104.047345	Fatty Acid Biosynthesis	7.3	1.12E+06	9.94	6.44E+06	9.37	2.74E+06
207	P	2	D-3-hydroxy-butyrates	C4H8O3	104.047345	Fatty Acid Biosynthesis	-	N	-	N	-	N
208	N	2	DL-3-aminobutyrate	C4H9NO2	103.063329		-	N	15.93	3.83E+05	-	N
209	P	2	DL-3-aminobutyrate	C4H9NO2	103.063329		19.25	1.85E+07	15.96	5.02E+07	5.61	2.57E+07
210	N	2	Deoxyribose	C5H10O4	134.05791	no	7.19	1.75E+05	8.87	1.99E+05	13.76	9.02E+05
211	P	2	Deoxyribose	C5H10O4	134.05791	no	-	N	-	N	-	N
212	N	2	L-Ornithine	C5H12N2O2	132.089878	Arginine and Proline Metabolism; Urea Cycle	29.11	1.57E+05	23.65	8.89E+05	5.03	1.02E+05
213	P	2	L-Ornithine	C5H12N2O2	132.089878	Arginine and Proline Metabolism; Urea Cycle	29.14	7.78E+06	23.63	2.65E+06	5.02	6.80E+06
214	N	2	Hypoxanthine	C5H4N4O	136.038511	Purine Metabolism	10.71	1.76E+07	10.57	7.23E+06	7.62	5.48E+06
215	P	2	Hypoxanthine	C5H4N4O	136.038511	Purine Metabolism	10.65	2.77E+07	10.55	1.67E+07	7.63	4.59E+06

No.	Polarity	Std. mix	Compound Name	Formula	MW	Pathway map	ZIC-HILIC		ZIC-pHILIC		C18	
							RT	peak	RT	peak	RT	Peak
216	N	2	Adenine	C5H5N5	135.054495	Purine Metabolism	16.82	1.34E+07	9.94	1.83E+07	6.23	1.17E+07
217	P	2	Adenine	C5H5N5	135.054495	Purine Metabolism	16.87	2.19E+07	9.81	3.27E+07	6.22	4.32E+07
218	N	2	Imidazole-4-acetate	C5H6N2O2	126.042928	Histidine Metabolism	17.79	1.25E+07	12.36	8.99E+06	5.89	1.16E+07
219	P	2	Imidazole-4-acetate	C5H6N2O2	126.042928	Histidine Metabolism	17.76	2.59E+07	12.37	8.91E+07	5.9	5.55E+07
220	N	2	N-Formyl-L-methionine	C6H11NO3S	177.045965	no	6.62	2.05E+07	7.85	1.11E+08	14.52	8.54E+07
221	P	2	N-Formyl-L-methionine	C6H11NO3S	177.045965	no	6.63	1.13E+06	5.42	4.34E+04	14.51	4.17E+06
222	N	2	O-Acetylcarnitine(+)	C9H18NO4	204.123584	Beta-Alanine Metabolism; Pantothenate and CoA Biosynthesis	15.19	2.99E+07	-	N	-	N
223	P	2	O-Acetylcarnitine(+)	C9H18NO4	204.123584	Beta-Alanine Metabolism; Pantothenate and CoA Biosynthesis	15.17	2.99E+07	11.51	1.76E+08	6.71	1.57E+07
224	N	2	2-Indolecarboxylicacid	C9H7NO2	161.047679	no	6.14	2.04E+07	7.8	8.99E+07	23.46	9.37E+07
225	P	2	2-Indolecarboxylicacid	C9H7NO2	161.047679	no	-	N	-	N	-	N
226	N	2	trans-cinnamic acid	C9H8O2	148.05243	no	6.12	3.66E+04	7.78	4.32E+07	24.02	2.42E+05
227	P	2	trans-cinnamic acid	C9H8O2	148.05243	no	6.08	4.71E+04	4.28	8.43E+03	24.01	9.33E+04
228	N	2	Caffeate	C9H8O4	180.04226	no	7.78	2.96E+07	12.2	4.27E+07	16.6	1.38E+08
229	P	2	Caffeate	C9H8O4	180.04226	no	7.88	1.18E+05	12.1	2.73E+04	16.58	4.50E+05
230	N	3	Sarcosine	C3H7NO2	89.047679	Glycine and Serine Metabolism	-	N	14.52	1.27E+06	-	N
231	P	3	Sarcosine	C3H7NO2	89.047679	Glycine and Serine Metabolism	18.27	2.57E+07	14.47	2.69E+07	5.47	1.97E+07
232	N	3	2-phosphoglycerate	C3H7O7P	185.992942	Glycine and Serine/Glycerolipid Metabolism and Glycolysis Gluconeogenesis	16.09	8.10E+06	17.64	6.97E+06	5.71	5.48E+06
233	P	3	2-phosphoglycerate	C3H7O7P	185.992942	Glycine and Serine/Glycerolipid Metabolism and Glycolysis Gluconeogenesis	16.07	1.86E+05	-	N	5.72	8.72E+04
234	N	3	xylose	C5H10O5	150.052825	no	13.77	2.03E+06	13.78	2.18E+05	5.71	4.70E+05
235	P	3	xylose	C5H10O5	150.052825	no	-	N	-	N	-	N

No.	Polarity	Std. mix	Compound Name	Formula	MW	Pathway map	ZIC-HILIC		ZIC-pHILIC		C18	
							RT	peak	RT	peak	RT	peak
236	N	3	D-Xylulose 5-phosphate	C5H11O8P	230.019157	Pentose Phosphate Pathway	15.74	9.97E+04	-	N	5.48	1.18E+06
237	P	3	D-Xylulose 5-phosphate	C5H11O8P	230.019157	Pentose Phosphate Pathway	-	N	-	N	-	N
238	N	3	Itaconate	C5H6O4	130.02661	no	7.5	2.02E+07	15.99	4.49E+07	12.63	5.15E+07
239	P	3	Itaconate	C5H6O4	130.02661	no	-	N	-	N	-	N
240	N	3	mannose	C6H12O6	180.06339	Fructose and Mannose Degradation; Galactose Metabolism	14.13	9.15E+06	14.38	1.78E+06	5.59	1.95E+06
241	P	3	mannose	C6H12O6	180.06339	Fructose and Mannose Degradation; Galactose Metabolism	-	N	-	N	-	N
242	N	3	galactose 1 phosphate	C6H13O9P	260.029722	Nucleotide Sugars Metabolism; Galactose Metabolism	16.88	1.14E+07	16.8	2.43E+06	5.23	2.13E+06
243	P	3	galactose 1 phosphate	C6H13O9P	260.029722	Nucleotide Sugars Metabolism; Galactose Metabolism	16.89	2.81E+05	16.79	3.54E+04	-	N
244	N	3	Picolinic acid	C6H5NO2	123.032029	no	-	N	9.29	8.41E+05	-	N
245	P	3	Picolinic acid	C6H5NO2	123.032029	no	-	N	9.28	4.45E+05	6.55	2.81E+06
246	N	3	D-Glucuronolactone	C6H8O6	176.03209	no	15.31	3.58E+06	16.21	5.01E+07	6.54	6.27E+06
247	P	3	D-Glucuronolactone	C6H8O6	176.03209	no	-	N	-	N	-	N
248	N	3	Paraxanthine	C7H8N4O2	180.064726		-	N	7.67	5.82E+06	-	N
249	P	3	Paraxanthine	C7H8N4O2	180.064726		7.7	3.27E+06	7.66	3.33E+05	13.65	8.69E+06
250	N	3	L-Kynurenine	C10H12N2O3	208.084793	Tryptophan Metabolism	14.27	1.24E+06	11.37	1.93E+06	12.86	9.91E+05
251	P	3	L-Kynurenine	C10H12N2O3	208.084793	Tryptophan Metabolism	14.25	8.99E+06	11.31	7.08E+06	12.89	8.77E+06
252	N	3	Guanosine	C10H13N5O5	283.09167	Purine Metabolism	13.49	8.20E+06	13.05	3.87E+06	10.1	2.92E+06
253	P	3	Guanosine	C10H13N5O5	283.09167	Purine Metabolism	13.46	8.86E+06	13.07	1.88E+06	7.47	6.82E+06
254	N	3	Thymidine	C10H14N2O5	242.090273	Pyrimidine Metabolism	8.19	2.22E+06	7.71	1.40E+07	11.38	2.63E+06
255	P	3	Thymidine	C10H14N2O5	242.090273	Pyrimidine Metabolism	8.21	2.43E+06	7.75	1.71E+05	11.41	8.83E+05

No.	Polarity	Std. mix	Compound Name	Formula	MW	Pathway map	ZIC-HILIC		ZIC-pHILIC		C18	
							RT	peak	RT	peak	RT	Peak
256	N	3	dAMP	C10H14N5O6P	331.068172	Purine Metabolism	17.85	1.35E+07	13.6	7.11E+06	6.36	2.45E+07
257	P	3	dAMP	C10H14N5O6P	331.068172	Purine Metabolism	17.82	2.55E+06	13.59	4.46E+06	6.35	4.61E+06
258	N	3	AMP	C10H14N5O7P	347.063087	Purine Metabolism	18.08	8.92E+06	14.52	5.14E+06	6.18	1.94E+07
259	P	3	AMP	C10H14N5O7P	347.063087	Purine Metabolism	18.11	1.53E+06	14.56	1.22E+06	6.17	3.66E+06
260	N	3	L-Metanephrine	C10H15NO3	197.105194	Tyrosine Metabolism	-	N	18.47	2.55E+04	-	N
261	P	3	L-Metanephrine	C10H15NO3	197.105194	Tyrosine Metabolism	17.23	1.75E+07	18.58	3.12E+07	7.47	3.34E+07
262	N	3	Spermine	C10H26N4	202.215746	Spermidine and Spermine Biosynthesis	-	N	-	N	-	N
263	P	3	Spermine	C10H26N4	202.215746	Spermidine and Spermine Biosynthesis	41.32	3.54E+05	-	N	4.29	1.58E+06
264	N	3	Kynurenic acid	C10H7NO3	189.042594	Tryptophan Metabolism	8.1	1.72E+07	7.69	4.95E+07	14.44	5.79E+07
265	P	3	Kynurenic acid	C10H7NO3	189.042594	Tryptophan Metabolism	8.16	3.25E+07	7.7	1.46E+07	14.45	1.83E+07
266	N	3	5-Hydroxyindoleacetate	C10H9NO3	191.058244	Tryptophan Metabolism	6.28	1.80E+05	5.03	6.66E+05	14.29	2.57E+06
267	P	3	5-Hydroxyindoleacetate	C10H9NO3	191.058244	Tryptophan Metabolism	6.11	5.23E+05	11.29	4.81E+05	-	N
268	N	3	L-Saccharopine	C11H20N2O6	276.132138	Lysine Degradation	22.87	2.71E+06	16.41	4.99E+06	5.41	8.58E+06
269	P	3	L-Saccharopine	C11H20N2O6	276.132138	Lysine Degradation	22.95	1.18E+06	16.42	2.19E+06	5.43	2.42E+06
270	N	3	NADPH	C21H30N7O17P3	745.091109	Histidine Metabolism; Glycerolipid Metabolism	-	N	18.03	4.47E+04	-	N
271	P	3	NADPH	C21H30N7O17P3	745.091109	Histidine Metabolism; Glycerolipid Metabolism	-	N	16.86	1.68E+03	-	N
272	N	3	Glycocholic acid	C26H43NO6	465.309039	Bile Acid Biosynthesis	6.58	1.32E+07	5.03	5.68E+07	22.12	5.64E+07
273	P	3	Glycocholic acid	C26H43NO6	465.309039	Bile Acid Biosynthesis	6.57	4.02E+06	5.04	1.98E+06	22.13	9.56E+06
274	N	3	Glycine	C2H5NO2	75.032029	Ammonia Recycling; Bile Acid Biosynthesis	-	N	-	N	-	N
275	P	3	Glycine	C2H5NO2	75.032029	Ammonia Recycling; Bile Acid Biosynthesis	19.68	5.82E+06	16.22	4.64E+05	5.4	2.14E+06
276	N	3	Pyruvate	C3H4O3	88.016045	Urea Cycle; Pyruvate Metabolism	8.35	4.05E+05	8.9	2.20E+07	6.52	8.58E+05

No.	Polarity	Std. mix	Compound Name	Formula	MW	Pathway map	ZIC-HILIC		ZIC-pHILIC		C18	
							RT	peak	RT	peak	RT	peak
277	P	3	Pyruvate	C3H4O3	88.016045	Urea Cycle; Pyruvate Metabolism	-	N	-	N	-	N
278	N	3	5-Oxoproline	C5H7NO3	129.042594	Glutathione Metabolism	8.35	3.11E+07	10.97	3.95E+07	7.45	2.18E+07
279	P	3	5-Oxoproline	C5H7NO3	129.042594	Glutathione Metabolism	8.37	3.33E+06	10.99	2.19E+05	7.44	1.52E+06
280	N	3	Histamine	C5H9N3	111.079647	Histidine Metabolism	-	N	25.86	2.04E+04	-	N
281	P	3	Histamine	C5H9N3	111.079647	Histidine Metabolism	35.33	9.26E+06	25.88	6.97E+06	4.84	1.10E+07
282	N	3	Acetylcysteine	C5H9NO3S	163.030315	no	8.15	3.42E+05	8.56	1.51E+07	19.5	6.98E+05
283	P	3	Acetylcysteine	C5H9NO3S	163.030315	no	-	N	8.57	1.03E+05	-	N
284	N	3	Galactarate	C6H10O8	210.03757	no	19.21	3.55E+06	18.1	1.14E+07	5.57	1.47E+07
285	P	3	Galactarate	C6H10O8	210.03757	no	-	N	-	N	-	N
286	N	3	D-Glucosamine	C6H13NO5	179.079374	Amino Sugar Metabolism	25.32	1.90E+05	14.34	9.14E+04	-	N
287	P	3	D-Glucosamine	C6H13NO5	179.079374	Amino Sugar Metabolism	25.35	3.74E+06	14.98	8.93E+05	5.36	1.74E+06
288	N	3	6-Phospho-D-gluconate	C6H13O10P	276.024637	Pentose Phosphate Pathway	20.16	5.57E+04	18.66	1.91E+05	5.68	3.04E+05
289	P	3	6-Phospho-D-gluconate	C6H13O10P	276.024637	Pentose Phosphate Pathway	-	N	-	N	-	N
290	N	3	L-Arginine	C6H14N4O2	174.111676	Urea Cycle; Arginine and Proline Metabolism	28.93	5.10E+06	26.45	1.41E+06	5.35	9.26E+05
291	P	3	L-Arginine	C6H14N4O2	174.111676	Urea Cycle; Arginine and Proline Metabolism	28.97	6.20E+06	26.47	3.18E+06	5.36	2.76E+06
292	N	3	D-Glucosamine 6-Phosphate	C6H14NO8P	259.045706	Amino Sugar Metabolism; Glutamate Metabolism	7.5	1.86E+05	13.25	3.83E+04	12.61	2.52E+05
293	P	3	D-Glucosamine 6-Phosphate	C6H14NO8P	259.045706	Amino Sugar Metabolism; Glutamate Metabolism	-	N	-	N	-	N
294	N	3	L-Histidine	C6H9N3O2	155.069477	Histidine Metabolism; Ammonia Recycling	27.49	1.39E+07	15.25	4.27E+06	5.07	1.59E+06
295	P	3	L-Histidine	C6H9N3O2	155.069477	Histidine Metabolism; Ammonia Recycling	27.48	9.95E+06	15.24	1.00E+07	5.08	1.87E+06
296	N	3	N-Acetyl-L-aspartate	C6H9NO5	175.048074	Aspartate Metabolism	8.49	3.80E+07	15.56	2.74E+07	7.41	1.81E+07
297	P	3	N-Acetyl-L-aspartate	C6H9NO5	175.048074	Aspartate Metabolism	8.48	3.42E+06	15.52	1.29E+05	7.4	1.09E+06

No.	Polarity	Std. mix	Compound Name	Formula	MW	Pathway map	ZIC-HILIC		ZIC-pHILIC		C18	
							RT	peak	RT	peak	RT	peak
298	N	3	N(pi)-Methyl-L-histidine	C7H11N3O2	169.085127	no	27.96	1.09E+07	13.6	2.61E+06	5.35	1.24E+06
299	P	3	N(pi)-Methyl-L-histidine	C7H11N3O2	169.085127	no	27.91	1.10E+07	13.61	2.28E+07	5.31	3.96E+06
300	N	3	N-Acetyl-L-glutamate	C7H11NO5	189.063724	no	8.24	3.50E+07	15.08	3.09E+07	7.45	2.52E+07
301	P	3	N-Acetyl-L-glutamate	C7H11NO5	189.063724	no	8.23	6.15E+06	15.07	5.52E+06	7.44	3.09E+06
302	N	3	Dopamine	C8H11NO2	153.078979	Tyrosine Metabolism; Catecholamine Biosynthesis	-	N	-	N	-	N
303	P	3	Dopamine	C8H11NO2	153.078979	Tyrosine Metabolism; Catecholamine Biosynthesis	-	N	29.48	3.27E+04	-	N
304	N	3	6-Hydroxydopamine(Oxidopamine) rapid brown	C8H11NO3	169.073894	no	-	N	8.28	3.77E+04	-	N
305	P	3	6-Hydroxydopamine(Oxidopamine) rapid brown	C8H11NO3	169.073894	no	18.02	7.98E+04	8.29	5.88E+05	-	N
306	N	3	Pyridoxamine	C8H12N2O2	168.089878	Vitamin B6 Metabolism	31.15	7.57E+04	12.02	1.05E+05	5.39	1.16E+05
307	P	3	Pyridoxamine	C8H12N2O2	168.089878	Vitamin B6 Metabolism	31.16	6.66E+06	11.91	8.12E+06	5.38	1.77E+07
308	N	3	Lipoate	C8H14O2S2	206.043522	Ammonia Recycling; Glycine and Serine Metabolism	6	2.61E+05	4.99	2.83E+07	26.58	2.51E+06
309	P	3	Lipoate	C8H14O2S2	206.043522	Ammonia Recycling; Glycine and Serine Metabolism	-	N	-	N	-	N
310	N	3	N6-Acetyl-L-Lysine	C8H16N2O3	188.116093	no	19.69	1.93E+07	15.53	1.02E+07	5.89	1.75E+07
311	P	3	N6-Acetyl-L-Lysine	C8H16N2O3	188.116093	no	19.68	2.26E+07	15.52	5.63E+07	5.9	3.94E+07
312	N	3	Phthalate	C8H6O4	166.02661	no	-	N	-	N	-	N
313	P	3	Phthalate	C8H6O4	166.02661	no	6.48	7.01E+05	14.75	1.68E+05	16.49	1.95E+06
314	N	3	Pyridoxal	C8H9NO3	167.058244	Vitamin B6 Metabolism	17.47	3.40E+05	4.91	5.08E+05	11.22	1.46E+05
315	P	3	Pyridoxal	C8H9NO3	167.058244	Vitamin B6 Metabolism	17.5	4.13E+05	5.75	4.37E+05	7.42	2.73E+05
316	N	3	Uridine	C9H12N2O6	244.069538	Pyrimidine Metabolism	10.18	9.75E+06	10.18	6.60E+06	7.43	3.88E+06
317	P	3	Uridine	C9H12N2O6	244.069538	Pyrimidine Metabolism	10.17	2.09E+06	-	N	7.44	6.39E+05

No.	Polarity	Std. mix	Compound Name	Formula	MW	Pathway map	ZIC-HILIC		ZIC-pHILIC		C18	
							RT	peak	RT	peak	RT	peak
318	N	3	Amphetamine	C9H13N	135.104799	no	-	N	-	N	-	N
319	P	3	Amphetamine	C9H13N	135.104799	no	13.96	6.84E+07	18.16	8.60E+07	14.34	1.15E+08
320	N	3	UMP	C9H13N2O9P	324.03587	Pyrimidine Metabolism;Lactose Synthesis	14.72	1.83E+07	15.94	4.76E+06	5.95	2.07E+07
321	P	3	UMP	C9H13N2O9P	324.03587	Pyrimidine Metabolism;Lactose Synthesis	14.75	7.57E+05	15.93	9.18E+04	5.97	3.36E+05
322	N	3	Cytidine	C9H13N3O5	243.085522	Pyrimidine Metabolism	20.64	8.18E+06	12.29	2.93E+06	6.2	2.99E+06
323	P	3	Cytidine	C9H13N3O5	243.085522	Pyrimidine Metabolism	20.6	1.19E+07	12.32	1.06E+07	6.19	1.43E+07
324	N	3	CDP	C9H15N3O11P2	403.018186	Pyrimidine Metabolism	30.2	2.14E+05	17.9	1.56E+06	5.64	1.47E+06
325	P	3	CDP	C9H15N3O11P2	403.018186	Pyrimidine Metabolism	-	N	17.93	1.64E+05	5.63	8.41E+04
326	N	3	CTP	C9H16N3O14P3	482.984518	Pyrimidine Metabolism; Amino Sugar Metabolism	-	N	19.38	1.16E+05	-	N
327	P	3	CTP	C9H16N3O14P3	482.984518	Pyrimidine Metabolism; Amino Sugar Metabolism	-	N	19.49	4.07E+03	-	N
328	N	3	O-Acetylcarnitine	C9H17NO4	203.115759	Beta Oxidation of Very Long Chain Fatty Acids	16.27	5.46E+04	11.46	1.87E+05	-	N
329	P	3	O-Acetylcarnitine	C9H17NO4	203.115759	Beta Oxidation of Very Long Chain Fatty Acids	16.3	2.18E+07	11.52	1.80E+08	7.44	2.87E+07
330	N	4	fructose	C6H12O6	180.06339	Starch and Sucrose Metabolism; Galactose Metabolism	13.7	4.97E+05	13.84	1.04E+06	-	N
331	P	4	fructose	C6H12O6	180.06339	Starch and Sucrose Metabolism; Galactose Metabolism	-	N	-	N	-	N
332	N	4	fructose 6 phosphate	C6H13O9P	260.029722	Glycolysis; Gluconeogenesis	16.56	1.06E+07	16.81	2.46E+06	5.41	1.03E+07
333	P	4	fructose 6 phosphate	C6H13O9P	260.029722	Glycolysis; Gluconeogenesis	16.5	4.72E+05	16.85	3.49E+04	5.4	1.93E+05
334	N	4	Octopamine	C8H11NO2	153.078979	no	-	N	20.47	6.91E+04	-	N
335	P	4	Octopamine	C8H11NO2	153.078979	no	18.57	1.16E+07	20.51	1.01E+07	6.34	1.21E+07
336	N	4	Tryptophanol	C10H11NO	161.084064	Tryptophan Metabolism	-	N	6.19	2.75E+05	-	N
337	P	4	Tryptophanol	C10H11NO	161.084064	Tryptophan Metabolism	6.26	2.56E+06	5.74	7.75E+05	21.76	8.20E+06

No.	Polarity	Std. mix	Compound Name	Formula	MW	Pathway map	ZIC-HILIC		ZIC-pHILIC		C18	
							RT	peak	RT	peak	RT	Peak
338	N	4	GMP	C10H14N5O8P	363.058002	Purine/Glutamate Metabolism	17.77	5.70E+06	17.52	2.99E+06	6.22	1.32E+07
339	P	4	GMP	C10H14N5O8P	363.058002	Purine/Glutamate Metabolism	17.66	8.57E+05	17.51	4.41E+05	6.23	1.16E+06
340	N	4	5-methylcytidine	C10H15N3O5	257.101172	Cancer	20.41	3.81E+06	11.05	4.29E+06	6.4	3.49E+06
341	P	4	5-methylcytidine	C10H15N3O5	257.101172	Cancer	20.4	8.44E+06	11.04	1.73E+07	6.41	6.73E+06
342	N	4	GDP	C10H15N5O11P2	443.024334		-	N	18.81	4.44E+05	-	N
343	P	4	GDP	C10H15N5O11P2	443.024334		-	N	18.8	5.29E+04	-	N
344	N	4	ATP	C10H16N5O13P3	506.995751	Citric Acid Cycle; Gluconeogenesis	-	N	17.53	1.25E+05	-	N
345	P	4	ATP	C10H16N5O13P3	506.995751	Citric Acid Cycle; Gluconeogenesis	-	N	17.63	4.13E+03	-	N
346	N	4	L-Glutathione oxidized	C20H32N6O12S2	612.151966	Glutamate Metabolism; Glutathione Metabolism	22.6	3.77E+06	18.28	1.70E+06	6.49	4.89E+06
347	P	4	L-Glutathione oxidized	C20H32N6O12S2	612.151966	Glutamate Metabolism; Glutathione Metabolism	22.58	3.80E+05	18.26	2.74E+05	6.52	3.43E+05
348	N	4	L-Tryptophan	C11H12N2O2	204.089878	Tryptophan Metabolism; Transcription/Translation	14.15	1.44E+05	12.15	6.69E+06	14.26	1.01E+07
349	P	4	L-Tryptophan	C11H12N2O2	204.089878	Tryptophan Metabolism; Transcription/Translation	14.21	1.17E+07	12.18	1.49E+07	14.24	3.79E+07
350	N	4	5'-Methylthioadenosine	C11H15N5O3S	297.089561	Methionine Metabolism; Spermidine and Spermine Biosynthesis	12.15	4.51E+05	7.71	4.62E+06	13.25	1.17E+06
351	P	4	5'-Methylthioadenosine	C11H15N5O3S	297.089561	Methionine Metabolism; Spermidine and Spermine Biosynthesis	12.18	1.45E+07	7.72	1.05E+07	13.28	2.38E+07
352	P	4	7-Methylguanosine(+)	C11H16N5O5	298.115145		19.95	4.89E+06	13.83	2.81E+07	7.5	1.40E+07
353	N	4	Thiamine (+)	C12H17N4OS	265.112307	Thiamine Metabolism	-	N	-	N	-	N
354	P	4	Thiamine (+)	C12H17N4OS	265.112307	Thiamine Metabolism	33.61	9.36E+06	21	1.16E+07	5.31	2.41E+07
355	N	4	Melatonin	C13H16N2O2	232.121178	Tryptophan Metabolism	6.34	1.97E+04	4.94	4.81E+06	20.47	1.05E+06
356	P	4	Melatonin	C13H16N2O2	232.121178	Tryptophan Metabolism	6.28	1.53E+07	4.91	4.30E+07	20.48	3.44E+07
357	N	4	S-Adenosyl-L-homocysteine	C14H20N6O5S	384.12159	Betaine Metabolism; Methionine Metabolism	23.39	9.18E+05	14.15	1.08E+06	6.33	2.37E+06

No.	Polarity	Std. mix	Compound Name	Formula	MW	Pathway map	ZIC-HILIC		ZIC-pHILIC		C18	
							RT	peak	RT	peak	RT	peak
358	P	4	S-Adenosyl-L-homocysteine	C14H20N6O5S	384.12159	Betaine Metabolism; Methionine Metabolism	23.29	2.12E+05	14.19	8.79E+05	6.32	6.70E+05
359	N	4	NAD+	C21H27N7O14P2	663.109127	Ammonia Recycling; Glycolysis	21.43	4.74E+05	14.86	6.07E+05	6.19	9.90E+05
360	P	4	NAD+	C21H27N7O14P2	663.109127	Ammonia Recycling; Glycolysis	21.72	7.16E+04	14.93	2.71E+05	6.18	3.98E+05
361	N	4	Cholate	C24H40O5	408.287575	Bile Acid Biosynthesis	6.27	3.07E+06	5.01	2.31E+07	24.61	8.84E+06
362	P	4	Cholate	C24H40O5	408.287575	Bile Acid Biosynthesis	6.28	6.15E+05	-	N	24.63	2.25E+06
363	N	4	taurocholate	C26H45NO7S	515.291675	Bile Acid Biosynthesis	8.16	4.10E+07	7.69	4.45E+07	20.25	4.19E+07
364	P	4	taurocholate	C26H45NO7S	515.291675	Bile Acid Biosynthesis	8.15	1.14E+06	4.93	1.08E+05	20.24	9.61E+05
365	N	4	Ethanolamine phosphate	C2H8NO4P	141.019096	Sphingolipid Metabolism	20.23	1.11E+07	16.65	2.51E+06	5.32	1.11E+07
366	P	4	Ethanolamine phosphate	C2H8NO4P	141.019096	Sphingolipid Metabolism	20.22	3.67E+06	16.69	8.47E+05	5.33	5.12E+06
367	N	4	Phosphocreatine	C4H10N3O5P	211.035809	Arginine and Proline Metabolism	16.33	4.09E+05	16.02	7.24E+05	5.7	1.79E+05
368	P	4	Phosphocreatine	C4H10N3O5P	211.035809	Arginine and Proline Metabolism	16.41	1.14E+05	16.01	2.52E+05	5.71	1.17E+05
369	N	4	(R)-Malate	C4H6O5	134.021525	no	10.76	1.21E+07	16.97	2.75E+07	6.55	7.66E+06
370	P	4	(R)-Malate	C4H6O5	134.021525	no	-	N	-	N	-	N
371	P	4	L-Homoserine Lactone	C4H7NO2	101.047679		20.67	1.77E+06	7.7	2.31E+05	5.49	1.74E+06
372	N	4	2-Hydroxybutanoic acid	C4H8O3	104.047345	no	6.89	8.79E+06	8.71	7.45E+06	10.52	1.83E+07
373	P	4	2-Hydroxybutanoic acid	C4H8O3	104.047345	no	-	N	-	N	-	N
374	N	4	L-Homocysteine	C4H9NO2S	135.0354	Methionine Metabolism; Glycine and Serine Metabolism	16.04	9.63E+05	13.66	2.11E+05	6.62	3.54E+05
375	P	4	L-Homocysteine	C4H9NO2S	135.0354	Methionine Metabolism; Glycine and Serine Metabolism	16.07	3.68E+06	13.62	4.97E+05	6.59	8.83E+05
376	N	4	Urate	C5H4N4O3	168.028341	Purine Metabolism	12.51	2.13E+06	-	N	7.45	2.77E+05
377	P	4	Urate	C5H4N4O3	168.028341	Purine Metabolism	12.52	3.18E+04	-	N	-	N
378	N	4	Guanine	C5H5N5O	151.04941	Purine Metabolism	16.2	2.09E+06	12.77	7.00E+05	6.24	7.45E+05

No.	Polarity	Std. mix	Compound Name	Formula	MW	Pathway map	ZIC-HILIC		ZIC-pHILIC		C18	
							RT	peak	RT	peak	RT	Peak
379	P	4	Guanine	C5H5N5O	151.04941	Purine Metabolism	16.19	2.39E+06	12.79	1.49E+06	6.23	3.07E+06
380	N	4	D-Galactono-1,4-lactone	C6H10O6	178.04774	no	10.76	2.62E+07	10.77	3.77E+06	6.17	1.30E+07
381	P	4	D-Galactono-1,4-lactone	C6H10O6	178.04774	no	10.82	1.62E+04	-	N	6.16	2.60E+05
382	N	4	D-Gluconic acid	C6H12O7	196.058305	no	18.54	5.32E+06	14.86	8.34E+06	5.59	1.32E+07
383	P	4	D-Gluconic acid	C6H12O7	196.058305	no	-	N	-	N	5.62	5.75E+04
384	N	4	L-Citrulline	C6H13N3O3	175.095692	Arginine and Proline Metabolism;Aspartate Metabolism	20.14	1.47E+07	16.44	6.39E+06	5.52	6.69E+06
385	P	4	L-Citrulline	C6H13N3O3	175.095692	Arginine and Proline Metabolism;Aspartate Metabolism	20.13	1.65E+07	16.47	1.44E+07	5.53	7.10E+06
386	N	4	L-Lysine	C6H14N2O2	146.105528	Lysine Degradation; Biotin Metabolism	28.98	2.15E+05	25.03	6.49E+05	4.98	2.86E+05
387	P	4	L-Lysine	C6H14N2O2	146.105528	Lysine Degradation; Biotin Metabolism	28.97	6.34E+06	25.07	1.77E+06	5.02	1.26E+07
388	N	4	beta-D-Fructose-1,6-bisphosphate	C6H14O12P2	339.996054	no	42.97	7.80E+04	19.36	7.07E+04	8.03	2.25E+05
389	P	4	beta-D-Fructose-1,6-bisphosphate	C6H14O12P2	339.996054	no	-	N	-	N	-	N
390	N	4	Triethanolamine	C6H15NO3	149.105194	no	-	N	9.92	9.91E+04	-	N
391	P	4	Triethanolamine	C6H15NO3	149.105194	no	20.86	3.27E+07	9.86	1.48E+08	5.44	3.56E+07
392	N	4	Nicotinamide	C6H6N2O	122.048013	Nicotinate and Nicotinamide Metabolism	-	N	7.73	3.51E+06	-	N
393	P	4	Nicotinamide	C6H6N2O	122.048013	Nicotinate and Nicotinamide Metabolism	10.66	3.63E+07	7.76	1.17E+07	7.26	6.32E+06
394	N	4	Cis-Aconitate	C6H6O6	174.01644	Citric Acid Cycle	8.23	4.69E+06	20.08	6.62E+05	10.43	6.04E+05
395	P	4	Cis-Aconitate	C6H6O6	174.01644	Citric Acid Cycle	-	N	-	N	-	N
396	N	4	N-Acetylglutamine	C7H12N2O4	188.079708	no	9.59	3.56E+07	10.79	1.55E+07	6.49	1.95E+07
397	P	4	N-Acetylglutamine	C7H12N2O4	188.079708	no	9.63	1.17E+07	10.89	2.36E+07	6.45	3.57E+06
398	N	4	Cystathionine	C7H14N2O4S	222.067429	Glycine and Serine Metabolism; Methionine Metabolism	23.93	1.13E+06	17.74	4.06E+05	5.25	1.17E+06

No.	Polarity	Std. mix	Compound Name	Formula	MW	Pathway map	ZIC-HILIC		ZIC-pHILIC		C18	
							RT	peak	RT	peak	RT	peak
399	P	4	Cystathionine	C7H14N2O4S	222.067429	Glycine and Serine Metabolism; Methionine Metabolism	23.92	3.22E+05	17.76	1.56E+05	5.26	6.02E+05
400	N	4	AcetylCholine	C7H15NO2	145.110279	Phospholipid Biosynthesis	-	N	-	N	-	N
401	P	4	AcetylCholine	C7H15NO2	145.110279	Phospholipid Biosynthesis	16.19	4.50E+06	15.33	3.16E+06	6.32	4.94E+06
402	N	4	methyl-L-lysine	C7H16N2O2	160.121178	no	28.41	3.35E+05	23.86	1.85E+06	5.03	1.93E+05
403	P	4	methyl-L-lysine	C7H16N2O2	160.121178	no	28.33	1.06E+07	23.87	1.34E+07	5.04	1.82E+07
404	N	4	Spermidine	C7H19N3	145.157897	Methionine Metabolism; Spermidine and Spermine Biosynthesis	-	N	-	N	-	N
405	P	4	Spermidine	C7H19N3	145.157897	Methionine Metabolism; Spermidine and Spermine Biosynthesis	-	N	15.65	8.93E+04	4.32	1.41E+07
406	N	4	Gallate	C7H6O5	170.021525	no	9.66	2.95E+07	18.86	7.81E+06	11.53	3.11E+07
407	N	4	2-(4-Hydroxyphenyl) ethanol	C8H10O2	138.06808	no	-	N	6.24	3.56E+05	-	N
408	P	4	2-(4-Hydroxyphenyl) ethanol	C8H10O2	138.06808	no	-	N	-	N	-	N
409	N	4	1-Phenylethylamine	C8H11N	121.089149	no	-	N	-	N	-	N
410	P	4	1-Phenylethylamine	C8H11N	121.089149	no	13.89	3.08E+07	21.14	2.31E+07	13.73	8.35E+07
411	N	4	L-Noradrenaline	C8H11NO3	169.073894	Catecholamine Biosynthesis; Tyrosine Metabolism	22.32	7.00E+06	24.96	7.27E+05	6.08	3.19E+06
412	P	4	L-Noradrenaline	C8H11NO3	169.073894	Catecholamine Biosynthesis; Tyrosine Metabolism	22.47	2.11E+06	24.7	1.29E+06	6.05	1.51E+07
413	N	4	N-Acetyl-D-glucosamine 6-phosphate	C8H16NO9P	301.056271	Glutamate Metabolism; Amino Sugar Metabolism	15.45	6.67E+06	15.97	2.65E+06	5.48	4.65E+06
414	P	4	N-Acetyl-D-glucosamine 6-phosphate	C8H16NO9P	301.056271	Glutamate Metabolism; Amino Sugar Metabolism	15.39	3.77E+05	16.01	1.63E+05	5.58	3.00E+05
415	N	4	Dimethyl-L-lysine	C8H18N2O2	174.136828		28.55	9.01E+04	21.93	1.14E+06	-	N
416	P	4	Dimethyl-L-lysine	C8H18N2O2	174.136828		28.54	1.24E+07	21.92	2.58E+07	5.17	1.84E+07
417	N	4	4-Hydroxyphenylacetate	C8H8O3	152.047345	Tyrosine Metabolism	6.46	2.11E+06	9.76	5.52E+06	17.3	2.70E+07
418	P	4	4-Hydroxyphenylacetate	C8H8O3	152.047345	Tyrosine Metabolism	-	N	-	N	-	N

No.	Polarity	Std. mix	Compound Name	Formula	MW	Pathway map	ZIC-HILIC		ZIC-pHILIC		C18	
							RT	peak	RT	peak	RT	Peak
419	N	4	Homogentisate	C8H8O4	168.04226	Phenylalanine and Tyrosine Metabolism; Tyrosine Metabolism	8.23	2.48E+07	9.81	2.95E+07	13	3.00E+07
420	P	4	Homogentisate	C8H8O4	168.04226	Phenylalanine and Tyrosine Metabolism; Tyrosine Metabolism	-	N	-	N	-	N
421	N	4	L-Phenylalanine	C9H11NO2	165.078979	Transcription/Translation; Phenylalanine and Tyrosine Metabolism	13.74	4.00E+04	10.75	6.42E+06	12.02	8.90E+05
422	P	4	L-Phenylalanine	C9H11NO2	165.078979	Transcription/Translation; Phenylalanine and Tyrosine Metabolism	13.66	1.85E+07	10.74	2.70E+07	11.94	2.95E+07
423	N	4	L-Tyrosine	C9H11NO3	181.073894	Tyrosine Metabolism; Phenylalanine and Tyrosine Metabolism	15.77	5.38E+06	13.54	1.29E+07	7.51	9.78E+06
424	P	4	L-Tyrosine	C9H11NO3	181.073894	Tyrosine Metabolism; Phenylalanine and Tyrosine Metabolism	15.8	2.42E+07	13.55	1.48E+07	7.5	4.55E+07
425	N	4	Dihydrobiopterin	C9H13N5O3	239.10184	Pterine Biosynthesis; Catecholamine Biosynthesis	14.68	8.87E+04	12.98	5.49E+05	6.8	1.56E+05
426	P	4	Dihydrobiopterin	C9H13N5O3	239.10184	Pterine Biosynthesis; Catecholamine Biosynthesis	14.53	2.82E+05	12.97	2.82E+06	7.46	1.32E+05
427	N	4	Phenylephrine	C9H13NO2	167.094629	no	-	N	-	N	-	N
428	P	4	Phenylephrine	C9H13NO2	167.094629	no	-	N	14.88	2.49E+04	11.09	7.95E+04
429	N	4	L-Adrenaline	C9H13NO3	183.089544	Tyrosine Metabolism; Catecholamine Biosynthesis	20.39	3.09E+06	25.51	7.91E+05	6.31	1.05E+07
430	P	4	L-Adrenaline	C9H13NO3	183.089544	Tyrosine Metabolism; Catecholamine Biosynthesis	20.36	6.49E+06	25.55	9.69E+06	6.3	3.08E+07
431	N	4	UDP	C9H14N2O12P2	404.002202	Pyrimidine Metabolism; Lactose Synthesis	26.02	4.61E+04	17.38	7.13E+05	-	N
432	P	4	UDP	C9H14N2O12P2	404.002202	Pyrimidine Metabolism; Lactose Synthesis	-	N	17.23	1.07E+04	-	N
433	N	4	CMP	C9H14N3O8P	323.051854	Pyrimidine Metabolism; Phosphatidylinositol Phosphate Metabolism	20.51	6.50E+06	16.63	2.31E+06	5.79	8.61E+06
434	P	4	CMP	C9H14N3O8P	323.051854	Pyrimidine Metabolism; Phosphatidylinositol Phosphate Metabolism	20.49	1.01E+06	16.67	2.83E+05	5.78	1.81E+06
435	N	4	L-Carnosine	C9H14N4O3	226.106591	Beta-Alanine Metabolism; Histidine Metabolism	30.67	1.13E+07	16.29	4.56E+06	4.98	9.83E+06

No.	Polarity	Std. mix	Compound Name	Formula	MW	Pathway map	ZIC-HILIC		ZIC-pHILIC		C18	
							RT	peak	RT	peak	RT	Peak
436	P	4	L-Carnosine	C9H14N4O3	226.106591	Beta-Alanine Metabolism; Histidine Metabolism	30.64	3.93E+06	16.28	5.17E+06	5.04	3.84E+06
437	N	4	Diethyl 2-oxoglutarate	C9H14O5	202.084125		-	N	4.34	4.31E+06	-	N
438	P	4	Diethyl 2-oxoglutarate	C9H14O5	202.084125		5.96	1.72E+05	4.33	5.05E+05	23.89	2.01E+05
439	N	4	UTP	C9H15N2O15P3	483.968534	Pyrimidine Metabolism; Amino Sugar Metabolism	-	N	18.72	3.63E+05	-	N
440	P	4	UTP	C9H15N2O15P3	483.968534	Pyrimidine Metabolism; Amino Sugar Metabolism	-	N	18.8	1.23E+03	-	N

Table 3-S1: Details of the urine samples for LC-MS running order.

Sample Number	Sample Name	Notes
01	P-1	Pooled-1 =50ul from each sample of 12 samples of LMS group)
02	Std. Mix1	Standard Mixture
03	Std. Mix2	Standard Mixture
04	LMS 2D3	VO ₂ max of LM = 53.4
05	LMS 1D1	
06	LMS 1D3	
07	LMS 2D1	
08	LMS 5D2	
09	LMS 3D1	
10	LMS 4D2	
11	LMS 4D1	
12	LMS 3D2	
13	LMS 5D1	
14	LMS 2D2	
15	LMS 1D2	
42	P-2	Pooled-2 =50ul from each sample of 12 samples of LMS group)
16	GSS 2D3	VO ₂ max of GS = 48.3
17	GSS 1D1	
18	GSS 1D3	
19	GSS 2D1	
20	GSS 5D2	
21	GSS 3D1	
22	GSS 4D2	
23	GSS 4D1	
24	GSS 3D2	
25	GSS 5D1	
26	GSS 2D2	
27	GSS 1D2	
28	P-3	Pooled-3 =50ul from each sample of 12 samples of MWS group)
29	MWS 2D3	VO ₂ max of MW = 43
30	MWS 1D1	
31	MWS 1D3	

32	MWS 2D1	
33	MWS 5D2	
34	MWS 3D1	
35	MWS 4D2	
36	MWS 4D1	
37	MWS 3D2	
38	MWS 5D1	
39	MWS 2D2	
40	MWS 1D2	
41	P-4	Pooled-2 (1)= 50ul of each sample from 12 samples of DMS group)
43	DMS 2D3	VO ₂ max of DM = 38.2
44	DMS 1D1	
45	DMS 1D3	
46	DMS 2D1	
47	DMS 5D2	
48	DMS 3D1	
49	DMS 4D2	
50	DMS 4D1	
51	DMS 3D2	
52	DMS 5D1	
53	DMS 2D2	
54	DMS 1D2	
55	P-5	Pooled-5= 50ul of each sample from 12 samples of CMS group)
56	Std. Mix3	Standard Mixture
57	CMS 2D3	VO ₂ max of CM = 40.7
58	CMS 1D1	
59	CMS 1D3	
60	CMS 2D1	
61	CMS 5D2	
62	CMS 3D1	
63	CMS 4D2	
64	CMS 4D1	
65	CMS 3D2	
66	CMS 5D1	
67	CMS 2D2	
68	CMS 1D2	

69	P-6	Pooled-6 = 50ul of each sample from 11 samples of MCS group)
70	MCS 2D3	VO ₂ max of MC = 33.5
71	MCS 1D1	
72	MCS 1D3	
73	MCS 2D1	
74	MCS 5D2	
75	MCS 3D1	
76	MCS 4D2	
77	MCS 4D1	
78	MCS 3D2	
79	MCS 5D1	
80	MCS 2D2	
81	MCS 1D2	
82	P-7	Pooled-7= 50ul of each sample from 12 samples of JWS group
83	JWS 2D3	VO ₂ max of JW = 41.7
84	JWS 1D1	
85	JWS 1D3	
86	JWS 2D1	
87	JWS 5D2	
88	JWS 3D1	
89	JWS 4D2	
90	JWS 4D1	
91	JWS 3D2	
92	JWS 5D1	
93	JWS 2D2	
94	JWS 1D2	
95	Std. Mix4	Standard Mixture
96	P- 8	Pooled- 8= 50ul of each sample from 12 sample of CES group
97	CES 2D3	VO ₂ max of = 40
98	CES 1D1	
99	CES 1D3	
100	CES 2D1	
101	CES 5D2	
102	CES 3D1	
103	CES 4D2	
104	CES 4D1	

105	CES 3D2	
106	CES 5D1	
107	CES 2D2	
108	CES 1D2	
109	P-9	Pooled- 9= 50ul of each sample from 12 sample of MBS group
110	MBS 2D3	VO ₂ max of MB = 40.4
111	MBS 1D1	
112	MBS 1D3	
113	MBS 2D1	
114	MBS 5D2	
115	MBS 3D1	
116	MBS 4D2	
117	MBS 4D1	
118	MBS 3D2	
119	MBS 5D1	
120	MBS 2D2	
121	MBS 1D2	
122	P-10	Pooled- 10= 50ul of each sample from 12 sample of NSS group
123	NSS 2D3	VO ₂ max of NS = 47.9
124	NSS 1D1	
125	NSS 1D3	
126	NSS 3D1	
127	NSS 5D2	
128	NSS 3D2	
129	NSS 4D2	
130	NSS 4D1	
131	NSS 5D1	
132	NSS 2D2	
133	NSS 1D2	

Table 3-S2: Metabolites with the highest correlation to the OPLSDA model for D2S3 vs D2S1. Metabolites with positive p (corr) values associate with D2S1 and metabolites with negative p (corr) values associate with D2S3.

m/z	RT	Molecular Formula	Metabolite	p-Value D2S3-D2S1	Ratio D2S3/D2S1	p(corr)
904.183	14.7	C22H28F2O5	Flumethasone	0.00001	0.24	0.89
583.312	10.3	C30H48O11	Cholicacid glucuronide	0.00009	0.27	0.63
407.164	15.2	C22H29O5Cl	Beclomethasone	0.00012	0.20	0.68
331.09	10.9	C13H21N2O4PS	Butamifos	0.00015	0.48	0.78
173.092	13.3	C7H12N2O3	Glycylproline	0.00015	0.54	0.75
477.147	12.8	C17H26N4O12	Glu-Thr-Asp-Asp	0.00026	0.42	0.72
291.15	10.2	C19H20N2O	16-Epivelloimine	0.00029	0.33	0.61
461.225	9.8	C19H34N4O9	Glu-Leu-Thr-Thr	0.00035	0.24	0.67
233.068	11.9	C9H14O7	trihomocitrate	0.00038	0.51	0.71
471.218	9.1	C30H32O5	[Fv]Euchrenonea14	0.00049	0.26	0.81
173.073	12.4	C10H10N2O	Indole-3-acetamide	0.00058	0.61	0.70
375.152	4.0	C26H20N2O	XE991	0.00073	0.10	0.65
407.281	6.6	C24H40O5	[ST trihydrox] 3Alpha,7Alpha,12Alpha-trihydroxy-5Beta-cholan-24-oic acid	0.00079	0.34	0.74
118.051	12.0	C4H9NO3	L-Threonine	0.00079	0.64	0.71
281.114	11.9	C13H18N2O5	Thr-Tyr	0.00082	0.39	0.68
322.09	11.2	C11H21N3O4S2	Met-Ala-Cys	0.00106	0.27	0.65
291.114	9.7	C18H16N2O2	INF271	0.00109	0.55	0.64
220.029	11.1	C7H11NO5S	S-(3-oxo-3-carboxy-n-propyl)cysteine	0.00111	0.21	0.63
288.124	12.1	C16H19NO4	3'-Demethoxypiplartine	0.00117	0.26	0.71
377.146	13.2	C17H22N4O6	Trp-Ser-Ser	0.00122	0.29	0.71
302.136	12.6	C12H21N3O6	Nicotianamine	0.00122	0.47	0.67
413.219	4.9	C21H34O8	[FA methyl(20:2)] methyl 5-hydroperoxy-6,8,9,11-bisepidioxy-12,14-eicosadienoate	0.00126	0.59	0.64
216.099	11.8	C8H15N3O4	N-Acetyl-L-citrulline	0.00132	0.60	0.63
334.055	10.8	C9H14N5O7P	Dihydroneopterin phosphate	0.00146	0.39	0.64
172.097	10.9	C8H13NO3	N-Butyryl-L-homoserine lactone	0.00147	0.60	0.67
389.179	8.3	C25H27N2Cl	Meclizine	0.00161	0.50	0.67
148.043	14.0	C5H11NO2S	L-Methionine	0.00165	0.58	0.63
399.124	12.9	C25H20O5	[Fv methoxy, methox] (S)-2,3-Dihydro-7-methoxy-2-[2-(4-methoxyphenyl)-5-benzofuranyl]-4H-1-benzopyran-4-one	0.00166	0.45	0.63

215.104	9.3	C9H16N2O4	gamma-Glutamyl-gamma-aminobutyraldehyde	0.00180	0.64	0.68
247.129	13.4	C10H18N2O5	Glu-Val	0.00187	0.40	0.62
583.312	11.5	C30H48O11	Cholicacidglucuronide	0.00253	0.23	0.50
321.089	14.1	C10H18N4O6S	Asn-Cys-Ser	0.00282	0.39	0.59
421.171	12.0	C19H26N4O7	Ala-Phe-Ala-Asp	0.00373	0.31	0.54
449.203	10.4	C21H30N4O7	Ala-Phe-Val-Asp	0.00400	0.32	0.74
388.168	10.2	C20H24FN3O4	Balofloxacin	0.00534	0.14	0.50
379.161	11.7	C17H24N4O6	Ala-Gln-Tyr	0.00542	0.35	0.63
191.103	9.8	C7H14N2O4	meso-2,6-Diaminoheptanedioate	0.00697	0.30	0.57
214.028	9.7	C9H10ClNO3	3-Chlorotyrosine	0.00697	0.23	0.59
142.051	9.6	C6H9NO3	Vinylacetyl glycine	0.00755	0.56	0.67
301.129	14.9	C15H18N4O3	Phe-His	0.00904	0.31	0.59
254.096	14.5	C13H18ClNO2	Hydroxybupropion	0.00917	0.49	0.63
261.144	5.6	C11H20N2O5	Glu-Leu	0.01123	0.31	0.60
322.133	9.0	C13H23NO4S2	S-Glutaryldihydrolipoamid	0.01264	0.47	0.58
403.161	11.1	C19H24N4O6	Glu-Ala-Trp	0.01338	0.26	0.65
258.108	15.7	C10H17N3O5	Gly-Pro-Ser	0.02019	0.25	0.50
421.228	4.4	C20H38O7S	1,4-Bis(2-ethylhexyl) sulfosuccinate	0.02783	0.33	0.51
218.139	6.0	C10H19NO4	O-Propanoylcarnitine	0.03150	0.36	0.45
147.066	11.1	C6H12O4	[FAMethyl,hydroxy(5:0)] 3R-methyl-3,5-dihydroxy-pentanoic acid	0.03859	0.61	0.55
297.181	4.6	C13H22N5O3	diphthamide	0.04240	0.47	0.46
386.145	15.5	C18H21N5O5	benzyladenine-7-N-glucoside	0.04767	0.34	0.57
379.168	12.0	C22H24N2O4	Vomicine	0.05349	0.34	0.58
469.16	4.5	C19H26N4O10	Asp-Ser-Ser-Tyr	0.09988	0.29	0.47
434.217	7.9	C19H29N7O5	Phe-Asn-Arg	0.14187	0.38	0.51
247.14	15.0	C9H18N4O4 N2	N2-(D-1-Carboxyethyl)-L-arginine	0.00001	2.23	0.89
178.072	10.8	C7H7N5O	6-methyl-H2-pterin	0.00007	3.94	0.90
182.997	17.0	C4H8SO6	hydroxybutyric acid sulfate	0.00008	2.17	0.85
250.105	10.8	C8H15N3O6	Gly-Ser-Ser	0.00010	3.43	0.87
137.046	10.8	C5H4N4O	Hypoxanthine	0.00011	3.75	0.89
190.072	9.6	C7H13NO5	2-amino-3,7-dideoxy-D-threo-hept-6-ulosonate	0.00073	1.42	0.77
217.083	10.9	C8H14N2O5	L-Ala-L-Glu	0.00096	1.76	0.73
240.102	9.1	C15H13NO2	N-Hydroxy-2-acetamidofluorene	0.00169	3.88	0.66
140.082	8.9	C6H9N3O	L-Histidinal	0.00201	4.27	0.67

240.001	15.7	C6H11NO5S2	3-Mercaptolactate-cysteinedisulfide	0.00246	1.53	0.68
202.109	5.8	C9H18NO4	O-Acetylcarnitine	0.00260	1.76	0.69
192.067	6.0	C10H11NO3	Phenylacetyl-glycine	0.00432	1.76	0.63
172.097	13.5	C8H13NO3	N-Butyryl-L-homoserine lactone	0.00546	3.77	0.58
555.245	8.8	C28H36N4O8	Asp-Leu-Phe-Tyr	0.00753	1.48	0.70
253.093	9.2	C10H12N4O4	Deoxyinosine	0.00884	4.97	0.76
314.234	5.6	C17H33NO4	[FA (10:0)] O-decanoyl-R-carnitine	0.00975	1.56	0.65
285.083	13.1	C10H12N4O6	Xanthosine	0.01137	2.33	0.61
391.019	17.0	C18H17O5Br	[Fv hydroxy,trimethox] 3'-Bromo-6'-hydroxy-2',4,4'-trimethoxychalcone	0.01425	1.79	0.57
231.009	4.1	C3H11N3O5PS	N-Phosphohypotaurocyamine	0.01992	1.59	0.64
168.066	8.0	C8H9NO3	Pyridoxal	0.02063	5.50	0.54
541.265	9.6	C24H34N10O5	His-Leu-His-His	0.02189	1.84	0.63
269.088	11.5	C9H16O9	Inosine	0.02489	16.27	0.55
197.046	9.8	C9H10O5	3-(3,4-Dihydroxyphenyl)lactate	0.02514	1.43	0.63
498.27	6.1	C26H35N5O5	Lys-Phe-Phe-Gly	0.03237	1.75	0.61
132.066	14.2	C5H9NO3	hydroxyproline	0.03886	18.28	0.46
161.038	19.7	C7H11O2Cl	[FA (7:0)] 7-chloro-2E-heptenoic acid	0.04844	1.90	0.51
221.092	6.8	C11H12N2O3	5-Hydroxy-L-tryptophan	0.05752	2.25	0.46
450.136	4.5	C20H25N3O7S	(1R)-Hydroxy-(2R)-glutathionyl-1,2-dihydronaphthalene	0.05860	1.98	- 0.56
198.113	16.8	C10H15NO3	L-Metanephrine	0.08210	3.00	- 0.39
395.071	11.3	C12H20N4O7S2	Asp-Cys-Cys-Gly	0.09705	2.66	- 0.62
420.223	4.5	C20H29N5O5	Lys-Trp-Ser	0.11143	2.04	- 0.58
173.092	14.9	C7H12N2O3	Glycylproline	0.11562	5.58	- 0.38
170.081	12.4	C8H11NO3	Pyridoxine	0.19003	2.05	- 0.32

Table 3-S 3: Metabolites with the highest correlation to the OPLSDA model for DIS3 vs DIS1. Metabolites with positive p (corr) values associate with DIS1 and metabolites with negative p(corr) values associate with DIS3.

m/z	RT	Molecular Formula	Metabolite	p-Value D2S3-D2S1	Ratio D2S3/D2S1	p(corr)
334.126	18.0	C12H21N3O89	N4-(Acetyl-beta-D-glucosaminyl)asparagine	0.00098	19.59	0.79
277.002	11.5	C9H10SO8	trihydroxyphenylpropionic acid sulfate or isomer	0.02027	22.15	0.84
330.118	10.8	C14H19NO8	Dopamineglucuronide	0.02707	4.62	0.50
379.122	5.4	C19H24O6S	[ST methoxy,hydroxy(3:0)] 2-methoxy-3-hydroxy-estra-1,3,5(10)-trien-17-one 3-sulfate	0.01368	6.81	0.73
409.136	8.7	C17H22N4O8	Asn-Asp-Tyr	0.05651	5.74	0.58
319.045	4.2	C15H12O8	Dihydromyricetin	0.04583	2.89	0.67
367.066	15.7	C10H15N4O9P	1-(5'-Phosphoribosyl)-5-formamido-4-imidazolecarboxamide	0.00296	6.45	0.74
240.101	10.8	C15H13NO2	N-Hydroxy-2-acetamidofluorene	0.00378	3.09	0.57
346.056	11.2	C10H14N5O7P	AMP	0.06766	6.58	0.56
490.216	5.1	C19H33N5O10	Glu-Lys-Thr-Asp	0.05040	3.00	0.51
234.077	9.5	C12H11NO4	2-Hydroxy-6-oxo-(2'-aminophenyl)-hexa-2,4-dienoate	0.00034	4.54	0.80
597.366	5.0	C33H48N4O6	L-Urobilinogen	0.00696	6.71	0.69
343.118	7.9	C19H18O6	[Fv Methyl,trimethox] 3,4-Methylenedioxy-2',4',6'-trimethoxychalcone	0.01677	5.06	0.63
367.104	6.4	C17H20O9	O-Feruloylquininate	0.01823	2.41	0.70
188.003	5.1	C6H7NO4S	2-Pyridyl hydroxymethane sulfonic acid	0.00313	2.56	0.73
200.175	12.1	C10H21N3O	Diethylcarbamazine	0.01824	4.84	0.62
381.18	14.2	C22H24N2O4	Vomicine	Vomicine	0.00890	0.60
240.109	10.8	C9H13N5O3	Dihydrobiopterin	0.00080	2.72	0.76
359.204	24.0	C14H26N6O5	Pro-Ser-Arg	0.00625	4.80	0.67
302.134	16.5	C12H19N3O6	Ala-Asp-Pro	0.00152	4.57	0.80
277.003	14.4	C9H10SO8	trihydroxyphenylpropionic acid sulfate or isomer	0.06894	3.20	0.51
385.144	6.4	C13H24N2O11	Macrozamin	0.00710	4.28	0.72
298.093	8.9	C13H17NO7	aminobenzoate-β-D-glucopyranosyl ester	0.01663	2.27	0.57
218.049	4.5	C8H11NO4S	Tyramine-O-sulfate	0.02041	2.32	0.66

295.087	7.8	C12H16N4O3S	5'-methylthiotubercidin	0.02420	3.72	0.39
302.087	13.7	C12H15NO8	4-Nitrophenol-alpha-D-galactopyranoside	0.00129	2.55	0.70
261.091	4.3	C10H16N2O4S	d-biotin d-sulfoxide	0.03123	1.94	0.63
176.001	5.6	C5H5NSO4	hydroxypyridine sulfate	0.07406	2.56	0.46
381.137	5.3	C22H23ClN2O2	Loratadine	0.00094	2.69	0.73
595.35	5.1	C33H46N4O6	L-Urobilin	0.00315	2.99	0.59
275.092	10.9	C15H16O5	Lactucin	0.04030	1.91	0.54
315.159	12.9	C19H22O4	[PR] 2,3-Didehydrogibberellin A	0.00014	2.12	0.74
234.077	12.7	C12H11NO4	2-Hydroxy-6-oxo-(2'-aminophenyl)-hexa-2,4-dienoate	0.00010	2.98	0.81
270.061	11.7	C11H13NO7	hydroxypyridine glucuronide	0.09258	2.11	0.57
163.052	8.8	C7H11O2Cl	[FA (7:0)] 7-chloro-2E-heptenoic acid	0.09062	2.00	0.51
446.152	16.4	C16H25N5O10	Ala-Asp-Asp-Gln	0.04092	3.77	0.53
156.077	17.2	C6H9N3O2	L-Histidine	0.00012	3.54	0.85
161.128	23.0	C7H16N2O2	N6-Methyl-L-lysine	0.00168	2.67	0.73
593.334	5.3	C32H48O10	Debromoaplysiatoxin	0.01163	2.41	0.53
173.987	5.6	C5H5NSO4	hydroxypyridine sulfate	0.03154	2.07	0.65
594.337	5.2	C26H43N9O7	Arg-Lys-Gln-Tyr	0.01468	2.29	0.50
411.122	6.0	C20H25O7Cl	Eupachlorin	0.01506	4.31	0.62
156.077	15.8	C6H9N3O2	L-Histidine	0.00002	2.63	0.87
327.072	13.9	C14H16O9	2-Succinyl-5-enolpyruvyl-6-hydroxy-3-cyclohexene-1-carboxylate	0.04770	2.09	0.46
221.081	6.0	C12H12O4	2,6-Dioxo-6-phenylhexanoate	0.04714	1.97	0.56
273.008	5.2	C10H10SO7	ferulic acid sulfate or isomer	0.21485	1.87	0.49
154.062	15.7	C6H9N3O2	L-Histidine	0.00166	2.73	0.72
196.026	13.5	C8H7NO5	3-Hydroxy-2-methylpyridine-4,5-dicarboxylate	0.05050	2.03	0.49
399.144	16.6	C22H22O7	Deoxypodophyllotoxin	0.00169	3.17	0.76
168.03	7.8	C7H7NO4	L-2,3 Dihydrodipicolinate	0.02339	1.98	0.60
214.027	14.0	C9H10ClNO3	3-Chlorotyrosine	0.00298	2.91	0.71
156.077	19.1	C6H9N3O2	L-Histidine	0.00007	1.99	0.78
169.051	7.9	C8H10O4	3,4-Dihydroxyphenylethyleneglycol	0.01602	2.17	0.63
260.053	12.7	C6H14NO8P	D-Glucosamine 6-phosphate	0.00029	2.14	0.78
154.062	17.2	C6H9N3O2	L-Histidine	0.00222	2.35	0.70
154.063	20.4	C6H9N3O2	L-Histidine	0.00026	2.10	0.79
207.077	4.9	C10H12N2O3	L-Kynurenine	0.01873	1.58	0.54
217.018	4.3	C8H10SO5	phenylethylene glycol sulfate	0.02391	2.08	0.64
309.076	5.1	C18H12O5	[Fv Methyl(9:1)] 3',4'-Methylenedioxy-[2'',3'':7,8]furanoflavanone	0.26933	2.04	0.39

175.119	25.3	C6H14N4O2	L-Arginine	0.02416	1.83	0.56
180.089	17.1	C7H10N5O	N1-hydroxyethyladenine	0.00002	2.11	0.82
174.057	9.3	C10H9NO2	Indole-3-acetate	0.01749	1.79	0.54
215.033	14.1	C5H13O7P	2-C-Methyl-D-erythritol 4-phosphate	0.01439	2.71	0.62
241.129	14.6	C10H16N4O3	Homocarnosine	0.05667	2.67	0.46
230.997	6.9	C8H8SO6	hydroxyphenyl acetic acid sulfate or isomer	0.03176	2.29	0.59
415.094	16.0	C15H20N4O8S	O-Carbamoyl-deacetylcephalosporin C	0.01044	2.53	0.58
234.077	16.3	C12H11NO4	2-Hydroxy-6-oxo-(2'-aminophenyl)-hexa-2,4-dienoate	0.00694	1.51	0.61
208.062	14.3	C10H11NO4	N-Benzoyloxycarbonylglycine	0.00070	1.75	0.69
116.035	14.1	C4H7NO3	L-2-Amino-3-oxobutanoic acid	0.00273	1.51	0.67
357.169	15.0	C21H24O5	[Fv Trihydroxy,trimethy] 2',4',4''-Trihydroxy-3',6'',6''-trimethylpyrano[2'',3''':6'',5'] dihydrochalcone	0.03435	2.01	0.52
170.092	13.5	C7H11N3O2	N(pi)-Methyl-L-histidine	0.00040	1.69	0.74
340.154	15.6	C20H21NO4	(S)-Canadine	0.00114	1.58	0.70
114.021	14.7	C4H5NO3	Maleamate	0.02136	1.55	0.55
285.119	14.8	C11H16N4O5	Coformycin	0.00560	2.27	0.62
234.077	18.0	C12H11NO4	2-Hydroxy-6-oxo-(2'-aminophenyl)-hexa-2,4-dienoate	0.00615	1.69	0.63
128.035	16.1	C5H7NO3	L-1-Pyrroline-3-hydroxy-5-carboxylate	0.00398	1.47	0.60
323.146	22.9	C12H24N2O8	Procollagen 5-(D-galactosyloxy)-L-lysine	0.05039	2.99	0.53
386.159	12.1	C21H23NO6	Polycarpine	0.00156	1.54	0.69
180.086	17.1	C6H13NO5	D-Glucosamine	0.00479	1.61	0.61
157.061	11.9	C6H8N2O3	4-Imidazolone-5-propanoate	0.00015	1.38	0.75
249.149	12.5	C15H20O3	[PR] 1,2-Dihydrosantonin	0.28230	2.11	0.40
267.138	6.8	C18H18O2	[ST hydroxy(5:0)] 3-hydroxy-estra-1,3,5(10),6,8-pentaen-17-one	0.00244	0.48	-0.66
275.151	7.4	C14H20N4O2	N-(4-Guanidinobutyl)-4-hydroxycinnamide	0.00465	0.39	-0.61
287.196	4.7	C14H26N2O4	N-Acetyl-leucyl-leucine	0.00226	0.53	-0.68
450.176	6.5	C15H27N7O7S	Arg-Asp-Cys-Gly	0.00170	0.51	-0.71
153.031	11.3	C6H6N2O3	Imidazol-5-yl-pyruvate	0.00346	0.46	-0.64
174.087	15.0	C6H11N3O3	5-Guanidino-2-oxopentanoate	0.00038	0.53	-0.73
494.239	5.0	C25H35NO9	Ryanodine	0.00242	0.48	-0.68
262.136	5.7	C14H19N3S	Methapyrilene	0.00094	0.56	-0.72
172.097	9.0	C8H13NO3	N-Butyryl-L-homoserine lactone	0.00021	0.50	-0.74
245.113	9.2	C10H16N2O5	Glu-Pro	0.00047	0.56	-0.74

451.166	8.0	C20H28N4O6S	Ala-Cys-Pro-Tyr	0.00380	0.39	-0.63
111.009	18.5	C5H4O3	2-Furoate	0.00253	0.48	-0.64
172.073	15.0	C6H11N3O3	5-Guanidino-2-oxopentanoate	0.00020	0.45	-0.76
500.239	4.5	C19H33N9O5S	Arg-Met-Gly-His	0.00248	0.52	-0.68
538.232	5.0	C24H35N5O7S	Gln-Met-Pro-Tyr	0.00016	0.39	-0.78
237.09	8.3	C8H16N2O4S	Met-Ser	0.00581	0.52	-0.61
522.197	5.6	C18H31N7O9S	Glu-Asp-Cys-Arg	0.00234	0.40	-0.69
210.062	5.0	C7H7O3N5	uric acid acetonitrile adduct	0.00074	0.52	-0.71
422.203	7.8	C19H27N5O6	Phe-Gln-Gln	0.00230	0.53	-0.65
492.224	5.0	C18H33N7O7S	Ala-Met-Asp-Arg	0.00130	0.50	-0.70
241.012	14.9	C6H11O8P	D-myo-Inositol 1,2-cyclic phosphate	0.00031	0.57	-0.73
434.217	7.5	C23H31NO7	Mycophenolate mofetil	0.00049	0.43	-0.70
102.066	16.8	C3H7N3O	N-acetylguanidine	0.00001	0.46	-0.83
156.078	10.0	C6H10N3O2	N3-hydroxyethylcytosine	0.00034	0.52	-0.74
448.203	6.1	C17H29N5O9	Ala-Lys-Asp-Asp	0.00023	0.48	-0.76
234.134	12.9	C10H19NO5	Hydroxypropionylcarnitine	0.00219	0.52	-0.66
176.103	16.2	C6H13N3O3	L-Citrulline	0.00044	0.59	-0.77
219.134	13.7	C9H18N2O4	N2-(D-1-Carboxyethyl)-L-lysine	0.00014	0.47	-0.77
138.091	22.4	C8H11NO	Tyramine	0.00118	0.53	-0.70
290.102	4.9	C15H15NO5	Acronycidine	0.00020	0.49	-0.77
336.217	6.2	C19H29NO4	Ankorine	0.00013	0.56	-0.77
189.123	13.6	C8H16N2O3	Glycyl-leucine	0.00013	0.54	-0.77
207.114	20.0	C11H14N2O2	Phenylethylmalonamide	0.00001	0.56	-0.85
374.254	7.2	C19H35NO6	Dodecanedioylcarnitine	0.00001	0.51	-0.84
173.009	18.4	C6H6O6	cis-Aconitate	0.00267	0.40	-0.64
129.019	18.5	C5H6O4	Mesaconate	0.00237	0.42	-0.65
278.198	5.2	C14H23N5O	EHNA	0.00034	0.41	-0.78
146.081	9.8	C6H11NO3	[FA oxo,amino(6:0)] 3-oxo-5S-amino-hexanoic acid	0.00013	0.54	-0.77
493.208	8.0	C25H34O10	Glauucarubinone	0.00082	0.20	-0.56
288.171	4.7	C16H21N3O2	Zolmitriptan	0.00195	0.51	-0.68
203.139	14.6	C9H18N2O3	Leu-Ala	0.00016	0.58	-0.79
476.199	5.5	C18H29N5O10	Asn-Leu-Asp-Asp	0.00415	0.48	-0.62
258.11	15.2	C8H20NO6P	sn-glycero-3-Phosphocholine	0.00108	0.55	-0.70
500.247	4.5	C20H33N7O8	Asp-Lys-Thr-His	0.00106	0.52	-0.72
334.203	6.2	C19H29NO4	Ankorine	0.00579	0.48	-0.59
220.029	15.6	C7H11NO5S	S-(3-oxo-3-carboxy-n-propyl)cysteine	0.00138	0.53	-0.70
218.114	11.8	C8H15N3O4	N-Acetyl-L-citrulline	0.00001	0.57	-0.83
490.207	5.0	C18H31N7O7S	Arg-Asp-Cys-Pro	0.00156	0.51	-0.71
178.107	16.2	C7H15NO4	validamine	0.00060	0.56	-0.75
221.092	10.7	C11H12N2O3	5-Hydroxy-L-tryptophan	0.00066	0.52	-0.74
165.075	13.4	C6H12O5	L-Rhamnose	0.00042	0.52	-0.74
233.114	10.9	C9H16N2O5	N2-Succinyl-L-ornithine	0.00196	0.52	-0.64
288.217	6.4	C15H29NO4	L-Octanoylcarnitine	0.00161	0.54	-0.69
283.129	5.5	C13H18N2O5	Thr-Tyr	0.00135	0.49	-0.71
219.081	14.9	C8H16N2O3S	Met-Ala	0.00027	0.52	-0.72

187.108	9.8	C8H14N2O3	Ala-Pro	0.00004	0.52	-0.81
295.132	6.0	C19H18O3	(2-Butylbenzofuran-3-yl)(4-hydroxyphenyl)ketone	0.00117	0.59	-0.69
145.014	16.2	C5H6O5	2-Oxoglutarate	0.00348	0.47	-0.63
480.187	7.9	C16H29N7O8S	Arg-Asp-Cys-Ser	0.00143	0.44	-0.70
220.118	13.2	C9H17NO5	Pantothenate	0.00146	0.53	-0.69
153.066	11.9	C7H8N2O2	N1-Methyl-2-pyridone-5-carboxamide	0.00096	0.52	-0.68
257.113	9.6	C11H16N2O5	1-(beta-D-Ribofuranosyl)-1,4-dihydrnicotinamide	0.00116	0.56	-0.71
450.235	5.5	C21H31N5O6	Ala-Phe-Val-Asn	0.00007	0.45	-0.78
248.113	14.1	C10H17NO6	Linamarin	0.00032	0.51	-0.75
350.16	7.2	C18H23NO6	Riddelline	0.00378	0.52	-0.64
217.129	15.6	C8H16N4O3	N-acetyl-(L)-arginine	0.00001	0.54	0.54
247.092	11.3	C9H14N2O6	5-6-Dihydrouridine	0.00016	0.55	-0.76
368.155	13.4	C14H25NO10	N-Acetyl-6-O-L-fucosyl-D-glucosamine	0.02483	0.33	-0.51
287.148	12.1	C10H20N6O4	Asn-Arg	0.00005	0.31	-0.79
204.134	12.7	C8H17N3O3	Lys-Gly	0.00142	0.52	-0.70
118.086	14.6	C5H11NO2	L-Valine	0.00124	0.52	-0.73
403.192	5.0	C26H28O4	[Fv] Boesenbergin A	0.00029	0.51	-0.73
245.15	8.8	C11H20N2O4	N-hexenoylglutamine	0.00007	0.48	-0.83
464.192	5.4	C16H29N7O7S	Ala-Asp-Cys-Arg	0.00097	0.48	-0.73
386.255	8.3	C21H31N5O2	Buspirone	0.00015	0.41	-0.75
310.113	14.2	C11H19NO9	N-Acetylneuraminate	0.00006	0.58	-0.78
163.108	9.8	C6H14N2O3	N6-Hydroxy-L-lysine	0.00004	0.44	-0.83
346.124	14.8	C15H24NO4PS	Isofenphos	0.00081	0.53	-0.71
288.171	8.8	C16H21N3O2	Zolmitriptan	0.00010	0.46	-0.76
313.062	11.2	C10H20O7P2	[PR] Geranyl pyrophosphate	0.00019	0.33	-0.74
288.125	12.0	C16H19NO4	3'-Demethoxyiplartine	0.00067	0.27	-0.64
167.021	13.5	C5H4N4O3	Urate	0.00019	0.53	-0.76
379.163	9.3	C17H24N4O6	Ala-Gln-Tyr	0.00302	0.48	-0.64
253.143	5.2	C14H20O4	ubiquinol-1	0.00007	0.53	-0.79
253.123	7.7	C17H16O2	cis-Hinokiresinol	0.00448	0.41	-0.64
417.211	7.2	C16H30N6O7	Ala-Lys-Asn-Ser	0.00094	0.40	-0.70
341.101	14.6	C19H16O6	Psorospermin	0.00568	0.44	-0.60
175.072	12.4	C6H12N2O4	Ala-Ser	0.00056	0.54	-0.71
431.177	4.0	C17H26N4O9	Glu-Ala-Asp-Pro	0.00143	0.48	-0.70
384.274	5.7	C21H37NO5	3-Hydroxy-5, 8-tetradecadiencarnitine	0.00018	0.50	-0.76
326.087	11.1	C14H15NO8	Pancratistatin	0.00045	0.52	-0.74
230.116	13.4	C9H16N5Cl	Propazine	0.00007	0.45	-0.79
402.285	6.4	C21H39NO6	[SP] Myriocin	0.00046	0.47	-0.74
175.108	9.3	C7H14N2O3	N-Acetylorntithine	0.00016	0.57	-0.77
131.118	20.5	C6H14N2O	N-Acetylputrescine	0.00331	0.55	-0.66
120.066	12.0	C4H9NO3	L-Threonine	0.00009	0.42	-0.80

327.139	14.2	C20H19FO3	2,2,4-Trimethyl-3-(4-fluorophenyl)-2H-1-benzopyran-7-ol acetate	0.00007	0.55	-0.78
205.035	17.8	C7H10O7	2-Hydroxybutane-1,2,4-tricarboxylate	0.00138	0.49	-0.73
487.256	8.1	C25H36N4O6	Ile-Pro-Pro-Ty	0.00153	0.25	-0.68
389.182	8.6	C19H26N4O5	Phe-Gln-Pro	0.00025	0.42	-0.74
227.127	22.4	C12H18O4	[FA oxo,hydroxy(5:1/5:0)] (1S,2R)-3-oxo-2-(5'-hydroxy-2'Z-pentenyl)-cyclopentaneacetic acid	0.00840	0.53	-0.60
336.158	7.7	C13H25N3O5S	Leu-Thr-Cys	0.00430	0.55	-0.63
274.092	14.1	C12H19NO2S2	Brugine	0.00003	0.48	-0.80
216.099	11.8	C8H15N3O4	N-Acetyl-L-citrulline	0.00501	0.55	-0.62
431.197	7.5	C18H32N4O6S	Cys-Leu-Thr-Pro	0.00444	0.47	-0.62
290.089	10.2	C11H17NO8	2,7-Anhydro-alpha-N-acetylneuraminic acid	0.01615	0.41	-0.59
157.992	7.5	C5H5NO3S 3	3-pyridinesulfonate	0.01051	0.42	-0.56
472.25	4.3	C19H33N7O7	Asn-Lys-Asn-Pro	0.00001	0.45	-0.83
235.092	12.8	C8H14N2O6	Glu-Ser	0.00007	0.52	-0.80
166.05	5.1	C8H7NO3	Formylanthranilate	0.00117	0.57	-0.69
260.089	15.6	C9H15N3O6	Ala-Asp-Gly	0.01361	0.44	-0.60
330.19	5.0	C16H27NO6	Europine	0.00011	0.49	-0.77
259.092	13.7	C10H14N2O6	(1-Ribosylimidazole)-4-acetate	0.00006	0.49	-0.80
494.193	5.7	C18H31N5O9S	Asp-Met-Thr-Gln	0.00334	0.20	-0.71
231.17	13.7	C11H22N2O3	Leu-Val	0.00024	0.46	-0.77
344.182	5.0	C15H25N3O6	Leu-Asp-Pro	0.00001	0.43	-0.83
247.132	8.4	C15H18O3	[PR] alpha-Santonin	0.00003	0.46	-0.80
282.12	13.9	C11H15N5O4	1-Methyladenosine	0.00042	0.52	-0.77
420.189	5.1	C19H25N5O6	Thr-Trp-Asn	0.00007	0.44	-0.81
272.172	5.3	C11H21N5O3	Pro-Arg	0.00012	0.41	-0.78
164.074	13.3	C6H13NO2S	S-Methyl-L-methionine	0.00105	0.49	-0.72
290.088	12.5	C11H17NO8	2,7-Anhydro-alpha-N-acetylneuraminic acid	0.00080	0.50	-0.69
283.123	13.9	C20H14N2	2,3-Diphenyl-3-(2-pyridinyl)acrylonitrile	0.00045	0.51	-0.76
217.118	9.3	C9H16N2O4	gamma-Glutamyl-gamma-aminobutyraldehyde	0.00006	0.51	-0.81
170.092	10.4	C7H11N3O2	N(pi)-Methyl-L-histidine	0.00002	0.44	-0.83
512.287	5.0	C27H37N5O5	Ala-Lys-Phe-Phe	0.00004	0.41	-0.82
360.24	5.2	C19H29N5O2	Loxidine	0.00237	0.57	-0.66
244.154	8.8	C12H21NO4	Tiglylcarnitine	0.00004	0.43	-0.82
221.096	12.9	C8H16N2O3S	Met-Ala	0.00294	0.52	-0.66
462.199	6.4	C21H27N5O7	Ala-Trp-Ala-Asp	0.00014	0.42	-0.81
312.13	9.2	C12H17N5O5	1-7-Dimethylguanosine	0.00255	0.56	-0.66
206.102	15.9	C8H15NO5	N-Acetyl-D-fucosamine	0.00054	0.45	-0.75
450.23	5.0	C16H31N7O8	Arg-Thr-Ser-Ser	0.00001	0.46	-0.84

261.145	8.9	C11H20N2O5	Glu-Leu	0.00006	0.43	-0.82
294.1	13.8	C14H16N3O2C 	Triadimefon	0.00410	0.48	-0.61
184.061	5.1	C8H9NO4	4-Pyridoxate	0.00054	0.53	-0.73
245.149	7.3	C11H20N2O4	N-hexenoylglutamine	0.00080	0.51	-0.71
232.129	10.9	C9H17N3O4	Ala-Ala-Ala	0.00077	0.46	-0.70
320.062	20.4	C11H15NO10	beta-Citryl-L-glutamic acid	0.14503	0.52	-0.57
188.057	14.9	C7H11NO5	N-Acetyl-L-glutamate	0.00005	0.40	-0.78
333.115	11.1	C13H21N4O2C 	Tos-Arg-CH2Cl	0.00362	0.46	-0.62
333.105	7.8	C11H18N4O8	Asn-Asp-Ser	0.00723	0.50	-0.58
526.265	5.5	C27H35N5O6	Asn-Phe-Phe-Val	0.00549	0.53	-0.62
357.213	14.3	C16H28N4O5	Leu-Gln-Pro	0.00013	0.47	-0.77
222.09	15.7	C8H16NO4P	D,L-cyclohexanephosphinothricin	0.00097	0.55	-0.69
392.155	12.5	C16H25NO10	Proacaciberin	0.00015	0.39	-0.78
234.145	9.3	C9H19N3O4	Lys-Ser	0.00008	0.45	0.45
296.136	17.8	C12H17N5O4	N6,N6-Dimethyladenosine	0.00195	0.49	-0.69
530.333	6.3	C28H43N5O5	Ile-Leu-Trp-Val	0.00106	0.50	-0.70
192.106	17.8	C8H17NO2S	trihomomethionine	0.00549	0.48	-0.60
478.192	9.8	C21H27N5O8	Ala-Trp-Asp-Ser	0.00201	0.34	-0.64
531.336	6.3	C21H42N10O6	Arg-Leu-Ser-Arg	0.00055	0.44	-0.73
400.27	6.3	C21H39NO6	[SP] Myriocin	0.00400	0.39	-0.60
790.56	3.8	C42H80NO10P	PS(18:0/18:1(9Z))	0.00432	0.53	-0.63
331.175	11.7	C16H26O7	8-Epiiridodial glucoside	0.00030	0.42	-0.73
220.12	14.1	C10H15N5O	Dihydrozeatin	0.00146	0.49	-0.66
271.165	5.2	C13H22N2O4	N-octadienoylglutamine	0.00001	0.44	-0.86
229.155	10.7	C11H20N2O3	Leu-Pro	0.00017	0.48	-0.79
258.17	8.1	C13H23NO4	2-Hexenoylcarnitine	0.00175	0.49	-0.68
237.077	10.8	C12H14O5	3-4-5-Trimethoxycinnamicacid	0.00069	0.44	-0.69
288.121	13.8	C11H19N3O6	Pro-Ser-Ser	0.00010	0.30	-0.72
474.231	4.5	C18H31N7O8	Ala-Gln-Gln-Gln	0.00002	0.44	-0.83
462.233	9.2	C22H31N5O6	Ala-Phe-Gln-Pro	0.00009	0.45	-0.81
218.156	13.2	C11H23NOS	Butylate	0.00029	0.51	-0.75
295.165	4.8	C13H22N5O3	diphthamide	0.00239	0.52	-0.64
217.155	13.2	C10H20N2O3	Val-Val	0.00009	0.45	-0.82
330.227	6.8	C17H31NO5	6-Keto-decanoylcarnitine	0.00003	0.45	-0.83
358.197	10.8	C16H27N3O6	Glu-Ile-Pro	0.00010	0.19	-0.76
199.083	11.2	C7H10N4O3	5-Acetylamino-6-amino-3-methyluracil	0.00001	0.48	-0.84
227.103	13.6	C10H16N2O4	(S)-ATPA	0.00063	0.44	-0.72
216.087	14.2	C9H13NO5	Succinyl proline	0.00173	0.40	-0.69
220.029	11.1	C7H11NO5S	S-(3-oxo-3-carboxy-n-propyl)cysteine	0.00024	0.23	-0.75
203.139	13.5	C9H18N2O3	Leu-Ala	0.00186	0.49	-0.70
261.122	15.1	C14H16N2O3	Maculosin	0.00056	0.37	-0.71
304.129	8.5	C15H17N3O4	indole-3-acetyl-glutamine	0.00098	0.49	-0.71

233.046	11.2	C12H10O5	2-Hydroxy-6-oxo-6-(2-hydroxyphenyl)-hexa-2,4-dienoate	0.00573	0.36	-0.58
262.038	16.0	C9H11NSO6	tyrosine sulfate	0.00029	0.46	-0.78
316.212	7.2	C16H29NO5	Butoctamide hydrogen succinate	0.00007	0.43	-0.81
174.041	15.3	C6H9NO5	[FA amino,oxo(6:0/2:0)] 2-amino-3-oxo-hexanedioic acid	0.00130	0.50	-0.69
261.138	12.8	C18H16N2	N,N'-Diphenyl-p-phenylenediamine	0.00049	0.51	-0.70
201.16	16.3	C10H20N2O2	dimethylsuberimidate	0.00075	0.43	-0.73
303.083	17.4	C11H16N2O8	N-Acetyl-aspartyl-glutamate	0.00514	0.38	-0.61
412.168	6.4	C22H25N3O3S	Ro 18-5364	0.00005	0.45	-0.82
255.097	24.5	C11H14N2O5	N-Ribosylnicotinamide	0.00083	0.46	-0.74
116.107	16.7	C6H13NO	Trimethylaminoacetone	0.00110	0.43	-0.71
188.056	13.9	C7H11NO5	N-Acetyl-L-glutamate	0.00155	0.52	-0.67
266.139	8.7	C14H19NO4	N(alpha)-Benzyloxycarbonyl-L-leucine	0.00026	0.42	-0.77
229.155	13.8	C11H20N2O3	Leu-Pro	0.00027	0.45	-0.78
724.528	4.0	C41H74NO7P	PE(18:3(6Z,9Z,12Z)/P-18:1(11Z))	0.00118	0.46	-0.70
279.064	16.0	C17H10O4	[Fv Hydrox] 4-Hydroxyfurano[2'',3'':6,7]auro ne	0.00028	0.44	0.44
475.247	7.0	C30H34O5	[Fv] Poinsettifolin B	0.00006	0.52	-0.79
412.23	7.4	C17H29N7O5	Lys-Gln-His	0.00019	0.20	-0.67
289.151	10.7	C11H20N4O5	Ala-Ala-Gln	0.00005	0.37	-0.82
484.31	4.4	C26H45NO5S	[ST hydrox] N-(3alpha-hydroxy-5beta-cholan-24-oyl)-taurine	0.00771	0.53	-0.60
242.066	19.5	C10H11NO6	N-(2,3-Dihydroxybenzoyl)-L-serine	0.00005	0.20	-0.82
228.103	14.6	C14H15NO2	thyronamine	0.00226	0.45	-0.66
301.18	8.3	C19H24O3	19-Oxoandrost-4-ene-3,17-dione	0.00001	0.39	-0.82
386.255	5.3	C21H31N5O2	Buspirone	0.00006	0.41	-0.82
296.091	16.0	C9H17N3O6S	Cys-Ser-Ser	0.00022	0.42	-0.80
221.081	11.4	C12H14O4	[FA (12:4/2:0)] 2E,4E,8E,10E-Dodecatetraenedioic acid	0.00116	0.44	-0.69
204.052	15.0	C8H15NOS2	Lipoamide	0.00189	0.46	-0.67
421.191	5.2	C20H28N4O4S	Leu-Trp-Cys	0.00013	0.30	-0.86
423.201	5.9	C22H30O8	Valtratum	0.00004	0.30	-0.90
230.186	16.2	C11H23N3O2	N1,N8-diacetylspermidine	0.00158	0.43	-0.70
402.198	15.0	C16H27N5O7	Ala-Gln-Pro-Ser	0.00014	0.24	-0.75
189.076	14.8	C8H14O5	(R)-3-((R)-3-Hydroxybutanoyloxy)butanoate	0.00044	0.46	-0.73
321.161	8.8	C19H25O2Cl	11beta-Chloromethylestradiol	0.00007	0.38	-0.82

506.296	4.8	C25H39N5O6	Asn-Leu-Leu-Phe	0.00008	0.32	-0.81
225.088	5.1	C10H12N2O4	3-Hydroxy-L-kynurenine	0.00001	0.36	-0.85
418.28	8.2	C21H39NO7	[SP amino, trihydroxy, hydroxy, methyl, oxo(20:0)] 2S-amino-3R,4R,5S trihydroxy-2-(hydroxymethyl)-14-oxo-eicos-6E-enoic acid	0.00001	0.31	-0.84
244.058	15.8	C8H11N3O6	6-aza-uridine	0.00037	0.16	-0.76
676.32	5.0	C33H41N9O7	Glu-Trp-Trp-Arg	0.00425	0.48	-0.63
504.282	4.6	C25H37N5O6	Gln-Leu-Phe-Pro	0.00001	0.30	-0.88
399.123	15.6	C25H20O5	[Fv methoxy, methox] (S)-2,3-Dihydro-7-methoxy-2-[2-(4-methoxyphenyl)-5-benzofuranyl]-4H-1-benzopyran-4-one	0.10096	0.42	-0.62
233.124	11.9	C8H16N4O4	(3R)-hydroxy-N-acetyl-(L)-arginine	0.00012	0.25	-0.80
454.256	9.1	C20H40NO8P	[PC (6:0/6:0)] 1,2-dihexanoyl-sn-glycero-3-phosphocholine	0.00237	0.21	-0.72
472.209	11.0	C17H29N9O5S	Arg-Cys-Gly-His	0.00031	0.22	-0.68
290.16	13.0	C13H23NO6	3-Methylglutaryl carnitine	0.00007	0.28	-0.83
514.265	8.3	C26H35N5O6	Lys-Phe-Gly-Tyr	0.00005	0.28	-0.85
384.122	15.2	C16H21N3O6S	Phe-Asp-Cys	0.00001	0.28	-0.85
330.165	7.5	C14H23N3O6	Val-Asp-Pro	0.00013	0.32	-0.87
517.321	4.6	C20H40N10O6	Arg-Val-Ser-Arg	0.00012	0.31	-0.81
516.317	4.6	C27H41N5O5	Ile-Trp-Val-Val	0.00009	0.31	-0.86
478.277	4.7	C22H35N7O5	Arg-Phe-Val-Gly	0.00014	0.30	-0.82
466.251	8.2	C19H31N9O5	Arg-Gly-Pro-His	0.00222	0.24	-0.63
376.193	13.3	C13H25N7O6	Asn-Ser-Arg	0.00139	0.18	-0.70
206.102	14.2	C8H15NO5	N-Acetyl-D-fucosamine	0.00007	0.24	-0.83
260.067	8.9	C10H14NO5P	p-Nitrophenyl-O-ethyl ethylphosphonate	0.00001	0.22	-0.91
242.066	14.1	C10H11NO6	N-(2,3-Dihydroxybenzoyl)-L-serine	0.00374	0.28	-0.62
496.276	8.8	C23H37N5O7	Lys-Phe-Thr-Thr	0.00082	0.12	-0.59
398.289	6.0	C22H39NO5	[FA trihydroxy(2:0)] N-(9S,11R,15S-trihydroxy-5Z,13E-prostadienoyl)-ethanolamine	0.00046	0.24	-0.79
424.183	14.7	C18H25N5O7	Asn-Gln-Tyr	0.00239	0.16	-0.62
506.194	5.1	C19H33N5O9S	Asp-Lys-Met-Asp	0.03757	0.30	-0.56
167.038	12.6	C5H12SO4	dihydroxypentenyl sulfate	0.00001	0.30	-0.78
504.266	8.9	C21H37N5O9	Glu-Leu-Lys-Asp	0.00037	0.28	-0.84
328.161	11.0	C13H21N5O5	Thr-Ala-His	0.00036	0.26	-0.62
260.115	13.7	C11H19NO6	Lotaustralin	0.00379	0.29	-0.71
327.073	17.2	C14H16O9	2-Succinyl-5-enolpyruvyl-6-hydroxy-3-cyclohexene-1-carboxylate	0.00157	0.30	-0.66

334.182	5.0	C22H25NO2	Lobelanine	0.02840	0.31	-0.57
257.165	5.3	C16H20N2O	Chanoclavine-I	0.00100	0.23	-0.72
305.045	13.2	C18H10O5	[Fv Methyl] 3',4'-Methylenedioxyfurano [2'',3'':6,7]aurone	0.00457	0.26	-0.71
357.083	18.8	C15H18O10	dihydroxyphenylpropionic acid glucuronide	0.00606	0.35	-0.68
320.092	12.0	C11H19N3O6S	gamma-L-Glutamyl-L-cysteinyl-beta-alanine	0.00142	0.29	-0.69
490.265	5.6	C24H35N5O6	Ala-Leu-Thr-Trp	0.00036	0.23	-0.76
784.586	4.1	C44H82NO8P	PC(18:2(9Z,12Z)/18:1(9Z))	0.00384	0.31	-0.65
336.164	14.5	C14H25NO8	validoxylamine A	0.00336	0.15	-0.73
293.087	15.8	C11H18O9	Tuliposide B	0.00635	0.28	-0.59
333.076	17.3	C20H14O5	19-Hydroxy-8-O-methyltetrangulol	0.00684	0.09	-0.58
283.059	21.2	C16H10O5	[Fv Methyl,hydrox] 4,5-Methylenedioxy-6-hydroxyaurone	0.01252	0.28	-0.56
554.296	5.2	C29H39N5O6	Gln-Leu-Phe-Phe	0.00302	0.25	-0.77
310.071	16.0	C17H11NO5	N-(6-Oxo-6H-dibenzo[b,d]pyran-3-yl)maleamic acid	0.00037	0.26	-0.84
328.115	12.1	C11H22NO8P	[PC acety] 1-acetyl-2-formyl-sn-glycero-3-phosphocholine	0.00044	0.15	-0.71
260.078	17.6	C10H15NO7	Hymexazol O-glucoside	0.00095	0.29	-0.70
534.314	5.7	C24H39N9O5	His-Leu-Lys-His	0.00276	0.25	-0.78
281.106	13.5	C11H20O6S	isopropyl 6-O-acetyl-β-D-thiogalactopyranoside	0.00005	0.18	-0.77
454.139	4.1	C18H25N5O7S	Asn-Cys-Gly-Tyr	0.00801	0.22	0.22
219.061	12.5	C7H12N2O6	Asp-Ser	0.00010	0.22	-0.74
556.313	5.1	C29H41N5O6	Lys-Phe-Val-Tyr	0.00018	0.26	-0.88
788.618	4.1	C44H86NO8P	[PC (18:0/18:1)] 1-octadecanoyl-2-(9Z-octadecenoyl)-sn-glycero-3-phosphocholine	0.00326	0.22	-0.65
362.15	12.1	C13H25N5O5S	Lys-Asn-Cys	0.00181	0.18	-0.77
167.036	12.8	C8H8O4	[PK] Orsellinic acid	0.00081	0.28	-0.74
276.017	15.9	C9H9NSO7	dihydrodopachrome sulfate	0.00364	0.16	-0.56
338.144	14.7	C13H23NO9	Streptobiosamine	0.00018	0.10	-0.54
237.079	13.7	C9H16O5S	2-(4'-methylthio)butylmalate	0.00393	0.15	0.15
243.1	4.0	C10H16N2O5	Glu-Pro	0.06619	0.34	-0.58
501.307	4.6	C26H44O9	Mupirocin	0.00176	0.30	-0.65
309.16	7.3	C19H22N2O2	Sarpagine	0.05433	0.35	-0.67
259.098	4.3	C15H16O4	[PR] Hemigossypol	0.01189	0.31	-0.65
583.312	11.5	C30H48O11	Cholicacidglucuronide	0.00590	0.17	-0.56

Table 4-S1: Summary of brain sample details: C=Control, D=Depression, S=Schizophrenic, B=Bipolar, DI=Diabetic. M=male and F=female.

Samples ID	Pathology	Brain section	Age (Year)	Sex	Year Of Collection
B1	Combined effects of chronic alcoholism and lithium use.	Frontal convexity and frontal parasagittal	57	F	2005
B2	Metastatic carcinoma of the breast.	Frontal convexity and frontal parasagittal	49	F	2010
B3	Suspension by ligature	Frontal convexity and frontal parasagittal	41	F	2007
B4	Hypertensive heart disease	Frontal convexity and frontal parasagittal	42	F	2006
B5	Suspension by a ligature.	Frontal convexity and frontal parasagittal	39	F	2011
B6	Bronchopneumonia.	Frontal convexity and frontal parasagittal	48	M	2011
C1	Pulmonary embolism. Deep vein thrombosis.	Frontal convexity and frontal parasagittal	70	M	2008
C2	Bilateral pulmonary embolism. Deep vein thrombosis. Combined effects of hypertensive heart disease and ischaemic heart	Frontal convexity and frontal parasagittal	22	M	2008
C3	Ischaemic heart disease.	Frontal convexity and frontal parasagittal	50	M	2010
C4	Sudden cardiac death.	Frontal convexity and frontal parasagittal	43	M	2010
C5	NA	Frontal convexity and frontal parasagittal	26	M	2009
C6	Multiple injuries	Frontal convexity and frontal parasagittal	46	M	2009

C7	NA	Frontal convexity and frontal parasagittal	39	M	2010
C8	Peritonitis. Bowel infarction.	Frontal convexity and frontal parasagittal	50	F	2011
C9	Ischaemic heart disease. Coronary artery atherosclerosis.	Frontal convexity and frontal parasagittal	43	M	2010
C10	NA	Frontal convexity and frontal parasagittal	38	M	2010
C11	Haemopericardium. Ruptured myocardial infarction. Coronary artery atherosclerosis. Hypertensive	Frontal convexity and frontal parasagittal	60	F	2009
C12	Bronchial asthma. Pulmonary congestion.	Frontal parasagittal	42	F	2011
C13	Ischaemic heart disease. Coronary artery atherosclerosis.	Frontal convexity and frontal parasagittal	65	M	2009
C14	Pulmonary thromboembolism. Deep vein thrombosis. Rupture of Achilles tendon.	Frontal convexity and frontal parasagittal	40	M	2010
C15	Ischaemic heart disease. Coronary artery atherosclerosis.	Frontal convexity and frontal parasagittal	74	M	2010
C16	Ischaemic heart disease. Coronary artery thrombosis. Coronary artery atherosclerosis.	Frontal convexity and frontal parasagittal	67	M	2009
C17	Myocardial re-infarction. Previous myocardial infarcts. Coronary atherosclerosis. Hypertensive heart disease.	Frontal convexity and frontal parasagittal	48	M	2010
C18	Ischaemic heart disease. Coronary artery atherosclerosis.	Frontal convexity and frontal parasagittal	53	M	2006
C19	NA	Frontal convexity and frontal parasagittal	26	M	2009
C20	Cardiomegaly. Ischaemic heart disease.	Frontal convexity and frontal parasagittal	36	M	2010

C21	NA	Frontal convexity and frontal parasagittal	39	M	2010
D1	Suspension by a ligature.	Frontal convexity and frontal parasagittal	53	M	2008
D2	Acute pulmonary oedema.	Frontal convexity and frontal parasagittal	24	M	2005
D3	Suspension by ligature	Frontal convexity and frontal parasagittal	24	F	2008
D4	Pulmonary embolism. Deep vein thrombosis.	Frontal convexity and frontal parasagittal	74	M	2011
D5	Suspension by a ligature.	Frontal convexity and frontal parasagittal	20	F	2008
D6	Suspension by a ligature.	Frontal convexity and frontal parasagittal	32	M	2009
D7	Pulmonary thromboembolism.	Frontal convexity and frontal parasagittal	57	F	2008
DI1	Diabetic ketoacidosis and morphine toxicity. Ischaemic heart disease.	Frontal convexity and frontal parasagittal	65	M	2010
DI2	Ischaemic heart disease. Coronary artery atherosclerosis. Diabetes mellitus.	Frontal convexity and frontal parasagittal	46	M	2008
DI3	Ischaemic & hypertensive heart disease. Type 1 diabetes. Liver cirrhosis.	Frontal convexity and frontal parasagittal	69	M	2010
DI4	Hypoglycaemia.	Frontal convexity and frontal parasagittal	38	M	2008
DI5	Combined effects of hypertensive heart disease and ischaemic heart disease. Diabetes (Type 1).	Frontal convexity and frontal parasagittal	45	M	2008
DI6	Hypertensive heart disease. Metastatic testicular tumour. COPD.	Frontal convexity and frontal parasagittal	38	M	2007
DI7	Hypoglycaemia.	Frontal convexity and frontal parasagittal	38	M	2008

DI8	Hyperglycaemic coma.	Frontal convexity and frontal parasagittal	20	M	2006
S1	Suspension by a ligature.	Frontal convexity and frontal parasagittal	25	M	2012
S2	Intra-cerebral haemorrhage. Ruptured intra-cerebral artery. Hypertension	Frontal convexity and frontal parasagittal	40	F	2009
S3	Acute combined morphine, methadone, diazepam and alcohol toxicity.	Frontal convexity and frontal parasagittal	50	M	2008
S4	Ischaemic heart disease. Severe coronary artery disease. Atherosclerosis. COPD. MS	Frontal convexity and frontal parasagittal	70	M	2007
S5	Pulmonary thromboembolism.	Frontal convexity and frontal parasagittal	42	M	2005
S6	Heart disease.	Frontal convexity and frontal parasagittal	25	M	2012
S7	Suspension by ligature.	Frontal convexity and frontal parasagittal	42	M	2009
S8	Unascertained pending laboratory studies.	Frontal convexity and frontal parasagittal	36	M	2011
S9	Hypertensive heart disease. Chronic obstructive pulmonary disease.	Frontal convexity and frontal parasagittal	69	M	2009
S10	Hypertensive heart disease. Hypertension.	Frontal convexity and frontal parasagittal	44	M	2006
S11	External asphyxia by inhalation of helium.	Frontal convexity and frontal parasagittal	41	M	2008

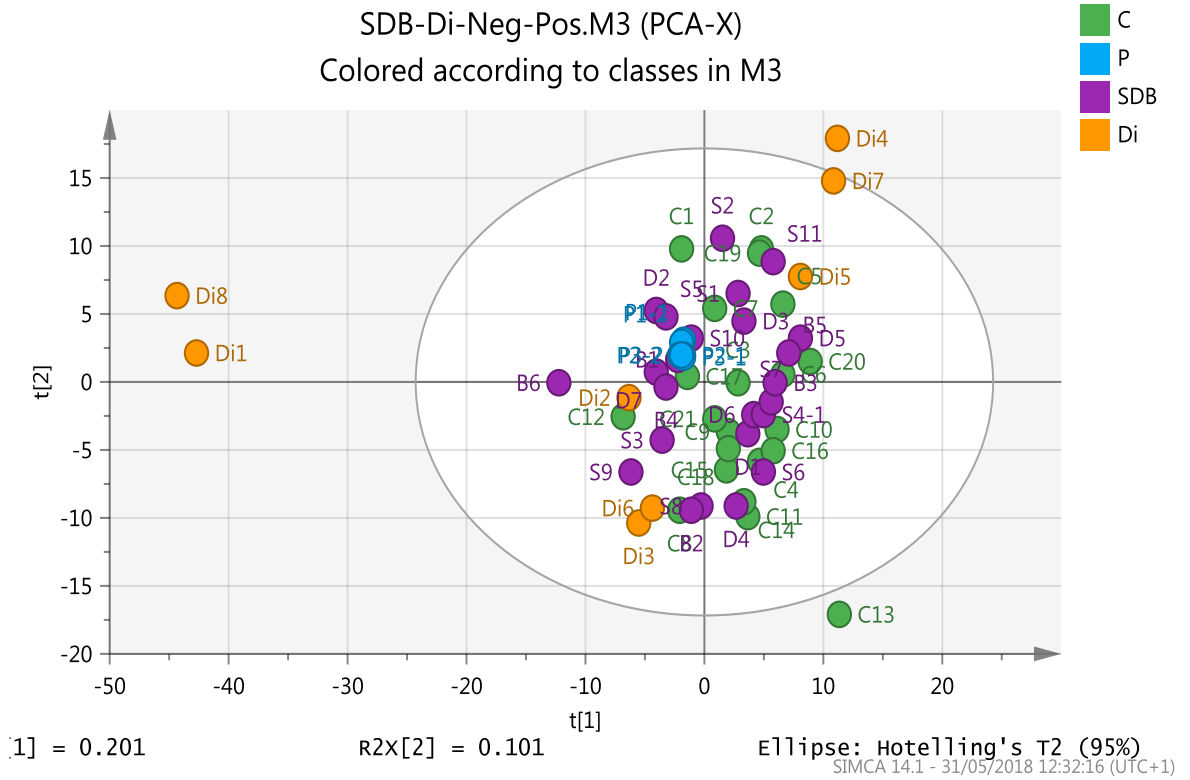


Figure 4-S1: PCA plot (R^2X (cum) 0.385, Q^2 (cum) 0.122, three components) based on 455 metabolites from positive and negative ion modes for control, SDB and DI samples produced on ZICHILIC column. Three of the DI samples (Di1, 4 and 8) lay outside of the ellipse and were omitted from the model. P = pooled sample used to check instrument stability over time. In this figure, the data produced from the analysis of the polar extracts on the ZICHILIC column were not satisfactory for producing separation in the sample sets.

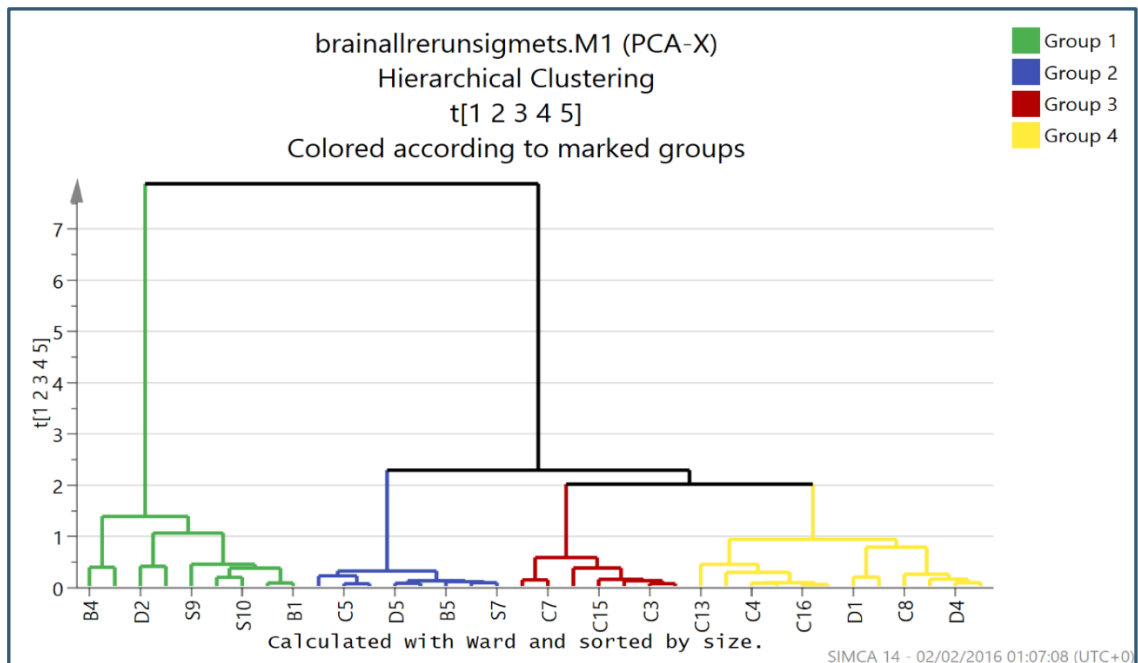


Figure 4-S2: HCA plot corresponding to figure 4-7.

Table 4-S2: Summary of univariate differences to extract the important metabolites with a *P* value < 0.05 between control and SDBDI brain samples. * Indicates that the retention time matches that of an authentic standard thus identification of MSI level 1. Application of the Benjamini-Hochberg procedure with a *Q* value of 0.1 indicates that the critical threshold for a regarding a *P* value as being significant is >0.05.

ID	M/Z	RT	Molecular Formula	Metabolite Name	P-value C and SDBDI	Ratio C/SD BDI
Neurotransmitter metabolism						
4191	146.0924	15.6	C5H11N3O2	4-Guanidinobutanoate	0.0002	0.714
4139	104.0706	15.9	C4H9NO2	4-Aminobutanoate*	0.005	0.854
767	248.0238	9.1	C8H11NO6S	Norepinephrinesulfate	0.008	0.489
776	248.0238	10.8	C8H11NO6S	Norepinephrinesulfate	0.01	0.526
25	164.072	10.4	C9H11NO2	Phenylalanine*	0.005	1.312
3337	260.0237	15.6	C9H11NSO6	tyrosine sulfate	0.009	1.319
50	180.0669	13.4	C9H11NO3	Tyrosine*	0.017	1.228
368	252.0882	8.1	C12H15NO5	N-Acetylvanilalanine	0.017	1.455
89	146.0461	11	C5H9NO4	Glutamate*	0.021	1.127
6505	189.087	10.9	C7H12N2O4	N-Acetylglutamine	0.045	1.233
67	203.083	12	C11H12N2O2	Tryptophan*	0.025	1.205
4366	161.1073	10.4	C10H12N2	Tryptamine	0.03	1.259
4307	305.0978	17.2	C11H16N2O8	N-Acetyl-aspartyl-glutamate*	0.029	0.489
2248	207.0778	9.4	C10H12N2O3	Kynurenine*	0.01	1.436
6253	165.1023	6.6	C9H12N2O	Kynuramine	0.048	1.462
Neutral lipophilic amino acids and metabolites						
20	116.0718	12.9	C5H11NO2	L-Valine*	0.0008	1.358
48	114.0561	13.2	C5H9NO2	L-Proline*	0.002	1.341
46	148.044	11.8	C5H11NO2S	L-Methionine*	0.004	1.297
11	130.0875	11.2	C6H13NO2	L-Leucine/isoleucine*	0.004	1.344
7122	174.1125	7.1	C8H15NO3	N-Acetyl-L-leucine	0.017	2.314
6004	204.0867	14.1	C8H13NO5	N2-Acetyl-L-aminoadipate	0.003	0.772
Polar amino acids						
2284	104.0354	16.1	C3H7NO3	L-Serine*	0.021	1.439
1034	118.0511	14.8	C4H9NO3	L-Threonine*	0.014	1.523
4160	90.05499	15.2	C3H7NO2	Sarcosine*	0.023	1.093
2299	231.099	16.8	C9H16N2O5	N2-Succinyl-L-ornithine	0.017	0.414
Sugar metabolism						
172	209.067	14.4	C7H14O7	Sedoheptulose*	0.0006	1.741
200	195.0513	14.4	C6H12O7	Gluconic/gulonic acid	0.001	2.203
154	121.0507	12.1	C4H10O4	Erythritol/threitol	0.001	1.574
266	215.0332	13.7	C6H11O6Cl	hexose chloride adduct	0.002	2.186
85	181.072	14.3	C6H14O6	Sorbitol/mannitol/adonitol/dulcitol	0.002	1.988
57	241.0123	17.4	C6H11O8P	D-myo-Inositol 1,2-cyclic phosphate	0.006	0.58
160	421.0761	17.4	C12H23O14P	Trehalose phosphate	0.009	0.623
169	209.0306	16	C6H10O8	Glucarate/galactarate	0.013	1.312
90	151.0614	13.2	C5H12O5	Xylitol/ribitol/arabinitol	0.017	1.144
1896	341.1095	15.6	C12H22O11	Sucrose	0.026	0.601
42	273.0385	15.7	C7H15O9P	1-Deoxy-D-altro-heptulose 7-phosphate	0.002	0.587
3327	177.0406	15.6	C6H10O6	D-Glucono-1,5-lactone	0.049	2.745

Purine and Pyrimidine Metabolism						
2485	347.0404	15.9	C10H13N4O8P	IMP*	0.051	0.678
4138	264.1094	11.4	C11H15N5O3	N6-Methyl-2'-deoxyadenosine	0.041	1.48
4221	284.0988	13	C10H13N5O5	Guanosine*	0.03	0.773
4152	269.0879	11.3	C9H16O9	Inosine*	0.019	0.804
192	167.0213	13	C5H4N4O3	Urate*	0.027	1.555
4480	152.0566	12.8	C5H5N5O	Guanine	0.026	0.702
596	113.0358	7.8	C4H6N2O2	5,6-Dihydrouracil	0.009	1.474
2167	245.0782	10.4	C9H14N2O6	5-6-Dihydrouridine	0.009	1.442
251	255.0991	9.4	C11H16N2O5	Methyluridine	0.008	1.399
4997	286.1032	8.5	C11H15N3O6	N4-Acetylcytidine	0.03	1.436
Amino sugar metabolism						
265	290.0887	13.6	C11H17NO8	Anhydro-alpha-N-acetylneuraminic acid	0.0005	0.77
1001	204.088	11.4	C8H15NO5	N-Acetyl-D-fucosamine	0.042	1.503
600	220.083	12.3	C8H15NO6	N-Acetyl-D-glucosamine	0.0005	1.244
3228	178.0724	12.9	C6H13NO5	D-Glucosamine	0.0008	1.845
7702	221.1132	14.1	C8H16N2O5	N-Acetyl-beta-D-glucosaminylamine	0.046	0.823
4642	260.0528	15.8	C6H14NO8P	D-Glucosamine 6-phosphate	0.032	1.566
Glycolysis and Krebs Cycle						
273	103.0038	16.1	C3H4O4	Malonate*	0.007	1.298
183	173.0094	12.1	C6H6O6	cis-Aconitate isomer	0.011	1.393
5302	277.0311	12.6	C6H13O10P	6-Phospho-D-gluconate isomer	0.015	0.256
225	173.0093	18.3	C6H6O6	cis-Aconitate*	0.007	0.644
3601	145.0144	6.3	C5H6O5	2-Oxoglutarate isomer	0.019	3.084
Carnitines						
122	202.1089	5.5	C9H18NO4	O-Acetylcarnitine isomer	0.007	1.486
7137	442.3526	5.1	C25H47NO5	3-Hydroxy-11Z-octadecenoylcarnitine	0.003	0.448
5789	290.1596	12.5	C13H23NO6	3-Methylglutarylcarnitine	0.011	0.684
281	368.2813	4	C21H39NO4	cis-5-Tetradecenoylcarnitine	0.017	0.493
957	202.1089	11.4	C9H18NO4	O-Acetylcarnitine*	0.041	1.361
5741	330.2637	4.2	C18H35NO4	undecanoylcarnitine	0.047	1.903
Glycerolipid metabolism						
1233	885.5504	3.9	C47H83O13P	[PI (18:0/20:4)] 1-octadecanoyl-2-(5Z,8Z,11Z,14Z-eicosatetraenoyl)-sn-glycero-3-phospho-(1'-myo-inositol)	0.001	1.714
6999	820.6219	4.1	C48H86NO7P	PC(22:4(7Z,10Z,13Z,16Z)/P-18:1(11Z))	0.04	0.645
4532	744.5905	4.3	C42H82NO7P	1-Hexadecanoyl-2-(9Z-octadecenoyl)-sn-glycero-3-phosphocholine	0.006	0.561
4229	786.6012	4.2	C44H84NO8P	[PC (18:1/18:1)] 1-(9Z-octadecenoyl)-2-(9Z-octadecenoyl)-sn-glycero-3-phosphocholine	0.008	0.87
7001	734.5701	4.3	C40H80NO8P	[PC (16:0/16:0)] 1-hexadecanoyl-2-hexadecanoyl-sn-glycero-3-phosphocholine	0.0009	1.327
4555	706.5384	4.3	C38H76NO8P	[PC (15:0/15:0)] 1,2-dipentadecanoyl-sn-glycero-3-phosphocholine	0.001	1.239

337	597.3056	4.5	C27H51O12P	[PI (18:0)] 1-(9Z-octadecenoyl)-sn-glycero-3-phospho-(1'-myo-inositol)	0.008	0.768
6550	720.5552	4.4	C39H78NO8P	[PC (15:0/16:0)] 1-pentadecanoyl-2-hexadecanoyl-sn-glycero-3-phosphocholine	0.012	1.507
4599	796.5856	4.1	C45H82NO8P	PE(18:0/22:4(7Z,10Z,13Z,16Z))	0.018	1.13
69	509.2892	4	C24H47O9P	[PG (18:0)] 1-(9E-octadecenoyl)-sn-glycero-3-phospho-(1'-sn-glycerol)	0.024	0.804
4554	511.3032	4	C24H47O9P	[PG (18:0)] 1-(9E-octadecenoyl)-sn-glycero-3-phospho-(1'-sn-glycerol)	0.032	0.817
4533	770.6065	4.2	C44H84NO7P	PC(18:1(11Z)/P-18:1(11Z))	0.037	0.513
4993	536.3348	4.4	C26H50NO8P	[PC acetyl(16:0)] 1-(9Z-hexadecenoyl)-2-acetyl-sn-glycero-3-phosphocholine	0.043	0.585
377	483.2738	4	C22H45O9P	[PG (16:0)] 1-hexadecanoyl-sn-glycero-3-phospho-(1'-sn-glycerol)	0.048	0.809
4744	258.11	14.9	C8H20NO6P	sn-glycero-3-Phosphocholine	0.042	1.606
4471	247.0576	13.2	C6H15O8P	Glycerophosphoglycerol	0.001	0.793
128	171.0066	14.9	C3H9O6P	sn-Glycerol 3-phosphate	0.034	1.684
Miscellaneous						
59	239.1154	16.6	C10H16N4O3	Homocarnosine	0.004	0.622
7071	227.1139	10.3	C9H14N4O3	Carnosine isomer (probably anserine)	0.0009	5.168
4239	170.0812	8.1	C8H11NO3	Pyridoxine	0.005	1.678
5958	169.0971	11.3	C8H12N2O2	Pyridoxamine	0.049	1.245
3	96.96983	13.6	H3O4P	Orthophosphate	0.005	1.168
3930	157.0872	5.5	C8H14O3	[FA oxo(8:0)] 3-oxo-octanoic acid	0.001	1.571
7654	316.2845	4	C18H37NO3	[SP hydrox] 6-hydroxysphing-4E-enine	0.005	1.611
5445	176.0554	15	C6H9NO5	[FA amino,oxo(6:0/2:0)] 2-amino-3-oxo-hexanedioic acid	0.008	0.611
1665	141.0923	4.6	C8H14O2	[FA (8:0)] 2Z-octenoic acid	0.012	1.442
558	159.1029	4.9	C8H16O3	Ethyl (R)-3-hydroxyhexanoate	0.015	2.012
1761	309.2229	4.2	C22H30O	[ST ethyl,methy] 13-ethyl-11-methylene-18,19-dinorpregn-4-en-20-yn-17alpha-ol	0.017	0.612
2237	315.2547	4.1	C18H36O4	[FA hydroxy(18:0)] 9,10-dihydroxy-octadecanoic acid	0.018	1.953
479	171.1029	4.7	C9H16O3	9-Oxononanoic acid	0.019	1.416
7062	188.103	12.5	C7H13N3O3	5-guanidino-3-methyl-2-oxo-pentanoate	0.021	1.443
355	131.0351	14	C5H8O4	2-Acetolactate	0.024	1.438
7036	223.0747	4.5	C7H14N2O4S	L-Cystathionine*	0.026	3.785
279	131.0715	6.2	C6H12O3	6-Hydroxyhexanoic acid	0.027	1.445
526	230.1513	24.2	C10H21N3O3	Gamma-Aminobutyryl-lysine	0.027	0.457
3230	351.2184	5.4	C20H32O5	[FA oxo,hydroxy(2:0)] 9-oxo-11R,15S-dihydroxy-5Z,13E-prostadienoic acid [PGE ₂]	0.027	10.749
276	131.0351	11	C5H8O4	2-Acetolactate	0.029	6.808
222	155.0464	8.5	C6H8N2O3	4-Imidazolone-5-propanoate	0.03	2.317
1186	572.0808	13.2	C16H25N5O14P2	GDP-3,6-dideoxy-D-galactose	0.033	0.654

981	145.0872	4.9	C7H14O3	[FA hydroxy(7:0)] 2-hydroxy-heptanoic acid	0.033	1.333
7167	257.1495	5.6	C12H20N2O4	N-heptadieneoylglutamine	0.034	1.661
275	295.2651	3.9	C19H36O2	[FA methyl(18:0)] 11R,12S-methylene-octadecanoic acid	0.037	0.811
2549	189.0044	12.2	C6H6O7	Oxalosuccinate	0.038	1.869
1676	335.2235	4.9	C20H32O4	Leukotriene B4	0.04	9.21
1522	219.015	12.1	C7H8O8	4-Carboxy-4-hydroxy-2-oxoadipate	0.042	1.752
661	171.0066	15.4	C3H9O6P	*sn-Glycerol 3-phosphate	0.045	0.598
1674	159.1028	6.4	C8H16O3	Ethyl (R)-3-hydroxyhexanoate	0.047	1.419
4370	648.6294	4	C42H81NO3	[SP (24:0)] N-(15Z-tetracosenoyl)-sphing-4-enine	0.05	0.622
3202	175.0978	5	C8H16O4	[FA hydroxy(8:0)] 6,8-dihydroxy-octanoic acid	0.05	1.598

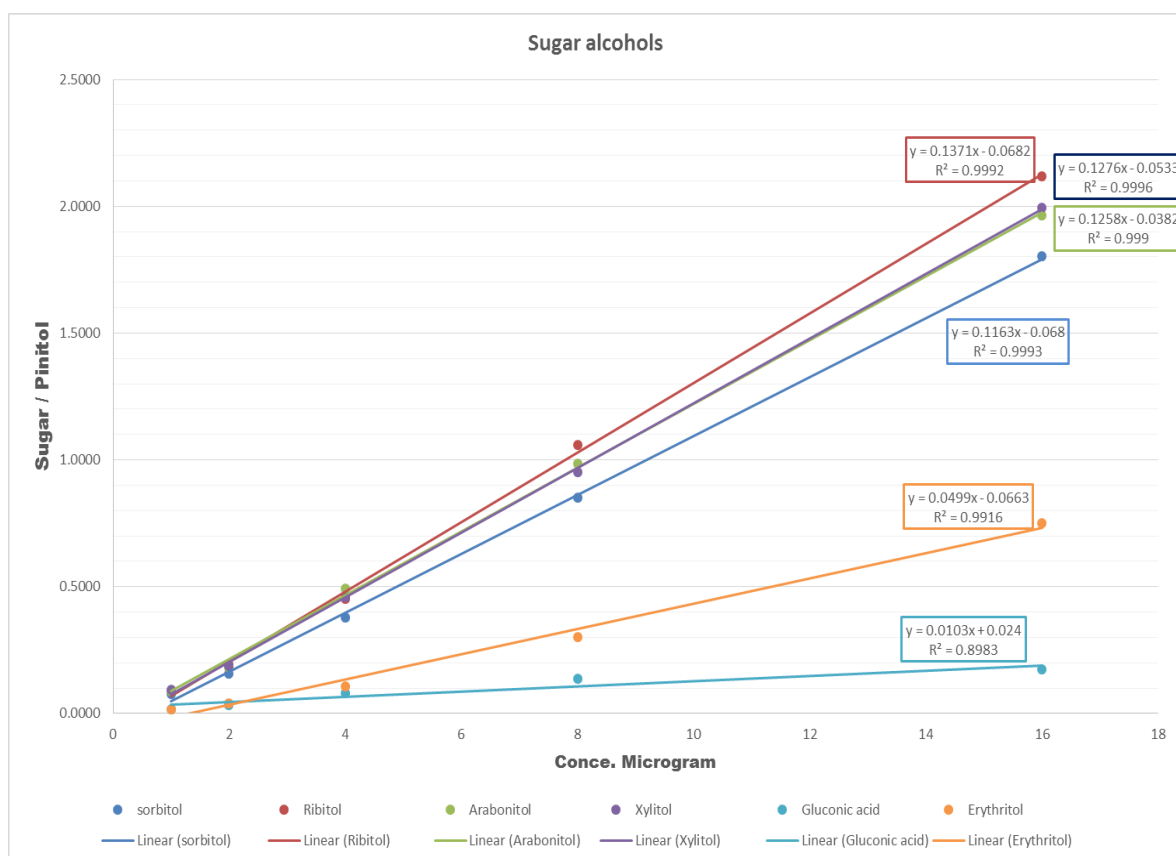


Figure 4-S3: Calibration curve for sugar alcohols and gluconic acid over the range (1-16 μg) with Pinitol (2μg) as an internal standard

Table 4-S3: The area of sugar alcohols and gluconic acid in the range 1–16 µg against 2 µg of pinitol as internal standard

Conce. µg	Area of Pinitol (P)	Area of Sorbitol (S)	Ratio of S/P	Area of Ribitol (R)	Ratio of A/P	Area of Arabinotol (Ar)	Ratio of Ar/P	Area of Xylitol (X)	Ratio of X/P	Area of Gluconic acid (Glu)	Ratio of Glu/P	Area of Erythritol (E)	Ratio of E/P
1	29246902	2222242	0.0760	2600391	0.0889	2558929	0.0875	2711408	0.0927	503593	0.0172	434780	0.0149
2	27630684	4372317	0.1582	5335317	0.1931	4987368	0.1805	5215643	0.1888	935997	0.0339	1113543	0.0403
4	14860830	5609983	0.3775	6694677	0.4505	7313337	0.4921	6836649	0.4600	1168034	0.0786	1608061	0.1082
8	28129739	23931582	0.8508	29751019	1.0576	27745172	0.9863	26742222	0.9507	3843943	0.1367	8426646	0.2996
16	30331954	54659844	1.8021	64241492	2.1179	59565375	1.9638	60527360	1.9955	5222257	0.1722	22802345	0.7518

Table 4-S4: The area of sugar alcohols and gluconic acid in post-mortem brain samples against 2 μ g of pinitol as internal standard.

Sample	Pinitol	Arabinitol	Ar/P	Adonitol	Ad/P	Erythritol	Er/P	Xylitol	Xy/P	Sorbitol	S/P	Gluconic Acid	Gl/P
B1	49463769	3604611	0.073	5097411	0.103	2049349	0.041	3228436	0.065	21198321	0.429	594346	0.012
B2	16895908	1805730	0.107	1849796	0.109	819101	0.048	532725	0.032	4319891	0.256	131270	0.008
B3	49534917	6013865	0.121	10732452	0.217	2913685	0.059	6391736	0.129	11210527	0.226	325877	0.007
B4	27788751	4216563	0.152	6461447	0.233	4034281	0.145	2580507	0.093	24730030	0.890	217161	0.008
B5	34537120	4699469	0.136	10613073	0.307	2387212	0.069	901651	0.026	6955652	0.201	124786	0.004
B6	19511972	2299906	0.118	4051826	0.208	3289464	0.169	2127584	0.109	16300095	0.835	233661	0.012
D1	32341711	4416339	0.137	6276363	0.194	2693246	0.083	1762358	0.054	11328290	0.350	69082	0.002
D2	19177281	2508697	0.131	4320544	0.225	1860891	0.097	1369439	0.071	8509613	0.444	163637	0.009
D3	27296454	6114593	0.224	6271914	0.230	1255571	0.046	642996	0.024	4864905	0.178	30033	0.001
D4	35171702	5216274	0.148	6651703	0.189	2732111	0.078	1439207	0.041	11875420	0.338	241657	0.007
D5	37685355	6371040	0.169	7993999	0.212	1282107	0.034	1058513	0.028	4332802	0.115	60427	0.002
D7	20869093	3884735	0.186	5467769	0.262	2129857	0.102	1642583	0.079	10307901	0.494	231359	0.011
Di2	27512530	2678160	0.097	3251397	0.118	2721541	0.099	2134272	0.078	27355126	0.994	320660	0.012
Di3	20369868	3790805	0.186	2756872	0.135	2051376	0.101	1349548	0.066	15717310	0.772	177627	0.009
Di5	58714088	10256210	0.175	12980324	0.221	2634587	0.045	1921198	0.033	4800748	0.082	76170	0.001

Sample	Pinitol	Arabinitol	Ar/P	Adonitol	Ad/P	Erythritol	Er/P	Xylitol	Xy/P	Sorbitol	S/P	Gluconic Acid	Gl/P
Di6	50273641	7087103	0.141	7987196	0.159	4093291	0.081	2274550	0.045	22021077	0.438	304395	0.006
Di7	41182923	3191585	0.077	4067621	0.099	1585011	0.038	248005	0.006	1477590	0.036	41725	0.001
S3	26670822	8451165	0.317	5198633	0.195	1888851	0.071	1895818	0.071	20436404	0.766	473418	0.018
S4	56988334	6034872	0.106	9869598	0.173	2997320	0.053	5066005	0.089	13117298	0.230	340261	0.006
S7	24218669	4936916	0.204	6604946	0.273	1684771	0.070	579882	0.024	6304182	0.260	80851	0.003
S8	32359521	4369720	0.135	7099697	0.219	1954873	0.060	1465976	0.045	17694742	0.547	352873	0.011
S9	16594314	2159994	0.130	2766985	0.167	1681827	0.101	1230161	0.074	6954518	0.419	355992	0.021
S10	22812876	3304467	0.145	5990359	0.263	2312883	0.101	1991229	0.087	19127513	0.838	316571	0.014
C1	11796227	1423441	0.121	1688187	0.143	647577	0.055	3899237	0.331	1948124	0.165	37073	0.003
C2	18742115	4098413	0.219	4714137	0.252	1342193	0.072	5524170	0.295	3701264	0.197	61999	0.003
C3	24603366	6385687	0.260	4681586	0.190	1799252	0.073	6137159	0.249	10624483	0.432	82511	0.003
C4	18382548	2603330	0.142	3319814	0.181	667939	0.036	2961012	0.161	1995806	0.109	18192	0.001
C5	34466189	4409590	0.128	6929314	0.201	2378638	0.069	8465885	0.246	8323814	0.242	140267	0.004
C7	10955146	1464021	0.134	1595705	0.146	548326	0.050	1506937	0.138	1964931	0.179	21858	0.002
C8	10744676	1807308	0.168	1801197	0.168	1213551	0.113	954276	0.089	8601267	0.801	67785	0.006
C9	18668043	3026922	0.162	3072049	0.165	945660	0.051	1684723	0.090	6873675	0.368	35274	0.002
C10	32495569	6433176	0.198	6078969	0.187	1489876	0.046	6064524	0.187	4056654	0.125	66559	0.002

Sample	Pinitol	Arabinitol	Ar/P	Adonitol	Ad/P	Erythritol	Er/P	Xylitol	Xy/P	Sorbitol	S/P	Gluconic Acid	Gl/P
C13	27524049	4642235	0.169	5266113	0.191	1741124	0.063	2468857	0.090	6161773	0.224	131579	0.005
C14	9786301	1943945	0.199	1591709	0.163	1023762	0.105	587563	0.060	2675732	0.273	20083	0.002
C15	46568409	7728720	0.166	6226777	0.134	2249712	0.048	5974265	0.128	6510806	0.140	270427	0.006
C16	31386724	4643842	0.148	6013478	0.192	1525747	0.049	1735633	0.055	5242321	0.167	67504	0.002
C18	31678993	5534263	0.175	5962034	0.188	1292198	0.041	913612	0.029	4478597	0.141	58639	0.002
C19	38696282	3885881	0.100	8384084	0.217	1910882	0.049	1569108	0.041	8074067	0.209	166051	0.004
C20	32937844	5490133	0.167	8970728	0.272	1564791	0.048	2907179	0.088	4069282	0.124	87594	0.003
C21	30303171	3702620	0.122	4790024	0.158	1503562	0.050	1648437	0.054	6697086	0.221	213116	0.007

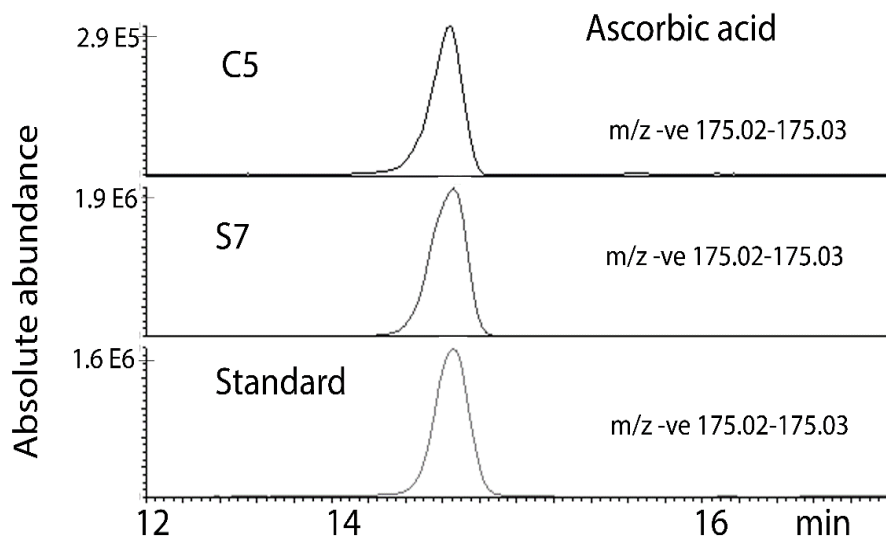


Figure 4-S4: Extracted ion trace showing ascorbic acid in C5 and S7 in comparison with a standard.

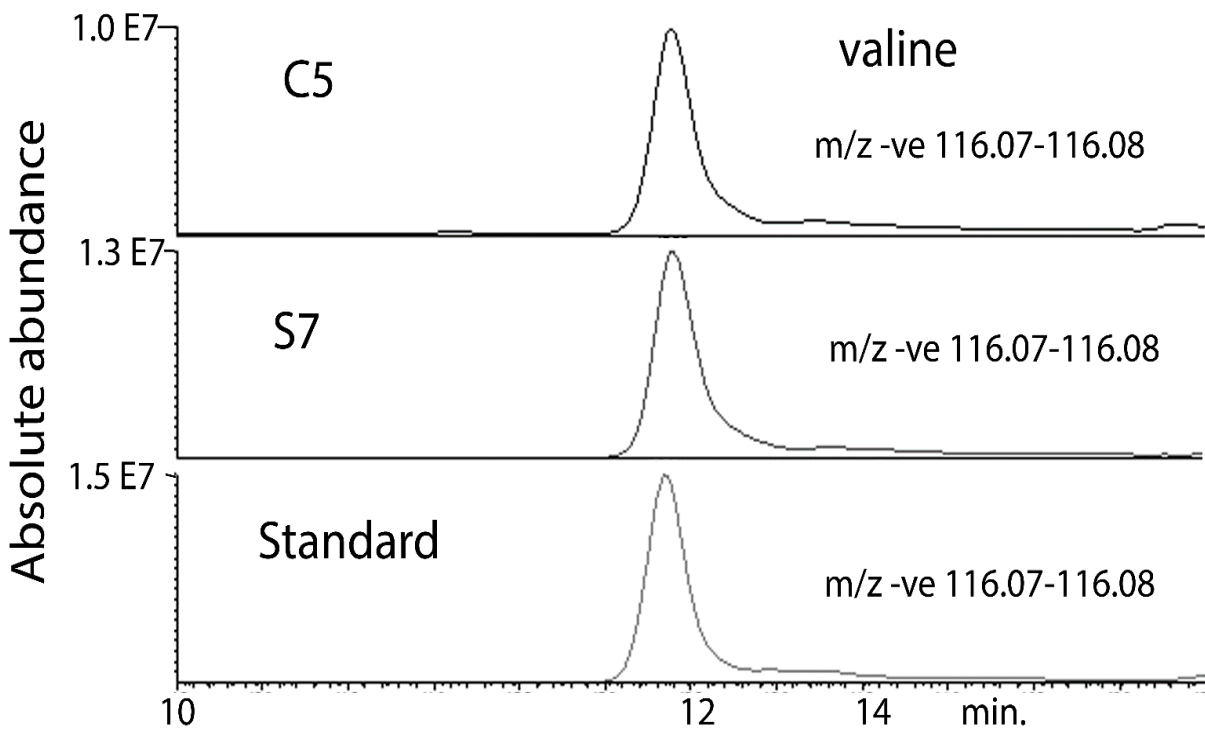


Figure 4-S5: Extracted ion trace showing valine in C5 and S7 in comparison with a standard.

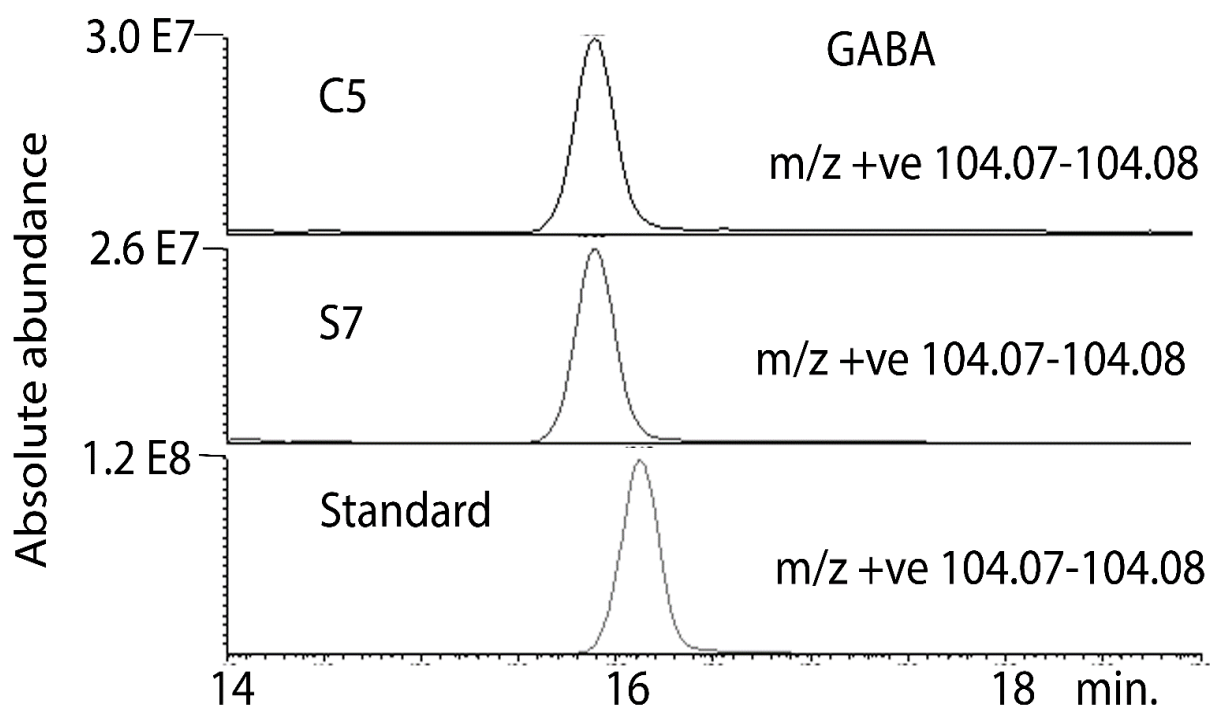


Figure 4-S6: Extracted ion trace showing GABA in C5 and S7 in comparison with a standard.

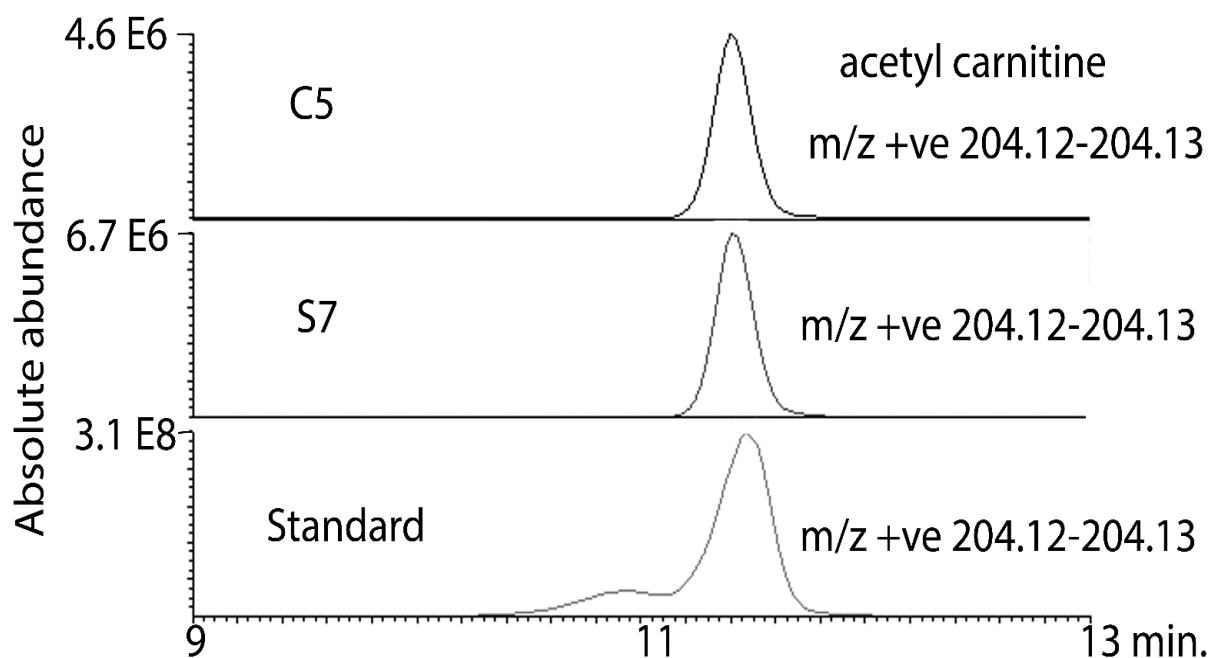


Figure 4-S7: Extracted ion trace showing acetyl carnitine in C5 and S7 in comparison with a standard.

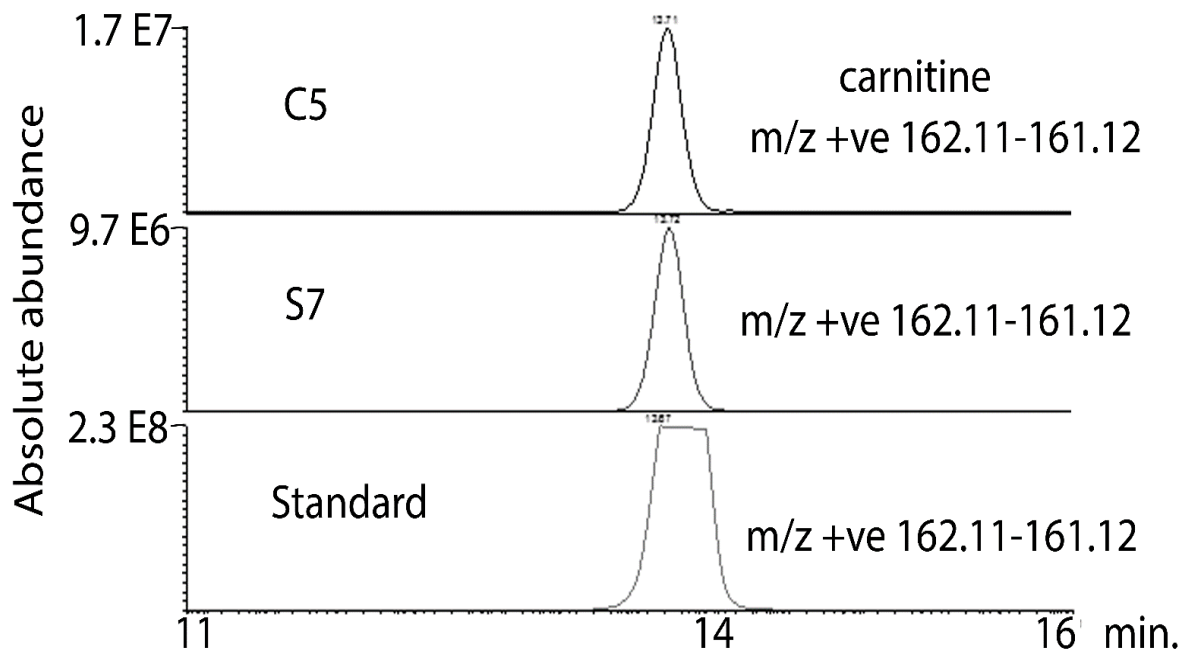


Figure 4-S8: Extracted ion trace showing carnitine in C5 and S7 in comparison with a standard.

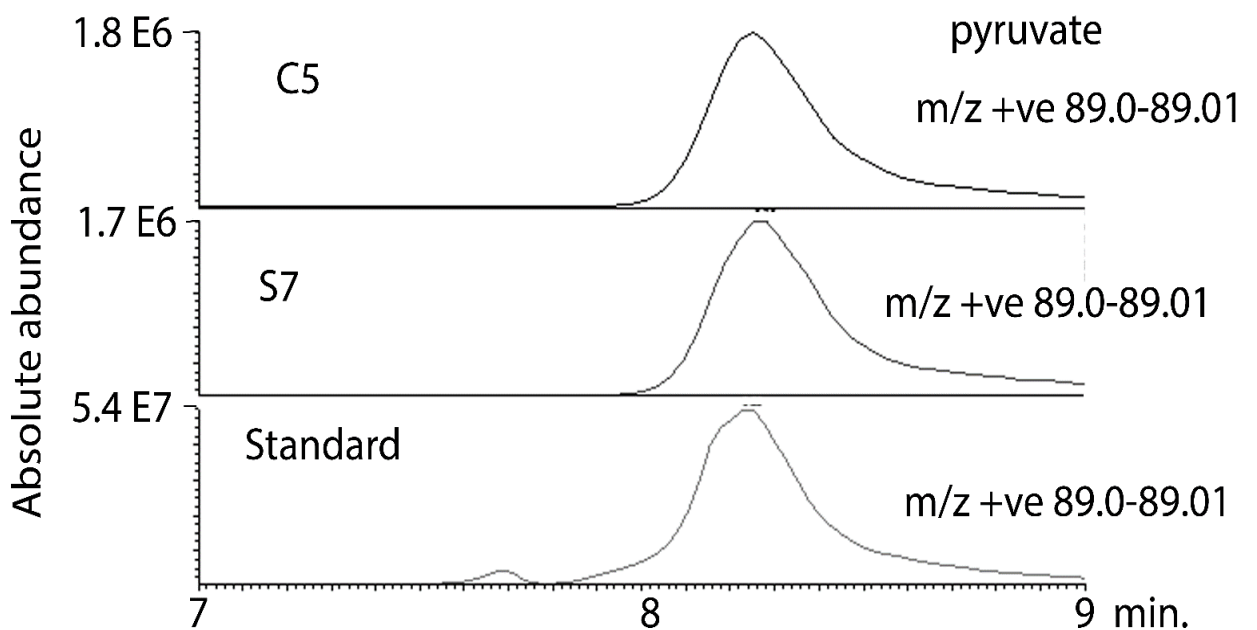
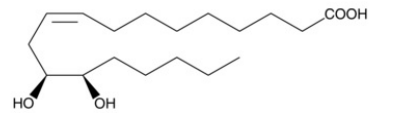
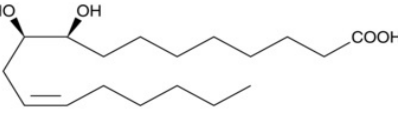
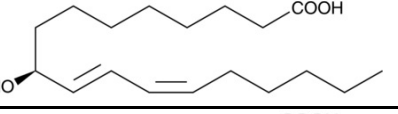
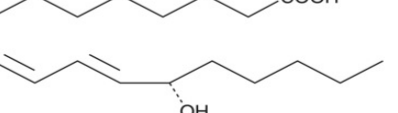
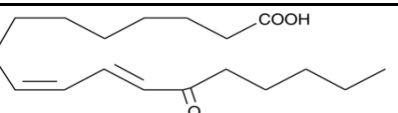
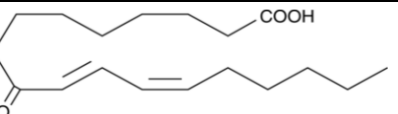
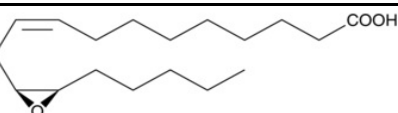
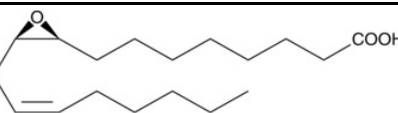
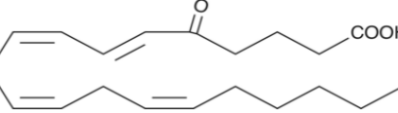
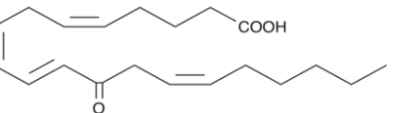

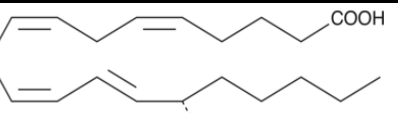
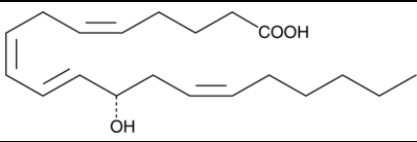
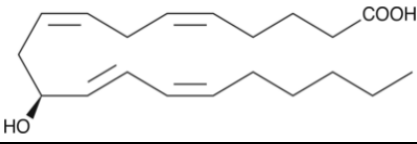
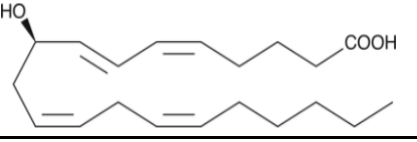
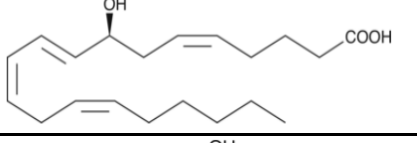
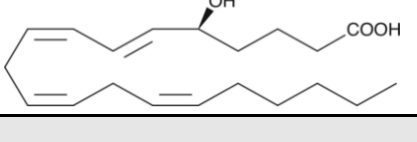
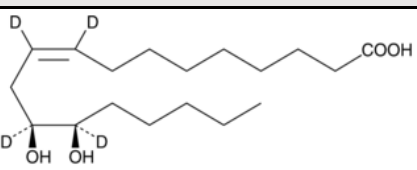
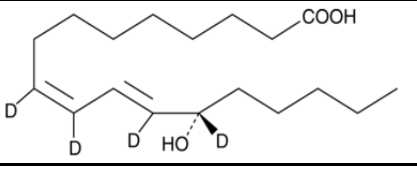
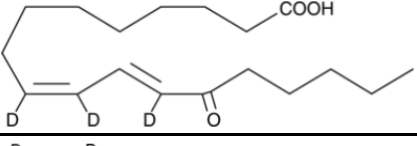
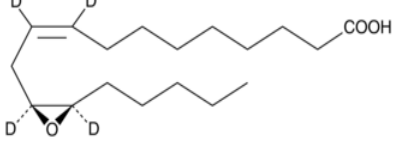


Figure 4-S9: Extracted ion trace showing pyruvate in C5 and S7 in comparison with a standard.

Table 6-S1: the name, molar mass and chemical formula and structure for underivatized oxylipins of LAO, ArAO and DLAO standard mixture.

Oxylipins Name	Abbreviation	Chemical Formula	Molar Mass	Chemical Structure
Linoleic Acid Oxylipin Mixture				
(±)12,13-dihydroxy-9Z-octadecenoic acid	(±)12(13)-DiHOME	C ₁₈ H ₃₄ O ₄	314.50	
(±)9,10-dihydroxy-12Z-octadecenoic acid	(±)9(10)-DiHOME	C ₁₈ H ₃₄ O ₄	314.50	
9S-hydroxy-10E,12Z-octadecadienoic acid	9(s)-HODE	C ₁₈ H ₃₂ O ₃	296.50	
13S-hydroxy-9Z,11E-octadecadienoic acid	13(s)-HODE	C ₁₈ H ₃₂ O ₃	296.50	
13-oxo-9Z,11E-octadecadienoic acid	13-OxoODE	C ₁₈ H ₃₀ O ₃	294.40	
9-oxo-10E,12Z-octadecadienoic acid	9-OxoODE	C ₁₈ H ₃₀ O ₃	294.40	
(±)12(13)epoxy-9Z-octadecenoic acid	(±)12(13)-EpOME	C ₁₈ H ₃₂ O ₃	296.50	
(±)9,10-epoxy-12Z-octadecenoic acid	(±)9(10)-EpOME	C ₁₈ H ₃₂ O ₃	296.50	
Arachidonic Acid Oxylipin Mixture				
5-oxo-6E,8Z,11Z,14Z-eicosatetraenoic acid	5-OxoETE	C ₂₀ H ₃₀ O ₃	404.33	
12-oxo-5Z,8Z,10E,14Z-eicosatetraenoic acid	12-OxoETE	C ₂₀ H ₃₀ O ₃	404.33	
15-oxo-5Z,8Z,11Z,13E-eicosatetraenoic acid	15-OxoETE	C ₂₀ H ₃₀ O ₃	404.33	
15S-hydroxy-5Z,8Z,11Z,13E-eicosatetraenoic acid	15(S)-HETE	C ₂₀ H ₃₂ O ₃	406.33	

12S-hydroxy-5Z,8Z,10E,14Z-eicosatetraenoic acid	12(S)-HETE	C ₂₀ H ₃₂ O ₃	406.33	
11S-hydroxy-5Z,8Z,12E,14Z-eicosatetraenoic acid	11(S)-HETE	C ₂₀ H ₃₂ O ₃	406.33	
9R-hydroxy-5Z,7E,11Z,14Z-eicosatetraenoic acid	9(R)-HETE	C ₂₀ H ₃₂ O ₃	406.33	
8S-hydroxy-5Z,9E,11Z,14Z-eicosatetraenoic acid	8(S)-HETE	C ₂₀ H ₃₂ O ₃	406.33	
5S-hydroxy-6E,8Z,11Z,14Z-eicosatetraenoic acid	5(S)-HETE	C ₂₀ H ₃₂ O ₃	406.33	
Deuterated Linoleic Acid Oxylipin Mixture				
(±)12,13-dihydroxy-9Z-octadecenoic-9,10,12,13-d4 acid	(±)12(13)-DiHOME-d ₄	C ₁₈ H ₃₀ D ₄ O ₄	318.50	
13S-hydroxy-9Z,11E-octadecadienoic-9,10,12,13-d4 acid	13(s)-HODE-d ₄	C ₁₈ H ₂₈ D ₄ O ₃	300.50	
13-oxo-9Z,11E-octadecadienoic-9,10,12,-d3- acid	13-OxoODE-d ₃	C ₁₈ H ₂₇ D ₃ O ₃	297.50	
(±)12(13)epoxy-9Z-octadecenoic-9,10,12,13-d4 acid	(±)12(13)-EpOME-d ₄	C ₁₈ H ₂₈ D ₄ O ₃	300.50	

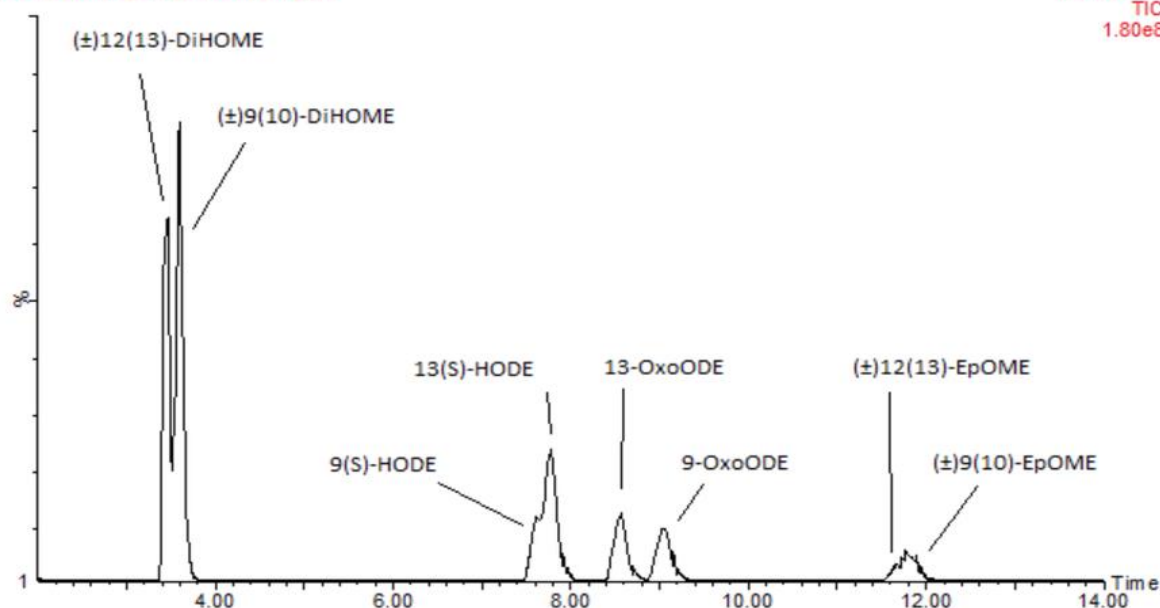


Figure 6-S1: differentiation among LAO isomers depended on product information provided by company under underivatized conditions ("Caymanchem.com, Linoleic Acid Oxylipins LC-MS Mixture, Item № 20794").

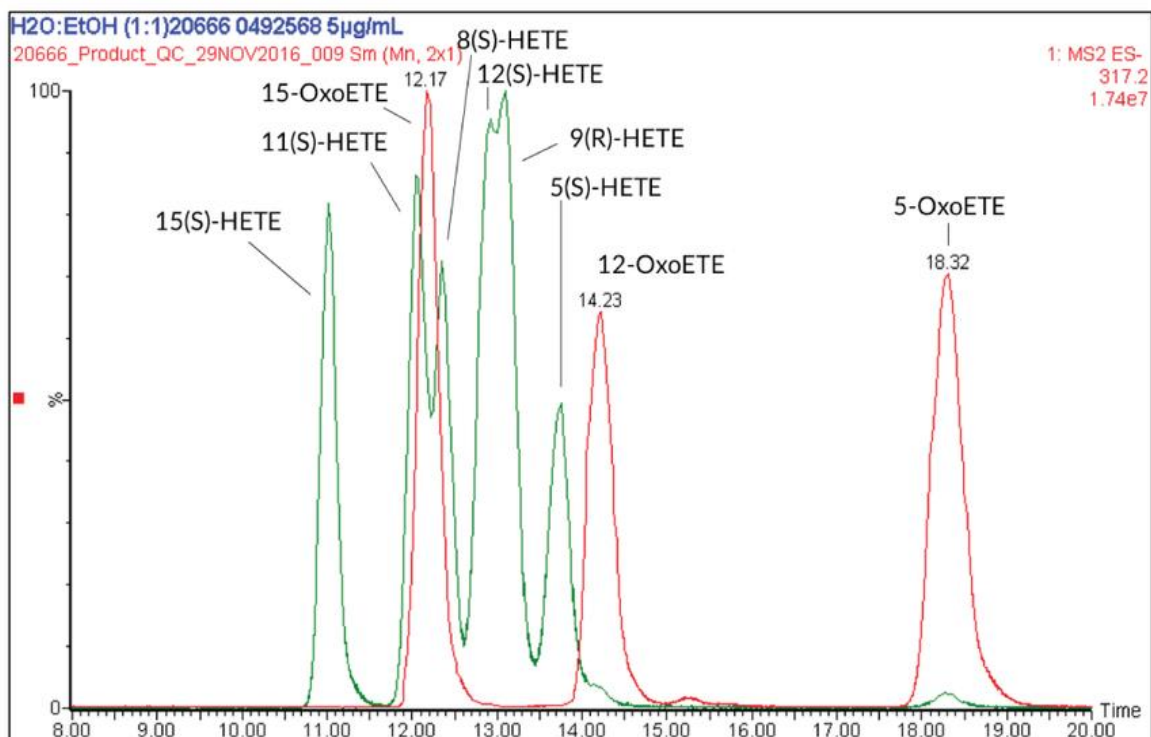


Figure 6-S2: Differentiation among LAO isomers depended on product information provided by company under underivatized conditions ("Caymanchem.com, Arachidonic Acid Oxylipins LC-MS Mixture, Item № 20666").

Appendix-II: Posters Presented in Conferences

1)

The Impact of Exercise on the Urinary Metabolome

Ali Muhsen Ali¹, Mia Burleigh², Evangelia Daskalaki³, Tong Zhang³, Chris Easton², David G Watson³

¹ Strathclyde Institute of Pharmacy and Biomedical Sciences, Glasgow G4 0RE and Thi-Qar University Iraq,
² Institute for Clinical Exercise and Health Science, University of the West of Scotland,
³ Strathclyde Institute of Pharmacy and Biomedical Sciences, Glasgow G4 0RE

Introduction

Regular exercise can modify but more importantly improve overall quality of life and life expectancy. However, questions remain with regard to adequate duration, frequency and intensity, as well as what type of exercise is optimal for individuals of different cohorts (e.g. sedentary vs. already active). A study was conducted with ten participants with a single 1 hour exercise intervention on day 2 and with measurement of VO₂max.

Materials & Methods

Ten health adult who were physically active participated in this study and their characteristics are explained in Table (1).

Participant Characteristics	
Number	10
Age	28.3 ± 6.7
Sex (F/M)	2/8
Stature (cm)	168 ± 30
Weight (kg)	68.33 ± 14.7
VO ₂ max (ml/kg ¹ /min ¹)	197 ± 5.4
Work rate max (W)	134 ± 61.3

Those participants underwent a two day (37 hour) trial where urine samples were collected at regular intervals as shown in figure (1). Aerobic exercise (VO₂max) was performed on bicycle ergometer. Analysis of urine samples was carried out on an Orbitrap Exactive instrument.

Results

Initially modelling was carried out on the first void samples versus the first post-exercise samples. PCA analysis revealed no separation on the basis of modelling based on raw peak areas. Each of the metabolites for each individual for day 1 and day 2 were then normalised to the total output for the metabolite over the day. On this basis the first void and first post exercise samples could be separated by PCA (figure 2) and OPLSDA modelling was used to highlight the most important metabolites (figure 3).

Figure 2 Separation of pre- and post-exercise samples by PCA.

Figure 3 Separation of pre- and post-exercise samples by OPLSDA.

There were many metabolites which were altered. For example the expected elevations in purines occurred post-exercise (table 2) although a wider range of purines are affected than reported previously. Metabolites which were altered included, steroids, bile acids and carnitines. There was also separation between the first and third samples on the non-exercise day and some of these changes were common to the same comparison on the exercise day. Thus two effects are evident, a diurnal variation for some metabolites and for metabolites which are altered by exercise.

Table 2: Alteration in purine metabolites between first void (D2S1) and first post-exercise (D2S3) samples

ID	m/z	Rt	Metabolite	P value D2S1:D2S3	Ratio D2S3:D2S1	VIP value	P(corr)
Purine metabolism							
290	137.046	10.8	Hypoxanthine	0.001	3.75	2.50	-0.89
397	152.057	13.1	Guanine	0.02	2.56	1.82	-0.51
11409	181.037	10.8	1-Methyluric acid	0.01	0.59	1.90	0.56
1154	253.093	9.2	Deoxyinosine	0.01	4.97	2.61	-0.76
1258	269.088	11.5	Inosine	0.02	16.27	3.54	-0.55
1373	285.083	13.1	Xanthosine	0.01	2.33	1.82	-0.61

The VO₂ max for the ten subjects could be correlated to a single metabolite oxoamino hexanoic acid and the model accommodated 22 of the day 2 samples with the post exercise samples correlating most closely. The marker metabolite is in the lysine degradation pathway. Figure 4 shows a plot for observed against predicted VO₂ max for these samples. Inclusion of other lysine degradation metabolites in the model and strengthened its predictive power to some extent. Lysine degradation generates NADPH and thus the marker might be related to efficiency in combating oxidative stress.

Figure 4 Predicted versus observed VO₂ max based on oxoamino hexanoic acid.

Ali Muhsen Ali^{1,2}, Christopher Monaghan³, Chris Easton³ and David G. Watson¹

1. Strathclyde Institute of Pharmacy and Biomedical Sciences, 161, Cathedral Street, Glasgow G4 0RE, Scotland, UK
2. Department of Clinical Biochemistry, Diabetes and Endocrinology Centre, Thi-Qar University, Iraq.
3. Institute for Clinical Exercise and Health Science, University of the West of Scotland

Introduction

The direct exposure to sunlight which is known as one of the main natural sources for producing ultraviolet (UV) radiation has beneficial and harmful effects on human health. UV radiation has been used to enhance the levels of vitamin D [1] and in the treatment of jaundice [2]. On another hand, the most common disorders caused by UV are eye damage and skin cancer which is listed as the cause of death 66,000 individuals annually of all global deaths according to WHO reports[3].

Several recent studies reported that the exposure to UV radiation can influence metabolic pathways in humans, animals and plants. The application of metabolomic analysis may be used as a tool to enhance the understanding of the damaging effects of UV radiation-exposure in human or its potential benefits in promoting nitric oxide production.

Thus, choosing of the potential specimen and appropriate approach is essential in the identification of these impacts on the changes of metabolic profile of human bio fluid samples and understanding the complete biochemical processes following this exposure

objective

Our study sought to compare between metabolomic changes of human urine and plasma to investigate which one can be used as the best tool to identify metabolomic profiling and novel biomarkers associated to the potential effects of ultraviolet-A radiation (UVA) exposure.

Materials and Methods

Human plasma and urine samples were collected from four adult healthy individuals.

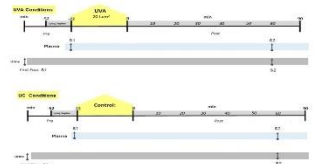


Figure 1: Indicative representation of plasma and urine collection schematic at two consecutive conditions: control conditions, without a dose of UVA light (UVA=0 U/cm²) and Ultraviolet-A conditions, with a dose of UVA light (UVA=20 U/cm²) which is approximately equivalent to 30 min in the sunshine in southern Europe, in summer. The first urine sample on each day was the first pass (typically: 6 am-8 am).

Results

Table 1 (A,2): The relevant important metabolites with high impact on the model separating non-exposure from exposure-UV in urine (Table 1) and plasma (Table 2) based on the critical threshold for a regarding a P-value as being significant is 0.05 and |V1|² > 0. N⁻ negative ion and P⁺ positive ion

Urine samples result							Plasma samples result						
MS/MS	RT	Retention	Name	Abundance	Ratio	MS/MS	RT	Retention	Name	Abundance	Ratio	MS/MS	RT
107.07	6.40	1789630	1-oxo-1,2-dihydro-3H-imidazo[4,5-b]pyridin-3-ylidenehydrazine	1.0401	1.705	1077	1.00	1789630	1-oxo-1,2-dihydro-3H-imidazo[4,5-b]pyridin-3-ylidenehydrazine	0.0002	0.000	1077	1.00
107.07	6.40	1789630	1-oxo-1,2-dihydro-3H-imidazo[4,5-b]pyridin-3-ylidenehydrazine	1.0401	1.705	1077	1.00	1789630	1-oxo-1,2-dihydro-3H-imidazo[4,5-b]pyridin-3-ylidenehydrazine	0.0002	0.000	1077	1.00
107.07	6.40	1789630	1-oxo-1,2-dihydro-3H-imidazo[4,5-b]pyridin-3-ylidenehydrazine	1.0401	1.705	1077	1.00	1789630	1-oxo-1,2-dihydro-3H-imidazo[4,5-b]pyridin-3-ylidenehydrazine	0.0002	0.000	1077	1.00
107.07	6.40	1789630	1-oxo-1,2-dihydro-3H-imidazo[4,5-b]pyridin-3-ylidenehydrazine	1.0401	1.705	1077	1.00	1789630	1-oxo-1,2-dihydro-3H-imidazo[4,5-b]pyridin-3-ylidenehydrazine	0.0002	0.000	1077	1.00
107.07	6.40	1789630	1-oxo-1,2-dihydro-3H-imidazo[4,5-b]pyridin-3-ylidenehydrazine	1.0401	1.705	1077	1.00	1789630	1-oxo-1,2-dihydro-3H-imidazo[4,5-b]pyridin-3-ylidenehydrazine	0.0002	0.000	1077	1.00
107.07	6.40	1789630	1-oxo-1,2-dihydro-3H-imidazo[4,5-b]pyridin-3-ylidenehydrazine	1.0401	1.705	1077	1.00	1789630	1-oxo-1,2-dihydro-3H-imidazo[4,5-b]pyridin-3-ylidenehydrazine	0.0002	0.000	1077	1.00
107.07	6.40	1789630	1-oxo-1,2-dihydro-3H-imidazo[4,5-b]pyridin-3-ylidenehydrazine	1.0401	1.705	1077	1.00	1789630	1-oxo-1,2-dihydro-3H-imidazo[4,5-b]pyridin-3-ylidenehydrazine	0.0002	0.000	1077	1.00
107.07	6.40	1789630	1-oxo-1,2-dihydro-3H-imidazo[4,5-b]pyridin-3-ylidenehydrazine	1.0401	1.705	1077	1.00	1789630	1-oxo-1,2-dihydro-3H-imidazo[4,5-b]pyridin-3-ylidenehydrazine	0.0002	0.000	1077	1.00
107.07	6.40	1789630	1-oxo-1,2-dihydro-3H-imidazo[4,5-b]pyridin-3-ylidenehydrazine	1.0401	1.705	1077	1.00	1789630	1-oxo-1,2-dihydro-3H-imidazo[4,5-b]pyridin-3-ylidenehydrazine	0.0002	0.000	1077	1.00
107.07	6.40	1789630	1-oxo-1,2-dihydro-3H-imidazo[4,5-b]pyridin-3-ylidenehydrazine	1.0401	1.705	1077	1.00	1789630	1-oxo-1,2-dihydro-3H-imidazo[4,5-b]pyridin-3-ylidenehydrazine	0.0002	0.000	1077	1.00
107.07	6.40	1789630	1-oxo-1,2-dihydro-3H-imidazo[4,5-b]pyridin-3-ylidenehydrazine	1.0401	1.705	1077	1.00	1789630	1-oxo-1,2-dihydro-3H-imidazo[4,5-b]pyridin-3-ylidenehydrazine	0.0002	0.000	1077	1.00
107.07	6.40	1789630	1-oxo-1,2-dihydro-3H-imidazo[4,5-b]pyridin-3-ylidenehydrazine	1.0401	1.705	1077	1.00	1789630	1-oxo-1,2-dihydro-3H-imidazo[4,5-b]pyridin-3-ylidenehydrazine	0.0002	0.000	1077	1.00
107.07	6.40	1789630	1-oxo-1,2-dihydro-3H-imidazo[4,5-b]pyridin-3-ylidenehydrazine	1.0401	1.705	1077	1.00	1789630	1-oxo-1,2-dihydro-3H-imidazo[4,5-b]pyridin-3-ylidenehydrazine	0.0002	0.000	1077	1.00
107.07	6.40	1789630	1-oxo-1,2-dihydro-3H-imidazo[4,5-b]pyridin-3-ylidenehydrazine	1.0401	1.705	1077	1.00	1789630	1-oxo-1,2-dihydro-3H-imidazo[4,5-b]pyridin-3-ylidenehydrazine	0.0002	0.000	1077	1.00
107.07	6.40	1789630	1-oxo-1,2-dihydro-3H-imidazo[4,5-b]pyridin-3-ylidenehydrazine	1.0401	1.705	1077	1.00	1789630	1-oxo-1,2-dihydro-3H-imidazo[4,5-b]pyridin-3-ylidenehydrazine	0.0002	0.000	1077	1.00
107.07	6.40	1789630	1-oxo-1,2-dihydro-3H-imidazo[4,5-b]pyridin-3-ylidenehydrazine	1.0401	1.705	1077	1.00	1789630	1-oxo-1,2-dihydro-3H-imidazo[4,5-b]pyridin-3-ylidenehydrazine	0.0002	0.000	1077	1.00
107.07	6.40	1789630	1-oxo-1,2-dihydro-3H-imidazo[4,5-b]pyridin-3-ylidenehydrazine	1.0401	1.705	1077	1.00	1789630	1-oxo-1,2-dihydro-3H-imidazo[4,5-b]pyridin-3-ylidenehydrazine	0.0002	0.000	1077	1.00
107.07	6.40	1789630	1-oxo-1,2-dihydro-3H-imidazo[4,5-b]pyridin-3-ylidenehydrazine	1.0401	1.705	1077	1.00	1789630	1-oxo-1,2-dihydro-3H-imidazo[4,5-b]pyridin-3-ylidenehydrazine	0.0002	0.000	1077	1.00
107.07	6.40	1789630	1-oxo-1,2-dihydro-3H-imidazo[4,5-b]pyridin-3-ylidenehydrazine	1.0401	1.705	1077	1.00	1789630	1-oxo-1,2-dihydro-3H-imidazo[4,5-b]pyridin-3-ylidenehydrazine	0.0002	0.000	1077	1.00
107.07	6.40	1789630	1-oxo-1,2-dihydro-3H-imidazo[4,5-b]pyridin-3-ylidenehydrazine	1.0401	1.705	1077	1.00	1789630	1-oxo-1,2-dihydro-3H-imidazo[4,5-b]pyridin-3-ylidenehydrazine	0.0002	0.000	1077	1.00
107.07	6.40	1789630	1-oxo-1,2-dihydro-3H-imidazo[4,5-b]pyridin-3-ylidenehydrazine	1.0401	1.705	1077	1.00	1789630	1-oxo-1,2-dihydro-3H-imidazo[4,5-b]pyridin-3-ylidenehydrazine	0.0002	0.000	1077	1.00
107.07	6.40	1789630	1-oxo-1,2-dihydro-3H-imidazo[4,5-b]pyridin-3-ylidenehydrazine	1.0401	1.705	1077	1.00	1789630	1-oxo-1,2-dihydro-3H-imidazo[4,5-b]pyridin-3-ylidenehydrazine	0.0002	0.000	1077	1.00
107.07	6.40	1789630	1-oxo-1,2-dihydro-3H-imidazo[4,5-b]pyridin-3-ylidenehydrazine	1.0401	1.705	1077	1.00	1789630	1-oxo-1,2-dihydro-3H-imidazo[4,5-b]pyridin-3-ylidenehydrazine	0.0002	0.000	1077	1.00
107.07	6.40	1789630	1-oxo-1,2-dihydro-3H-imidazo[4,5-b]pyridin-3-ylidenehydrazine	1.0401	1.705	1077	1.00	1789630	1-oxo-1,2-dihydro-3H-imidazo[4,5-b]pyridin-3-ylidenehydrazine	0.0002	0.000	1077	1.00
107.07	6.40	1789630	1-oxo-1,2-dihydro-3H-imidazo[4,5-b]pyridin-3-ylidenehydrazine	1.0401	1.705	1077	1.00	1789630	1-oxo-1,2-dihydro-3H-imidazo[4,5-b]pyridin-3-ylidenehydrazine	0.0002	0.000	1077	1.00
107.07	6.40	1789630	1-oxo-1,2-dihydro-3H-imidazo[4,5-b]pyridin-3-ylidenehydrazine	1.0401	1.705	1077	1.00	1789630	1-oxo-1,2-dihydro-3H-imidazo[4,5-b]pyridin-3-ylidenehydrazine	0.0002	0.000	1077	1.00
107.07	6.40	1789630	1-oxo-1,2-dihydro-3H-imidazo[4,5-b]pyridin-3-ylidenehydrazine	1.0401	1.705	1077	1.00	1789630	1-oxo-1,2-dihydro-3H-imidazo[4,5-b]pyridin-3-ylidenehydrazine	0.0002	0.000	1077	1.00
107.07	6.40	1789630	1-oxo-1,2-dihydro-3H-imidazo[4,5-b]pyridin-3-ylidenehydrazine	1.0401	1.705	1077	1.00	1789630	1-oxo-1,2-dihydro-3H-imidazo[4,5-b]pyridin-3-ylidenehydrazine	0.0002	0.000	1077	1.00
107.07	6.40	1789630	1-oxo-1,2-dihydro-3H-imidazo[4,5-b]pyridin-3-ylidenehydrazine	1.0401	1.705	1077	1.00	1789630	1-oxo-1,2-dihydro-3H-imidazo[4,5-b]pyridin-3-ylidenehydrazine	0.0002	0.000	1077	1.00
107.07	6.40	1789630	1-oxo-1,2-dihydro-3H-imidazo[4,5-b]pyridin-3-ylidenehydrazine	1.0401	1.705	1077	1.00	1789630	1-oxo-1,2-dihydro-3H-imidazo[4,5-b]pyridin-3-ylidenehydrazine	0.0002	0.000	1077	1.00
107.07	6.40	1789630	1-oxo-1,2-dihydro-3H-imidazo[4,5-b]pyridin-3-ylidenehydrazine	1.0401	1.705	1077	1.00	1789630	1-oxo-1,2-dihydro-3H-imidazo[4,5-b]pyridin-3-ylidenehydrazine	0.0002	0.000	1077	1.00
107.07	6.40	1789630	1-oxo-1,2-dihydro-3H-imidazo[4,5-b]pyridin-3-ylidenehydrazine	1.0401	1.705	1077	1.00	1789630	1-oxo-1,2-dihydro-3H-imidazo[4,5-b]pyridin-3-ylidenehydrazine	0.0002	0.000	1077	1.00
107.07	6.40	1789630	1-oxo-1,2-dihydro-3H-imidazo[4,5-b]pyridin-3-ylidenehydrazine	1.0401	1.705	1077	1.00	1789630	1-oxo-1,2-dihydro-3H-imidazo[4,5-b]pyridin-3-ylidenehydrazine	0.0002	0.000	1077	1.00
107.07	6.40	1789630	1-oxo-1,2-dihydro-3H-imidazo[4,5-b]pyridin-3-ylidenehydrazine	1.0401	1.705	1077	1.00	1789630	1-oxo-1,2-dihydro-3H-imidazo[4,5-b]pyridin-3-ylidenehydrazine	0.0002	0.000	1077	1.00
107.07	6.40	1789630	1-oxo-1,2-dihydro-3H-imidazo[4,5-b]pyridin-3-ylidenehydrazine	1.0401	1.705	1077	1.00	1789630	1-oxo-1,2-dihydro-3H-imidazo[4,5-b]pyridin-3-ylidenehydrazine	0.0002	0.000	1077	1.00
107.07	6.40	1789630	1-oxo-1,2-dihydro-3H-imidazo[4,5-b]pyridin-3-ylidenehydrazine	1.0401	1.705	1077	1.00	1789630	1-oxo-1,2-dihydro-3H-imidazo[4,5-b]pyridin-3-ylidenehydrazine	0.0002	0.000	1077	1.00
107.07	6.40	1789630	1-oxo-1,2-dihydro-3H-imidazo[4,5-b]pyridin-3-ylidenehydrazine	1.0401	1.705	1077	1.00	1789630	1-oxo-1,2-dihydro-3H-imidazo[4,5-b]pyridin-3-ylidenehydrazine	0.0002	0.000	1077	1.00
107.07	6.40	1789630	1-oxo-1,2-dihydro-3H-imidazo[4,5-b]pyridin-3-ylidenehydrazine	1.0401	1.705	1077	1.00	1789630	1-oxo-1,2-dihydro-3H-imidazo[4,5-b]pyridin-3-ylidenehydrazine	0.0002	0.000	1077	1.00
107.07	6.40	1789630	1-oxo-1,2-dihydro-3H-imidazo[4,5-b]pyridin-3-ylidenehydrazine	1.0401	1.705	1077	1.00	1789630	1-oxo-1,2-dihydro-3H-imidazo[4,5-b]pyridin-3-ylidenehydrazine	0.0002	0.000	1077	1.00
107.07	6.40	1789630	1-oxo-1,2-dihydro-3H-imidazo[4,5-b]pyridin-3-ylidenehydrazine	1.0401	1.705	1077	1.00	1789630	1-oxo-1,2-dihydro-3H-imidazo[4,5-b]pyridin-3-ylidenehydrazine	0.0002	0.000	1077	1.00
107.07	6.40	1789630	1-oxo-1,2-dihydro-3H-imidazo[4,5-b]pyridin-3-ylidenehydrazine	1.0401	1.705	1077	1.00	1789630	1-oxo-1,2-dihydro-3H-imidazo[4,5-b]pyridin-3-ylidenehydrazine	0.0002	0.000	1077	1.00
107.07	6.40	1789630	1-oxo-1,2-dihydro-3H-imidazo[4,5-b]pyridin-3-ylidenehydrazine	1.0401	1.705	1077	1.00	1789630	1-oxo-1,2-dihydro-3H-imidazo[4,5-b]pyridin-3-ylidenehydrazine	0.0002	0.000	1077	1.00
107.07	6.40	1789630	1-oxo-1,2-dihydro-3H-imidazo[4,5-b]pyridin-3-ylidenehydrazine	1.0401	1.705	1077	1.00	1789630	1-oxo-1,2-dihydro-3H-imidazo[4,5-b]pyridin-3-ylidenehydrazine	0.0002	0.000	1077	1.00
107.07	6.40	1789630	1-oxo-1,2-dihydro-3H-imidazo[4,5-b]pyridin-3-ylidenehydrazine	1.0401	1.705	1077	1.00	1789630	1-oxo-1,2-dihydro-3H-imidazo[4,5-b]pyridin-3-ylidenehydrazine	0.0002	0.000	1077	1.00
107.07	6.40	1789630	1-oxo-1,2-dihydro-3H-imidazo[4,5-b]pyridin-3-ylidenehydrazine	1.0401	1.705	1077	1.00	1789630	1-oxo-1,2-dihydro-3H-imidazo[4,5-b]pyridin-3-ylidenehydrazine	0.0002	0.000	1077	1.00
107.07	6.40	1789630	1-oxo-1,2-dihydro-3H-imidazo[4,5-b]pyridin-3-ylidenehydrazine	1.0401	1.705	1077	1.00	1789630	1-oxo-1,2-dihydro-3H-imidazo[4,5-b]pyridin-3-ylidenehydrazine	0.0002	0.000	1077	1.00
107.07	6.40	1789630	1-oxo-1,2-dihydro-3H-imidazo[4,5-b]pyridin-3-ylidenehydrazine	1.0401	1.705	1077	1.00	1789630	1-oxo-1,2-dihydro-3H-imidazo[4,5-b]pyridin-3-ylidenehydrazine	0.0002	0.000	1077	1.00
107.07	6.40	1789630	1-oxo-1,2-dihydro-3H-imidazo[4,5-b]pyridin-3-ylidenehydrazine	1.0401	1.705	1077	1.00	1789630	1-oxo-1,2-dihydro-3H-imidazo[4,5-b]pyridin-3-ylidenehydrazine	0.0002	0.000	1077	1.00



An Enhanced LC-MS Approach to Detection Carboxylic Acid and Its Oxidised in Biological Samples by Derivatisation with Choline Coupling

Ali Muhsen Ali^{1,2} and David G. Watson¹

1. Strathclyde Institute of Pharmacy and Biomedical Sciences, 161, Cathedral Street, Glasgow G4 0RE, Scotland, UK
2. Department of Clinical Biochemistry, College of science , Thi-Qar University, Iraq.



Introduction

Fatty acids and other metabolites containing a carboxyl group is of high interest in biomedicine because of their major role in metabolic pathways. Many instrumental techniques such as gas chromatography (GC), high-performance liquid chromatography (HPLC) were applied in the analysis of carboxylic acids containing. In target metabolomics approaches, Liquid chromatography-mass spectrometry (LC-MS) is one of the most prominent analytical techniques [1]. However, these methods lack sensitivity and selectivity [2].

Derivatization reactions are widely used in analytical chemistry and instrumental analysis to improve analytical capabilities and are frequently used to enhance ionization or introduce a specific mass shift to the sample ions that becomes evident in the mass spectrum. Traditional derivatization by silylation or methylation in GC/MS methods was employed in the analysis of fatty acids [3]. In LC-MS, chemical derivatizations to tag carboxylic acid compounds with a permanent positive charge such as quaternary ammonium compounds will increase the sensitivity and selectivity of LC-MS detection. This strategy will cause targeted carboxylic acid compounds have a positive charge in both acidic as well as mobile phases.

Objective : The objective of this study describes a new and novel strategy for quantification and analysing carboxyl-containing compounds in biological samples by soft ionization (ESI).

Materials and Methods

The coupling of choline to fatty acids was performed by using FDMP coupling reagent. The reaction outline and LC-MS condition for this method are illustrated in figure (1).

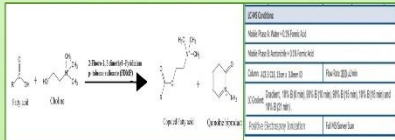


Figure 1: Choline coupling to derivatise fatty acids.

Human plasma samples were collected from seven adult healthy individuals after beetroot ingestion (figure 2).

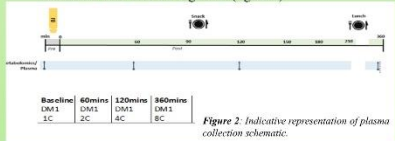


Figure 2: Indicative representation of plasma collection schematic.

Solutions of the linoleic acid oxylipins (MixS1-LAO), standard mixture, and deuterated linoleic acid oxylipins (MixS2-DLA), internal standards, were obtained from Cayman Chemical Company

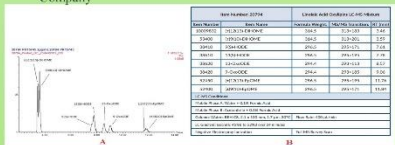


Figure 3: Description of the extracted ion chromatograms (A) and product information (B) for the linoleic acid oxylipins LC-MS mixture (LAO) [4].

Results

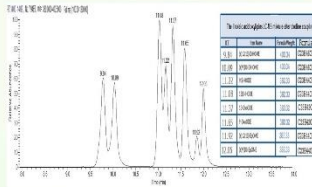


Figure 4: The extracted ion chromatograms and details for the linoleic acid oxylipins LC-MS mixture (LAO) in derivatization method of the coupling of choline to fatty acids.

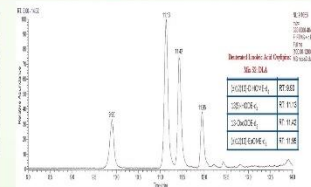


Figure 5: The extracted ion deuterated linoleic acid oxylipins (DLA), internal standards, in derivatization method of the coupling of choline to fatty acids.

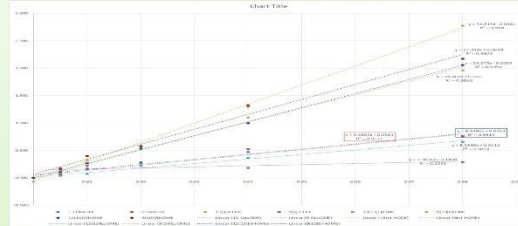


Figure 6: Calibration curve for the LAO mixture against the internal standard, DLA mixture.

Table 1: Calibration data based on ratio of response of derivatized LAO to response for derivatized DLA over the range 0.005–0.08 µg.

LAO Mixture	Equation of the line	(R ²)
(+)-12,13-dihydroxy-9Z-octadecenoic acid [12(13)DiHOME]	Y=25.679X - 0.0025	0.9994
(+)-9,10-dihydroxy-12Z-octadecenoic acid [9(10)DiHOME]	Y=27.314X + 0.0649	0.9871
9S-hydroxy-10E,12Z-octadecadienoic acid [9(s)-HODE]	Y=1.9876X + 0.1404	0.3235
13S-hydroxy-9Z,11E-octadecadienoic acid [13(s)-HODE]	Y=24.804X + 0.026	0.9953
13-oxo-9Z,11E-octadecadienoic acid [13-OxoODE]	Y=9.4486X + 0.0414	0.9819
9-oxo-10E,12Z-octadecadienoic acid [9-OxoODE]	Y=9.3852X + 0.0561	0.9571
(±)12(13)epoxy-9Z-octadecenoic acid [12(13)EpOME]	Y=8.2993X + 0.0112	0.9874
(±)9,10-epoxy-12Z-octadecenoic acid [9(10)EpOME]	Y=34.815X - 0.0481	0.998

Table 2: Average of calculated amount (µg) of oxylipin in 100µl of plasma samples from beetroot study and the ratio and p-value based on the critical threshold 0.05.

oxylipin	Average of calculated amount µg ± RSD								Ratio	P-Value
	Baseline (C1)	60min (C2)	120min (C4)	360min (C8)	C2/C1	C4/C1	C8/C1	C1-C2		
13-OxoODE	0.0045 ± 0.69	0.0045 ± 2.23	0.0045 ± 1.56	0.0045 ± 1.18	1.011	1.003	1.007	0.2763	0.6294	0.2256
9-OxoODE	0.0061 ± 0.81	0.0061 ± 0.64	0.0061 ± 0.72	0.0061 ± 0.75	0.999	0.998	0.997	0.8257	0.5940	0.4835
13(s)-HODE	0.0011 ± 1.72	0.0012 ± 5.35	0.0012 ± 3.66	0.0012 ± 3.27	1.079	1.043	1.062	0.0102	0.0266	0.0023
9(s)-HODE	0.0717 ± 0.50	0.0733 ± 2.83	0.0727 ± 1.41	0.0728 ± 1.65	1.023	1.014	1.015	0.0852	0.0485	0.0627
12(13) EpOME	0.0014 ± 2.15	0.0014 ± 2.68	0.0014 ± 2.64	0.0014 ± 3.63	1.028	1.013	1.033	0.0609	0.4285	0.0753
9(10) EpOME	0.0014 ± 0.47	0.0014 ± 0.70	0.0014 ± 0.52	0.0014 ± 1.28	1.001	0.999	1.007	0.7797	0.6377	0.2440

Conclusion

In this study, A new and easy strategy was developed to detect and quantify carboxylic acid derivatives in biological samples. The method proved to be precise and reproducible and can quantify oxidised fatty acids compounds to 5 Nano grams. Six oxylipins,13-OxoODE, 9-OxoODE, 13(s)-HODE, 9(s)-HODE, 12(13) EpOME and 9(10) EpOME, were quantified in beetroot plasma samples.

References

1. Qi, B.-L., et al., Derivatization for liquid chromatography-mass spectrometry. TrAC Trends in Analytical Chemistry, 2014. 59; p. 121-132.
2. Chen, S.-H. and Y.-J. Chang, Analysis of fatty acids by column liquid chromatography. Analytica Chimica Acta, 2002. 465(1-2): p. 145-155.
3. Brooks, C.J.W., et al., Derivatives suitable for GC-MS. Chemistry and Physics of Lipids, 1978. 21(4): p. 403-416.
4. Caymanchem.com, Linoleic Acid Oxylipins LC-MS Mixture, Item No 20794. <https://www.caymanchem.com/product/20794/image/>.